VOLUME 64
NUMBER 9 / NUMÉRO 9
SEPTEMBER / SEPTEMBRE
2007

Canadian Journal of
FISHERIES AND AQUATIC SCIENCES
cjfas.nrc.ca

An NRC Research Press
JOURNAL
Une REVUE des
Presses scientifiques du CNRC

Journal canadien des
SCIENCES HALIEUTIQUES ET AQUATIQUES
jcsha.cnrc.ca

National Research Council Canada
Conseil national de recherches Canada
NRC·CNRC

ISSN 0706-652X / CJFSDX 64(9) 1157–1289 (2007)

The *Canadian Journal of Fisheries and Aquatic Sciences*, previously published as *Contributions to Canadian Biology* 1901–1925, *Contributions to Canadian Biology and Fisheries* 1926–1934, *Journal of the Biological Board of Canada* 1934–1937, and *Journal of the Fisheries Research Board of Canada* 1938–1979, is issued monthly to form annual volumes of 12 numbers plus supplements.

Editorial policy. The Journal publishes original research articles, perspectives (syntheses, critiques, reevaluations), discussions (comment and reply), and rapid communications. Manuscripts may concern cells, organisms, populations, communities, ecosystems, or processes that affect aquatic systems. They may cover a range of disciplines including biology and ecology of marine and freshwater organisms, limnology, oceanography, physiology, toxicology, genetics, economics, disease, and management. Preference will be given to manuscripts that emphasize understanding of observed phenomena and interpretation of experimental results. The Journal encourages papers that lead from clearly stated purpose or rationale and from testable hypotheses, concepts, or questions to identifiable conclusions or syntheses. Such papers may amplify, modify, question, or redirect accumulated knowledge embodied in contemporary perceptions of a particular state of aquatic sciences. The Journal discourages papers that are essentially descriptive, except in emerging disciplines; have only site-specific or local applications (a certain year, place, taxon, chemical compound, etc.); only confirm previously established principles; or apply standard techniques without breaking new methodological ground.

Manuscripts for publication should be submitted to the Editorial Office via NRC Research Press' online submission and peer review system (**OSPR**EY) at http://pubs.nrc-cnrc.gc.ca/cjfas/osprey. Alternatively, manuscripts may be submitted to the Editor, *Canadian Journal of Fisheries and Aquatic Sciences*, Department of Ecology and Evolutionary Biology, University of Toronto, Toronto, ON M5S 3G5, Canada (416-946-0609; fax: 866-523-4174 (Canada and United States) or 416-946-0509; e-mail: cjfas@utoronto.ca).

Submissions in either English or French are acceptable. The information must be original, that is, not copyrighted, published, or submitted elsewhere except in abstract form or unless by written consent of the Editor.

Correspondence concerning accepted manuscripts and corrected proofs should be sent to NRC Research Press, National Research Council of Canada, Ottawa, ON K1A 0R6, Canada (fax: 613-952-7656; e-mail: pubs@nrc-cnrc.gc.ca).

Instructions to Authors are published once a year in the first issue of each volume. Copies are available from NRC Research Press or at cjfas.nrc.ca. The **Publication Policy** of NRC Research Press is available at pubs.nrc-cnrc.gc.ca.

Microfilm. Issues from 1934 through the current volume can be purchased on 16- or 35-mm microfilm. Photocopies of individual articles or issues can be purchased from University Microfilms International, 330 North Zeeb Road, Ann Arbor, MI 48106, USA.

The *Canadian Journal of Fisheries and Aquatic Sciences*, ISSN 0706-652X, is published monthly, 12 times per year, by NRC Research Press, c/o USACAN Media Dist. Srv. Corp. at 26 Power Dam Way, Suite S1-S3, Plattsburgh, NY 12901, USA. Periodicals postage paid at Plattsburgh, NY. POSTMASTER: Send address changes to *Canadian Journal of Fisheries and Aquatic Sciences*, c/o NRC, P.O. Box 2888, Plattsburgh, NY 12901, USA.

Publié sans interruption depuis 1901, le *Journal canadien des sciences halieutiques et aquatiques* a paru sous plusieurs titres : *Contributions to Canadian Biology* 1901–1925, *Contributions to Canadian Biology and Fisheries* 1926–1934, *Journal of the Biological Board of Canada* 1934–1937, et *Journal of the Fisheries Research Board of Canada* 1938–1979. Le Journal paraît tous les mois, formant ainsi un volume de 12 numéros, et offre en plus jusqu'à deux suppléments par année.

Politique éditoriale. On publie, dans le Journal, des articles rendant compte de recherche originale, des perspectives (synthèses, critiques et réévaluations), des discussions (commentaires et réponses) et des communications rapides. Les documents peuvent porter sur les cellules, organismes, populations, communautés, écosystèmes ou processus qui affectent les systèmes aquatiques. Ils peuvent relever de divers domaines y compris la biologie et l'écologie des organismes marins et d'eau douce, la limnologie, l'océanographie, la physiologie, la toxicologie, la génétique, l'économie, la pathologie et la gestion. On accorde la préséance aux articles qui contribuent à la compréhension de phénomènes observés et à l'interprétation de résultats expérimentaux. On invite les auteurs à soumettre des articles ayant des objectifs précis ou relevant d'hypothèses, de concepts ou de questions vérifiables et se terminant par de solides conclusions ou d'utiles synthèses. Ces articles enrichissent, changent, mettent en question ou réorientent les connaissances acquises sur divers aspects des sciences aquatiques. On décourage toutefois la soumission d'articles simplement descriptifs (à moins qu'il ne s'agisse de nouvelles disciplines), d'application très limitée (applicables à une seule année, une seule région ou un seul taxon, portant sur un unique composé chimique, etc.); d'articles qui ne font que reprendre les principes énoncés dans des articles précédents; et d'articles rendant compte de l'application de normes sans gain de méthodologie.

Les auteurs sont invités à soumettre leur **manuscrit** au Bureau de la rédaction par le truchement du Système de soumission et d'examen en direct des articles (**OSPR**EY) des Presses scientifique du CNRC à http://pubs.nrc-cnrc.gc.ca/jcsha/osprey. Sinon, ils peuvent transmettre leur manuscrit par la poste au directeur scientifique, *Journal canadien des sciences halieutiques et aquatiques*, Département d'écologie et de biologie évolutive, Université de Toronto, Toronto, ON M5S 3G5, Canada (416-946-0609; télécopieur : 866-523-4174 (Canada et États-Unis) ou 416-946-0509; courriel : cjfas@utoronto.ca).

Les contributions peuvent être en anglais ou en français. Elles doivent être originales, c.-à.-d. qu'elles ne doivent pas avoir fait l'objet d'un copyright, avoir été publiées ou soumises ailleurs, sauf sous forme abrégée ou avec le consentement du rédacteur. Le CNRC ne se tient en aucune façon responsable des opinions exprimées par un collaborateur ou des déclarations qui pourrait faire ce dernier.

La correspondance ayant trait aux manuscrits acceptés et les **épreuves corrigés** doivent être envoyées aux Presses scientifiques du CNRC, Conseil national de recherches du Canada, Ottawa, ON K1A 0R6, Canada (télécopieur : 613-952-7656; courriel : pubs@nrc-cnrc.gc.ca).

Les Recommandations aux auteurs sont publiées une fois par année dans le premier numéro de chaque volume. Des copies sont disponibles auprès du Bureau de la rédaction aux Presses scientifiques du CNRC ou au jcsha.cnrc.ca. **La Politique de publication** est disponible auprès des Presses scientifiques du CNRC ou au pubs.nrc-cnrc.gc.ca.

Microfilms. On peut acheter sur microfilms de 16 ou 35 mm tous les numéros depuis 1934. Des photocopies d'articles ou de numéros individuels sont aussi en vente auprès de University Microfilms International, 330 North Zeeb Road, Ann Arbor, MI 48106, É.-U.

This Journal is indexed or abstracted in / Cette revue est signalée ou résumée dans
ABSEARCH; Applied Science and Technology Index and Abstracts; Aquatic Sciences and Fisheries Abstracts; Biological Abstracts; Biological and Agricultural Abstracts; CAB Abstracts; Chemical Abstracts; Current Contents; Elsevier BIOBASE; Environmental Abstracts; ETDE Energy Database; General Science Index and Abstracts; GEOBASE; GeoRef; Life Sciences Collection; Meteorological and Geoastrophysical Abstracts; Oceanic Abstracts; PASCAL Database; Science Citation Index.

Volume 64, Number 9, September 2007

Canadian Journal of Fisheries and Aquatic Sciences

Published by the National Research Council of Canada

Volume 64, numéro 9, septembre 2007

Journal canadien des sciences halieutiques et aquatiques

Publié par le Conseil national de recherches du Canada

Editor / Directeur scientifique Don Jackson

Vice-editor / Vice-directeur scientifique

Rolf Vinebrooke, *University of Alberta*

Assistant to the Editors / Adjointe aux directeurs scientifiques **Holly Foster**

Associate Editors / Directeurs scientifiques associés

D. Boisclair, *Université de Montréal*
U. Borgmann, *Environment Canada, Burlington*
M.J. Bradford, *DFO/MPO and Simon Fraser University*
S.E. Campana, *DFO/MPO, Dartmouth*
Y. Chen, *University of Maine, Orono, Maine*
J.W.A. Grant, *Concordia University*
M.M. Hansen, *Danish Institute for Fisheries Research, Silkeborg, Denmark*
R. Hilborn, *University of Washington*
J.M. Jech, *NFSC/NOAA, Woods Hole, Mass.*
B. Jonsson, *Norwegian Institute for Nature Research, Oslo, Norway*
K.A. Kidd, *University of New Brunswick*
D.L. MacLatchy, *University of New Brunswick, Saint John*
P. Magnan, *Université du Québec à Trois Rivières*
C.T. Marshall, *University of Aberdeen*
Y.T. Prairie, *Université du Québec à Montréal*
T.J. Quinn II, *University of Alaska–Fairbanks, Juneau, Alaska*
T.P. Quinn, *University of Washington*
C.W. Ramcharan, *Laurentian University*
J.S. Richardson, *The University of British Columbia*
K. Rose, *Louisiana State University, Baton Rouge, La.*
B. Sainte-Marie, *DFO/MPO, Mont-Joli*
R.E.H. Smith, *University of Waterloo*
S.J. Smith, *DFO/MPO, Dartmouth*
E.B. Taylor, *The University of British Columbia*
C.J. Walters, *The University of British Columbia*
G. Weyhenmeyer, *Swedish University of Agricultural Sciences, Uppsala, Sweden*
B. de Young, *Memorial University of Newfoundland*

NRC Research Press / Presses scientifiques du CNRC

Fax / Télécopieur : 613-952-7656; e-mail / courriel : pubs@nrc-cnrc.gc.ca; URL / URL : pubs.nrc-cnrc.gc.ca
Editor-in-Chief / Directeur scientifique en chef **Bruce P. Dancik**
Assistant Editor-in-Chief / Adjoint au directeur scientifique en chef **Donald S. Mavinic**
Director / Directeur **Cameron D. Macdonald**

Acting Business Manager / Gestionnaire des affaires commerciales par intérim **Mike Boroczki**
Advertising and reprints / Annonces publicitaires et tirés à part **Roxanne Landriault** (613-990-2254)
Subscriptions / Abonnements **Eileen Evans-Nantais** (613-990-7873), **André Séguin** (613-993-9084)

Manager, Journals Program / Gestionnaire du Programme des revues **Carolyn Brown**
Managing Editor / Rédactrice administrative **Cecily M. Pearson** (613-993-9099)
Publication Officers / Agents de publication **Jennifer McColl, Thad Costigan**
Editorial Publication Assistants / Adjoints à la publication **Diana Leck, Luc Julien**

Production Manager / Gestionnaire de la production **Brad Stoppa**
Production Application Support Technician / Technicienne au soutien de la production **Judy Hum**
Desktop Publishing Technician / Technicienne en éditique **Lisette Séguin**
Graphics Technician / Technicien en graphisme **Dario Ferrara**
Web Technician / Technicien Web **Dennis Cafferty**

The National Research Council of Canada accepts no responsibility for statements or opinions expressed by a contributor. Acceptance of an advertisement, announcement, or other material does not imply endorsement by either the Journal's Senior Editor or the National Research Council.

© National Research Council of Canada 2007. All rights reserved.

No part of this publication may be reproduced, stored, or transmitted in any form or by any means, without the written permission of the publisher, except as stated below.

The National Research Council of Canada grants **permission*** to individuals to make single copies of articles for personal use. Any person may reproduce short excerpts from articles in the journal for any purpose that respects the moral rights of authors, provided that the source is fully acknowledged. As a courtesy, the consent of authors of such material should be obtained directly from the author.

Authorization to reproduce items for other than personal use, as stated above, is granted by the National Research Council of Canada provided that the copyright fee of $7.00 per copy is paid directly to Access Copyright, The Canadian Copyright Licensing Agency, One Yonge Street, Suite 800, Toronto, ON M5E 1E5, Canada.

*The above permission does not extend to other kinds of copying, such as copying for general distribution, for advertising, or promotional purposes, for creating new collective works, or for resale. For such copying, arrangements must be made with the publisher, National Research Council of Canada, Ottawa, ON K1A 0R6, Canada.

Subscription information

The *Canadian Journal of Fisheries and Aquatic Sciences* (ISSN 0706-652X) is published monthly by the National Research Council of Canada. The 2007 annual subscription rates (second class postage) for Canada are $1051CAN institutional and $325CAN personal, for US & foreign $1051US institutional and $325US personal. For air mail add $150US to foreign rate. Canadian customers please include 6% GST (business no. 12149 1807 RT 0275). Subscriptions are entered for the calendar year. Remittances should be made payable to the Receiver General for Canada, credit NRC. Price for regular single issues: institutional, $110.00; personal, $35.00. Supplements will be priced separately. Special rates apply to members of Canadian scientific and engineering societies if they subscribe through their respective societies.

There are no refunds on cancelled subscriptions once delivery has begun. Claims for missing issues should be made within four months (North America) or six months (outside North America) following the date of publication. The publisher expects to supply missing issues only when losses have occurred in transit and when the reserve stock will permit. For change of address and subscription enquiries: Subscription Office, NRC Research Press, National Research Council of Canada, Ottawa, ON K1A 0R6, Canada; tel.: 613-993-9084; fax: 613-952-7656; e-mail: pubs@nrc-cnrc.gc.ca.

Microform backfiles are available from UMI, P.O. Box 1346, Ann Arbor, MI 48106-1346, USA, and Micromedia Ltd., 20 Victoria St., Toronto, ON M5C 2N8, Canada.

All issues of the *Canadian Journal of Fisheries and Aquatic Sciences* since 1996 are available on the Web. Pricing information can be found at pubs.nrc-cnrc.gc.ca.

Le Conseil national de recherches du Canada ne se tient en aucune façon responsable des opinions exprimées par un collaborateur ou des déclarations que pourrait faire ce dernier. La publication d'annonces publicitaires, d'avis et autres n'implique pas l'endossement de leur contenu par la directrice principale de la Revue ou le CNRC.

© Conseil national de recherches du Canada 2007. Tous droits réservés.

Il est interdit de reproduire, de sauvegarder ou de transmettre quelque partie de la présente publication dans quelque format ou de quelque façon sans le consentement écrit de l'éditeur, à l'exception des conditions suivantes.

Le Conseil national de recherches du Canada accorde aux particuliers le droit de faire des copies individuelles pour leur usage personnel. Toute personne peut reproduire de courts extraits des articles de la Revue pour autant que les droits moraux de l'auteur soient respectés et que la mention de provenance soit clairement indiquée. Il est de convenance de demander le consentement de l'auteur avant de faire mention de son travail.

On obtiendra l'autorisation de reproduire des articles à d'autres fins que l'usage personnel (tel qu'on l'a décrit ci-dessus) auprès du Conseil national de recherches du Canada pour autant que des redevances de droits d'auteurs de 7,00 $/copie soient versées au Access Copyright, The Canadian Copyright Licensing Agency, 1, rue Yonge, bureau 800, Toronto, ON M5E 1E5, Canada.

*La permission ci-dessus ne s'applique pas à la reproduction à grande échelle, telle que la reproduction aux fins de distribution générale, publicitaire ou promotionnelle, de compilation de nouveaux ouvrages collectifs ou de revente. Dans de tels cas, il faudra ratifier une entente particulière avec l'éditeur, le Conseil national de recherches du Canada, Ottawa, ON K1A 0R6, Canada.

Renseignements sur l'abonnement

Journal canadien des sciences halieutiques et aquatiques (ISSN 0706-652X) est une publication mensuelle du Conseil national de recherches du Canada. Le prix de l'abonnement annuel en 2007 au Canada (courrier de deuxième classe) est de 1051 $CAN pour les organismes et de 325 $CAN pour les particuliers. À l'étranger (y compris les É.-U.), le prix de l'abonnement est de 1051 $US pour les organismes et de 325 $US pour les particuliers. L'expédition par avion exige des frais de 150 $US en sus du prix d'abonnement à l'étranger. Les clients du Canada doivent ajouter la TPS de 6 % (numéro d'entreprise 12149 1807 RT 0275). Les abonnements sont pour l'année civile. Tout paiement doit être adressé au Receveur général du Canada, crédit du CNRC. Le prix par numéro est de 110 $ pour les organismes et de 35 $ pour les particuliers. Le prix des hors-série varie. Les membres des sociétés canadiennes de sciences et de génie bénéficient de taux préférentiels en s'abonnant via leurs sociétés respectives.

Aucun remboursement ne sera accordé ni aucune annulation acceptée une fois que les livraisons auront commencé. Les réclamations de numéros manquants devront être soumises dans les quatre mois (Amérique du Nord) ou dans les six mois (à l'extérieur de l'Amérique du Nord) suivant la date de publication. L'éditeur ne fournira de numéros manquants que si le document a été perdu pendant l'expédition et que si le stock le permet. Adressez tout changement d'adresse ou toute question quant à l'abonnement au : Bureau des abonnements, Presses scientifiques du CNRC, Conseil national de recherches Canada, Ottawa, ON K1A 0R6, Canada; téléphone : 613-993-9084; télécopieur : 613-952-7656; courriel : pubs@nrc-cnrc.gc.ca.

On peut obtenir les fichiers rétrospectifs sur **microforme** auprès de UMI, P.O. Box 1346, Ann Arbor, MI 48106-1346, É.-U., et auprès de Micromedia Ltée, 20, rue Victoria, Toronto, ON M5C 2N8, Canada.

À partir de 1996, tous les numéros de *Journal canadien des sciences halieutiques et aquatiques* sont accessibles sur le Web. On trouvera des renseignements sur les tarifs à pubs.nrc-cnrc.gc.ca.

Modeling fish numbers dynamically by age and length: partitioning cohorts into “slices”

Richard McGarvey, John E. Feenstra, and Qifeng Ye

Abstract: Fishery processes of selectivity and recruitment to legal size vary with fish length and are mediated by fish growth. Yet most fishery models are age-based. To model length-dependent change within each cohort, fish numbers must vary dynamically with length as well as with age in the model population array. The fishery model formalism described here achieves this by a partition of the continuous length-at-age distribution. This method is computationally efficient and cleanly differentiates legal from sublegal fish. Fish numbers within each cohort are partitioned into length bins, called slices. A slice is defined and calculated as the fish in each cohort length-at-age distribution that have grown into legal size since the start of the previous time step. When growth is estimated from catch length and age samples separately from the stock assessment, biases result from the implicit assumption that catch samples are representative of the population and from ignoring length-dependent change within cohorts. These biases are avoided by integrating recruitment, growth, and selectivity estimation into a stock assessment likelihood that represents changing population numbers by both age and length. Size dependence also permits a natural extension of fishery models to trophic interactions with the surrounding ecosystem.

Résumé : Les processus halieutiques de sélectivité et de recrutement jusqu’à la taille légale de capture varient en fonction de la longueur des poissons et sont gérés par la croissance. Néanmoins, la plupart des modèles de la pêche sont basés sur l’âge. Afin de pouvoir modéliser le changement en fonction de la longueur dans chaque cohorte, il faut que les nombres de poissons varient de façon dynamique en fonction de la longueur aussi bien qu’en fonction de l’âge dans la matrice de la population modèle. Le formalisme du modèle de pêche que nous décrivons atteint ce but par une partition de la distribution continue des longueurs en fonction de l’âge. Cette méthode est efficace à l’ordinateur et distingue nettement les poissons légaux et sub-légaux. Les nombres de poissons dans chaque cohorte sont répartis en casiers de longueurs appelés tranches. Une tranche se définit et se calcule d’après les poissons dans chaque cohorte de longueur en fonction de l’âge qui ont atteint la taille légale depuis le début de l’étape temporelle précédente. Quand la croissance est estimée d’après des échantillons des longueurs et des âges dans les captures séparément de l’évaluation du stock, il résulte des erreurs de la présupposition implicite que les échantillons de capture sont représentatifs de la population ainsi que de la négligence des changements reliés à la longueur dans les cohortes. On peut éviter ces erreurs en intégrant les estimations du recrutement, de la croissance et de la sélectivité dans une vraisemblance de l’estimation du stock qui représente les densités changeantes de la population en fonction de l’âge et de la longueur. La dépendance de la taille permet aussi aux modèles de pêche d’être étendus naturellement aux interactions trophiques avec l’écosystème environnant.

[Traduit par la Rédaction]

Introduction

The length of a fish is the sample measure of population structure that is among the least expensive to obtain. Nearly all fish that are aged are also measured for length, and usually length samples are several times larger than the subsamples that are aged. Thus, sample data of measured fish lengths, generally of the catch, are abundant.

Yet in most fishery models, fish population numbers varying through time are broken down by age, but not also by fish size. Length dependence is often accounted for by the use of empirical age–length keys (Methot 1990). This description is accurate, being directly from data, but it is static with regard to length because the time-dependent model population array is not a function of fish body size. Growth is usually estimated separately, previous to the stock assessment, by fitting to length-at-age samples of the catch.

Representing fish population numbers through time by both age and length thus presents an opportunity to improve stock assessment model accuracy. It gives fishery models the possibility of accounting for dynamic change in cohort length-at-age distributions, that is, to model rates of change in population numbers that differ by fish body length within each age group. In particular, because faster-growing fish

Received 18 July 2006. Accepted 22 March 2007. Published on the NRC Research Press Web site at cjfas.nrc.ca on 15 August 2007.
J19427

R. McGarvey,[1] J.E. Feenstra, and Q. Ye. South Australian Research and Development Institute (SARDI), Aquatic Sciences, West Beach, South Australia 5024, Australia.

[1] Corresponding author (e-mail: mcgarvey.richard@saugov.sa.gov.au).

Can. J. Fish. Aquat. Sci. **64**: 1157–1173 (2007) doi:10.1139/F07-080

reach legal or gear-selected size at a younger age, they incur higher rates of fishing mortality sooner. Thus, the impact of fishing is asymmetric with length for fish of given age by more rapidly reducing fish numbers in the upper tail of the length-at-age distribution. This length asymmetry in mortality is greatest while cohorts are recruiting to legal size.

Models that can account for this length asymmetry by a dynamic, length-specific rendering of fish numbers in a cohort will predict size-dependent quantities more accurately. Two principal fishery data sources, catch total in weight and catch proportions-at-age for partially recruited ages, are strongly population size-dependent. By accounting for length in the model population array, and thus predicting change in fish numbers by length more accurately, better model predictions are fitted to these two critical data inputs, yielding more accurate stock assessment estimates overall.

Fishery models that represent both age and length structure fall into two basic categories: (*i*) those that represent the spread of fish by length in each cohort (age group) as a continuous distribution and (*ii*) those that partition each cohort into discrete length bins. The models of Deriso and Parma (1988; Parma and Deriso 1990) and models (both steady-state (Smith and Botsford 1998) and dynamic (Banks et al. 1991; Kristensen et al. 2006) that solve the von Foerster equation) retain a continuous distribution of lengths at age. Growth-transition models (Fleksibest, Frøysa et al. 2002) and growth groups (Punt et al. 2002) partition lengths into discrete bins. MULTIFAN (Fournier et al. 1990, 1998) is age based and distributes fish normally by length into discrete bins.

Most fishery models used in stock assessment practice are coded and solved numerically and assume a discrete model time step. A discrete time step can lead naturally to discrete length bins, via growth. We present a new method to partition a continuous length distribution into discrete length bins. This provides a natural link from the continuous length-at-age growth description of each cohort to a set of length bins defined discretely for use inside a discrete-time stock assessment model.

Rather than uniform fixed bins of, for example, 1 cm width, we allow the partition lengths separating neighboring bins to vary as needed in order to grow continuously and smoothly with each fish cohort over time. These growing length bins of variable width are called slices, by the manner in which each slice is created. Thus, to represent the growth of each cohort, rather than moving fish among fixed length bins in each model time step, for example using length-transition matrices, the fish remain in each slice from the time it is first created, when those fish reach legal size. Thus, the length bins themselves grow, rather than moving fish among fixed bins.

By analogy, imagine slicing the cohort length distribution as one would slice a loaf of bread. In each discrete model time step, we advance the normally shaped bread and widen it with the standard deviation of fish lengths, as determined by the underlying growth submodel. A new portion of fish thus grows into legal size in each model time step. The slicing knife is positioned at legal minimum length (LML). As the new portion of fish in the cohort is grown across LML (Fig. 1), the slicing knife descends and a new slice of fish is defined. One new slice is thereby created in each model time step. This definition for newly created slices is sufficient to

Fig. 1. Slice partition of a growing cohort of female southern sea garfish (*Hyporhamphus melanochir*) in Gulf St. Vincent. Normal probability densities (length-at-age distributions, as pdfs, $p(l\,|\,\theta;\,a)$) are plotted for each half-yearly model time step and thus for each half-yearly cohort age a. The portion of the cohort newly growing past legal minimum length (LML) in each cohort age is shown as a new "slice" of fish, enumerated by the slice number, s = 1, etc. The probability under the curve within each slice subinterval of fish length equals $P_{slice}(a)$ and is the proportion of fish assigned to that slice as it is created, with one new slice for each cohort age.

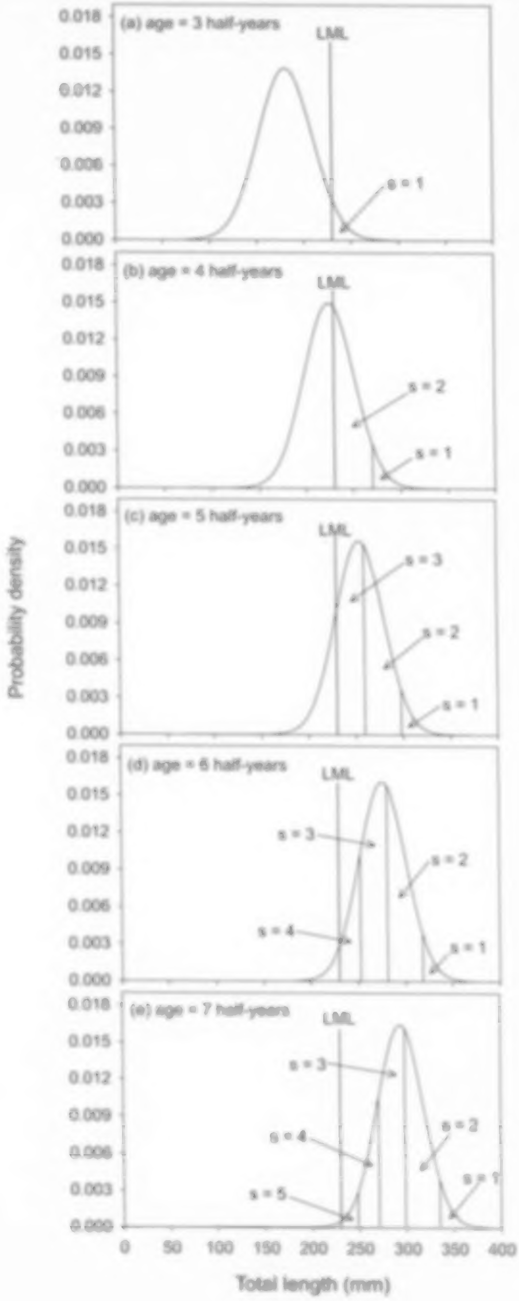

uniquely specify a fish number proportion and a length subinterval of fish for each newly created slice.

An algorithm is then needed to extend this definition to infer all other slice partition points (fish lengths separating neighboring slices), thereby specifying the length partition for each age group. This algorithm, based on the growth submodel, was defined to achieve two objectives: for each cohort age, (*i*) to permit the creation of one new length bin (i.e., one new slice) in each model time step, while (*ii*) cleanly separating model fish above and below LML. Based on this algorithm (detailed in Materials and methods and in Appendix A), as each cohort grows into legally harvestable size, a calculated number of the still sublegal fish are transferred to a newly created length slice. In subsequent time steps, fish numbers in each (by definition, legal size) slice are reduced by natural and fishing mortality. Because slices give legal fish numbers by length, the slice formalism can account for variation in capture selectivity, and thus mortality, by length. The slice partition is computationally efficient and can be integrated into a currently age-based stock assessment model. We applied the slice-based modeling approach to a garfish (*Hyporhamphus melanochir*) stock in South Australia.

Materials and methods

We first present a general description and the principal assumptions of an age- and length-based stock assessment model employing a slice partition. Second, we describe the slice partition algorithm, specifically how the fish in each age group are divided into variable length bins. Third, we present an application of slice partition to stock assessment of southern sea garfish (*Hyporhamphus melanochir*). Last, we address bias in growth estimation.

Modeling length dependence: growth, selectivity, recruitment, and mortality

The starting point and basis of the slice approach for partitioning fish cohorts by length is the length-at-age growth submodel. A statistical growth submodel is needed, which describes the full distribution of fish lengths for each model age. This growth submodel is assumed to represent the distribution of fish by length in each cohort that would be observed in the absence of length-asymmetric mortality. (Length-selective capture mortality will subsequently be imposed on these model cohorts, partitioned by slice, when used in the stock assessment model.) This growth submodel, a set of probability density functions (pdfs) over length, one for each model age, is specified by the estimated growth parameters. We used a normal length-at-age pdf, which permitted computational efficiencies (Appendix A), though in theory, the slice method can employ any distribution function for which integral equations can be solved numerically for lower integration limits. To model mean fish length $\bar{l}$, the mean of the normal length-at-age pdf, for any cohort age a, we employed a four-parameter, exponent-generalized von Bertalanffy mean length-at-age curve (McGarvey and Fowler 2002):

$$\bar{l}(a) = L_\infty \left\{ 1 - \exp\left[-K\left(\frac{a - t_0}{12} \right) \right] \right\}^{r}$$

Two additional parameters quantified the dependence of the standard deviation $\sigma(a)$ of normally distributed lengths for each age given as an allometric function of mean length:

$$\sigma(a) = \sigma_0 [\bar{l}(a)]^{\sigma_1}$$

The growth parameters can be estimated by fitting to length-at-age samples (*i*) previous to or (*ii*) by integrating growth estimation into the stock assessment likelihood. We did both in that order. First, we fitted the growth submodel directly to catch lengths-at-age. This gave an approximate, though biased, growth estimate as argued in Slice partition algorithm below. To correct for this bias, we then integrated growth submodel estimation into the stock assessment likelihood, specifically re-estimating the two parameters, von Bertalanffy's K and the normal length-at-age standard deviation coefficient σ_0 (McGarvey and Fowler 2002), which most directly determine the mean rate of growth and spread of lengths at each age.

Starting from this growth submodel, an algorithm (described below) was devised to effectively "slice off" the length subintervals of fish that have grown past LML in each model time step. Once this population number is assigned to each newly created slice bin by transferring these fish from the sublegal component, there is no subsequent diffusion of fish, as with von Foerster methods, or further exchange of fish between length bins, unlike with length-transition growth submodels. Fish within slices can only die (and in spatial models, move). The simplification of neglecting growth diffusion among length bins affords the slice approach large reductions in computation time compared with, for example, a length-transition approach, which requires $(n_L)^2$ growth-transition multiplications in each model time step, where n_L is the number of length bins. In a slice partition model, growth is quantified as the increasing length range with age of each slice subinterval, and no computation is needed to shift fish among bins.

Recruitment is defined as the creation of the (normal) length-at-age cohort at some age where it makes sense to describe fish lengths by a specified continuous distribution. This "birth" age can be sensibly chosen as the fishery model cohort age when the fastest-growing fish first reach legal size. The number of fish in each cohort at this specified age of birth, a_b, serves as the model estimate of yearly recruitment. Each yearly recruit number is a freely estimated model parameter. The legal-size fish (i.e., those longer than LML) in this first model age are quantified and defined as the first newly created slice. In subsequent model time steps, new slices are created as the calculated proportion of sublegal fish in each cohort that have grown into legal size since the previous time step, thus explicitly representing the gradual recruitment of each cohort to fishable sizes over the number of model time steps required, as determined by the growth submodel.

Mortality is differentiated for legal and sublegal fish. Legal-size fish, partitioned into length slices, are subject to both fishing and natural mortality. Length-dependent gear selectivity and any other length-dependent mortality processes are applied to the length-partitioned fish numbers, specifically in the legal size range. Thus, in addition to the capture selectivity that results from knife-edge cut-off in catches at LML, a varying capture selectivity can be imposed on the legal slices of each model cohort, applying a selectivity function, often a logistic, to the mean or midpoint lengths of each slice length bin. Sublegal population numbers (fish below the legal size limit) incur only natural mortality.

Slice partition algorithm

We now describe the mathematical basis of the slice partition algorithm. The principal inputs to this algorithm are LML and the growth submodel, specified by the growth parameters. We need three numerical outputs (a vector and two triangular matrices) from this algorithm, call them slice objects, as subsequent input into stock assessment models that implement a slice partition age- and length-based method: (*i*) a vector of proportions of fish transferring from the sublegal component to each newly created legal slice, subscripted by the age when each slice is created; (*ii*) the slice partition lengths, one vector of slice left-hand-side partition points for each cohort age, subscripted by age and slice number; and (*iii*) the mean weight of fish in each (legal size) slice, also given by slice number and age. The slice partition lengths change with model age because fish grow, and one new slice is added for each model age, up to the maximum (plus group) age, $a_{\max}$. If the model time step is monthly or yearly, then fish cohort age also increases in monthly or yearly increments. A set of slice partition objects are needed for each set of growth parameters, notably when growth varies by region or sex and, if legal size regulations change, for each LML.

The growth submodel specifies a length-at-age probability density, $p(l|\theta; a)$, of fish numbers per unit length for any continuous age a. The selected normal probability density of fish lengths for each cohort, $p(l|\theta; a)$, was specified by the parameters θ giving the mean and standard deviation as a continuous function of age a. In the slice partition algorithm, a discrete set of the length-at-age pdfs are evaluated at the full set of discrete model ages, understood as the ages of cohorts at the start of each model time step.

As a first step in the slice partition algorithm, the length pdf is partitioned into legal and sublegal length ranges for all model ages a. The two probabilities of legal ($P_{\text{legal}}(a)$) and sublegal ($P_{\text{sublegal}}(a)$) size ranges sum to 1 for all model ages ($P_{\text{legal}}(a) = 1 - P_{\text{sublegal}}(a)$) and thus constitute a first level of partition. The sublegal probability for each age a is defined as the integral under the length-at-age pdf for all fish lengths below LML:

$$(1) \qquad P_{\text{sublegal}}(a) = \int_{-\infty}^{\text{LML}} p(l|\theta; a)\,\mathrm{d}l$$

The algorithm must calculate the probabilities of all legal slices, $\{P_{\text{slice}}(a)\}$. It is a basic assumption of the slice partition algorithm that these slice probabilities will not change with age. Let us henceforth assume that the birth age is chosen to be the youngest age at which a measurable fraction of the faster-growing fish has reached legal size. Therefore, the probability of the first (upper tail) slice in each cohort, which comprises the legal-size fish at the birth age, is

$$\begin{aligned} P_{\text{slice}}(a_{\text{b}}) &= \int_{\text{LML}}^{\infty} p(l|\theta; a_{\text{b}})\,\mathrm{d}l = P_{\text{legal}}(a_{\text{b}}) \\ &= 1 - P_{\text{sublegal}}(a_{\text{b}}) = 1 - \int_{-\infty}^{\text{LML}} p(l|\theta; a_{\text{b}})\,\mathrm{d}l \end{aligned}$$

For all subsequent ages, the probability under the curve of each slice is most simply derived as a difference of legal probabilities. Thus, $P_{\text{slice}}(a)$, the proportion newly legal fish at the start of model age a, was calculated as the legal proportion of the cohort in the current age (a) minus the proportion that was legal at the start of the preceding age ($a - 1$):

$$(2) \qquad P_{\text{slice}}(a) = P_{\text{legal}}(a) - P_{\text{legal}}(a-1), \quad a = a_{\text{b}} + 1, \ldots, a_{\max}$$

At each cohort age, the sum of P_{slice} probabilities over all legal slices plus the probability of sublegal fish (P_{sublegal}) equals 1. This constitutes a partition of the length distribution, one length partition of the cohort for each age in the model population. The age a designating each slice in the $P_{\text{slice}}(a)$ vector is the slice-creation age when those fish reached legal size.

Given slice probabilities, we can derive the multiplying coefficients needed to populate each newly created slice inside the stock assessment estimator by transferring fish as they grow from the sublegal component. The proportion of sublegal model fish assigned to each newly created legal-size slice in each time step, call it the transfer coefficient $f_{\text{transfer}}(a)$, was defined as a ratio of two probabilities: the newly created slice probability in the current age divided by the sublegal probability from the previous age:

$$(3) \qquad f_{\text{transfer}}(a) = \frac{P_{\text{slice}}(a)}{P_{\text{sublegal}}(a-1)}$$

In the population model, new slices are created from the sublegal survivors of the previous model time step. Multiplying the sublegal population number at the end of the previous time step (cohort at age $a - 1$) by $f_{\text{transfer}}(a)$ transfers the correct (P_{slice}-proportional) number of sublegal fish into the new legal slice for the start of the current time step (cohort at age a).

The number of legal slices equals the number of ages, and thus also the number of model time steps, that the cohort has had a legal component, starting from a_{b}, when there is just one legal slice, $n_s(a_{\text{b}}) = 1$. Thus, the function specifying the number of slices $n_s(a)$ for any age a can be written as

$$(4) \qquad n_s(a) = a - a_{\text{b}} + 1, \quad a = a_{\text{b}}, \ldots, a_{\max}$$

In the model population array, slices are enumerated (i.e., subscripted), starting with $s = 1$ to designate the first slice created, at age a_{b}, which comprises the fastest-growing fish in the upper tail of the length-at-age distribution. At older ages, $s = 1$ continues to refer to this same first-created slice, fish of longest length in each cohort. Similarly, $s = 2$ designates the second slice created, of fish in the next length subinterval to the left of the upper tail slice, and so on.

The full set of slice length partition points can then be derived. The left-hand-side partition point for all newly created slice subintervals is the LML. For the birth age a_{b} when the first slice is created, we can notate this as $l_{\text{lhs}}(a_b, s = 1) =$ LML. Indeed, for all ages $a = a_b, \ldots, a_{\max}$, the new slice in each partition will have LML as its left-hand subinterval boundary: $l_{\text{lhs}}(a, s = n_s(a)) =$ LML.

All other slice left-hand-side partition points were derived by conserving the $P_{\text{slice}}(a)$ probabilities. For example, consider the upper tail slice $s = 1$ for the second legal cohort age. (This cohort age will have two legal slices, the other newly created slice, $s = 2$, having LML as its left-hand side.) The left-hand-side partition point of the upper tail slice for the second legal-size age, $a_b + 1$, $l_{\text{lhs}}(a_b + 1, s = 1)$ is exactly solved for as the only unknown, the lower integration limit, in the integral equation

$$P_{\text{slice}}(a_b) = \int_{l_{\text{lhs}}(a_b+1,1)}^{\infty} p(l \mid \theta; a_b + 1)\,\mathrm{d}l$$

where the $s = 1$ slice probability, $P_{\text{slice}}(a_b)$, is fixed through time. This integral equation method can be used to calculate the slice partition left-hand-side length for the upper tail slice of all ages a of the population by solving for $l_{\text{lhs}}(a, 1)$ in

$$(5)\qquad P_{\text{slice}}(a_b) = \int_{l_{\text{lhs}}(a,1)}^{\infty} p(l \mid \theta; a)\,\mathrm{d}l$$

To estimate subsequent (non-upper-tail) slice left-hand-side partition lengths for ages greater than $a_b + 1$, a similar integral equation can be solved to derive lower integration limits, $l_{\text{lhs}}(a, s)$:

$$(6)\qquad P_{\text{slice}}(a_b - 1 + s) = \int_{l_{\text{lhs}}(a,s)}^{l_{\text{lhs}}(a,s-1)} p(l \mid \theta; a)\,\mathrm{d}l$$

for ages $a = a_b + 2, \ldots, a_{\max}$ and $s = 2, \ldots, n_s(a) - 1$. Because the upper integration bound in eq. 6, the right-hand partition length for each slice, was derived in each previous iterative integral equation solution as the left-hand side of the slice immediately to its right, $s - 1$, these integral equations for successive slices can be solved iteratively starting with the right-hand tail slice ($s = 1$) and progressing to the left. By an iterative sequence of integral equation solutions, ending with the left-hand side of the second youngest slice in each age, together with LML, which is always the left-hand side of the youngest slice, all slice left-hand-side partition points can be calculated.

The mean weight of fish in each slice can be derived as an exact quantity by integrating the weight-versus-length relationship across each slice length subinterval

$$(7)\qquad w(a, s) = \int_{l_{\text{lhs}}(a,s)}^{l_{\text{lhs}}(a,s-1)} \alpha l^{\beta} p(l \mid \theta; a)\,\mathrm{d}l$$

where an allometric αl^{β} (or other) weight–length conversion function is required with estimated parameters α and β.

The slice partition has been applied to three South Australian fish stocks. The integral equation algorithm described above was implemented using Mathematica software (Wolfram Research Inc., Champaign, Illinois) for the King George whiting (*Sillaginodes punctata*) stock assessment model in which growth and slice partition quantities were computed previous to use as inputs in the stock assessment estimator. This permitted exact integrated probability solutions for transfer coefficients, slice partition points, and mean weights.

For garfish, growth estimation was integrated into the stock assessment likelihood, and a more efficient algorithm was sought. This computationally more efficient slice partition algorithm does not require solving integral equations for the lower limit of integration but assumes (initially) normally distributed lengths (Appendix A). When growth is integrated, the growth and slice-algorithm quantities must be recomputed in each log-likelihood function evaluation, because these depend on estimated growth parameters. The mean weights of each non-upper-tail slice were approximately calculated from the slice midpoint length rather than integrating across the slice subinterval. For the right-hand tail slice, we defined the central length by the median length at which the tail-slice probability is divided evenly into two. Pseudo-code for this more efficient slice partition algorithm is given in Appendix A.

Application: southern sea garfish

The slice partition was applied in a stock assessment model of southern sea garfish in South Australia. Being a species of modest landed value, yearly ongoing catch monitoring is not undertaken. In 1997–1998, the market catch of garfish was systematically sampled by length, with approximately 15% of those subsampled for ageing by otoliths.

The fishery is highly seasonal. Fishers target spawning aggregations of predominantly female garfish inshore over the 6 months spanning summer (October–March). In winter (April–September), catch rates approximately double and both sexes are taken. The garfish model thus employs two half-yearly time steps per year. Growth varied by sex and between the two principal regions: Gulf St. Vincent and Spencer Gulf. LML was raised from 21 to 23 cm in 2001. With two sexes, two regions, and two LMLs, eight sets of slice-algorithm outputs were required.

There were three data types: (*i*) half-yearly totals of reported catch (kg) and effort (fisher-days) by region and effort type, October 1983 – September 2005; (*ii*) sampled garfish catch length proportions by region and effort type ($n = 7646$); and (*iii*) catch proportions by age and sex ($n = 1627$), aged by otoliths, subsampled from the length-measured garfish. Assuming no fish movement, stock assessments in each region are effectively independent. Model equations for the fishery population dynamics and likelihood are given in Appendix B.

Principal features of the garfish model are as follows. (*i*) The birth age (a_b) of new cohorts to the model population was at 1 year after spawning, when the fastest-growing fish have just started reaching legal size. (*ii*) Four catch and effort (i.e., effort-type) categories were defined, differing by gear, target species, and sector. (*iii*) Logistic length-selectivity was estimated. (*iv*) Capture vulnerability parameters were also estimated by effort type, sex, half-yearly season, and region.

(*v*) Yearly recruit numbers were estimated by region and separably by sex. (*vi*) Length distributions were fitted using the four moment properties (mean, standard deviation, skewness, and kurtosis), following Fournier and Doonan (1987), who fitted to the central moments. (*vii*) A method was implemented to correct for nonuniform subsampling of ages from the representative sample of lengths, permitting a sample size increase by 46% from 1114 to 1627 otolith-aged garfish. The model is (*viii*) effort-conditioned and uses a (*ix*) lognormal likelihood for fits to catch weight totals by effort type and a (*x*) two-dimensional, multinomial likelihood for simultaneous fit to proportions by both sex and age in each region for the two half-yearly time steps when catch sample data were collected.

The stock assessment negative log-likelihood was minimized using the AD Model Builder parameter estimation software (otter-rsch.com/admodel.htm).

Growth estimation bias

Growth estimates based on catch length-at-age samples can be biased (overestimating growth) when the lower capture selectivity of smaller fish is ignored (Troynikov 1999; Taylor et al. 2005; Punt et al. 2006*a*). When this selectivity variation by length is due to a legal size limit, the slice method naturally models the knife-edge cut-off in capture probability at LML. A zero probability of capture of fish smaller than LML in the catch sample growth data was made explicit as a truncated likelihood in the growth submodel pdf (McGarvey and Fowler 2002), thus accounting for the absence of sublegal fish in the sample and thereby obviating this first source of growth estimation bias. In the garfish model, by fitting model to data catch lengths in the stock assessment estimator, we further modeled logistic capture selectivity and its influence on growth estimates for fish above LML. In this way, we accounted for and thus corrected this first kind of growth estimation bias resulting from a sample, as catch, which differs from the population overall.

In addition, we argue that a second kind of growth estimation bias results from change through time in the shape of the length distribution of cohorts, specifically of growth bias resulting from length-asymmetric mortality (i.e., faster-growing fish being harvested sooner). This second cause of bias has the opposite effect of underestimating growth and would result even if samples were representative from the population. Relatively more surviving, slower-growing fish in these samples will be interpreted to reflect slower growth, a bias not incurred when mortality is uniform with length. This effect of asymmetric mortality changing the shape of the length distribution is not reflective of the growth of individual fish. When growth estimation can be integrated into a fully age- and length-based population model, length-asymmetric mortality and the changes it induces in the population can be modeled and this bias thereby alleviated.

In summary, by (*i*) representing population numbers by length in each cohort, (*ii*) fitting to lengths for each age separately, and (*iii*) integrating growth estimation, both growth biases resulting from length-asymmetric harvest are corrected or greatly reduced.

Fig. 2. Length partition of a Gulf St. Vincent female model cohort that has been of legal size for three half-yearly time steps. The estimated normal length-at-age pdf, $p(l|\theta; a)$, for these garfish (*Hyporhamphus melanochir*) aged 5 half-years, is shown in both panels. (*a*) The slice probability (P_{slice}) equals the area under the pdf curve in each slice subinterval to the right of legal minimum length (LML). The shaded area equals $P_{\text{slice}}(a_5)$, which is the probability of the upper-tail slice, subscripted as $s = 1$. (*b*) As each slice is created, fish are transferred from the sublegal component to the newly created slice adjacent to LML, here shown as the dotted line bar for slice $s = 3$. The greater reduction in numbers of faster-growing fish, having been subject to harvesting for a longer time, is shown by the relative heights of solid versus dotted line bars, where dotted line bars equal the probabilities under the curve when each slice is created (P_{slice}), and the solid line bars are proportional to the model population numbers by slice after mortality has occurred in the (October–March 2004) time step.

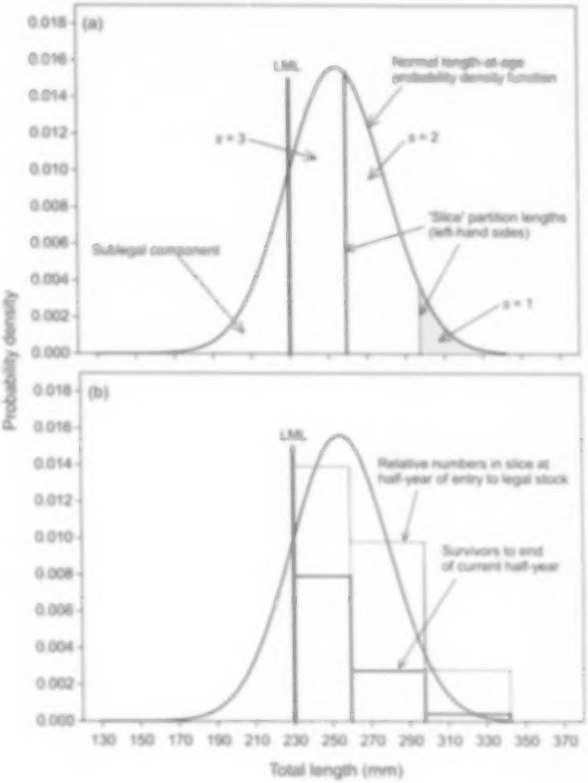

Results

The garfish model solution exemplifies a slice partition of cohorts by length. Population numbers by slice for females from Gulf St. Vincent aged 5 half-years were plotted together with the underlying normal length-at-age pdf from which these slices were partitioned (Fig. 2). Because faster-growing fish were removed more rapidly, having reached legal size sooner, the upper tail is relatively much reduced (solid line bars compared with dotted line bars in Fig. 2*b*), skewing the previously normal distribution of population numbers by length to the left. This fishery gear- or LML-induced skewness of the population length-at-age distributions causes the second form of growth bias, underestimation, when not accounted for.

We illustrate the extent of the two kinds of growth bias on Gulf St. Vincent garfish (Fig. 3). The top row of growth fits (Figs. 3*a* and 3*b*) were to catch data, previous to stock assessment. Comparing dotted with dashed plots shows the correction of type 1 growth bias. The dotted curve expresses type 1 overestimation bias because, with no accounting for capture selectivity, it ignores the under-representation of smaller (sublegal) fish in catch samples. The LML-truncated growth estimation (dashed curve) has most type 1 growth bias removed because the truncated growth submodel accounts for the absence of smaller fish (those below legal size) in the catch sample. However, the improved (dashed) curve underestimates growth as type 2 growth bias because accounting for the cumulative harvest of faster-growing fish requires that growth estimation be integrated into the stock assessment model. The middle row (Figs. 3*c* and 3*d*) illustrates the correction of type 2 growth bias made possible by integrating growth estimation, where the solid curve is from integrated growth estimates. For the relatively high levels of exploitation encountered by southern sea garfish in South Australia, type 2 growth bias was the larger of the two biases shown by the larger differences evident in the middle row of graphs compared with the top row. In the bottom row, we investigated the effect of varying levels of fishing mortality on type 2 growth bias. As anticipated, as mortality rates decline (with *F* lowered by 50% and 10%, while leaving all other parameters, including growth, freely estimated), the extent of type 2 growth bias declines accordingly, and growth integrated estimates approach those of (LML-truncated) fits directly to catch data, because this second source of bias is due to the difference in mortality rate between fish above and below harvestable size.

The impact of length-asymmetric mortality on population numbers by length can be seen in a typical cohort. For the 2001 cohort of Gulf St. Vincent females after three half-yearly time steps in legal size (Fig. 2), the legal-size mean length of modeled garfish was 255.3 mm when the more rapid removal of larger fish was accounted for (solid line bars, Fig. 2*b*), compared with 263.6 mm when it was not (dotted line bars formed directly from the normal length curve, Fig. 2*b*, which implicitly ignores length-dependent differences in mortality history over time). The estimated mean weight of legal fish was similarly reduced from 80.1 to 72.8 g, a 10% (type 2) growth bias correction by weight. Similar, 8%–9% bias corrections for mean catch weights were also observed when comparing growth-integrated estimates with the previous, nonintegrated (but truncated, and thus type-1-bias-corrected) growth curves. Thus, accounting for length-asymmetric mortality produced a roughly 10% correction in model-predicted catch in weight in this fishery with relatively high fishing mortality rates.

A visual comparison of the model and data length frequencies, specifically of model catch number proportions by slice with the data proportions in 1 cm length bins (Fig. 4), provides confirmation that the garfish slice-based length partition as estimated using moment property fits and the growth submodel is accurate. Model fits to catch proportions by age (Fig. 5) and to sex ratio (not shown) were close. The general agreement of the slice-model length and age breakdowns with data, in both Gulf St. Vincent (Figs. 4 and 5) and Spencer Gulf (not shown), indicate a successful description of garfish population structure by both age and length. The estimated garfish time series for Gulf St. Vincent of yearly recruitment and half-yearly biomass and harvest fraction are shown with 95% confidence intervals (Fig. 6).

Discussion

The garfish application illustrates two kinds of growth estimation bias, both of which are due to asymmetric capture selectivity by length, which characterizes nearly all fishery cohorts as fish recruit to a legal or gear-selected size range.

The first kind of growth bias is due to the length-at-age sample being not representative of the population, because it comes from the catch where smaller and thus slower-growing fish are under-represented. Previous studies have addressed this first kind of bias in stand-alone growth estimates, undertaken previous to use inside a stock assessment. Dow (1992), Troynikov (1999), and Punt et al. (2006*a*) used tag–recovery data. For growth estimation applied to catch length-at-age samples to obviate type 1 growth bias, McGarvey and Fowler (2002) assumed a knife-edge selectivity at LML. These approaches generally provide only a partial bias correction, because the selectivity and growth estimates obtained external to the stock assessment from the same length-at-age data would be partially confounding, without the additional knowledge of underlying population numbers that the full stock assessment provides. Moreover, growth estimation external to a stock assessment cannot account for the second kind of growth bias due to cumulative length-asymmetric changes to the underlying population (Taylor et al. 2005), which requires dynamically varying cohort fish numbers by length.

Thus, a superior (because more complete) approach is to integrate growth into the stock assessment model that has a length- and age-dependent population array and all available data sets to account for and thus correct for all modeled processes that can influence either (*i*) the fitted sample of lengths-at-age or (*ii*) the underlying population structure by length of each cohort.

Recruitment, defined as the yearly growth of fish into the legal or capture-selected body size range, is also linked to growth. When fish can be aged, recruitment is mainly inferred from catch sample proportions by age. Quantifying more precisely the proportion of a newly recruiting cohort that has reached harvestable lengths can make a large difference when analyzing catch proportions-at-age in estimates of recruitment and total mortality. This primarily affects the most recent year class or two in a stock assessment, which are often the most abundant and whose estimates can sometimes be most important for management decision makers when used, for example, in estimating current biomass. This most recent year class is also the most poorly estimated, precisely because it is only partially recruited.

Fig. 3. Estimated growth curves for male and female southern sea garfish (*Hyporhamphus melanochir*) in Gulf St. Vincent, as mean length versus half-yearly age, comparing growth-integrated estimates and previous growth fits. The top row of graphs (*a* and *b*) shows two growth curves estimated by fitting directly to catch data: one unmodified to account for gear selectivity (dotted line plots) and the other accounting for the knife-edge selectivity (dashed line in panels *a*–*d*) at legal minimum length. The growth-integrated curves (solid line with circle point markers and error bars as 95% CI, middle and bottom rows, panels *c*–*f*) were obtained by re-estimating K and σ_0 in the overall stock assessment likelihood. Differences between growth curves in the middle row (panels *c* and *d*) quantify the effect of integrating growth estimation, thereby correcting type 2 growth bias. The sensitivity of type 2 growth bias to varying fishing mortality (bottom row, panels *e* and *f*) is indicated by the evident reduced bias as less correction that would have been needed had fishing mortality been 50% (dot-dashed line) and 90% (dot-dot-dashed line) lower than estimated, reflecting the dependence of type 2 growth bias on differences in cumulative mortality of faster-growing versus slower-growing fish in each cohort.

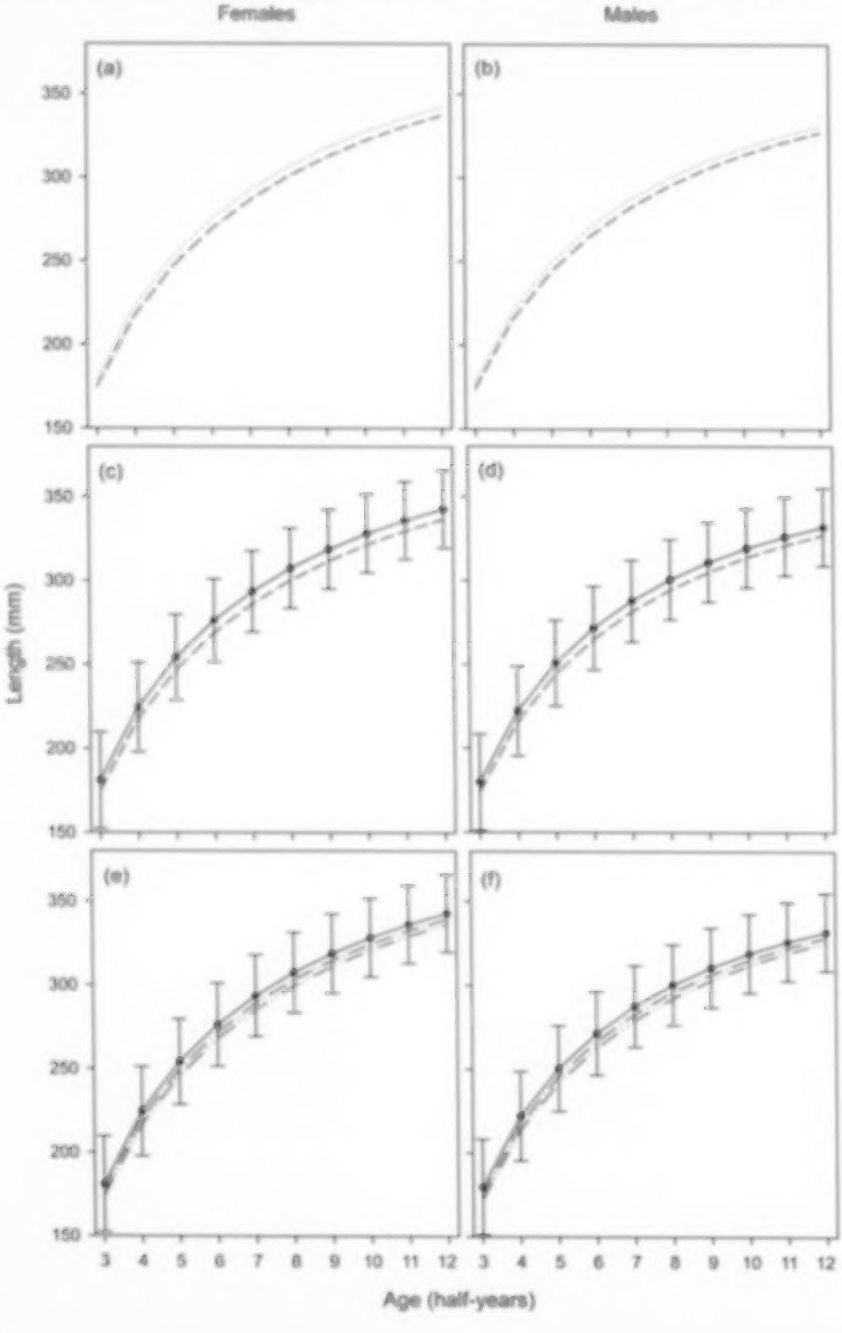

Fig. 4. Length frequencies of sample data and model slices by age. Gulf St. Vincent, 1997–1998 haul-net southern sea garfish (*Hyporhamphus melanochir*) catch market subsampling-corrected proportions in 1 cm length bins (bars) and model-predicted garfish number proportions by slice (line and circle markers) in the landed commercial catch for all half-yearly model ages.

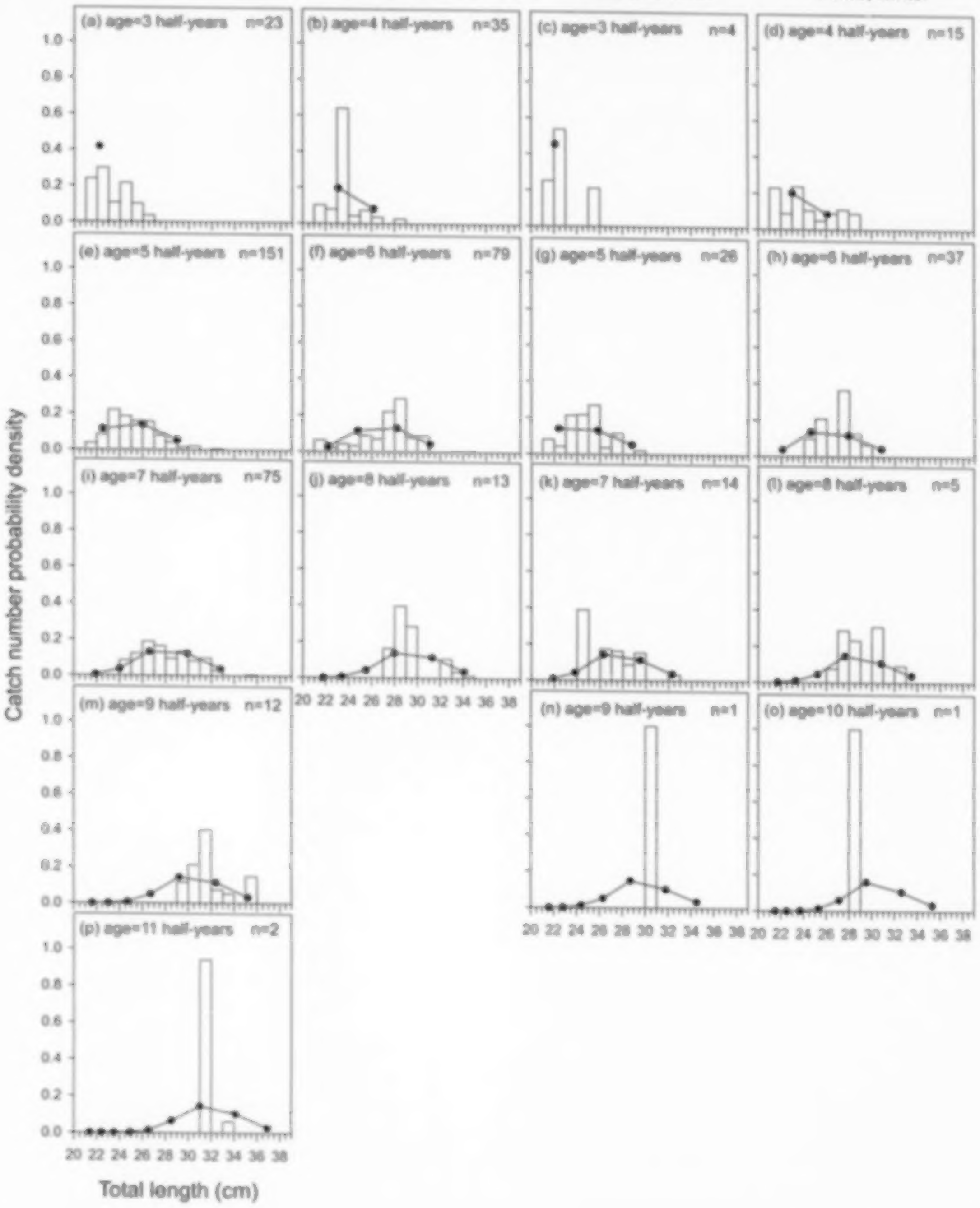

Thus, two aspects of slice partition make it suitable as an accurate way to model this growth-dependent recruitment process: (*i*) It explicitly models the growth of each cohort into the legal size range as cohorts grow past LML. (*ii*) By further breaking down the legal size range of fish into length bins, capture selectivity functions can be applied to length-specific population numbers, and capture selectivity estimates can be more accurately inferred. Better growth and

Fig. 5. Model fits to catch proportions-at-age from haul nets. Open circles correspond to catch sample data; solid circles with lines show the model-fitted proportions by age.

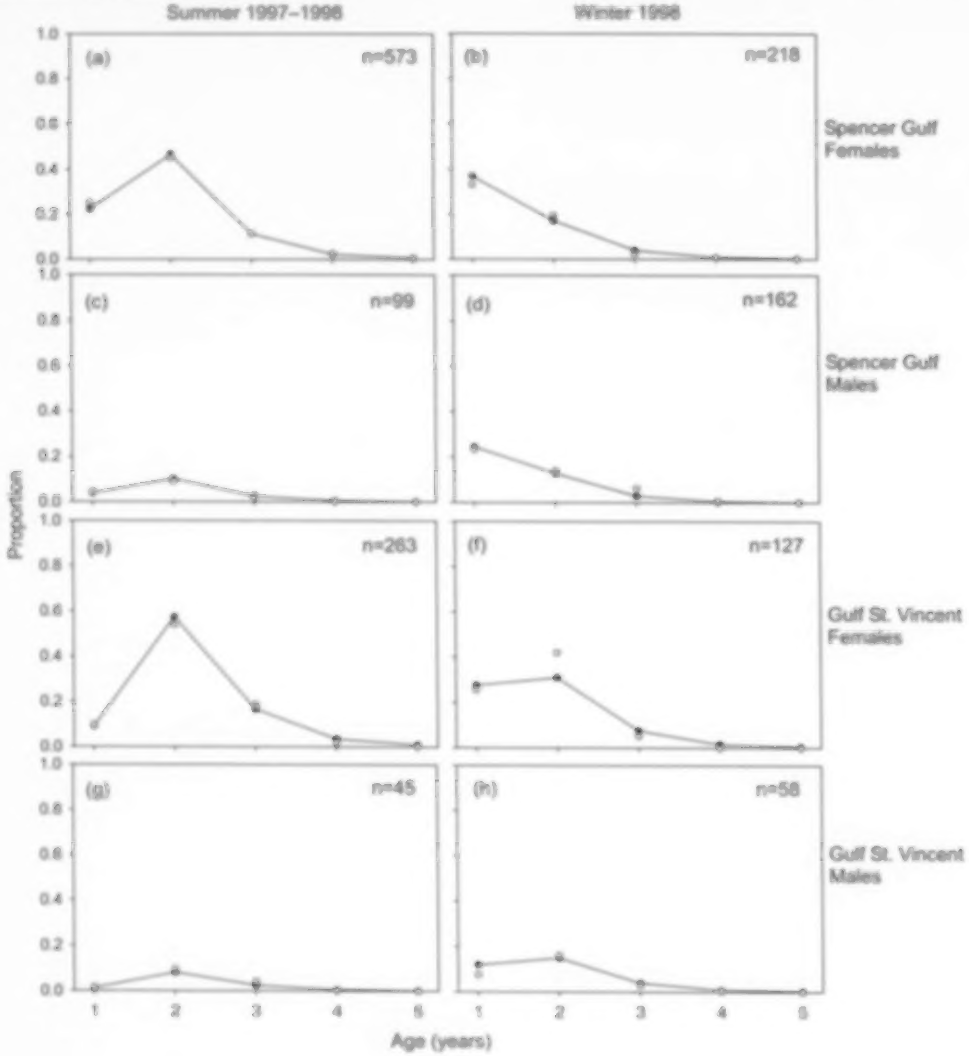

capture selectivity estimates will in turn yield more accurate recruitment estimates.

With growth, selectivity, and recruitment being more accurately described by a length- and age-based fishery model approach, the overall stock assessment is more accurately informed by the data. These inter-related, length-dependent processes all influence model-predicted quantities that are fitted to fishery data. More accurate predictions of catch totals by weight, catch proportions by age, and catch proportions by length (-at-age) should yield more accurate stock assessment estimates overall. Just as integrating effort standardization into the stock assessment improves both estimations because they mutually interact (Maunder 2001), insofar as changing levels of stock size estimated in the stock assessment inform standardization inference and vice versa, integrating growth improves both the stock assessment and the growth estimation and thus all size-dependent inferences.

Integrating growth has not been generally possible to date because, in particular using length-transition matrices, it has been too computationally intensive. However, the garfish model, with growth integrated, converged in 2–5 min, suggesting run time is not an obstacle to implementing a length- and age-based model formalism. Slice partition thus provides a computationally efficient method to represent population numbers by age and by length, in turn permitting growth estimation to be integrated into the stock assessment likelihood.

Extensions of this approach are plausible. The slice partition can be extended to fish of length less than LML. This would be useful with fisheries, where undersize discard mortality is substantial (e.g., Punt et al. 2006*b*). Moreover, the

Fig. 6. Estimated population and fishery time series indices for southern sea garfish (*Hyporhamphus melanochir*) in Gulf St. Vincent, 1984–2005: (*a*) yearly recruit numbers, (*b*) legal-size biomass at the start of each half-year, and (*c*) exploitation rate as the half-yearly model catch divided by the start-of-half-year legal-size biomass. Error bars as 95% confidence intervals were obtained as delta approximations from maximum likelihood variance matrix (numerical inverse Hessian) standard errors.

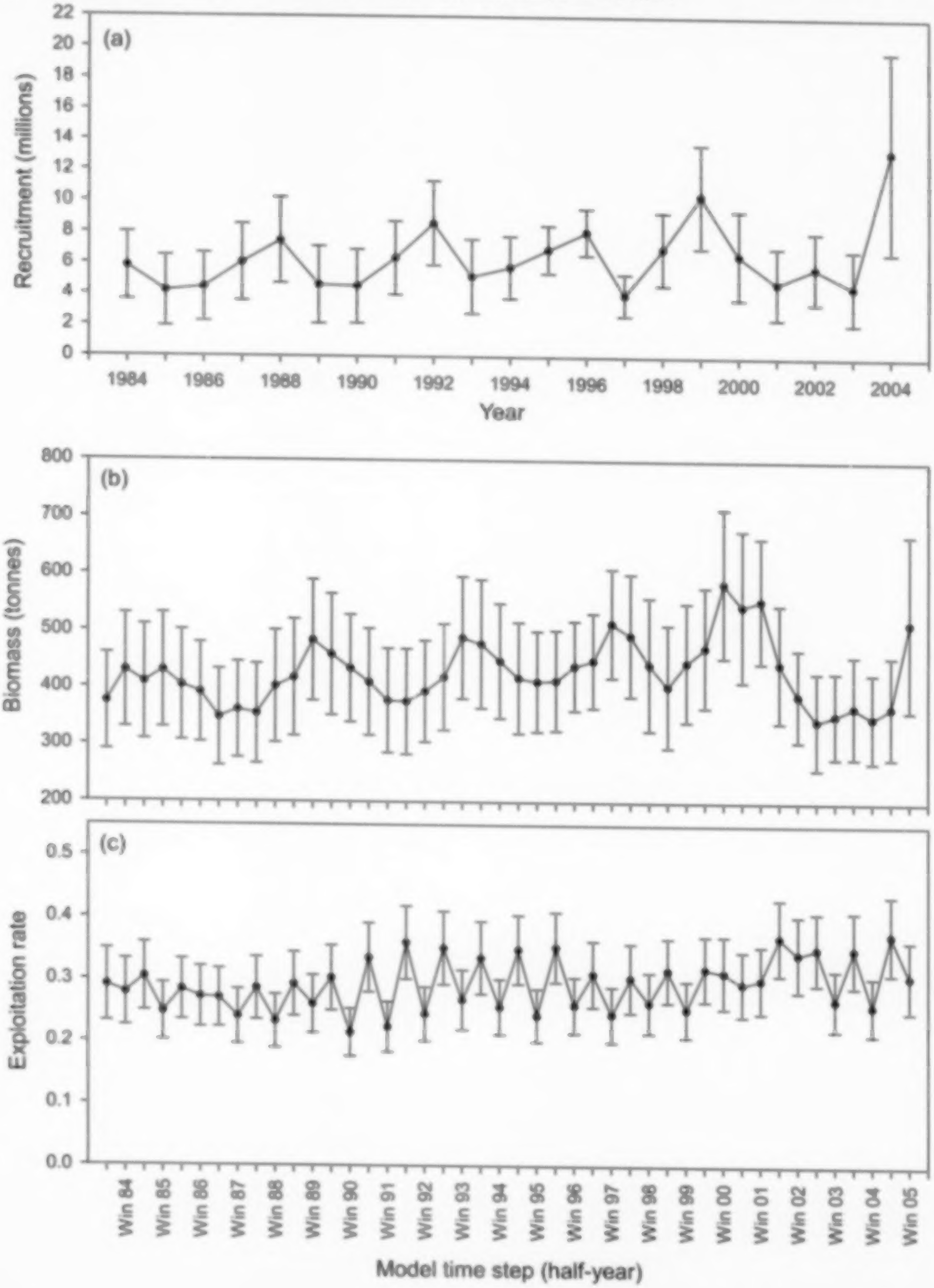

specific body length chosen to define a slice partition does not have to be LML; it can be any characteristic species length.

Comparison with age–length keys

Traditional age–length key models condition on age–length sample data, taking the normalized age–length sample matrix as observed. In some fishery data situations, these age–length keys can be superior to a full dynamic (e.g., slice) description of fish population numbers by age and length, because as with conditioning by catch, age–length keys impose the observed histograms probability mass functions of sample length proportions.

But unlike catch totals, age and length sample data are subject to quite high sample variances (Pennington and Vølstad 1994; Pennington et al. 2002), which must manifest directly in empirical age–length keys. The variation by length of garfish market samples is shown herein by comparison with the modeled, more smoothly varying slice proportions. When conditioned upon, random errors in these sample age–length histograms will be imposed on the stock assessment model inference. When age–length samples are sparse, model estimates can thus be improved by modeling length-specific population change based on growth estimates from years when samples were larger or more representative, especially for older, less populated age groups.

Recent approaches smooth age–length keys by combining external growth pdf estimates and integrating across fixed length bins (Salthaug 2003), while also accounting for ageing imprecision (Fournier and Archibald 1982; Methot 1990), in multinomial fits to rather than by conditioning on age–length samples. But because fish numbers by length do not vary dynamically in most model population arrays, correcting type 2 growth bias and its onflow to estimates of mortality, selectivity, and recent recruitment is not possible.

Moreover, in years or regions when no age–length samples have been gathered, age–length models such as slice partition can restore length dependence of the model description. In effect, the model creates and populates its own age–length keys as model population numbers by age and slice, based on an underlying growth model. The model can thereby account for length-dependent processes in describing model population numbers changing through time in time steps or subregions where no age samples were taken. Similarly, for stock assessment models that project into the future (e.g., in quota setting), age–length keys are not possible because age–length data do not yet exist. The length dependence of change in future populations can be modeled by an age- and length-based approach.

Another advantage over age–length keys is obtained for fishery gears or sectors or time periods when only samples of fish numbers by length, but not age, are available. In this case, slice (or other model) numbers by length can be fitted to the sampled length proportions (Fournier et al. 1990), thereby potentially obtaining estimates of mortality and other inferences that age samples would otherwise provide.

Disadvantages of a slice-growth model approach

With slices, computational complexity increases when length partitions must be changed or combined: (*i*) when the minimum length regulation changes, (*ii*) when fish move from one growth region to another, or (*iii*) when fitting to age-aggregated length frequencies.

A new LML requires a new slice partition. In the model time step when LML is changed, the fish in each cohort must be reallocated from the previous LML's slice partition to the new one. We constructed a LML-change algorithm based on proportional allocation from old to new slices, by either integrating over overlapping slice subintervals or taking simple linear proportions by length of fish from each old slice bin into each overlapping, newly defined slice bin. Similar fish reassignment procedures are needed if fish move among growth regions or for summing length frequencies of fish across age and between sexes if their growth differs by sex. This complication would presumably apply to most other age- and length-based model formulations, except those using fixed bins.

A second constraint applies specifically to the slice approach. The number of slices partitioning each cohort equals the number of model time steps over which it has been recruiting to legal size. To obtain higher length resolution, for example in estimating selectivity ogives, more time steps per year are required, which results in each cohort being partitioned into thinner, more numerous slices. With both more length bins per cohort and more time steps per model run, this causes fairly rapid increases in computation time. With King George whiting, this problem was addressed by recombining fish from all the length slices into a single postlegal cohort once the cohort had become fully (>98%) recruited to legal size. This computational savings permitted a monthly time step in a 13-cell spatial model needed to describe (*i*) yearly pulses of high fishing mortality in winter, (*ii*) seasonal recruitment to legal size as fish grow fastest in late summer, and (*iii*) yearly summer migration rates estimated using a method unbiased by tag nonreporting (McGarvey and Feenstra 2002). However, for King George whiting growth estimated externally, type 2 growth bias was not addressed.

Implications for fishery and ecosystem modeling

While beyond the scope of this paper, testing with simulated data and systematic comparison with age-only models are needed to rigorously quantify the accuracy improvements in model estimates that we claim. But the benefits of explicitly modeling dependence of population numbers on body size extend beyond technical improvements in the stock assessment estimator. With many critical influences on exploited marine populations being dependent on body length, notably capture rates determined by regulations (LML) or gear mesh size, and with fundamental population measures of fecundity and catch in weight being nonlinear (approximately cubic) functions of body length, it is plainly desirable to achieve population models that break down age groups by length. Modeling differing rates of mortality by length is important in fishery models because so many critical population processes either affect that length-specific population breakdown or they and their inferences are strongly affected by it. Most importantly, data on fish length are relatively abundant and thus are sufficient to inform a more refined, dynamic, length-dependent stock assessment inference.

In future extensions of fishery models to include the marine food web undertaken, for example, to assess environmental and ecosystem impacts of harvesting (Hall et al.

2006), organism body size is the natural independent variable. This is because trophic predation among organisms in the aquatic food web is known to be body-size selective (Hansen et al. 1994; Scharf et al. 2000; Brose et al. 2006*b*), strongly influencing ecosystem dynamics (Jennings et al. 2002; Layman et al. 2005). Moreover, ageing methods for most or all other species are not likely to be available as they are for exploited fish, while body size can often be measured for most or all of the trophic species in a food web, increasingly with automated or remote measurement technologies. By making both size and age dependence explicit for fish (or other) species in a food web, life history shifts in the size range and species of selected prey can be accommodated.

Moreover, powerful rules relating an astonishingly broad range of relationships among ecological quantities have been uncovered (Peters 1983) that exhibit allometric dependence on body size. Ecological processes that show clear, allometric, body-weight dependence include metabolism (Kleiber 1932; Hemmingsen 1960), intrinsic growth rate (Fenchel 1974; Savage et al. 2004), natural mortality (Pauly 1980), and predation rates (Peters 1983). Fishery ecosystem models currently can exhibit a very wide range of possible solutions (Koen-Alonso and Yodzis 2005) because data are not usually sufficient to constrain the range of solutions. Incorporating allometric relationships with body size (Kerr 1974; Cohen et al. 2003), which appear accurate though logarithmically variable, over a very wide range of species and orders of magnitude in organism body weight (Brown et al. 2004) will be a critical component of ecosystem models (Kerr and Dickie 2001; Brown and Gillooly 2003; Koen-Alonso and Yodzis 2005). This will constrain the range of solutions while adding important information about realistic ecosystem structure (Loeuille and Loreau 2005; Brose et al. 2006*a*), notably for dependence of predation rates and energy budgets on size and thus of energetic flows up the food chain. Incorporating these allometric relationships requires a model breakdown of predators and prey by body size.

Modeling populations by length as well as by age can permit smooth integration of fishery with ecosystem models. Fishery models are principally age-based, while ecosystem models, especially in aquatic environments, have been and will be size-based (Kerr and Dickie 2001; Brown and Gillooly 2003; Jennings 2005). Thus, one strategy for unification is to generalize fishery models by adding explicit dependence on size. Slice partition offers one avenue for extending fishery models to the dynamic age- and size-based formulation that future models will require.

Acknowledgements

André Punt and Tony Fowler provided advice in several stages of model development and exposition. Dave Short aged most garfish. Moira Ferguson, Pierre Pepin, Barry Smith, and three anonymous reviewers provided essential comments. This work was supported by the Australian Fisheries Research and Development Corporation, Project Nos. 95/008, 97/133, and 1999/145.

References

Banks, H.T., Botsford, L.W., Kappel, F., and Wang, C. 1991. Estimation of growth and survival in size-structured cohort data: an application to larval striped bass (*Morone saxatilis*). J. Math. Biol. **30**: 125–150.

Brose, U., Williams, R.J., and Martinez, N.D. 2006*a*. Allometric scaling enhances stability in complex food webs. Ecol. Lett. **9**: 1228–1236.

Brose, U., Jonsson, T., Berlow, E.L., Warren, P., Banasek-Richter, C., Bersier, L.-F., Blanchard, J.L., Brey, T., Carpenter, S.R., Blandenier, M.-F.C., Cushing, L., Dawah, H.A., Dell, T., Edwards, F., Harper-Smith, S., Jacob, U., Ledger, M.E., Martinez, N.D., Memmott, J., Mintenbeck, K., Pinnegar, J.K., Rall, B.C., Raynor, T.S., Reuman, D.C., Ruess, L., Ulrich, W., Williams, R.J., Woodward, G., and Cohen, J.E. 2006*b*. Consumer–resource body-size relationships in natural food webs. Ecology, **87**: 2411–2417.

Brown, J.H., and Gillooly, J.F. 2003. Ecological food webs: high-quality data facilitate theoretical unification. Proc. Natl. Acad. Sci. U.S.A. **100**: 1467–1468.

Brown, J.H., Gillooly, J.F., Allen, A.P., Savage, V.M., and West, G.B. 2004. Toward a metabolic theory of ecology. Ecology, **85**: 1771–1789.

Cohen, J.E., Jonsson, T., and Carpenter, S.R. 2003. Ecological community description using the food web, species abundance, and body size. Proc. Natl. Acad. Sci. U.S.A. **100**: 1781–1786.

Deriso, R.B., and Parma, A.M. 1988. Dynamics of age and size for a stochastic population model. Can. J. Fish. Aquat. Sci. **45**: 1054–1068.

Dow, N.G. 1992. Growth parameter estimation from tagging and aging data. *In* The measurement of age and growth in fish and shellfish. *Edited by* D.A. Hancock. Bureau of Rural Resources, Canberra, Australia. Bureau of Rural Resources Proceedings No. 12. pp. 185–192.

Fenchel, T. 1974. Intrinsic rate of natural increase: the relationship with body size. Oecologia, **14**: 317–326.

Fournier, D., and Archibald, C.P. 1982. A general theory for analyzing catch at age data. Can. J. Fish. Aquat. Sci. **39**: 1195–1207.

Fournier, D.A., and Doonan, I.J. 1987. A length-based stock assessment method utilizing a generalized delay-difference model. Can. J. Fish. Aquat. Sci. **44**: 422–437.

Fournier, D., Sibert, J.R., Majkowski, J., and Hampton, J. 1990. MULTIFAN a likelihood-based method for estimating growth parameters and age composition from multiple length frequency data sets illustrated using data for southern bluefin tuna (*Thunnus maccoyii*). Can. J. Fish. Aquat. Sci. **47**: 301–317.

Fournier, D., Hampton, J., and Sibert, J.R. 1998. MULTIFAN-CL: a length-based, age-structured model for fisheries stock assessment, with application to South Pacific albacore, *Thunnus alalunga*. Can. J. Fish. Aquat. Sci. **55**: 2105–2116.

Frøysa, K.G., Bogstad, B., and Skagen, D.W. 2002. Fleksibest — an age–length structured stock assessment model. Fish. Res. **55**: 87–101.

Hall, S.J., Collie, J.S., Duplisea, D.E., Jennings, S., Bravington, M., and Link, J. 2006. A length-based multispecies model for evaluating community responses to fishing. Can. J. Fish. Aquat. Sci. **63**: 1344–1359.

Hansen, B., Bjørnsen, P.K., and Hansen, P.J. 1994. The size ratio between planktonic predators and their prey. Limnol. Oceanogr. **39**: 395–403.

Hemmingsen, A.M. 1960. Energy metabolism as related to body size and respiratory surfaces, and its evolution. Reports of the Steno Memorial Hospital and the Nordisk Insulinlaboratorium (Copenhagen), **9**: 6–110.

Jennings, S. 2005. Size-based analyses of aquatic food webs. *In* Aquatic food webs. *Edited by* A. Belgrano, U.M. Scharler, J.

Dunne, and R.E. Ulanowicz. Oxford University Press, Oxford. pp. 86–97.

Jennings, S., Pinnegar, J.K., Polunin, N.V.C., and Warr, K.J. 2002. Linking size-based and trophic analyses of benthic community structure. Mar. Ecol. Prog. Ser. **226**: 77–85.

Kerr, S.R. 1974. Theory of size distribution in ecological communities. J. Fish. Res. Board Can. **31**: 1859–1862.

Kerr, S.R., and Dickie, L.M. 2001. The biomass spectrum. Columbia University Press, New York.

Kleiber, M. 1932. Body size and metabolism. Hilgardia, **6**: 315–353.

Koen-Alonso, M., and Yodzis, P. 2005. Multispecies modelling of some components of the marine community of northern and central Patagonia, Argentina. Can. J. Fish. Aquat. Sci. **62**: 1490–1512.

Kristensen, K., Lewy, P., and Beyer, J.E. 2006. How to validate a length-based model of single-species fish stock dynamics. Can. J. Fish. Aquat. Sci. **63**: 2531–2542.

Layman, C.A., Langerhans, R.B., and Winemiller, K.O. 2005. Body size, not other morphological traits, characterizes cascading effects in fish assemblage composition following commercial netting. Can. J. Fish. Aquat. Sci. **62**: 2802–2810.

Loeuille, N., and Loreau, M. 2005. Evolutionary emergence of size-structured food webs. Proc. Nat. Acad. Sci. U.S.A. **102**: 5761–5766.

Maunder, M.N. 2001. A general framework for integrating the standardization of catch-per-unit-effort into stock assessment models. Can. J. Fish. Aquat. Sci. **58**: 795–803.

McGarvey, R., and Feenstra, J.E. 2002. Estimating rates of fish movement from tag-recoveries: conditioning by recapture. Can. J. Fish. Aquat. Sci. **59**: 1054–1064.

McGarvey, R., and Fowler, A.J. 2002. Seasonal growth of King George whiting (*Sillaginodes punctata*) from length-at-age samples truncated by legal minimum size. Fish. Bull. **100**: 545–558.

Methot, R.D. 1990. Synthesis model: an adaptable framework for analysis of diverse stock assessment data. Int. North Pacif. Fish. Comm. Bull. **50**: 259–277.

Parma, A.M., and Deriso, R.B. 1990. Dynamics of age and size composition in a population subject to size-selective mortality: effects of phenotypic variability in growth. Can. J. Fish. Aquat. Sci. **47**: 274–289.

Pauly, D. 1980. On the interrelationships between natural mortality, growth parameters, and mean environmental temperature in 175 fish stocks. J. Cons. Int. Explor. Mer. **39**: 175–192.

Pennington, M., and Vølstad, J.H. 1994. Assessing the effect of intra-haul correlation and variable density on estimates of population characteristics from marine surveys. Biometrics, **50**: 725–732.

Pennington, M., Burmeister, L.-M., and Hjellvik, V. 2002. Assessing the precision of frequency distributions estimated from trawl-survey samples. Fish. Bull. **100**: 74–80.

Peters, R.H. 1983. The ecological implications of body size. Cambridge University Press, Cambridge, UK.

Punt, A.E., Smith, D.M., and Cui, G. 2002. Evaluation of management tools for Australia's south east fishery 1. Modelling the south east fishery taking account of technical interactions. Mar. Freshw. Res. **53**: 615–629.

Punt, A.E., Hobday, D., Gerhard, J., and Troynikov, V.S. 2006*a*. Modelling growth of rock lobsters, *Jasus edwardsii*, off Victoria, Australia using models that allow for individual variation in growth parameters. Fish. Res. **82**: 119–130.

Punt, A.E., Smith, D.C., Tuck, G.N., and Methot, R.D. 2006*b*. Including discard data in fisheries stock assessments: two case studies from south-eastern Australia. Fish. Res. **79**: 239–250.

Salthaug, A. 2003. Dynamic age–length keys. Fish. Bull. **101**: 451–456.

Savage, V.M., Gillooly, J.F., Brown, J.H., West, G.B., and Charnov, E.L. 2004. Effects of body size and temperature on population growth. Am. Nat. **163**: 429–441.

Scharf, F.S., Juanes, F., and Rountree, R.A. 2000. Predator size – prey size relationships of marine fish predators: interspecific variation and effects of ontogeny and body size on trophic-niche breadth. Mar. Ecol. Prog. Ser. **208**: 229–248.

Smith, B.D., and Botsford, L.W. 1998. Interpretation of growth, mortality, and recruitment patterns in size-at-age, growth increment, and size frequency data. *In* Proceedings of the North Pacific Symposium on Invertebrate Stock Assessment and Management, 6–10 March 1995, Nanaimo, British Columbia, Canada. *Edited by* G.S. Jamieson and A. Campbell. Can. Spec. Publ. Fish. Aquat. Sci. **125**: 125–139.

Taylor, N.G., Walters, C.J., and Martell, S.J.D. 2005. A new likelihood for simultaneously estimating von Bertalanffy growth parameters, gear selectivity, and natural and fishing mortality. Can. J. Fish. Aquat. Sci. **62**: 215–223.

Troynikov, V.S. 1999. Use of Bayes theorem to correct size-specific sampling bias in growth data. Bull. Math. Biol. **61**: 355–363.

Appendix A. Slice partition pseudo-code

The programming steps for calculating the three slice partition quantities are outlined in this appendix. Here, we summarize a relatively efficient coding algorithm for implementing a slice partition in an age-based model. It does not require (*i*) solving of integral equations for a lower integration limit or (*ii*) integrating an allometric function for weight versus length across each slice subinterval, as the slice partition was mathematically defined in Materials and methods. This algorithm does require the calculation of cumulative probabilities of a standardized normal and the inverse calculation of a standardized normal z value given upper tail probability. Both of these are numerically well approximated by a polynomial and thus can be feasibly integrated into a stock assessment model likelihood.

Computational efficiency was achieved by (1) employing the normal score for each slice partition point and (2) making midpoint approximations in place of more exact integrals under the pdf (for mean weights). (1) The standardized normal variate (the z score or normal score) is formed as the relative position of LML along the standardized normal length-at-age pdf, designating the left boundary of each slice, in the age it is created. This normal score value is unchanged thereafter, though the mean and standard deviation of the cohort length pdfs do naturally change (grow) with age. Thus, given the mean and standard deviation for each legal cohort age, the fish lengths specifying slice left-hand partition points are calculated from the z scores for all (legal-size) slices. The use of the normal score obviates the need for solving integral equations for lower limits of integration. However, this shortcut assumes normally distributed fish lengths because it relies on using the standardized normal to specify each slice partition length. If fish lengths are non-normally distributed at time of recruitment, unless a way to extend the normal score approach were devised, iterative solving for lower integration limits, as described in Materials and methods, would be needed. A fixed P_{slice} probability of each slice for all ages underlies the definition of slices and also explains why the z scores uniquely specify the slice partition for any chosen model age. (2) The fish mean weight in each slice is approximated by the weight–length function evaluated at the midpoint length of each slice (or, for the upper-tail slice, the median probability length) rather than numerically integrating weight versus length across each slice subinterval.

The slice partition algorithm has six basic steps, coded by six iteration loops. In each loop, calculations iterate over cohort age (for each region, sex, etc.):

Step 1. Calculate the (1.1) mean length, $\bar{l}(a)$, and (1.2) standard deviation, $\sigma(a)$, and thus also the (1.3) z score, $z(a) = [\text{LML} - \bar{l}(a)]/\sigma(a)$, for every age ($a$) of growth. This step requires the input of growth submodel parameters specifying $\bar{l}$ and σ, given a. In this loop, calculate also (1.4) $P_{\text{sublegal}}(a) = \int_{-\infty}^{\text{LML}} p(l \mid \theta; a)\,dl$ and (1.5) $P_{\text{legal}}(a) = 1 - P_{\text{sublegal}}(a)$. For calculating the $P_{\text{sublegal}}(a)$ normal cumulative probabilities, we used the AD Model Builder cumd_norm function, which encapsulates the Abramowitz and Stegan (1965; formula 26.2.17) polynomial approximation and takes the standardized z score as input.

Step 2. Calculate slice probabilities, $P_{\text{slice}}(a)$, the proportions of the cohort reaching legal size in each model age: $P_{\text{slice}}(a) = P_{\text{legal}}(a) - P_{\text{legal}}(a-1)$, $a = a_b + 1, \ldots, a_{\max}$.

Step 3. Calculate the first of three output quantities, the fish transfer coefficients, $f_{\text{transfer}}(a) = P_{\text{slice}}(a)/P_{\text{sublegal}}(a-1)$, $a = a_b + 1, \ldots, a_{\max}$. No transfer coefficient is needed for birth age (a_b) cohorts, with the population number for their one legal (upper tail) slice given by $P_{\text{slice}}(a_b)$ ($= P_{\text{legal}}(a_b)$) times the total recruit number estimated for that cohort.

Step 4. Calculate the slice partition points, specifically the left-hand sides of each slice subinterval, stored as a triangular matrix by age and slice number, $l_{\text{lhs}}(a, s)$. The number of slices for each legal cohort age is given by $n_s(a) = a - a_b + 1$, $a = a_b, \ldots, a_{\max}$. (4.1.) For newly created slices, whose slice subscript number equals the total number of legal slices, $n_s(a)$, the left-hand-side partition point is, by definition, the legal minimum length (LML): $l_{\text{lhs}}(a, s = n_s(a)) = \text{LML}$, $a = a_b, \ldots, a_{\max}$. (4.2) Looping over all other slices in each cohort age group, $s = 1$ to $n_s(a) - 1$, the slice left-hand-sides are derived using the z scores: $l_{\text{lhs}}(a, s) = \bar{l}(a) + \sigma(a)\, z(s - 1 + a_b)$.

Step 5. Calculate the second slice partition output quantity, the triangular matrix of central lengths for each slice, $l(a, s)$. (5.1) For all slices except upper-tail slices, the midpoints were used: $l(a, s) = [l_{\text{lhs}}(a, s) + l_{\text{lhs}}(a, s-1)]/2$. (5.2) For the upper-tail slices, the central length was chosen to be the median probability value of the upper tail, whose z score was calculated by $z_{\text{median}}(a, s = 1) = \text{inv\_cumd\_norm}(1 - P_{\text{legal}}(a_b)/2)$. The inv_cumd_norm function in AD Model Builder (Abramowitz and Stegan 1965, formula 26.2.23) gives a standardized normal z value for any given probability.

Step 6. Calculate the mean weights by evaluating the weight–length formula at each slice central length: $w(a, s) = \alpha[l(a, s)]^{\beta}$.

Appendix A reference

Abramowitz, M., and Stegan, I.A. 1965. Handbook of mathematical functions. Dover Publications, Inc., New York.

Appendix B. Garfish stock assessment model

The stock assessment model has three principal submodels: (*i*) recruitment, (*ii*) growth, via the slice formalism, and (*iii*) harvest and natural mortality. The recruitment and slice-growth submodels were described in Materials and methods and Appendix A. Here, we detail equations for harvest and mortality and the model-fitting likelihood.

Model population array

The model garfish population array $N(t, r, x, c, s)$ is five-dimensional, with fish numbers broken down by (*i*) half-yearly model time step t, (*ii*) spatial region r, (*iii*) sex x, (*iv*) cohort (i.e., year class, given by year of spawning) c, and (*v*) slice s.

Variable subscripts for winter or summer half-year (t_{season}) and cohort age in half-years (a) were calculated as functions of t and c. Ages ran from 3 to 12+ half-years, the oldest age being a "plus" group. Garfish catch and effort, for data and model, were divided into four effort types, i_E: (*i*) haul nets targeting garfish, (*ii*) haul nets not targeting garfish, (*iii*) dab nets and minor gears, and (*iv*) recreationals. The two commercial gears, g, each with separate length selectivity, are haul net and dab net. Data quantities, such as reported effort, $\tilde{E}$, are denoted by a tilde.

Effort and catch

The catch equations were effort-conditioned. Thus, fishing mortality was written as a linear function of reported fishing effort for each component of catch:

$$\text{(B.1)}\quad F(t, r, x, c, s, i_E) = q(r, t_{\text{season}}, x, i_E)\, \tilde{E}(t, r, i_E)\, s_{\text{len}}(g(i_E), s)$$

The catchability, q, was assumed to vary with region, season, sex, and effort type. Length selectivity, s_{len}, by gear type followed a logistic function of fish length, the latter specified by the midpoint of each slice. For commercial effort, the catchability was written as

$$\text{(B.2)}\quad q(r, t_{\text{season}}, x, i_E) = q_{\text{CSE}}(r, t_{\text{season}}, i_E) \times s_{\text{SS}}(t_{\text{season}}, x)[1 + q'(t - t_{\text{mid}})]$$

with q_{CSE} being the absolute catchability given as function of region, season, and effort type; with a relative selectivity coefficient $s_{\text{SS}}(t_{\text{season}}, x)$ describing the specifically sex-dependent seasonality of catchability, notably strong differences in sex ratios in the catch between summer and winter; and where a half-yearly linear rate of increase in catchability (changing effective effort) is estimated by q', the median catchability level given when t equals the middle time step, t_{mid}, in the estimated time series range.

The instantaneous fishing mortality rate for each element of the population array is given by a sum of fishing mortalities over all fishing effort types:

$$\text{(B.3)}\quad F(t,r,x,c,s) = \sum_{i_E=1}^{n_E} F(t,r,x,c,s,i_E)$$

Mortality

The Baranov depletion equation for each element of the population array was written as

$$\text{(B.4)}\quad N(t+1,r,x,c,s) = N(t,r,x,c,s)\exp\{-[M + F(t,r,x,c,s)]\,p_{\text{year}}(t)\}$$

where $p_{\text{year}}(t)$ quantifies the proportion of a year spanned by the days in each half-yearly time step. Natural mortality rate was taken as constant, $M = 0.4$ (Jones 1990).

Parameters

Estimated parameters for the model fall into seven general categories: (1) yearly recruit numbers by region, (2) recruitment female sex proportion by region, (3) catchabilities, (4) relative selectivities by sex and season, (5) logistic length selectivity, (6) growth, and (7) likelihood standard deviations of fits to half-yearly catch totals.

Model likelihood

The model likelihood (Fournier and Archibald 1982) was fitted to (*i*) catch proportions by age and sex, (*ii*) half-yearly catch totals by weight, and (*iii*) catch length samples by age.

Catch totals by weight

Model commercial catch totals by weight (kg) were fitted to data using a lognormal likelihood. The catch by weight was calculated using the standard Baranov formula as

$$\text{(B.5)}\quad \hat{C}(t,r,x,c,s,i_E) = N(t,r,x,c,s)\,w(a(t,c),s)\,\frac{F(t,r,x,c,s,i_E)}{M + F(t,r,x,c,s)}\,(1 - \exp\{-[M + F(t,r,x,c,s)]\,p_{\text{year}}(t)\})$$

where the weights by age and slice $w(a(t,c),s)$ were derived in Appendix A.

The likelihood factor for each combination of region, r, and commercial effort type (i_E up to $n_E - 1$), was written as

$$\text{(B.6)}\quad L_C = \prod_{t=1}^{n_t}\prod_{i_E=1}^{n_E-1}\prod_{r=1}^{n_r}\frac{1}{\sqrt{2\pi}\,\sigma_C\,\tilde{C}(t,r,i_E)}\exp\left(-\frac{1}{2}\left\{\frac{\ln[\tilde{C}(t,r,i_E)] - \ln[\hat{C}(t,r,i_E)]}{\sigma_C}\right\}^2\right)$$

where σ_C is the estimated catch-likelihood standard deviation parameter; $\tilde{C}(t,r,i_E)$ is reported catch by weight for each time step, t, region, r, and effort type, i_E; and $\hat{C}(t,r,i_E)$ is model-predicted catch by weight for each t, r, and i_E.

This lognormal likelihood form was also fitted to recreational ($i_E = n_E$) catch survey numbers.

Catch samples by age and sex

A two-dimensional multinomial likelihood was used to fit to catch-sample proportions by sex and age, since both are attributes of a single catch sample data set. The fitted data from the principal gear (haul nets), in the two time steps and regions where catch was monitored, consisted of the counts of sampled fish falling into each possible combination of sex and half-yearly age, $\tilde{n}(a,x;t,r)$. The multinomial likelihood factor was written as

$$\text{(B.7)}\quad L_{AX} = \prod_{i_{AX}=1}^{n_{AX}}\prod_{a=a_0}^{12+}\prod_{x=0}^{1}\hat{p}(a,x;i_{AX})^{\tilde{n}(a,x;i_{AX})}$$

where i_{AX} is the index over the set of n_{AX} catch samples of fish age and sex; $\hat{p}(a,x;i_{AX})$ is the two-dimensional array of model-predicted fish proportions captured by age and sex for each sampled half-year and region, indexed by i_{AX}; $\tilde{n}(a,x;i_{AX})$ are fish numbers for each age and sex, observed in the catch-at-age sample i_{AX}.

Catch samples by length

A normal likelihood was applied to fit the data and model moment properties, mean, standard deviation, skewness, and kurtosis. Fournier and Doonan (1987) developed this approach and also fitted a normal likelihood, but to the central moments rather than moment properties. The likelihood for the length moment fit was written as

$$(\mathrm{B.8})\quad L_{\mathrm{mp}} = \prod_{i_{\mathrm{AX}}=1}^{n_{\mathrm{AX}}(i_{\mathrm{mp}})} \prod_{i_{\mathrm{mp}}=1}^{4} \prod_{\mathrm{sex}=0}^{1} \prod_{a=a_r}^{12+} \prod_{g=1}^{2} \left[\frac{\exp\left(-\frac{1}{2} \left\{ \frac{[\tilde{b}(i_{\mathrm{mp}}, x, a, g; i_{\mathrm{AX}}) - \hat{b}(i_{\mathrm{mp}}, x, a, g; i_{\mathrm{AX}})]}{\sigma_{\mathrm{mp}}(g)} \right\}^2 \right)}{\sqrt{2\pi}\,\sigma_{\mathrm{mp}}(g)} \right]^{\tilde{n}_a(x,a,g;i_{\mathrm{AX}})}$$

We weighted each factor in the log-likelihood by the sample size ($\tilde{n}_a(x, a, g; i_{\mathrm{AX}})$). Higher moment properties require more data to be informative. We therefore set criteria for exclusion of smaller catch sample data sets, i_{AX}, from the L_{mp} likelihood, depending on the moment property fitted. Thus, the number of qualifying data sets, $n_{\mathrm{AX}}(i_{\mathrm{mp}})$, decreased with moment property i_{mp}. We required at least 16 aged fish for kurtosis, eight for skewness, four for standard deviation, and one for fitting to mean length. Similarly we required four model slices for kurtosis, three for skewness, two for standard deviation, and one for fitting mean length.

Appendix B references

Fournier, D., and Archibald, C.P. 1982. A general theory for analyzing catch at age data. Can. J. Fish. Aquat. Sci. **39**: 1195–1207.

Fournier, D.A., and Doonan, I.J. 1987. A length-based stock assessment method utilizing a generalized delay-difference model. Can. J. Fish. Aquat. Sci. **44**: 422–437.

Jones, G.K. 1990. Growth and mortality in a lightly fished population of garfish (*Hyporhamphus melanochir*), in Baird Bay, South Australia. Trans. R. Soc. S. Aust. **114**: 37–45.

The lampricide 3-trifluoromethyl-4-nitrophenol (TFM) interferes with intermediary metabolism and glucose homeostasis, but not with ion balance, in larval sea lamprey (*Petromyzon marinus*)

Michael P. Wilkie, John A. Holmes, and John H. Youson

Abstract: Although treatment of streams with the lampricide 3-trifluoromethyl-4-nitrophenol (TFM) has been highly effective for sea lamprey (*Petromyzon marinus*) population control in the Great Lakes, little is known about its mechanism(s) of toxicity. We investigated two hypotheses of TFM toxicity in larval sea lamprey exposed to TFM for 12 h. The first was that TFM interferes with oxidative ATP production by mitochondria, causing depletion of fuel stores in the body. The second was that TFM interferes with gill-mediated ion exchange, which eventually causes circulatory collapse. While exposure of larvae to TFM (2 $mg \cdot L^{-1}$) did not disturb tissue ATP stores, it led to a sustained 60% reduction in phosphocreatine (PCr) after 6 h. This was accompanied by 6- to 10-fold increases in plasma and tissue lactate, which persisted through 12 h. By 12 h, plasma glucose was nearly depleted in the five surviving lamprey, but TFM caused no appreciable changes in plasma Cl^-, haematocrit, haemoglobin, or ammonia concentration. We conclude that TFM-mediated gill damage and ionic failure are not underlying mechanisms of TFM toxicity. Rather, TFM likely interferes with oxidative ATP production, leading to reduced tissue PCr stores and eventually profound hypoglycaemia that starves the nervous system of glucose, causing death.

Résumé : Bien que le traitement des cours d'eau au lampricide 3-trifluorométhyl-4-nitrophénol (TFM) ait été très efficace pour le contrôle de la grande lamproie marine (*Petromyzon marinus*) dans les Grands Lacs, on connaît mal son ou ses mécanismes de toxicité. Nous explorons deux hypothèses concernant la toxicité de TFM chez des larves de grandes lamproies marines exposées au TFM pendant 12 h. La première veut que le TFM interfère avec la production oxydative d'ATP par les mitochondries, ce qui réduit les réserves de carburant du corps. La seconde soutient qu'il interfère avec les échanges ioniques sous le contrôle des branchies, ce qui éventuellement cause un effondrement circulatoire. Alors que l'exposition des larves au TFM (2 $mg \cdot L^{-1}$) n'affecte pas les réserves tissulaires d'ATP, elle cause une réduction prolongée de 60 % de la phosphocréatine (PCr) au bout de 6 h. Ceci s'accompagne d'augmentations de 6 à 10 fois du lactate dans le plasma et les tissus qui persistent au cours des 12 h. Au bout de 12 h, il y a un épuisement presque total du glucose plasmatique chez les cinq lamproies survivantes; cependant, le TFM n'entraîne pas de changement appréciable du Cl^- plasmatique, de l'hématocrite et des concentrations d'hémoglobine et d'ammoniaque. Nous concluons que le dommage aux branchies sous l'action du TFM et l'effondrement ionique ne sont pas les mécanismes sous-jacents de la toxicité du TFM. En revanche, le TFM interfère vraisemblablement avec la production oxydative d'ATP, ce qui réduit les réserves de PCr et, en fin de compte, mène à une hypoglycémie profonde qui prive le système nerveux de glucose, provoquant ainsi la mort.

[Traduit par la Rédaction]

Introduction

The sea lamprey (*Petromyzon marinus*) spends 3–7 years burrowed in the sediments of streams as a suspension-feeding larva before entering a complex metamorphosis characterized by a reorganization of both internal and external features of the body (Beamish and Potter 1975; Youson 2003). Postmetamorphic lamprey then migrate to lakes or the sea, where they begin the 1- to 2-year parasitic phase of their life cycle (Beamish and Potter 1975). Such parasitism (or predation when the host is killed) contributed to massive declines in Great Lakes fish stocks, especially lake trout (*Salvelinus namaycush*), in the early to mid-1900s (Applegate 1950; Smith and Tibbles 1980). In 1958, the

---

Received 25 September 2006. Accepted 20 April 2007. Published on the NRC Research Press Web site at cjfas.nrc.ca on 18 August 2007.
J19558

M.P. Wilkie,[1,2] J.A. Holmes,[3] and J.H. Youson. Department of Life Sciences, University of Toronto at Scarborough, Toronto, ON M1C 1A4, Canada.

[1] Corresponding author (e-mail: mwilkie@wlu.ca).
[2] Present address: Department of Biology, Wilfrid Laurier University, Waterloo, ON N2L 3C5, Canada.
[3] Present address: Fisheries and Oceans Canada, 3190 Hammond Bay Road, Nanaimo, BC V9T 6N7, Canada.

Can. J. Fish. Aquat. Sci. **64**: 1174–1182 (2007) doi:10.1139/F07-082

halogenated phenol, 3-trifluoromethyl-4-nitrophenol (TFM) was first applied as a selective lampricide to nursery streams containing larval sea lamprey in Lake Superior. The use of TFM was later expanded to tributaries of Lakes Huron, Michigan, Ontario, and finally to Lake Erie (Howell et al. 1980), which contributed to the partial recovery of many fisheries (e.g., Smith and Tibbles 1980; Heinrich et al. 2003; Morse et al. 2003).

Although other methods of sea lamprey control have been implemented, including barriers, traps, and sterile male release, the primary means of sea lamprey population control remains TFM or mixtures of TFM plus niclosamide (1%–2%) in the Great Lakes and in a few other infested watersheds, including Lake Champlain in northeastern USA (Brege et al. 2003). Owing to ongoing public concern regarding pesticide use, increasing costs, and potential nontarget effects on other aquatic organisms, an objective of the Great Lakes Fishery Commission (GLFC), a binational body that oversees sea lamprey control in the Great Lakes, is to reduce its reliance on TFM (GLFC 1992, 2001). As surprisingly little is known about TFM's mode of toxic action, a better understanding of this process could provide insight on how to reduce TFM use while still effectively controlling larval sea lamprey populations.

Applegate et al. (1966) proposed that TFM impaired ATP production in larval lamprey because of its similarity to compounds known to uncouple oxidative phosphorylation in the mitochondria of cells (e.g., 2,4-dinitrophenol). To date, the only direct evidence of uncoupling was provided by Niblett and Ballantyne (1976), who used isolated rat mitochondria to demonstrate that TFM exposure led to greater oxygen consumption per molecule of ATP synthesized (decreased ADP/O ratio), a characteristic of uncoupled mitochondria. Neither the effects of TFM upon oxidative phosphorylation in mitochondria nor its impact upon actual fuel stores and metabolites in the body has been examined in larval lamprey, however. Based on its predicted effects upon mitochondrial function, a central objective of our study was to test the hypothesis that TFM caused death in larval lamprey by interfering with intermediary metabolism.

A second hypothesis of TFM toxicity is that it causes disturbances to internal osmotic and ionic status based on ultrastructural changes reported in the mitochondria-rich cells (MRC) of larval lamprey gills (Mallatt et al. 1985, 1994). There is little information about the effects of TFM upon internal water and ionic status in larval lamprey and nontarget fishes, however. Thus, the second objective of our study was to test the hypothesis that TFM causes haematological, ionic, and osmotic disturbances in larval sea lamprey.

After performing preliminary acute TFM toxicity experiments, our experimental approach was to test both hypotheses simultaneously by collecting blood and tissue samples at regular intervals (3, 6, 9, 12 h) from larval sea lamprey exposed to near-lethal concentrations of TFM (2 mg·L^{-1}). This time frame was chosen because field applications of TFM typically last 10–12 h (Bills et al. 2003). As indices of gill function and electrolyte balance, blood samples were analyzed for haematocrit, haemoglobin, plasma Cl$^-$ concentration, and plasma ammonia concentration. Plasma glucose and lactate and tissue ATP, phosphocreatine (PCr), glycogen, lactate, and pyruvate measurements were used to determine if TFM interfered with intermediary metabolism.

Materials and methods

Experimental animals and holding

Larval sea lamprey (*P. marinus*) were collected by pulsed DC electrofishing from Putnam Creek (Lake Champlain), New York, in summer 1995, transported to the University of Toronto at Scarborough (UTSC) in well-insulated containers, and held in aerated, flowing dechlorinated municipal tap water (pH ~ 8.0; titratable alkalinity ~ 87 mg CaCO$_3$·L^{-1}; hardness ~ 1.4 mequiv. CaCO$_3$·L^{-1}; temperature ~ 15 °C) under a 12 h light : 12 h dark photoperiod. Holding tanks were lined with sand (4–5 cm depth) to provide substrate for the burrow-dwelling larval lamprey. The lamprey were fed a weekly slurry of bakers yeast (2 g per animal; Holmes and Youson 1994), which remained in the tanks for approximately 12 h after water flow had been cut off.

Two experiments were conducted. In the first, the acute toxicity of the lampricide TFM to larval sea lamprey (N = 48; mass = 1.2 ± 0.1 g) was determined over a 24 h exposure period. Acute toxicity data was then used to determine a TFM exposure concentration to which larval lamprey could be exposed for 12 h to determine its effects on internal ion, osmotic, and nitrogen balance and metabolic status (N = 45; mass = 1.7 ± 0.1 g). All experiments followed guidelines of the Canadian Council on Animal Care and were approved by the UTSC Animal Care Committee.

Experimental protocol

Acute toxicity of TFM

One week prior to testing, larval sea lamprey were randomly assigned in groups of six to one of eight rectangular containers (1 L; temperature = 18 °C). The containers contained sand at a depth of approximately 4–5 cm and were well aerated to ensure there was uniform mixing of TFM in the static exposure setups. For determination of acute TFM toxicity, lamprey were either held under control conditions (no TFM) or exposed to nominal TFM concentrations of 2, 4, or 8 mg·L^{-1} for 24 h. Because treatments were in duplicate, a total of 12 larval lamprey were exposed to each treatment condition. The TFM concentrations chosen represented ranges used in typical lampricide treatments of streams in the Great Lake's region (e.g., Bills et al. 2003). Field formulation TFM was used for all experiments (38% active ingredient dissolved in isopropanol; provided courtesy of Fisheries and Oceans Canada), which was diluted in water to yield a 2 g·L^{-1} stock solution. On the day of experiments, appropriate amounts of the stock solution were added to each treatment container to yield nominal TFM concentrations of 2, 4, or 8 mg·L^{-1} TFM, and survival was monitored at 0.25, 0.5, 1.0, 1.5, 2.0, 3.0, 4.0, 8.0, 12.0, and 24.0 h. Water samples were also collected for later determination of the water TFM concentration. Log-probit analysis was then used to calculate the concentration lethal to 50% of individuals (LC$_{50}$) (Sprague 1969) for TFM, which allowed us to choose a TFM concentration to which a large proportion of larval lamprey could survive for 9–12 h, but still exhibit the key physiological disturbances that would be characteristic of TFM toxicity.

Physiological effects of TFM

Based on the data from the acute toxicity study, larval lamprey were exposed to a nominal TFM concentration of 2 mg·L^{-1} for 12 h to determine the effects of TFM on haematology (haematocrit, haemoglobin), electrolyte, and water balance (plasma Cl$^-$ concentration, tissue water); fuel stores (plasma glucose and tissue glycogen, ATP, and PCr); and metabolites (plasma ammonia and lactate, tissue pyruvate and lactate). Animals were acclimated to the experimental temperature (18 °C) for 3 weeks, and 1 day before experiments, they were transferred in groups of three to the aerated, rectangular experimental containers (1.0 L), receiving water at approximately 250 mL·min^{-1}. Animals were not fed 7–10 days prior to experiments to minimize the accumulation of ammonia over the 12 h TFM exposure period, when water flow was cut off to the containers. Although each container held three lamprey, we estimated that total ammonia never exceeded 10 μmol·L^{-1} in each container because of the low basal rates of ammonia excretion that are characteristic of this life stage (20–50 nmol N·g^{-1}·h^{-1}; Wilkie et al. 2006). Thus, it is highly unlikely that the accumulation of ammonia in the water would have exacerbated TFM toxicity. Each experimental container was darkened and contained diffusely distributed cotton to provide burrowing substrate to calm the burrow-dwelling larvae (thigmokinesis; Rovainen and Scheiber 1975). The cotton substrate, plus the small volume of the containers, also expedited sampling by making it easier to locate and retrieve the animals.

Larval lamprey were terminally sampled (three animals at a time) in the absence of TFM at time zero (controls) or after 3, 6, 9, or 12 h of TFM exposure. The intent of this sampling regimen was to establish how TFM toxicity progressed over 12 h, which is approximately the length of a typical TFM treatment in the field (Bills et al. 2003). As oxygen consumption and the metabolic parameters examined (e.g., ATP, PCr, glycogen, lactate) are stable in larval lamprey for at least 24 h under similar holding conditions (e.g., Wilkie et al. 2001; P.G. Bradshaw and M.P. Wilkie, unpublished data), we were confident that comparisons between the control animals sampled at time zero were directly comparable to measurements made in the TFM-treated animals sampled 3, 6, 9, or 12 h later. A total of nine animals were sampled at each interval following MS-222 (tricaine methanesulfonate) anaesthesia (1.5 g·L^{-1} buffered with 3.0 g·L^{-1} of $NaHCO_3$; Sigma Chemical Co.; Wilkie et al. 2001), except at 12 h (N = 5) when there were four mortalities caused by TFM. After each animal was immobilized by the anaesthetic, they were removed from the water and an incision made through the heart from which blood was collected using non-heparinized haematocrit tubes. As tubes were filled with blood, they were capped with plasticene (Critoseal) and placed on ice until sampling was completed (~5 min). Immediately following blood collection, the trunks of the animals (the region immediately posterior to the last (7th) branchiopore, including internal organs) were snap-frozen in liquid N_2 using precooled aluminum tongs (freeze-clamped) to preserve the concentrations of labile fuels and metabolites such as ATP, PCr, glycogen, pyruvate, and lactate (e.g., Wang et al. 1994*a*). Aliquots of whole blood were added to Drabkin's solution (5–10 μL) for later haemoglobin determination. The remaining blood (50–100 μL) was centrifuged in a haematocrit centrifuge at 3000*g* for 5 min, and where a sufficient volume of blood was available, it was used for the immediate determination of haematocrit. Aliquots of plasma were then drawn off and either frozen (–80 °C) for later determination of glucose, ammonia, and Cl$^-$ concentration or added to equal volumes of 8% perchloric acid (15–25 μL) for later determination of plasma lactate concentration.

Analytical techniques

Well-established procedures were used in the analysis of blood and tissue samples, and more detailed descriptions can be found in Wilkie et al. (1997) and Bergmeyer (1983). Briefly, blood haemoglobin concentration was determined using the cyanomethaemoglobin method and commercial reagents (Sigma Chemical Co.). Plasma glucose, lactate, and ammonia concentrations were determined spectrophotometrically using hexokinase, lactate dehydrogenase, and glutamate dehydrogenase, respectively (Bergmeyer 1983). Plasma Cl$^-$ was determined using the mercuric thiocyanate assay (Zall et al. 1956). The mean cell haemoglobin concentration (MCHC) of the blood was determined by dividing the blood haemoglobin concentration by the haematocrit.

Processing of tissue for determination of fuel and metabolite concentrations is described by Wilkie et al. (1997, 2001) and can be summarized as follows. The trunks of the lamprey were initially pulverized to smaller chunks of tissue using a hammer and then quickly transferred to a liquid N_2-cooled mortar. The frozen pieces of trunk tissue were then ground to a fine power under liquid N_2, followed by deproteinization in four volumes of 8% perchloric acid, which contained 1 mmol·L^{-1} ethylenediaminetetraacetic acid (EDTA). The extract was then continuously mixed for 5 min at 4 °C and then centrifuged at 10 000*g* for 2 min. The supernatant was drawn off, neutralized with 1.5 volumes of KOH (2 mmol·L^{-1}) solution (composed of 0.4 mmol·L^{-1} imidazole and 0.4 mmol·L^{-1} KCl), vortexed, and then centrifuged for 30 s. The supernatant was then transferred to 1.5 mL centrifuge tubes and frozen at –80 °C. This extract was subsequently analyzed enzymatically as described by Bergmeyer (1983) for ATP (hexokinase, using glucose-6-phosphatase as a linking enzyme), PCr (creatine kinase), pyruvate (lactate dehydrogenase), and lactate (lactate dehydrogenase). Trunk tissue glycogen content was determined on a neutralized extract that had been digested in five volumes of 30% KOH, using the amyloglucosidase–hexokinase assay (Hassid and Abraham 1957). Tissue water content was determined by drying powdered tissue (initial mass ~100 mg) to constant mass in an oven at 80 °C and was expressed as mL·g^{-1} dry tissue.

Calculations and statistics

Determination of the 12 h LC_{50} for larval lamprey exposed to TFM was done by probit analysis (Sprague 1969) using software provided by the United States Environmental Protection Agency (EPA Probit Analysis Program, version 1.5). All physiological data are presented as the mean ± 1 standard error of the mean (SEM). All comparisons were unpaired and analyzed using one-way analysis of variance

(ANOVA). When significant variability was observed, statistical significance between means was assessed using the Tukey–Kramer test at the $P < 0.05$ level. When the requirement for homogeneity of variance was not satisfied, a nonparametric ANOVA was used, followed by Dunn's test where appropriate.

Results

Acute toxicity of TFM

The respective nominal TFM concentrations of 2, 4, and 8 mg·L^{-1} in the water of each exposure container were reflected by measured TFM concentrations of 2.0 ± 0.2, 3.7 ± 0.2, and 8.1 ± 0.1 mg·L^{-1} (data not shown). At a nominal TFM concentration of 2 mg·L^{-1}, 100% of larval sea lamprey survived for 6 h, but by 8 h there was 50% mortality, and 83.3% mortality after 12 h. By 24 h all animals exposed to 2 mg·L^{-1} of TFM had died. No larval lamprey survived beyond 6 and 3 h at nominal TFM concentrations of 4 and 8 mg·L^{-1}, respectively (data not shown). Over 12 h, the corresponding LC_{50} for TFM was calculated to be 1.6 mg·L^{-1} (data not shown). Based on this mortality data, larval sea lamprey were subsequently exposed to a nominal TFM concentration of 2 mg·L^{-1} to shed light on its physiological effects.

Physiological effects of TFM

In these experiments, no mortality was observed after 3, 6, or 9 h of exposure to a nominal TFM concentration of 2 mg·L^{-1} (actual [TFM] = 2.1 ± 0.04 mg·L^{-1}), but four of the nine animals to be terminally sampled at 12 h died before this time. Exposure to TFM substantially altered intermediary metabolism but had little effect on plasma electrolyte balance, haematology, or water balance. Although tissue ATP concentrations were unaffected by TFM, averaging approximately 2.0–2.8 μmol·g^{-1} wet tissue in control and treatment animals (Fig. 1*a*), the concentrations of PCr dropped significantly after 3 h (Fig. 1*b*). At this time, PCr was approximately 25% lower compared with control values of 20 μmol·g^{-1} wet tissue (Fig. 1*b*) and declined further between 6 and 12 h to concentrations that were approximately 60% lower than controls (Fig. 1*b*).

Disturbances to high energy phosphates were accompanied by marked changes in tissue lactate, but not glycogen, concentration, which was variable but not significantly altered by TFM (Figs. 2*a*, 2*b*). Tissue lactate was initially unaffected by TFM exposure, averaging 0.5–1.5 μmol·g^{-1} wet tissue in controls and in animals exposed to TFM for 3 h (Fig. 2*b*). By 6 h, however, there was a 10-fold elevation of tissue lactate, which was sustained through to the 12 h sample period (Fig. 2*b*). Tissue pyruvate concentration, the immediate precursor for lactate arising from the glycolytic pathway, was unaltered by TFM exposure averaging approximately 0.12–0.15 μmol·g^{-1} wet tissue in controls and TFM-treated animals alike (Fig. 2*c*).

The metabolic disturbances observed in the tissues extended to the plasma. Plasma glucose averaged 0.9 mmol·L^{-1} in control larvae and over the first 9 h of TFM exposure was unaltered. At 12 h, however, there was a precipitous decrease in glucose to approximately zero in all five remaining animals (Fig. 3*a*). Plasma lactate did not initially change, but after approximately 6 h of TFM it was fivefold greater than control values, dropped at 9 h, but was again significantly greater after 12 h (Fig. 3*b*).

Fig. 1. Changes in the whole-body concentrations of (*a*) adenosine triphosphate (ATP) and (*b*) phosphocreatine (PCr) in resting larval sea lamprey (*Petromyzon marinus*) following exposure to 3-trifluoromethyl-4-nitrophenol (TFM; hatched bars) at a nominal concentration of 2 mg·L^{-1} for 3, 6, 9, or 12 h. Control animals (open bars) were sampled at time zero, under the same static conditions, in the absence of TFM. Data is expressed as the mean + 1 standard error of the mean ($N = 9$ under control conditions and after 3, 6, and 9 h of TFM exposure; $N = 5$ after 12 h because of TFM-induced mortality in four lamprey). Mean data sharing the same letter are not significantly different ($P < 0.05$).

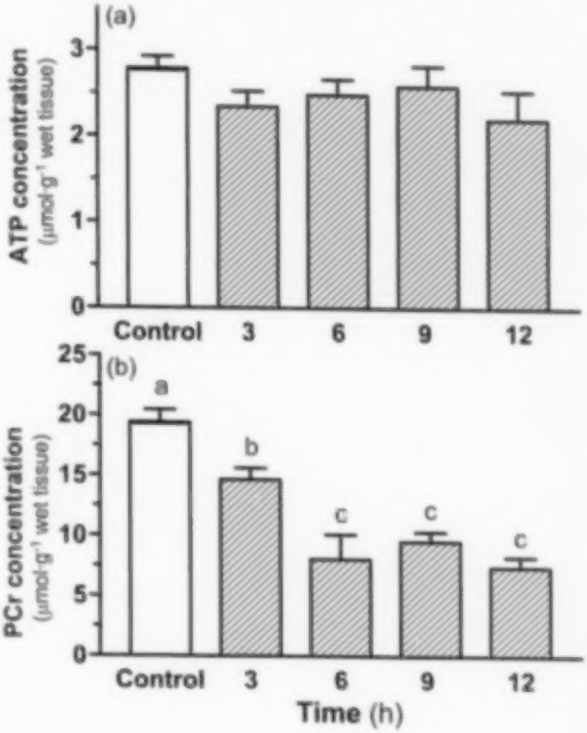

In contrast with intermediary metabolism, gill-mediated processes such as ion exchange, osmoregulation, and nitrogenous waste excretion appeared to be unaffected by TFM. There were no significant differences in plasma Cl$^-$ concentration, which averaged 95 mmol·L^{-1} in control animals and ranged from 91 to 98 mmol·L^{-1} in the TFM-exposed larvae (Fig. 4*a*). Similarly, there were no changes in plasma ammonia, which averaged 0.35–0.40 mmol·L^{-1} in control and treatment animals (Fig. 4*b*). Blood haematocrit averaged 26% in control animals, which was also not significantly different from TFM-treated animals (Table 1). Haemoglobin and MCHC were also unaltered compared with controls (Table 1). The lack of change in red blood cell volume extended to the tissues, where the water content averaged 5.8 mL·g^{-1} dry tissue in control animals and was not significantly different from values measured in TFM-treated larval sea lamprey (Table 1).

Fig. 2. Changes in the whole-body concentrations of (*a*) glycogen, (*b*) lactate, and (*c*) pyruvate in resting larval sea lamprey (*Petromyzon marinus*) following exposure to 3-trifluoromethyl-4-nitrophenol (TFM; hatched bars) at a nominal concentration of 2 mg·L^{-1} for 3, 6, 9, or 12 h. Control animals (open bars) were sampled at time zero, under the same static conditions, in the absence of TFM. Data is expressed as the mean + 1 standard error of the mean (N = 6–9 under control conditions and after 3, 6, and 9 h of TFM exposure; N = 5 for tissue lactate and pyruvate, and N = 2 for tissue glycogen, after 12 h). Mean data sharing the same letter(s) are not significantly different ($P < 0.05$).

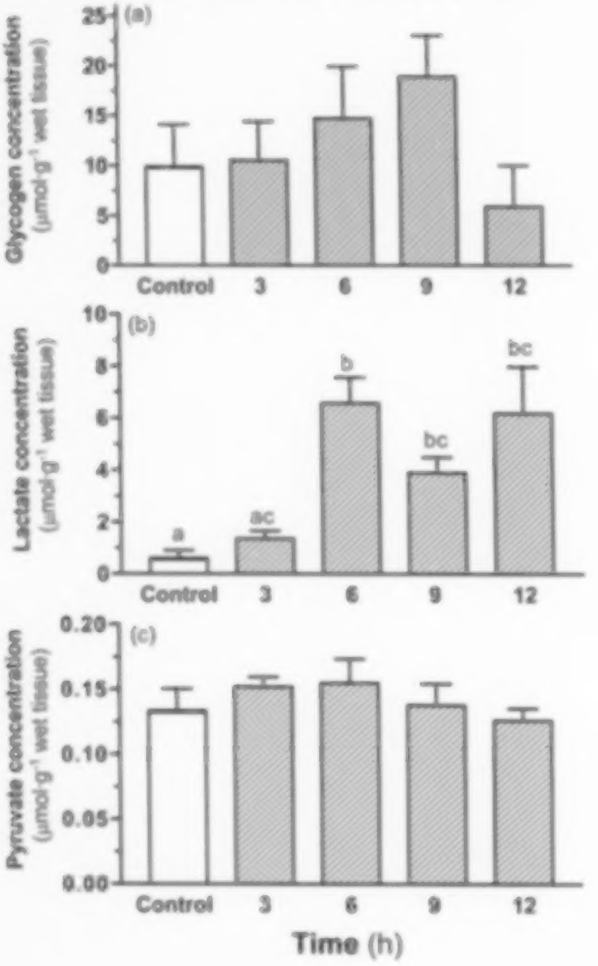

Discussion

Acute toxicity of TFM

The first goal of our experiment was to identify a TFM concentration that caused physiological disturbances similar to those experienced by larval sea lamprey following TFM treatments in the field, but did not cause substantial mortality prior to 12 h. Our bioassay protocol, though not as refined as that used by sea lamprey control agents of the GLFC for TFM treatments, was successful in this regard.

Fig. 3. Changes in the plasma concentrations of (*a*) glucose and (*b*) lactate in resting larval sea lamprey (*Petromyzon marinus*) following exposure to 3-trifluoromethyl-4-nitrophenol (TFM; hatched bars) at a nominal concentration of 2 mg·L^{-1} for 3, 6, 9, or 12 h. Control animals (open bars) were sampled at time zero, under the same static conditions, in the absence of TFM. Data is expressed as the mean + 1 standard error of the mean (N = 7–9 under control conditions and after 3, 6, and 9 h of TFM exposure; N = 5 after 12 h because of TFM-induced mortality in four lamprey). Mean data sharing the same letter are not significantly different ($P < 0.05$).

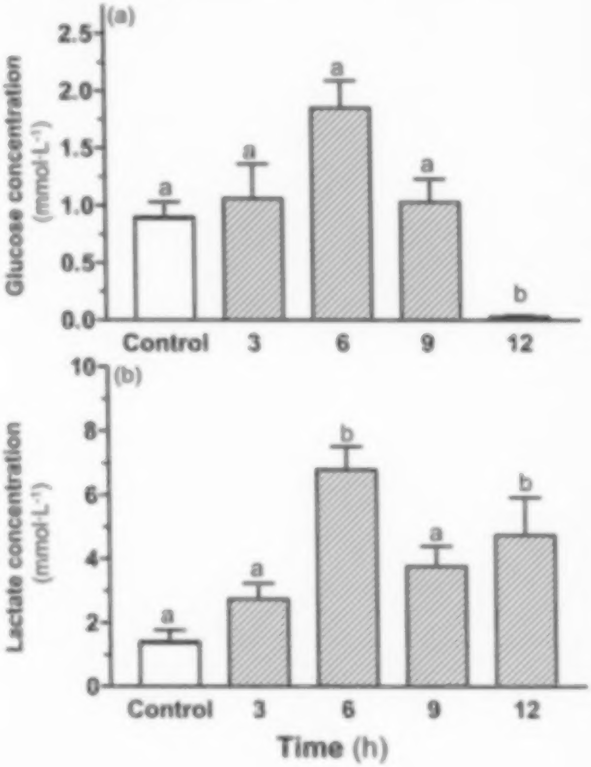

The 12 h LC_{50} of 1.6 mg·L^{-1}, determined for larval lamprey at pH 8.0 and a titration alkalinity of 87 mg $CaCO_3$·L^{-1}, was in good agreement with that reported by Bills et al. (2003) (12 h LC_{50} = 1.23 mg·L^{-1}) in water of similar composition (pH = 8.03, titration alkalinity = 83 mg·L^{-1}) using a flow-through protocol.

It was notable that mortality in the acute toxicity experiment was greater in larval lamprey exposed to nominal TFM concentrations of 2 mg·L^{-1} in sand substrate, compared with those exposed to the same TFM concentration in cotton substrate for the physiological effects study (see below). Differences in actual TFM dose do not explain these observations, nor do differences in water quality (e.g., dissolved oxygen, ionic content, pH), because the animals were exposed to TFM in waters of identical composition and temperature. However, the body masses of larval lamprey exposed to TFM in the acute toxicity study were approximately 30% less than those used in the physiological effects study (1.2 vs. 1.7 g; $P < 0.0005$ (unpaired t test)). As with other fishes,

Fig. 4. Changes in the plasma concentrations of (*a*) chloride and (*b*) ammonia in resting larval sea lamprey (*Petromyzon marinus*) following exposure to 3-trifluoromethyl-4-nitrophenol (TFM; hatched bars) at a nominal concentration of 2 mg·L^{-1} for 3, 6, 9, or 12 h. Control animals (open bars) were sampled at time zero, under the same static conditions, in the absence of TFM. Data is expressed as the mean + 1 standard error of the mean (N = 7–9 under control conditions and after 3, 6, and 9 h of TFM exposure; N = 5 after 12 h because of TFM-induced mortality in four lamprey).

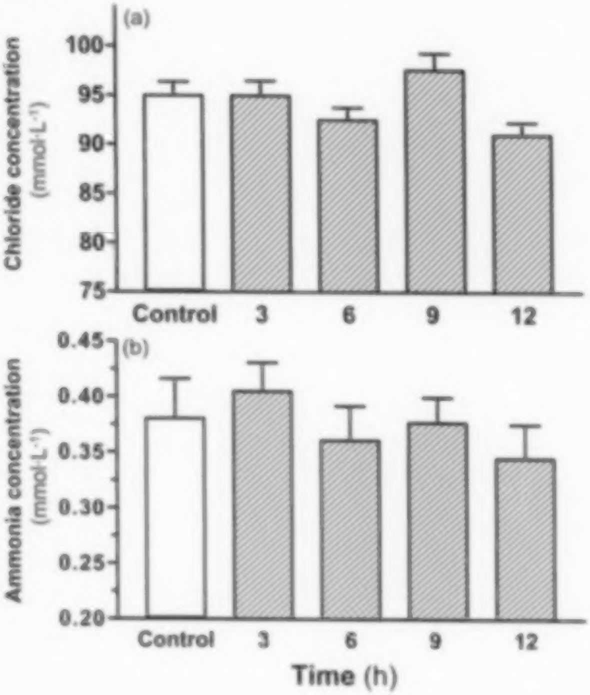

the metabolic rate of larval lamprey inversely scales with body size, in which rates of oxygen consumption are higher in smaller compared with larger animals (e.g., Lewis 1980; Holmes and Lin 1994; Wilkie et al. 2001). Moreover, the relative surface area of the gills is also likely greater in smaller than in larger larval sea lamprey, as described for larvae of the European river lamprey (*Lampetra fluviatilis*; Lewis 1980). Together, greater rates of ventilation and gill surface area could have resulted in higher rates of TFM uptake in the smaller group of larval lamprey, leading to greater toxicity. Despite the possibility of such size-dependent effects, these experiments still permitted us to identify a TFM concentration (2 mg·L^{-1}) to which larval sea lamprey could survive for 9–12 h.

TFM interferes with intermediary metabolism

The analysis of ATP, PCr, glycogen, and lactate represents the respective concentration of each in all tissues and organs of the trunk combined (e.g., liver, kidney, gastrointestinal tract, muscle). However, it is probable that these measures mainly reflected fuel and metabolite concentrations in the muscle, which is approximately 75% of the total body mass of larval lamprey (Bull and Morris 1967).

The present findings are evidence that TFM interferes with oxidative ATP production in larval lamprey. Although tissue ATP concentrations were unaltered in the larval lamprey, it is important to note that as ATP is consumed, it is rapidly replenished by the hydrolysis of PCr via creatine phosphokinase (CPK; Hochachka 1991). Thus, any interference with ATP production would be preceded by decreases in PCr, which was observed from 3 to 12 h of TFM exposure. Under such circumstances, PCr concentrations would have to be almost completely exhausted before declines in ATP were observed (Hochachka 1991). Although PCr concentrations were lower, sufficient amounts of this phosphagen were likely available to ensure that ATP concentrations remained relatively stable in the body. This is also often the case during vigorous exercise in teleost fishes (e.g., Wang et al. 1994*b*) and larval sea lamprey (Wilkie et al. 2001), in which ATP concentrations in the muscle are frequently maintained despite substantial (>50%) reductions in PCr concentration. It is unlikely that observed declines in PCr resulted from greater ATP consumption because no changes in overall activity levels were noted between the TFM-treated versus control larvae, both of which remained embedded in the cotton that was added to the containers as burrowing substrate. This response differs slightly from that in the field, in which lampricide causes emergence of larvae from their burrows (Bills et al. 2003).

The decrease in PCr observed in the present study was greater and much more sustained than that observed in vigorously exercised larval lamprey, in which PCr dropped by 50% but was rapidly replenished within 30 min of post-exercise recovery (Wilkie et al. 2001). In the case of exercised larvae, replenishment of PCr was likely the result of the CPK shuttle, in which ATP generated via oxidative phosphorylation on the inner mitochondrial membrane drives the CPK reaction in the direction of PCr synthesis (Hochachka 1991). Since larval lamprey muscle is a mixture of oxidative muscle fibres (red fibres) and glycolytic muscle fibres (white fibres) (Peters and MacKay 1961; Meyer 1979), there are likely sufficient mitochondria to quickly generate the ATP needed to replenish PCr following vigorous exercise (Wilkie et al. 2001). However, if oxidative phosphorylation were uncoupled by TFM, this means of ATP-mediated PCr regeneration would be short-circuited, resulting in the sustained decreases in the body's PCr reserves we observed during the TFM exposure period. The substantial increases in tissue lactate suggest that complete depletion of PCr was prevented by increased reliance on anaerobic glycolysis, which would provide some of the needed ATP, provided there was sufficient glycogen. Since the tissue analyzed was mainly muscle (~75%; see above), it is likely that glycogen in this compartment was sufficient to prevent complete depletion of muscle PCr. Glycogen concentrations in both control and TFM-exposed larval sea lamprey were approximately 5–10 µmol·g^{-1} wet tissue in the present study and in good agreement with previous measurements (O'Boyle and Beamish 1977; Wilkie et al. 2001).

Given the above scenario, it is not surprising that glycogen stores were not depleted in muscle during TFM exposure, even in moribund animals that were approaching death at 12 h, because muscle generally represents the largest glycogen reserve in teleosts (see Moyes and West 1995; Kieffer

Table 1. Haematocrit, haemoglobin, mean cell haemoglobin concentration (MCHC), and tissue water content in larval sea lamprey (*Petromyzon marinus*) exposed to 3-trifluoromethyl-4-nitrophenol (TFM; 2 $mg \cdot L^{-1}$) for 12 h.

	Control	3 h	6 h	9 h	12 h
Haematocrit (%)	26.4±0.6abc (9)	22.5±0.8ab (9)	30.8±1.7ac (8)	31.4±2.3ac (8)	25.1±3.2abc (5)
Haemoglobin ($g \cdot L^{-1}$)	76±4abc (7)	58±6ab (5)	95±7ac (5)	94±6ac (7)	68±11abc (4)
MCHC ($g \cdot L^{-1}$)	290±16 (7)	255±25 (5)	327±18 (5)	314±23 (7)	269±32 (4)
Tissue H_2O ($mL \cdot g^{-1}$ dry weight)	5.8±0.5 (9)	6.1±0.6 (9)	7.5±1.5 (9)	5.4±0.7 (9)	5.1±0.8 (4)

Note: Mean data sharing the same letters are not significantly different ($P < 0.05$). Numbers in parentheses indicate the number of sea lamprey used.

2000 for reviews) and in larval lamprey (O'Boyle and Beamish 1977). Further, glycogen is generally retained in the muscle as a fuel reserve for burst exercise (Moyes and West 1995; Kieffer 2000). Although not examined directly in the present study, we suggest that glycogen may have been depleted in tissues other than muscle, including the kidney, liver, brain, and associated meninges. Unlike muscle, these tissues possess glucose-6-phosphatase, which converts glucose-6-phosphate to glucose for export to the extracellular fluid (Panserat et al. 2000). These extramuscular tissues therefore play an important role in glucose homeostasis in lamprey (Rovainen 1970; Murat et al. 1979; Hardisty and Baker 1982) and could be particularly sensitive to TFM.

TFM causes profound hypoglycaemia in larval lamprey

The profound hypoglycemia observed following TFM treatment likely extended to the central nervous system (CNS) and ultimately led to death in the larval sea lamprey by depriving the CNS of its main fuel, glucose. A number of studies have demonstrated that the lamprey CNS depends upon glucose, including those of Rovainen (Rovainen 1970; Rovainen et al. 1971), who demonstrated that larval and upstream migrant sea lamprey had very high glycogen reserves and glucose-6-phosphatase activities in the meninges of the brain. Using incubated brain pieces, Foster et al. (1993) demonstrated that the brain of upstream migrant sea lamprey not only oxidized glucose, but that their brains had substantial gluconeogenic and glyconeogenic capabilities. While it is clear that the lamprey CNS depends upon glucose for ATP production, quantification of glucose and glycogen reserves in lamprey brain tissue during TFM exposure is needed to confirm our hypothesis that TFM causes death by starving the CNS of glucose.

Anaerobic glycolysis likely explains the greater lactate in the tissues and plasma of larval lamprey exposed to TFM (see above). By serving as a substrate for both gluconeogenesis and glyconeogenesis, lactate production would have also contributed to the maintenance of glucose–glycogen supply in the earlier stages of TFM exposure, especially in the brain, which preferentially uses lactate for these processes in sea lamprey (Foster et al. 1993). However, both gluconeogenesis and glyconeogenesis are ATP-consuming processes and would eventually shut down, as ATP supply could no longer meet ATP demands. Thus, the precipitous decline in blood glucose at 12 h was likely due to a combination of greater glucose consumption via anaerobic glycolysis, the eventual cessation of gluconeogenesis–glyconeogenesis, and the depletion of readily available glycogen reserves in tissues such as the liver, kidney, and brain. As the large amounts of glycogen in the somatic muscle, which cannot provide extracellular glucose (see above), likely obscured changes in hepatic, renal, and CNS glycogen stores, there is a need to examine the tissue-specific effects of TFM on glycogen stores and glucose homeostasis.

Although TFM has been reported to damage the gills of larval lamprey (Christie and Battle 1963; Mallat et al. 1994), it is less likely that impaired oxygen uptake and (or) delivery to the mitochondria contributed to the observed lactate buildup. If TFM were to impair oxygen uptake, TFM toxicity should be exacerbated in waters that are deficient in oxygen. However, exposure of larval sea lamprey to TFM plus low dissolved oxygen (as low as 30% saturation) has no major effect on toxicity (Seelye and Scholefield 1990). Further, TFM actually stimulates oxygen consumption in lamprey (Schnick 1972), which is more consistent with the hypothesis that TFM uncouples oxidative phosphorylation (Kawatski and McDonald 1974; Kawatski et al. 1974).

TFM has minimal effects on plasma Cl^- balance, haematology, and water content

The absence of any disturbances to plasma Cl^- concentration, haemoglobin, haematocrit, MCHC and tissue water content, and plasma ammonia concentration does not support the hypothesis that TFM has physiologically important effects on gill-mediated ionic or osmotic regulation or on nitrogenous waste excretion in larval lamprey. Exposure of larval sea lamprey to TFM or mixtures of TFM–niclosamide does cause marked histological damage to the gills, especially to the MRCs (Mallat et al. 1985, 1994). Like teleosts, these MRCs, which are also known as ion uptake cells (Mallat et al. 1994), MR platelet cells (Youson and Freeman 1976), and ammocoete MR cells (Bartels and Potter 2004), are probably important for ion uptake in fresh water (Bartels and Potter 2004). Damage to the MRCs caused by TFM included cellular swelling, loss of apical microvilli, mitochondrial swelling, and the appearance of cytoplasmic vacuoles (Mallat et al. 1985, 1994). Based on these observations, Mallat et al. (1994) proposed that an alternate or additional mechanism of TFM toxicity was ionoregulatory failure. While TFM may interfere with ion uptake by the gill, the present findings indicate that such effects would not be of sufficient magnitude over a 10–12 h exposure period to cause measurable changes to internal ion or osmotic homeostasis.

TFM susceptibility, toxicity, and detoxification in larval lamprey versus nontarget fishes

It is likely that TFM impairs ATP production in invertebrate and vertebrate nontarget organisms by the same mechanism (e.g., Kawatski et al. 1974; Viant et al. 2001), but most of these animals are less susceptible to TFM because of their greater ability to detoxify TFM in liver via processes such as glucoronidation (Kawatski and McDonald 1974;

Lech and Statham 1975; Kane et al. 1994). For instance, nontarget fishes such as rainbow trout (*Oncorhynchus mykiss*) and channel catfish (*Ictalurus punctatus*) rapidly clear TFM and TFM–glucoronide (within 24 h) from the muscle when exposed to TFM in the field or the laboratory (Sills and Allen 1975; Vue et al. 2002; Hubert 2005). Larval and parasitic lamprey, on the other hand, have a much lower capacity to convert TFM to TFM–glucoronide compared with these and other nontarget fishes (Lech and Statham 1975; Kane et al. 1994). Of the few studies that have looked at the kinetics of TFM elimination by lamprey, Lech and Statham (1975) reported that larval and parasitic sea lamprey accumulated low concentrations of TFM–glucoronide in the blood and that TFM–glucoronide excretion was undetectable. In other words, biologically active TFM is retained for longer periods in sea lamprey.

If biologically active TFM is retained for longer periods in larval sea lamprey, its impairment of ATP production might persist beyond the period of TFM application. Further studies are therefore needed to determine if disturbances to glucose homeostasis and intermediary metabolism continue following shorter TFM exposure periods. Similar approaches could be used to compare the impact that TFM treatments have on the physiology of nontarget organisms and other life history stages of the lamprey. Such knowledge may make it possible to adjust TFM dosing regimens to reduce TFM exposure times (and consumption) while protecting sensitive nontarget organisms, such as larval lake sturgeon (*Acipenser fulvescens*) and mudpuppies (*Necturus maculosus*; Boogaard et al. 2003). Reductions in the TFM needed to effectively control sea lamprey populations would also be in accord with the goal of further reducing TFM use because of concerns about rising costs, nontarget mortality, and public anxiety about pesticide use (GLFC 2001).

Acknowledgements

We thank Fisheries and Oceans Canada for generously donating the field-grade TFM used in this study. We are also grateful to Dr. Clair Hasenkampf (UTSC) for the use of her plate spectrophotometer and to Dr. Grant McClelland (McMaster University), who provided valuable feedback on earlier versions of this manuscript. The comments and suggestions of two anonymous referees are also appreciated. Research was partially funded by a Natural Sciences and Engineering Research Council of Canada (NSERC) grant to JHY and an NSERC postdoctoral scholarship to MPW.

References

Applegate, V.C. 1950. Natural history of the sea lamprey (*Petromyzon marinus*) in Michigan. U.S. Fish Wildl. Serv. Spec. Sci. Rep. Fish. No. 55.

Applegate, V.C., Johnson, B.G.H., and Smith, M.A. 1966. The relation between molecular structure and biological activity among mono-nitrophenols containing halogens. Gt. Lakes Fish. Comm. Tech. Rep. 11. pp. 1–19.

Bartels, H., and Potter, I.C. 2004. Cellular composition and ultrastructure of the gill epithelium. J. Exp. Biol. **207**: 3447–3462.

Beamish, F.W.H., and Potter, I.C. 1975. The biology of the anadromous sea lamprey (*Petromyzon marinus*) in New Brunswick. J. Zool. **177**: 57–72.

Bergmeyer, H.L. 1983. Methods for enzymatic analysis. Academic Press, New York.

Bills, T.D., Boogard, M.A., Johnson, D.A., Brege, D.C., Scholefield, R.J., Westman, R.W., and Stephens, B.E. 2003. Development of a pH/alkalinity treatment model for applications of the lampricide TFM to streams tributary to the Great Lakes. J. Gt. Lakes Res. **29**(Suppl. 1): 510–520.

Boogaard, M.A. Bills, T.D., and Johnson, D.A. 2003. Acute toxicity of TFM and a TFM/niclosamide mixture to selected species of fish, including the lake sturgeon (*Acipenser fulvescens*) and mudpuppies (*Necturus maculosus*), in laboratory and field studies. J. Gt. Lakes Res. **29**(Suppl. 1): 519–541.

Brege, D.C., Davis, D.M., Genovese, J.H., McAuley, T.C., Stephens, B.E., and Westman, R.W. 2003. Factors responsible for the reduction of the quantity of the lampricide, TFM, applied annually to streams tributary to the Great Lakes from 1979 to 1999. J. Gt. Lakes Res. **29**(Suppl. 1): 500–509.

Bull, J.M., and Morris, R. 1967. Studies on freshwater osmoregulation in the ammocoete larva of *Lampetra planeri* (Bloch). I. Ionic constituents, fluid compartments and water balance. J. Exp. Biol. **47**: 485–494.

Christie, R.M., and Battle, H.I. 1963. Histological effects of 3-trifluoromethyl-4-nitrophenol (TFM) on larval lamprey and trout. Can. J. Zool. **41**: 51–61.

Foster, G.D., Youson, J.H., and Moon, T.W. 1993. Carbohydrate metabolism in the brain of the adult lamprey. J. Exp. Zool. **267**: 27–32.

GLFC. 1992. Strategic vision of the Great Lakes Fishery Commission for the decade of the 1990s. Great Lakes Fishery Commission, Ann Arbor, Mich. Available from www.glfc.org/pubs/viscon/html [accessed 1 June 2006].

GLFC. 2001. Strategic Vision of the Great Lakes Fishery Commission for the First Decade of the New Millenium. Great Lakes Fishery Commission, Ann Arbor, Mich. Available from www.glfc.org/pubs/viscon/html [accessed 1 June 2006].

Hardisty, M.W., and Baker, B.I. 1982. Endocrinology of lampreys. *In* The biology of lampreys. Vol. 4B. *Edited by* M.W. Hardisty and I.C. Potter. Academic Press, New York. pp. 1–115.

Hassid, W.Z., and Abraham, S. 1957. Chemical procedures for analysis of polysaccharides. *In* Methods of enzymology. *Edited by* S.P. Colowick and N.O. Kaplan. Academic Press, New York. pp. 34–37.

Heinrich, J.W., Mullet, K.M., Hansen, M.J., Adams, J.V., Klar, G.T., Johnson, D.A., Christie, G.C., and Young, R.J. 2003. Sea lamprey abundance and management in Lake Superior 1957–1999. J. Gt. Lakes Res. **29**(Suppl. 1): 566–583.

Hochachka, P.W. 1991. Design of energy metabolism. *In* Comparative animal physiology. 4th ed. Environmental and metabolic animal physiology. *Edited by* C. Ladd Prosser. Wiley-Liss, New York. pp. 325–351.

Holmes, J.A., and Lin, P. 1994. Thermal niche of the larval sea lamprey, *Petromyzon marinus*. Can. J. Fish. Aquat. Sci. **51**: 253–262.

Holmes, J.A., and Youson, J.H. 1994. Fall condition factor and temperature influence the incidence of metamorphosis in sea lampreys, *Petromyzon marinus*. Can. J. Zool. **72**: 1134–1140.

Howell, J.H., Lech, J.J., and Allen, J.L. 1980. Development of sea lamprey larvicides. Can. J. Fish. Aquat. Sci. **37**: 2103–2107.

Hubert, T.D. 2005. Residues of the lampricides 3-trifluoromethyl-4-nitrophenol and niclosamide in muscle tissue of rainbow trout. J. Agric. Food Chem. **53**: 5342–5346.

Kane, A.S., Kahng, M.W., and Reimschuessel, R. 1994. UDP-glucoronyltransferase kinetics for 3-trifluoromethyl-4-nitrophenol (TFM) in fish. Trans. Am. Fish. Soc. **123**: 217–222.

Kawatski, J.A., and McDonald, J. 1974. Effect of 3-trifluoromethyl-4-nitrophenol on *in vitro* tissue respiration of four species of fish with preliminary notes on *in vitro* biotransformation. Comp. Gen. Pharmacol. **5**: 67–76.

Kawatski, J.A., Dawson, V.K., and Ruevers, M.L. 1974. Effect of TFM and Bayer 73 on *in vivo* oxygen consumption of the aquatic midge *Chironomus tentans*. Trans. Am. Fish. Soc. **3**: 551–556.

Kieffer, J.D. 2000. Limits to exhaustive exercise in fish. Comp. Biochem. Physiol. A, **126**: 161–179.

Lech, J.J., and Statham, C. 1975. Role of glucoronide formation in the selective toxicity of 3-trifluoromethyl-4-nitrophenol (TFM) for the sea lamprey: comparative aspects of TFM uptake and conjugation in sea lamprey and rainbow trout. Toxicol. Appl. Pharmacol. **31**: 150–158.

Lewis, S.V. 1980. Respiration of lampreys. Can. J. Fish. Aquat. Sci. **37**: 1711–1722.

Mallatt, J., Ridgeway, R.L., and Paulsen, C. 1985. Ultrastructural effects of 3-trifluoromethyl-4-nitrophenol on gills of the larval lamprey (*Petromyzon marinus*). Can. J. Zool. **63**: 155–164.

Mallatt, J., McCall, R.D., Bailey, J.F., and Seelye, J. 1994. Effects of lampricides on the gill ultrastructure of larval sea lampreys and rainbow trout fry. Can. J. Zool. **72**: 1653–1664.

Meyer, W. 1979. Oxidative enzymes and myosin-ATPase in the trunk musculature of the river lamprey (*Lampetra fluviatilis*). Histochem. J. **11**: 187–195

Morse, T.J., Ebener, M.P., Koon, E.M., Morkwert, S.B., Johnson, D.A., Cuddy, D.W., Weisser, J.W., Mullet, K.M., and Genovese, J.H. 2003. A case history of sea lamprey control in Lake Huron: 1979–1999. J. Gt. Lakes Res. **29**(Suppl. 1): 599–614.

Moyes, C.D., and West, T.G. 1995. Exercise metabolism in fish. *In* Biochemistry and molecular biology of fishes. Vol. 4. *Edited by* P.W. Hochachka and T.P. Mommsen. Elsevier, New York. pp. 367–392.

Murat, A., Plisetskaya, E.M., and Soltitskaya, L.P. 1979. Glucose-6-phosphatase activity in kidney of the river lamprey (*Lampetra fluviatilis* L.). Gen. Comp. Endocrinol. **39**: 115–117.

Niblett, P.D., and Ballantyne, J.S. 1976. Uncoupling of oxidative phosphorylation in rat liver mitochondria by the lamprey larvicide TFM (3-trifluoromethyl-4-nitrophenol). Pest. Biochem. Physiol. **6**: 363–366.

O'Boyle, R.N., and Beamish, F.W.H. 1977. Growth and intermediary metabolism of larval and metamorphosing stages of the landlocked sea lamprey, *Petromyzon marinus* L. Environ. Biol. Fishes, **2**: 103–120.

Panserat, S., Médale, F., Brèque, J., Plagnes-Juan, E., and Kaushik, S. 2000. Lack of significant long-term effect of dietary carbohydrates on hepatic glucose-6-phosphate expression in rainbow trout (*Oncorhynchus mykiss*). J. Nutr. Biochem. **11**: 22–29.

Peters, A., and Mackay, B. 1961. The structure and innervation of the myotomes of the lamprey. J. Anat. **95**: 575–585.

Rovainen, C.M. 1970. Glucose production by lamprey meninges. Science (Washington, D.C.), **167**: 889–890.

Rovainen, C.M., and Scheiber, M.H. 1975. Ventilation of larval lampreys. J. Comp. Physiol. **104**: 185–203.

Rovainen, C.M., Lemcoe, G.E., and Peterson, A. 1971. Structure and chemistry of glucose-producing cells in meningeal tissue of the lamprey. Brain Res. **30**: 99–118.

Schnick, R.A. 1972. A review of the literature on TFM (3-trifluoromethyl-4-nitrophenol) as a lamprey larvicide. Investigations in Fish Control 44. United States Department of the Interior, Fish and Wildlife Service, Washington, D.C.

Seelye, J.G., and Scholefield, R.J. 1990. Effects of changes in dissolved oxygen on the toxicity of 3-trifluoromethyl-4-nitrophenol (TFM) to sea lamprey and rainbow trout. Gt. Lakes Fish. Comm. Tech. Rep. 56.

Sills, J.B., and Allen, J.L. 1975. Accumulation and loss of residues of 3-trifluoromethyl-4-nitrophenol (TFM) in fish muscle tissue: laboratory studies. Investigations in Fish Control No. 65. United States Department of the Interior, Fish and Wildlife Service, Washington, D.C.

Smith, B.R., and Tibbles, J.J. 1980. Sea lamprey (*Petromyzon marinus*) in Lakes Huron, Michigan, and Superior: history of invasion and control, 1936–1978. Can. J. Fish. Aquat. Sci. **37**: 1780–1801.

Sprague, J.B. 1969. Measurement of pollutant toxicity to fish. I. Methods for acute toxicity. Water Res. **3**: 793–821.

Viant, M.R., Walton, J.H., and Tjeerdema, R.S. 2001. Comparative sub-lethal actions of 3-trifluoromethyl-4-nitrophenol in marine molluscs as measured by *in vivo* ^{31}P NMR. Pest. Biochem. Physiol. **71**: 40–47.

Vue, C., Bernardy, J.A., Hubert, T.D., Gingerich, W.H., and Stehly, G.R. 2002. Relatively rapid loss of lampricide residues from fillet tissue of fish after routine treatment. J. Agric. Food Chem. **50**: 6786–6789.

Wang, Y., Wilkie, M.P., Heigenhauser, G.J.F., and Wood, C.M. 1994*a*. The analysis of metabolites in rainbow trout white muscle: a comparison of different sampling and processing methods. J. Fish Biol. **45**: 855–873.

Wang, Y., Heigenhauser, G.J.F., and Wood, C.M. 1994*b*. Integrated responses to exhaustive exercise and recovery in rainbow trout white muscle: acid–base, phosphagen, carbohydrate, lipid, ammonia, fluid and electrolyte metabolism. J. Exp. Biol. **195**: 227–258.

Wilkie, M.P., Brobbel, C.M., Forsyth, L., Davidson, K., and Tufts, B.L. 1997. The influence of temperature on the postexercise physiology and survival of Atlantic salmon (*Salmo salar*). Can. J. Fish. Aquat. Sci. **54**: 503–511.

Wilkie, M.P., Bradshaw, P.G., Joanis, V., Claude, J.F., and Swindell, S.L. 2001. Rapid metabolic recovery following vigorous exercise in burrow-dwelling larval sea lampreys (*Petromyzon marinus*). Physiol. Biochem. Zool. **74**: 261–272.

Wilkie, M.P., Claude, J.F., Cockshutt, A., Holmes, J.A., Wang, Y.S., Youson, J.H., and Walsh, P.J. 2006. Shifting patterns of nitrogenous waste excretion and amino acid catabolism capacity during the life cycle of the sea lamprey (*Petromyzon marinus*). Physiol. Biochem. Zool. **79**: 885–898.

Youson, J.H. 2003. The biology of metamorphosis in sea lampreys: endocrine, environmental and physiological cues and events, and their potential application to lamprey control. J. Gt. Lakes Res. **29**(Suppl. 1): 26–49.

Youson, J.H., and Freeman, P.A. 1976. Morphology of the gills of larval and parasitic adult sea lamprey, *Petromyzon marinus* L. J. Morphol. **149**: 73–104.

Zall, D.M., Fisher, M.D., and Garner, Q.M. 1956. Photometric determination of chlorides in water. Analyt. Chem. **28**: 1665–1678.

Effects of marine conditions, fishing, and smolt traits on the survival of tagged, hatchery-reared sea trout (*Salmo trutta trutta*) in the Baltic Sea

Irma Kallio-Nyberg, Irma Saloniemi, Eero Jutila, and Ari Saura

Abstract: The marine survival of tagged sea trout (*Salmo trutta trutta*) smolt groups ($n = 236$) stocked from 1970 to 2001 in the Baltic Sea was analysed using a linear mixed model. The response variable, survival rate, was associated with smolt size, release date, sea surface temperature in May, and prey fish abundance, and interactions among these factors. The effect of smolt size was in interaction with Baltic herring (*Clupea harengus membras*) abundance; smolt size had an optimum of about 22 cm in years when herring were abundant, but when herring were less abundant, the survival of larger smolts was higher. Early stocking in warm springs or late stocking in cold springs gave the best survival rates for trout. Changes in return activity or fishing methods have made tag returns a less reliable way of estimating survival during the last 30 years. The actual return rate of undersized fish (<40 cm) compared with their estimated proportion among captured fish decreased over time, which suggests that the survival rate for the later years was probably underestimated. It is likely that we were unable to include all the relevant explanatory variables in the model, as year effects remained significant, suggesting unknown annual variation affecting survival.

Résumé : Nous avons analysé à l'aide d'un modèle de mélange linéaire la survie en mer de groupes ($n = 236$) de saumoneaux de truites de mer (*Salmo trutta trutta*) marqués et ensemencés dans la Baltique de 1970 à 2001. La variable dépendante, le taux de survie, est associée à la taille des saumoneaux, la date de libération, la température de surface de la mer en mai et l'abondance des poissons proies, ainsi qu'aux interactions entre ces facteurs. L'effet de la taille des saumoneaux est en interaction avec l'abondance des harengs de la Baltique (*Clupea harengus membras*); l'optimum de taille des saumoneaux est d'environ 22 cm lors des années de forte abondance des harengs; lors des années d'abondance moindre des harengs, la survie des saumoneaux plus grands est supérieure. Les empoissonnements hâtifs des printemps chauds et les empoissonnements tardifs des printemps froids donnent les meilleurs taux de survie chez la truite. Des changements dans les activités de retour et dans les méthodes de pêche au cours des 30 dernières années font que l'analyse des retours d'étiquettes est devenue une méthode moins fiable pour estimer la survie. Le taux de retour réel des poissons de taille inférieure au seuil (<40 cm) comparé à leur proportion estimée parmi les poissons capturés décline en fonction du temps, ce qui laisse croire que les taux de survie aux âges plus avancés sont probablement sous-estimés. Comme les effets des années demeurent significatifs, il est probable que nous ayons été incapables d'inclure toutes les variables explicatives pertinentes dans le modèle; il y aurait peut-être une variation annuelle inconnue qui affecte la survie.

[Traduit par la Rédaction]

Introduction

Sea trout (*Salmo trutta trutta*) are common fish in the streams flowing into the Baltic Sea. Mainly owing to human impact (dams that prevent spawning migration, overexploitation, pollution), the wild populations of sea trout have drastically declined since the 1960s (Jutila et al. 2006). To compensate for the lost natural production, artificial production is largely used, and now about 90% of sea trout smolts entering the Baltic Sea are produced in hatcheries (ICES 2005*a*). Annual extensive sea trout stocking in the Baltic Sea started in the 1960s. In the northern parts of the Baltic Sea, the recapture rate generally varied between 5% and 15% in the 1980s and early 1990s (ICES 2005*a*), but since then the recapture rates both of sea trout (Jutila et al. 2006) and Atlantic salmon (*Salmo salar*) (Kallio-Nyberg et al. 2004) have declined to 1%–5%. The reasons for the low recapture rate of sea trout are unknown.

There are indications that the smolts of salmonid fishes suffer high mortality at the beginning of their sea life (Salminen et al. 1995; Hansen and Quinn 1998; Dieperink et al. 2002). Large annual and long-term changes in survival are also typical for salmonids (Friedland et al. 1993, 1998; Jonsson and Jonsson 2004). The annual fluctuations in the

Received 22 May 2006. Accepted 18 April 2007. Published on the NRC Research Press Web site at cjfas.nrc.ca on 28 August 2007.
J19327

I. Kallio-Nyberg.[1] Finnish Game and Fisheries Research Institute, Quark Fisheries Research Station, Korsholmanpuistikko 16, FIN-65100 Vaasa, Finland.
I. Saloniemi. University of Turku, Department of Biology, Laboratory of Genetics, FIN-20014 Turku, Finland.
E. Jutila and A. Saura. Finnish Game and Fisheries Research Institute, P.O. Box 2, FIN-00791 Helsinki, Finland.

[1] Corresponding author (e-mail: irma.kallio-nyberg@rktl.fi).

Can. J. Fish. Aquat. Sci. **64**: 1183–1198 (2007) doi:10.1139/F07-084

survival of salmonids appear to be influenced by climatic factors, such as the sea surface temperature (SST) and the North Atlantic Oscillation (NAO) (Friedland et al. 1998, 2000, 2003), or by biotic factors such as prey fish abundance (Salminen et al. 1995; Kallio-Nyberg et al. 2004). Human-controlled factors such as the size, quality, and breeding history of hatchery-reared fish or the date and site of smolt release may also explain the success of fish in the wild (Berg and Berg 1987; McKinnell and Lundqvist 2000; Saloniemi et al. 2004). Atlantic salmon smolt survival is affected by a limited period of readiness (a physiological "smolt window") and the timing of seawater entry in relation to environmental conditions such as temperature, food, and predators (an ecological "smolt window") (McCormick et al. 1998). The survival estimate may also depend on the distribution of fishing and on the return rate of tags if the estimate is based on tag recapture data.

The simultaneous fluctuations in the tag recapture rate among different Atlantic salmon stocks in the Baltic Sea (McKinnell and Karlström 1999) suggest that common marine factors affect their recapture rate in the critical postsmolt phase. The decrease in salinity in the Baltic Sea during last 30 years appears to have affected the zooplankton community structure (Rönkkönen et al. 2004), which has further affected the diet composition of planktivorous fish species such as the Baltic herring (*Clupea harengus membras*) and European sprat (*Sprattus sprattus sprattus*) (Möllmann et al. 2004). Salmonids are, for at least part of their life, at the top of the food chain, mainly feeding on herring and sprat in the Baltic Sea (Haluch and Skóra 1997; Karlsson et al. 1999). The growth rate and survival of Atantic salmon postsmolts correlate positively with herring abundance in the Baltic Sea (Salminen et al. 1995).

This study analysed whether the observed environmental conditions in the marine environment in the postsmolt year (SST, NAO index, salinity, herring and sprat abundance), water temperature at the release site, the release date, and fishing variables are linked with the variability in the recapture rate of Isojoki sea trout. The studied Isojoki sea trout may be subjected to these marine factors because they undergo their feeding migration both in coastal waters and offshore (Kallio-Nyberg et al. 2002). The sea trout groups stocked in the Gulf of Finland (GF) and in the southern Bothnian Sea (BS) in 1970–2001 were included.

The proportion of recaptured fish in each group was assumed to be related to survival, assuming that the exploitation rate has been constant and fishing has been nonselective with respect to the size of released fish. The fish may, however, also recruit to the fishery in relation to their smolt size, which may increase the return rate of the fish with a large smolt size. Mortalities among the trout after the postsmolt phase were mostly caused by fishing (Jutila et al. 2006). The fishing pressure on young sea trout was so high in the study period that nearly all fish were caught before their first spawning migration, and in practice no fish survive their whole natural life cycle of 6–8 years with several spawning migrations (Jutila et al. 2006). If changes in postsmolt mortality before fishing mortality are mainly due to natural mortality (predation, starving) during the postsmolt phase, the recapture rate of captured fish may indicate the postsmolt mortality. The fishing of sea trout and the temporal and spatial distribution of recaptures were analyzed by using tag recoveries from experiments carried out in 1980–2001.

Because it is likely that the return activity of recaptured tagged fish may to some extent affect the return rate, factors related to annual fishing, such as the proportion of undersized fish returned and the estimated proportion of small fish in the recruiting population, were included in the data and models. It is also important to examine whether the decrease in recapture rate is due to an increase in natural mortality or a decrease in return activity.

Material and methods

Study area and tagged sea trout groups

The sea trout stock used in the stocking experiment originated from the Isojoki River, which discharges into the southern Gulf of Bothnia (62°30′N, 21°25′E) (Fig. 1). In nature, sea trout live 3–5 years in a stream before smoltification and sea migration. Typical behaviour for sea trout is to visit the home site annually in autumn, although they have no intention to spawn. Sea trout usually spawn for the first time after three sea years (Haikonen et al. 2002). The experimental groups were established from the offspring of spawners from Isojoki brood stocks kept at different hatcheries in central and southern Finland. Trout were raised for 2 or 3 years, and variation in rearing conditions among the hatcheries was possible. The older smolts were longer than the 2-year-old smolts in the groups released in 1989–2000 in the GF (2-year-olds: mean ± standard deviation (SD), 23.3 ± 1.5 cm, $n = 93$; 3-year-olds: 28.6 ± 4.0 cm, $n = 10$; t test: $P < 0.01$). One to six months before release, fish were individually marked with external Carlin tags under MS-222 (tricaine methanesulfonate) anaesthesia. During tagging, the total length (mm) of each fish and the weight (g) of 100 randomly selected fish per group were recorded. Tagged groups were released in April, May, or June as smolts.

The groups used in survival analysis ($n = 236$) were released into the different estuaries and coastal waters of two sub-basins of the Baltic Sea: the GF and the BS (Table 1) (Fig. 1). The average number of fish released in each group was 770 individuals (±331 SD) (minimum 199, maximum 2000 fish per group). The migration and fishing of sea trout were studied from individual recapture data. The smolts (BS: 79 groups, 68 722 tagged smolts; GF: 125 groups, 90 074 tagged smolts) were released in 1980–2001. The groups were nearly the same as used in the survival study of the same period. The smolt length of recaptured and nonrecaptured fish was compared with sea trout released ($n = 18\,241$) in 1988–2001 into the GF. The fishermen along the migration routes of the sea trout in the Baltic Sea area returned tags from captured fish, and the tagging office of the Finnish Game and Fisheries Research Institute compiled data from these tags.

Statistical analyses

Our aim was to identify factors that would explain the changes in tag return and trout survival between 1970 and 2001 in the main bays (BS and GF) of the Baltic Sea. The differences in median recapture rate for groups released at different times were analyzed by using the Kruskal–Wallis test of the NPAR1WAY procedure (SAS Institute, Inc. 2001).

Fig. 1. Map of Baltic Sea showing sub-basins (Baltic Proper (= Main Basin), Gulf of Finland, Gulf of Bothnia, and some smaller sub-basins) and the location of estuaries of Kokemäenjoki (river basin 35), Karvianjoki (36), Isojoki (37), and Kyrönjoki (42) rivers flowing into the Bothnian Sea and the location of Kymijoki (14), Mustijoki (19), Vantaanjoki (21), and Fiskarsinjoki (23) rivers flowing into the Gulf of Finland. The sea trout (*Salmo trutta trutta*) groups were released into the estuaries of these rivers or coastal waters. The locations of the Valassaaret (V), Seili (S), and Tvärminne (T) stations are also shown.

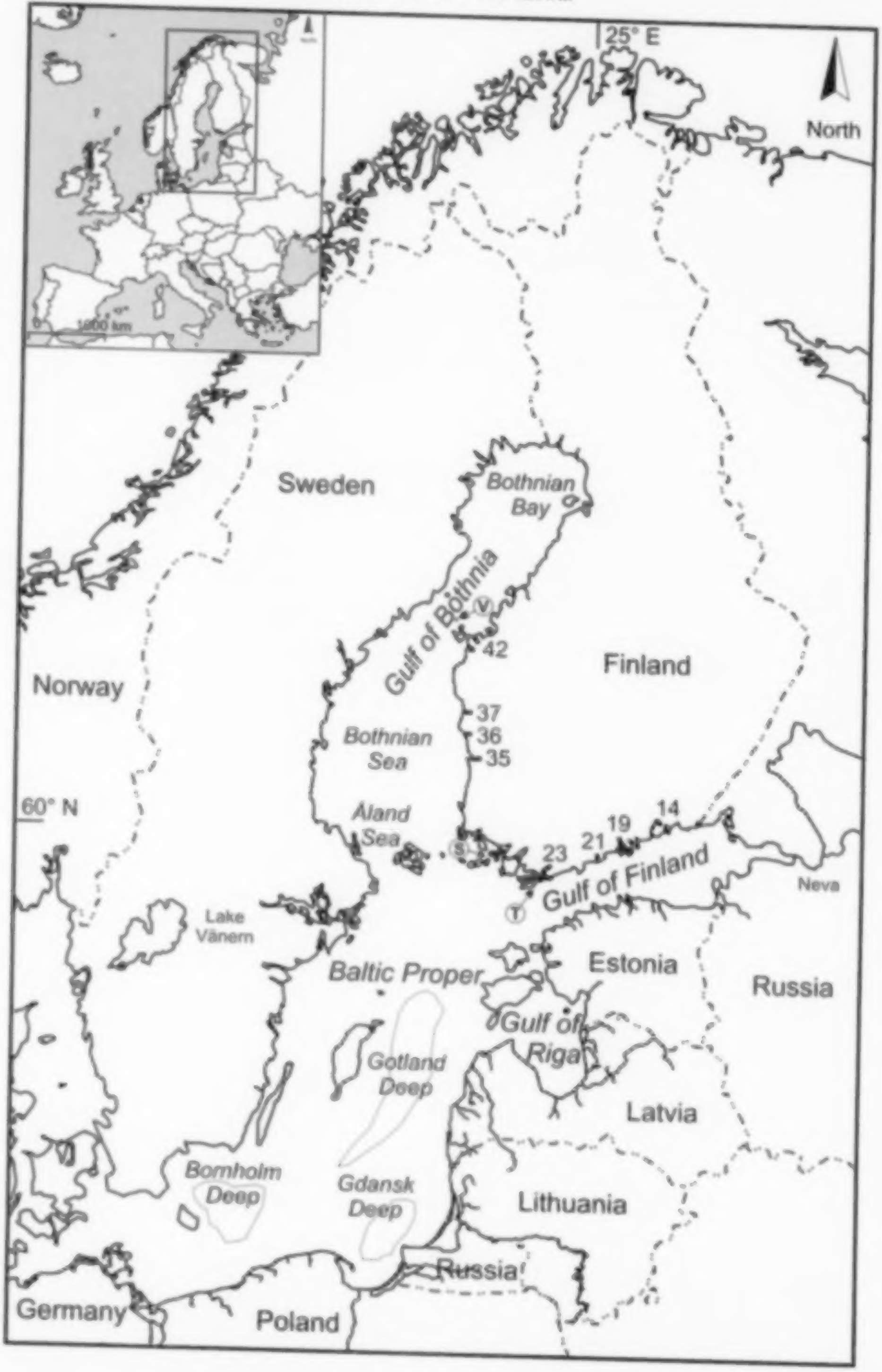
1000 km
25° E
North
Sweden
Bothnian Bay
Gulf of Bothnia
V
42
Finland
Norway
37
36
35
Bothnian Sea
60° N
Åland Sea
S
14
19
21
23
Gulf of Finland
Neva
T
Lake Vänern
Baltic Proper
Estonia
Russia
Gulf of Riga
Gotland Deep
Latvia
Bornholm Deep
Gdansk Deep
Lithuania
Russia
Germany
Poland

Table 1. The recapture rate (%) and mean smolt size (cm) of sea trout (*Salmo trutta trutta*) groups released in the Bothnian Sea (BS) and in the Gulf of Bothnia (GF) from 1970 to 2001.

Sea	Groups	Recapture rate			Groups	Mean smolt length		
	n	Mean±SD	Min.	Max.	n	Mean±SD	Min.	Max.
BS	86	8.9±6.2	1.1	25.4	81	22.4±2.2	18.6	27.7
GF	150	8.6±5.1	0.4	24.6	149	22.7±2.9	16.3	34.6

Note: The means indicate variability among groups.

The effects of single predictors such as smolt size or annual gill proportion on tag return rates were analyzed by using the REG procedure (SAS Institute, Inc. 2001).

As the study the combines effects of several predictors, the proportions in each tagging group (Fig. 2*a*) were normalized using arcsine transformation in the models. Data analysis was performed with the SAS statistical package by using the MIXED procedure (SAS Institute, Inc. 2001) with the repeated option for release groups of the same year. To account for dependences between years, we allowed tag recaptures to depend on each other via the autoregressive option type = AR(1). With this option, correlations between successive years decreased with time (1 year, σ; 2 years, σ^2; 3 years, σ^3; etc.). The AR(1) error structure model was chosen after a comparison with likelihood ratios.

The survival of the groups released in the 1970s and later (1980–2001) was analysed separately because of their different nature and the lack of some explanatory variables (prey fish abundance and fishing variables) in the 1970s. In total, 25 groups (1970s) and 192 groups (1980–2001) with a mean smolt size under 300 mm were used in the survival analysis.

Normality of the length distributions of recaptured fish was tested using the Kolmogorov–Smirnov test (univariate procedure of SAS). The aim was to examine the lower tail of the distribution, representing undersized fish whose tag may not be returned. The nontransformed size distributions were used in later analyses of the proportions of undersized fish despite certain groups showing some deviations from the theoretical normal distribution (Table 2). The length of each the group was standardized (z = (400 mean length)/SD) and compared with the theoretical normalized distribution to obtain the proportion of undersized fish. The minimum legal size for trout is 40 cm. For example, if $z = 1.12$, the proportion of undersized fish is 0.5 + 0.3686, or 86.86%. If $z = -1.12$, the proportion is 100 – 86.86 = 13.14%. The trend in the proportion of undersized returned trout was explained by the estimated proportion of undersized fish using linear regression (REG procedure of SAS).

The survival of tagged fish released in the GF during 1988–2001 was analyzed in more detail by comparing the effects of fishing on different size classes. We applied the SAS Genmod procedure to the data for individual fish by assuming the tag returns to show a binary distribution, as used by Saloniemi et al. (2004). Only the year, smolt length, and their interaction were used as predictors in this model.

Smolt background and climatic and oceanographic explanatory variables

The explanatory variables used were the mean smolt length (total) of the tagged group (Fig. 2*b*), release site (GF, BS), monthly SST in May and June, release date, water temperature on release, NAO index, salinity (Fig. 3*a*), the condition factor of the group, and prey fish abundance (Fig. 3*b*). The condition factor (K) for each group was calculated by $K = W/(L/10)^3 \times 100$, where W is the mean weight of the group (g), and L is the mean total length of the group (mm). We did not have the smolt age for the groups, but in most cases 2-year-old smolts were used.

The monthly SST used as an explanatory variable was measured at a depth of 1 m by the Finnish Institute of Marine Research at two field stations in Seili and Valassaaret in the BS and one station in Tvärminne in the GF (Fig. 1). Because the annual fluctuations in monthly SST between the GF and BS were positively correlated in May and June (Spearman correlation; May: $r = 0.73$, $P < 0.001$, $n = 25$; June: $r = 0.42$, $P < 0.05$, $n = 31$), one mean SST for May and one mean SST for June measured in these two sea areas were used in the analyses (Fig. 3*a*). The release date was a running number from the beginning of the year. The water temperature at the release site was available for 100 groups.

The seasonal NAO index in April to June was included as a factor to explain the survival of sea trout (Fig. 3*a*). A positive seasonal NAO in spring means that westerly winds and a mild marine climate are dominant, while a negative seasonal NAO index indicates that a continental climate dominates in Europe (Hurrell 1995).

The salinity of the water in June and in July was used as an explanatory variable (Fig. 3*a*). Values were measured by the Finnish Institute of Marine Research at two field stations in Seili and Tvärminne (Fig. 1). One mean of three values per month (April to August) was used.

The abundance of 0+ herring or sprat at the end of the year in the Baltic Main Basin and BS was included as an explanatory variable (Fig. 3*b*) (ICES 2005*b*). The herring and sprat abundance estimates were $\log_{10}$-transformed for analysis because of their high annual variation.

The climatic and oceanographic explanatory variables during the postsmolt period were selected, because natural mortality due to environmental factors was assumed to be highest soon after release during the first sea summer. The monthly SST used as explanatory variable included the release months. The seasonal NAO index in April–June also indicated conditions in the spring of release. The salinity values were measured in the spring and summer of the release year. 0+ herring and 0+ sprat are suitable prey fish based on their prevalence and adequate size for sea trout postsmolts when they switch from invertebrates to a fish diet in their first summer in the sea (Salminen et al. 2001).

Fishing variables and recovery data

The fishing variables taken into account for survival analysis were the proportion of undersized fish among the tag re-

Fig. 2. The mean annual recapture rate (*a*) and mean annual smolt length (total) (*b*) for sea trout (*Salmo trutta trutta*) groups released in the Gulf of Finland (GF) (squares) and in the Bothnian Sea (BS) (triangles). Linear regressions are as follows: Isojoki GF: recapture rate = 441.22 – 0.2176 × year, $F_{[1,27]} = 15.1$, $P < 0.001$, $r^2 = 0.36$; Isojoki BS: recapture rate = 178.61 – 0.0857 × year, $F_{[1,22]} = 0.4$, $P = 0.502$, $r^2 = 0.02$; Isojoki GF: mean size = –3348.3 + 1.795 × year, $F_{[1,24]} = 38.5$, $P < 0.001$, $r^2 = 0.64$; Isojoki BS: mean size = –3988.6 + 2.115 × year, $F_{[1,20]} = 40.8$, $P < 0.001$, $r^2 = 0.67$.

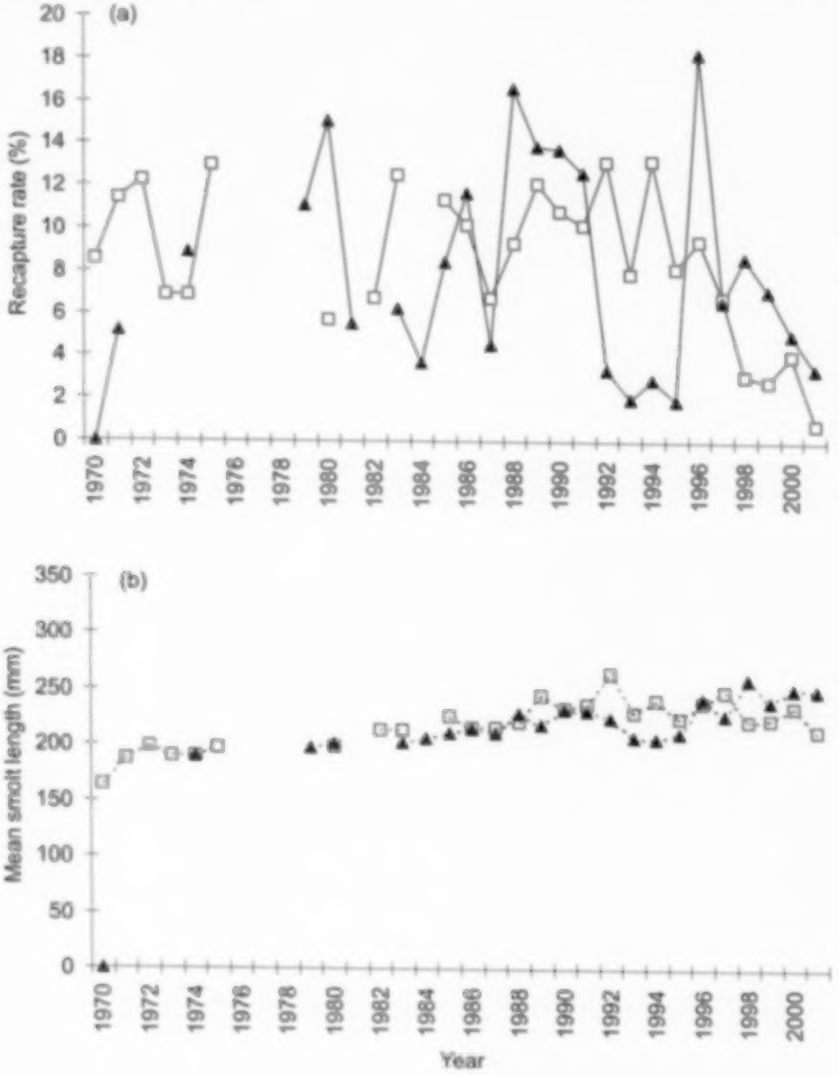

captures (Figs. 4*a* and 4*b*), the proportion of undersized fish estimated from the size distribution (Figs. 4*a* and 4*b*), and the proportion of the catch taken by bottom gill nets (Fig. 4*c*).

Because the fishing and reporting activity of tags may influence the recapture rate and the survival estimate, annual factors from fishing both in the GF and in the BS were included. Released sea trout recruited to the fishery at an average 3–5 months after release (i.e., in September or October) (Table 3). The sea trout recaptured in the first sea year were on average 8–16 cm longer than smolts at tagging. The recaptured fish were larger (mean length ± SD: 24.1 ± 3.8 cm, $n = 1404$) than nonrecaptured fish (22.7 ± 3.2 cm, $n = 16\,837$) (t test: $P < 0.001$; groups released in 1988–2001 in the GF).

The majority of sea trout were recaptured in the area where they were released (Table 4) and before their third sea year (Fig. 5*a*). The sea trout were mainly captured by gill nets (Fig. 5*b*). The relative proportion of the bottom gill net catch increased, while the proportion of the trap catch decreased in the GF from 1980 to 2001 (Fig. 5*b*).

The mean annual length of the captured sea trout decreased during the period 1980–2001 (linear regression, GF: annual mean length = 9963.00 – 4.75 × year, $F_{[1,20]} = 6.91$, $P < 0.05$, $r^2 = 0.26$; BS: annual mean length = 4802.90 – 2.19 × year, $F_{[1,20]} = 6.39$, $P < 0.05$, $r^2 = 0.24$) (Table 2) be-

Table 2. The catch length of sea trout (*Salmo trutta trutta*) released in 1980–2001 in the Gulf of Finland and Bothnian Sea.

Year	Gulf of Finland					Bothnian Sea				
	n	Mean±SD (cm)	Md (cm)	Skew	*P*	*n*	Mean±SD (cm)	Md (cm)	Skew	*P*
1980	81	54±14	55	0.306	0.125	241	45±13	44	0.097	<0.010
1981	12	43±21	39	–0.447	>0.150	153	47±13	47	0.372	0.011
1982	23	60±12	61	–0.344	0.016	19	44±10	44	0.177	>0.150
1983	83	57±16	61	–0.953	<0.010	47	48±14	51	–0.217	0.049
1984	6	44±14	44	–0.529	0.064	53	45±18	48	0.121	0.013
1985	119	61±14	62	–0.687	<0.010	294	49±12	50	–0.193	<0.010
1986	114	58±14	59	–0.256	>0.150	123	49±11	48	0.521	<0.010
1987	117	60±14	60	–0.411	0.087	113	42±12	42	0.186	>0.150
1988	561	57±14	60	–0.435	<0.010	496	50±12	48	–0.042	<0.010
1989	808	55±11	55	0.102	<0.010	608	48±12	45	0.320	<0.010
1990	643	52±11	50	0.432	<0.010	451	44±10	43	0.688	<0.010
1991	670	53±12	52	–0.057	<0.010	368	45±12	44	0.529	<0.010
1992	546	52±10	51	–0.241	<0.010	60	46±15	45	0.043	>0.150
1993	475	44±11	46	0.111	<0.010	46	40±11	40	–0.024	>0.150
1994	383	49±12	48	–0.089	<0.010	62	39±11	40	0.197	0.055
1995	362	51±12	50	0.477	<0.010	18	46±9	45	0.841	>0.150
1996	579	48±10	45	0.205	<0.010	227	41±11	42	0.181	<0.010
1997	278	49±8	48	0.419	<0.010	263	44±12	42	0.340	<0.010
1998	106	50±11	48	0.961	<0.010	176	45±12	45	0.554	>0.150
1999	71	49±10	47	–0.045	0.1211	136	43±13	45	–0.142	<0.010
2000	164	47±7	47	–1.071	<0.010	142	42±12	41	0.899	<0.010
2001	19	38±10	41	–0.670	0.019	91	43±12	45	–0.028	0.037

Note: Md, median; Skew, skewness of the length distribution; *n*, number of fish recaptured. *P* values are from the Kolmogorov–Smirnov test of normality. When $P < 0.010$, the length distribution differed from the normal distribution.

cause fish were caught younger. In the 1980s, the sea trout migrated 18–19 months in the sea before recapture, but in the 1990s the respective migration time was 11–14 months. The length of recaptured fish decreased in the bottom gill net catch (linear regression, GF: length = 9352 – 4.4 × year, $F = 23.3_{[1,2198]}$, $P < 0.001$; BS: length = 5399 – 2.5 × year, $F = 28.9_{[1,2039]}$, $P < 0.001$) and floating gill net catch (GF: $P < 0.01$; BS: $P < 0.05$) in both sea areas (tagged and recaptured in these areas), when all fish independent of sea year were included. The length of fish caught by trap gears decreased significantly in the GF (length = 13 579 – 6.5 × year, $F = 22.2_{[1,683]}$, $P < 0.001$), but not in the BS (length = 2897 – 1.2 × year, $F = 0.57_{[1,257]}$, $P = 0.451$).

The sea trout recaptured in the release year by different gears usually had a similar mean length. However, fish recaptured in the second sea year by bottom gill nets were smaller than fish caught by floating gill nets or traps (*t* test: $P < 0.1–0.001$). The sea trout recaptured by bottom gill nets in the release year usually had a larger smolt length than fish recaptured later, except in the BS in the 1980s (Fig. 6).

The minimum legal size for trout has been 40 cm since 1983, but was 35 cm before then. If fishermen do not return tagged fish, survival is underestimated. The supposition is that the fish recaptured with a size under 40 cm are returned at a relatively lower rate than recaptured fish of a legal size. Thus, when the mean length and standard deviation of captured fish were known (Table 2), the proportion of undersized fish (<40 cm) could be estimated by assuming normality of the size distribution of the returned sea trout (Table 2).

Results

Recapture rate and smolt traits of tagged groups

The recapture rate showed a decreasing trend for sea trout released into the GF, but not for groups released in the BS, when the trends were calculated from annual means (percentage of recaptured fish) (Fig. 2*a*). The variation in the recapture rate was higher in the BS than in the GF ($F_{[85,149]} = 1.5$, $P = 0.032$). The Spearman correlation between annual recapture rates for groups released in the BS and in the GF was low ($r = 0.01$, $n = 21$).

The mean smolt length of the sea trout groups released increased by about 2 mm·year^{-1} in both the GF and the BS (1970–2001) (Fig. 2*b*). The percentage of sea trout caught increased with an increase in the mean smolt length (GF: recapture rate = –6.07 + 0.06 × smolt size, $F_{[1,147]} = 23.4$, $P < 0.001$, $r^2 = 0.14$; BS: recapture rate = –14.73 + 0.10 × size, $F_{[1,79]} = 13.1$, $P < 0.001$, $r^2 = 0.14$), when all groups stocked in 1970–2001 were included in the model. The recapture rate of sea trout groups increased with an increase in the mean smolt size in the 1980s (linear regression, $P < 0.001$), when mean length was 21.4 ± 1.5 cm ($n = 31$), but not for groups released in 1995–2001 ($P = 0.184$), when the mean length was 23.8 ± 2.1 cm ($n = 29$) in the BS.

To study the effect of smolt length on the recapture rate in more detail, we also used the individual data available for these release groups (GF, 1988–2001). In the logistic regression model, only the year was significant ($P = 0.002$), but not smolt length ($P = 0.091$) or the interaction between variables ($P = 0.087$). The analysis showed that at least between

Fig. 3. (*a*) Mean monthly sea surface temperature (SST, °C) in May (solid squares), in June (solid triangles), and surface water (1 m) salinity (‰) (open triangles) in the Gulf of Finland and in the Bothnian Sea (BS), as well as the seasonal North Atlantic Oscillation (NAO) index in April to June (open squares) in 1970–2001. (*b*) Estimated abundance of 0+ year Baltic herring (*Clupea harengus membras*) (subdivisions 25–29 and 32, excluding the Gulf of Riga) (solid triangles) and European sprat (*Sprattus sprattus sprattus*) (open triangles) (subdivisions 22–32) in the Baltic Main Basin (MB) and estimation of the abundance of 0+ year herring in the BS (subdivision 30; southern Gulf of Bothnia) (solid squares) in 1970–2001. Estimates of prey fish abundances (million individuals) were $\log_{10}$-transformed. Linear regressions are as follows: SST June = 3.39 – 0.004 × year, $F_{[1,27]} = 0.01$, $P = 0.907$, $r^2 = 0.001$; SST May = 36.82 – 0.016 × year, $F_{[1,22]} = 0.2$, $P = 0.656$, $r^2 = 0.01$; NAO = 71.17 – 0.035 × year, $F_{[1,30]} = 1.4$, $P = 0.236$, $r^2 = 0.05$; salinity June–July = 29.72 – 0.011 × year, $F_{[1,30]} = 4.8$, $P = 0.036$, $r^2 = 0.14$; herring abundance in the MB = 53.83 – 0.022 × year, $F_{[1,24]} = 10.0$, $P = 0.004$, $r^2 = 0.29$; herring abundance in the BS = –62.28 + 0.035 × year, $F_{[1,25]} = 17.7$, $P < 0.001$, $r^2 = 0.42$; sprat abundance = –36.90 + 0.024 × year, $F_{[1,24]} = 1.6$, $P = 0.215$, $r^2 = 0.06$.

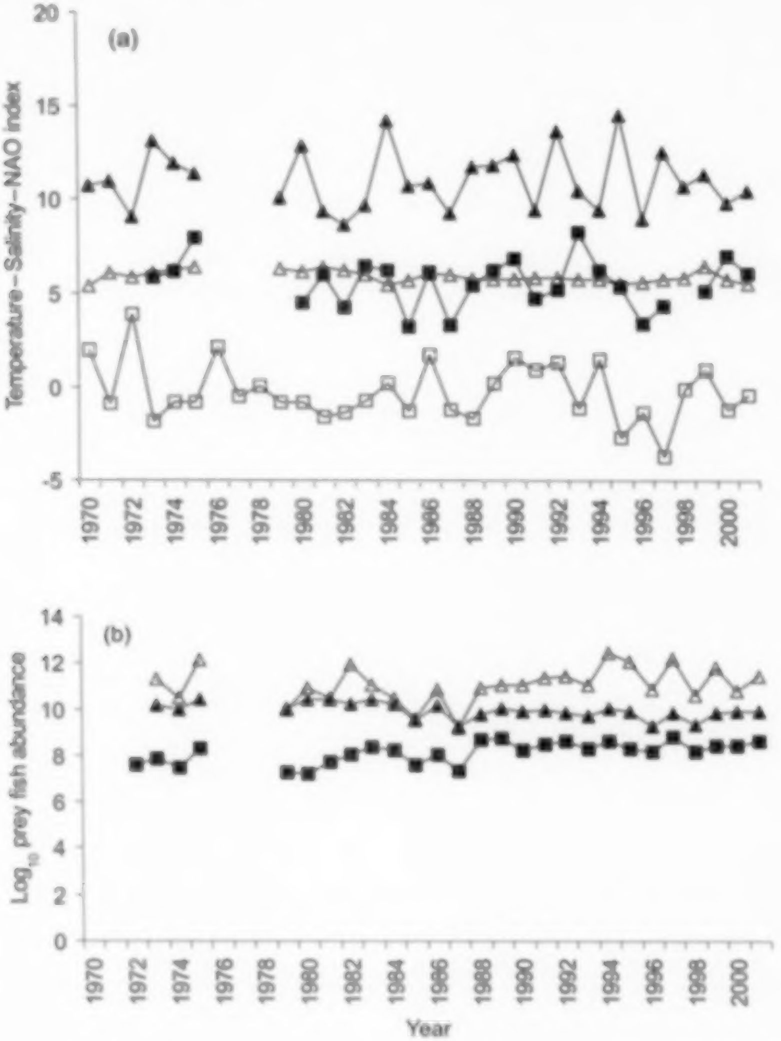

1988 and 2001, the recapture rate decreased independently of smolt size from year to year, and the recapture rate increased with an increase in the size at release.

The condition factor for the all tagged groups slightly increased from 1970 to 2001 ($K = -3.33 + 0.002 \times$ year, $F_{[1,195]} = 3.54$, $P = 0.061$, $r^2 = 0.18$), being 0.95 (median) (lower (25%) – upper (75%) quartiles: 0.93–0.96, $n = 2$), 1.04 (0.99–1.10, $n = 55$), and 1.07 (1.02–1.12, $n = 140$) in the 1970s, 1980s, and 1990s, respectively. The condition factor increased among the groups released in the BS, but did not rise among groups released in the GF (BS: $K = -5.69 + 0.0034 \times$ year, $F_{[1,77]} = 4.0$, $P = 0.047$, $r^2 = 0.05$; GF: $K = -2.59 + 0.0018 \times$ year, $F_{[1,119]} = 1.1$, $P = 0.278$, $r^2 = 0.01$).

Marine and fishing variables in relation to recapture rate

The median recapture rate for groups released (GF + BS) at a water temperature of 4–16 °C was on average higher (7%–9%) than that for groups released at colder or warmer

Fig. 4. The recapture rate (%) of undersized fish based on the number of returned fish (squares) or estimation of the size distribution of caught fish (solid triangles) in the Bothnian Sea (BS) (*a*) and Gulf of Finland (GF) (*b*) and the percentage of the sea trout (*Salmo trutta trutta*) catch taken by bottom gill nets for groups released in the GF (triangles) and in the BS (squares) in 1980–2000 (*c*). Linear regressions for estimated undersized fish are as follows: BS, annual proportion = –1219.97 + 0.631 × year, $F_{[1,19]} = 4.2$, $P = 0.055$, $r^2 = 0.18$; GF, annual proportion = –1577.49 + 0.801 × year, $F_{[1,18]} = 3.8$, $P = 0.067$, $r^2 = 0.17$. Linear regressions for undersized fish returned: BS, annual proportion = –1279.61 + 0.661 × year, $F_{[1,19]} = 4.53$, $P = 0.046$, $r^2 = 0.19$; GF, annual proportion = –1825.15 + 0.927 × year, $F_{[1,18]} = 4.09$, $P = 0.058$, $r^2 = 0.19$. The groups included separately into the analysis are as follows: GF, annual gill net proportion = –3015.57 + 1.542 × year, $F_{[1,10]} = 22.4$, $P = 0.0002$, $r^2 = 0.55$; BS, annual gill net proportion = –607.28 + 0.339 × year, $F_{[1,19]} = 0.9$, $P = 0.352$, $r^2 = 0.05$.

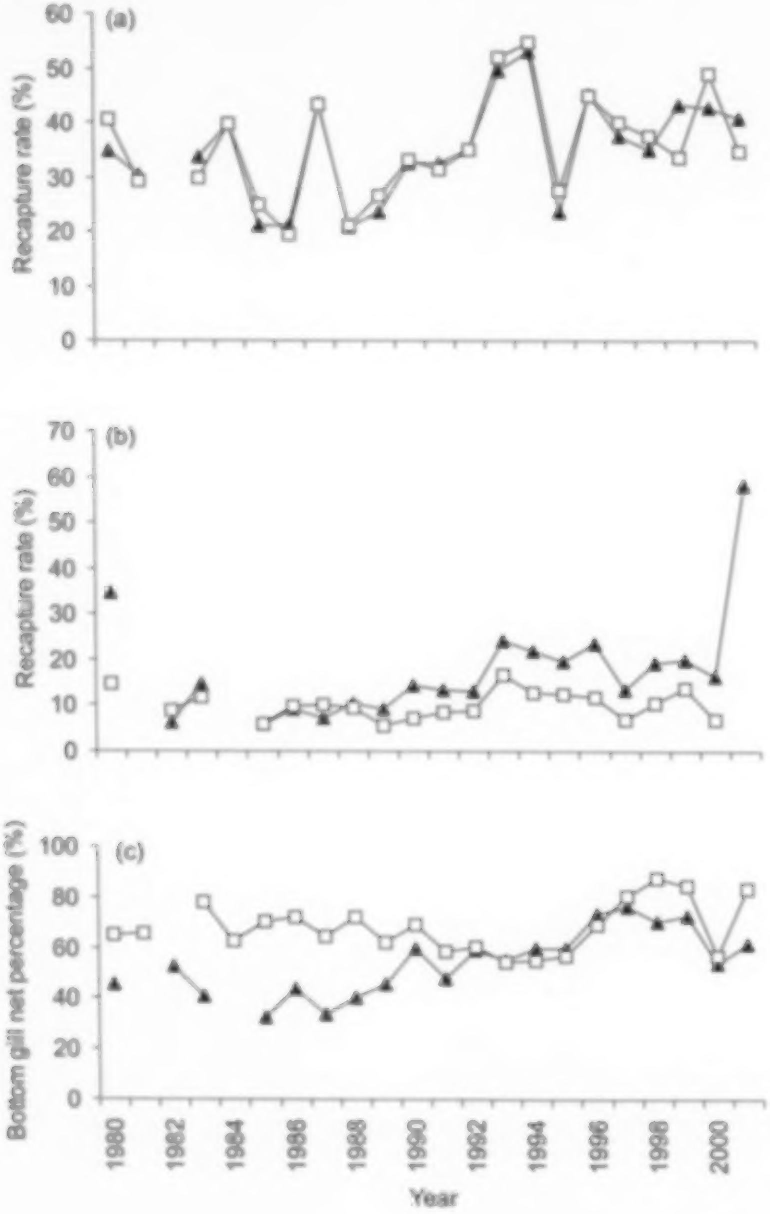

Table 3. The mean recruit time (months at sea) and recruit length for sea trout (*Salmo trutta trutta*) in the first sea year and the smolt length at tagging.

Sea	Time	Months		Recruit length (mm)		Smolt length (mm)	
		n	Mean±SD	*n*	Mean±SD	*n*	Mean±SD
GF	1980s	452	4.2±2.5	268	377±95	452	244±40
	1990s	1803	5.4±2.1	1344	418±82	1801	254±39
BS	1980s	419	3.9±2.3	266	328±93	419	221±25
	1990s	1377	3.3±2.1	947	330±79	1377	251±29

Note: The 1980s and 1990s and the Gulf of Finland (GF) and Bothnian Sea (BS) (released in this area) are shown separately. *n*, number of fish.

Table 4. Spatial distribution of sea trout (*Salmo trutta trutta*) released into the estuaries of the Gulf of Finland (GF) and estuaries of the Bothnian Sea (BS) in 1980–2001.

		Recapture areas					
Site	Recapture year	SMB (%)	NMB (%)	GB (%)	GF (%)	Estuaries (%)	*n*
GF	1	0	3	0	83	14	2291
BS	1	0	1	66	0	33	1936
GF	2	1	8	2	87	2	3425
BS	2	0	2	93	0	5	2695

Note: SMB, southern Main Basin; NMB, northern Main Basin; GB, Gulf of Bothnia. Estuaries refers to estuaries of different rivers. *n*, number of fish recaptured.

water temperatures (3%–4%) (Kruskal–Wallis) (Fig. 7*a*). Moreover, the median recapture rate for groups released in May was on average higher (10%) than that for groups released in April or in June (4%–8%) Kruskal–Wallis, $P < 0.05$) (Fig. 7*b*).

The median release date of all groups in 1970–2001 was 15 May (25%–75% quartiles: 31 April – 30 May, $n = 247$). The groups were released most frequently at the end of May in the 1980s (mean release date, BS: 30 May; GF: 20 May), but at the beginning of May in the 1990s (BS: 11 May; GF: 6 May) (Fig. 8). The recapture rate of sea trout groups in the BS in the 1980s was at the highest at the end of May (13.1%, $n = 9$; Kruskal–Wallis, $P < 0.10$) and highest in the 1990s at the beginning of May (8.7%, $n = 20$; Kruskal–Wallis, $P < 0.10$) (Fig. 8).

During the study period, the abundance of Baltic herring decreased in the Baltic Main Basin (including the GF), but increased in the BS (Fig. 3*b*). The increase in 0+ herring abundance in the Main Basin seemed to cause a slight increase in the recapture rate of sea trout in the GF, but not in the BS (GF recapture rate = −17.27 + 2.62 × herring abundance, $F_{[1,129]} = 3.06$, $P = 0.082$, $r^2 = 0.023$; BS recapture rate = 34.22 – 2.56 × abundance, $F_{[1,82]} = 1.17$, $P = 0.192$, $r^2 = 0.021$). The increase in 0+ sprat in the Baltic Sea was linked with the decrease in the recapture rate of sea trout (recapture rate = 17.85 – 0.83 × sprat, $F_{[1,213]} = 3.08$, $P = 0.081$, $r^2 = 0.014$).

There was a weak increasing trend in the percentage of undersized fish in the catch and in also in the percent evaluated from the size distribution of recaptured fish in 1980–2001 in both areas (linear regression, $P < 0.1$) (Figs. 4*a* and 4*b*). The annual percentage of returned undersized fish was lower (about 5%–10%) than that estimated from the size distribution in the GF (linear regression: proportion of undersized returned = 5.289 + 0.309 × estimated proportion of undersized, $F_{[1,17]} = 20.6$, $P < 0.001$, $r^2 = 0.55$), but not in the BS (proportion of undersized returned = 2.342 + 0.945 × estimated proportion of undersized, $F_{[1,19]} = 112.1$, $P < 0.001$, $r^2 = 0.85$). The estimated proportions match with normally distributed length distribution of recaptured fish for most of the years (Table 2). The correlations between estimated and actual percentages of fish were high both in the BS (Spearman correlation: $r = 0.92$, $P < 0.001$, $n = 21$) and in the GF ($r = 0.74$, $P < 0.001$, $n = 19$) (Figs. 4*a* and 4*b*). The percentage of the catch taken by bottom gill nets significantly increased in the period from 1980 to 2000 in the GF, but not in the BS (Fig. 4*c*).

Survival models

To determine the best mixed model for predicting the survival rate of the Isojoki stock, all climatic and oceanographic factors (SST in May, SST in June, seasonal NAO (April–June) index, release date, salinity), prey fish abundance (herring abundance in the BS and Main Basin and sprat abundance in the Main Basin), and fishing variables (returned and estimated proportion of undersized fish and catch proportion taken by bottom gill nets) were included into the model, together with the mean smolt length, condition factor, sea area (GF or BS), and year. The groups released in the 1970s and later (1980–2001) were separately analysed because of their different nature and lack of some explanatory variables (prey fish abundances and fishing variables) in the 1970s (Table 5).

In the model for the first decade (1970–1979), only smolt year, mean smolt size, and their interaction remained in model when all nonsignificant predictors and their interactions were excluded. An increase in smolt length tended to increase the recapture rate ($F_{[1,23]} = 10.5$, $P = 0.004$, $r^2 =$

Fig. 5. (*a*) Temporal distribution of sea trout (*Salmo trutta trutta*) recaptures in first (open bars), second (dotted), third (horizontal lines), fourth (vertical lines), fifth–ninth (gray–black) sea years. (*b*) The proportion of captured fish taken by different gears in four time periods (1980–1984 = 80; 1985–1989 = 85; 1990–1994 = 90; 1995–2001 = 95) from groups released into the Gulf of Finland (GF) and the Bothnian Sea (BS). Gears are as follows: bottom gill net (open bars), floating gill net (dots), longline (horizontal lines), trap net (vertical lines), rod (gray), others (solid). The numbers of recaptures are shown at the bottom of the columns.

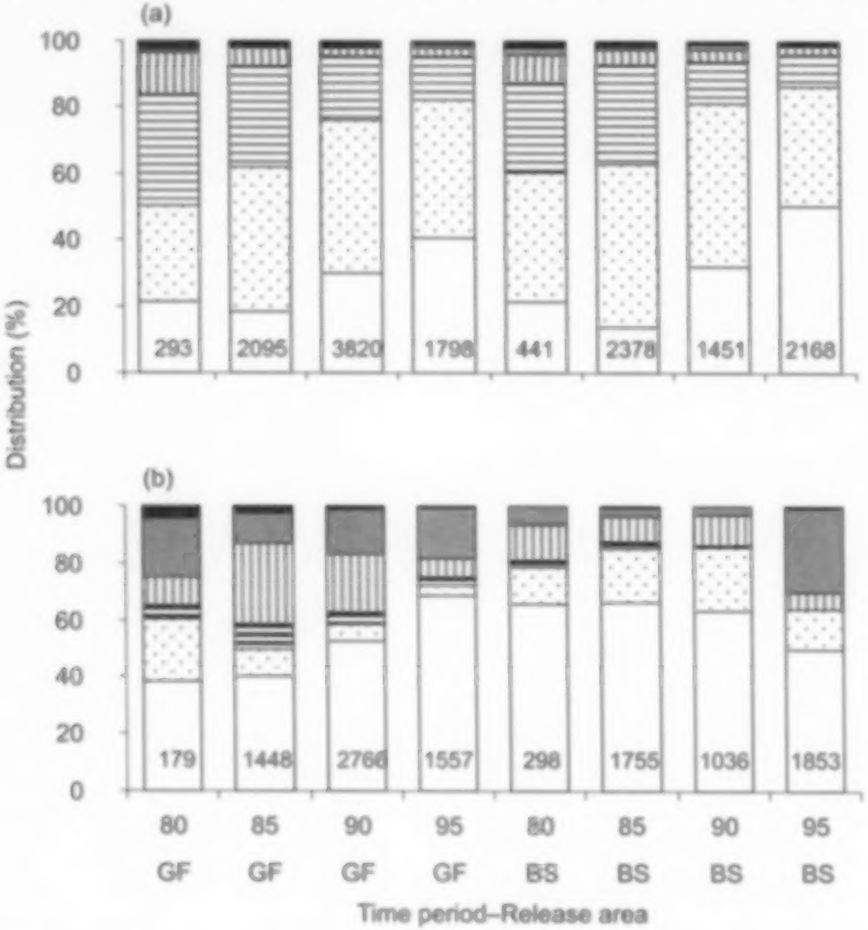

0.31, $Y = -31.7 + 0.22 \times$ smolt length). The smolt year in the model showed that some unknown annual factors also explain the survival rate (Table 5).

The oceanographic factors (salinity), fishing variables (returned and estimated proportion of undersized fish, catch proportion taken by bottom gill nets), condition factor, and release area had no effect on the survival rate of groups released in 1980–2001. In contrast, smolt size, release date, SST in May, herring abundance in the BS, year, or interactions among these variables had a significant influence on the survival of sea trout smolt groups (Table 5). The recapture rate increased with a later release date from the beginning of April to 15 May ($F_{[1,100]} = 15.4$, $P = 0.0002$, $r^2 = 0.13$, $Y = -8.67 + 0.14 \times$ date), but decreased slowly from 15 May to the end of June, concurrent with an increase in the SST ($F_{[1,98]} = 0.8$, $P = 0.366$, $r^2 = 0.01$, $Y = 15.6 - 0.04 \times$ date). The interaction between release date and SST in May was due to the survival rate being better in the early releases (in April) if the spring was warm, but better in the late releases (in June) if the spring was cold (Figs. 9*a* and 9*b*).

Survival increased with an increase in the smolt size when the herring abundance was low. When herring abundance was high, the survival rate was highest for smolts of 22 cm in length (Figs. 9*a* and 9*b*). Herring abundance was low in the 1980s, but high in the 1990s (Fig. 3*b*). The increase in the SST in May had a positive impact on the survival rate in years with either low or high herring abundance (Figs. 9*a* and 9*b*). When the stocking was carried out late, the survival of large smolts was nearly the same in both cold and warm springs and also in years with either high or low herring abundance. The smolt year in the model may indicate that there are also other annual explanatory factors besides those included in the model. If the salinity, condition factor, sprat abundance, NAO index, release site, and fishing variables are additionally present in the previous accepted model, all the new explanatory variables are nonsignificant, but the old

Fig. 6. The smolt length (mean ± standard deviation) of sea trout (*Salmo trutta trutta*) recaptured by bottom gill nets in the release year (1–8 months at sea; solid) and in the second (9–20 months, open) and third sea years (21–32 months, hatched). The 1980s and 1990s and both sea areas (GF, Gulf of Finland; BS, Bothnian Sea) are shown separately.

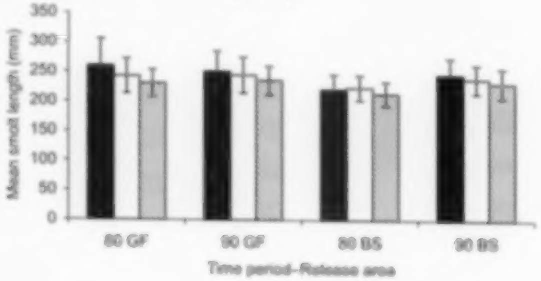

ones are significant, except the SST in May. The correlation analysis (Spearman) among annual mean condition factor, NAO index, salinity, SST in May, 1+ sprat abundance in the Main Basin, and 0+ herring abundance in the BS revealed a significant correlation between condition factor and salinity ($r = -0.435$, $P = 0.049$, $n = 21$) and between herring and salinity ($r = -414$, $P = 0.032$, $n = 27$), but not between other variables.

The years 1997–2001 may be exceptional because of changes in return activity, fishing methods, and very long smolt lengths. If this time period is excluded, the accepted model changes. Smolt length is no longer significant, but year ($P < 0.001$), smolt length ($P < 0.001$), release date ($P = 0.055$), SST in May ($P < 0.033$), herring abundance ($P < 0.035$), and the interaction between release date and SST in May ($P = 0.021$) remain in the model.

Discussion

Effect of smolt traits on survival

In our data, the survival rate depended on both human-controlled (smolt size, release date, return activity) and marine conditions (SST, herring abundance, smolt year). The mean smolt size of the released sea trout groups increased on average by 2 cm·decade^{-1}. The increase in smolt size was probably intentional and linked with better growth conditions in the hatcheries (Kallio-Nyberg and Koljonen 1997). The smolt size of sea trout had a positive influence on their survival rate as earlier observed in both hatchery-reared Atlantic salmon (Salminen et al. 1994, 1995; Saloniemi et al. 2004) and in wild-descending sea trout (Berg and Berg 1987). Berg and Berg (1987) observed that small smolts suffered from tagging, but not large ones. The lower smolt length of the nonrecaptured versus the recaptured fish in the study indicated that especially small smolts tend to die before recruiting to the fishery. Small smolts have more predators than large smolts (Hyvärinen and Vehanen 2004) and may have a higher likelihood of starving. They were particularly unaccounted for in cold springs, when invertebrate abundance was probably low. The large smolts were recruited to the fishery earlier than the small ones in this study, as was earlier observed in Atlantic salmon (Salminen et al. 1995). The small smolts probably suffered a higher level of natural mortality during the postsmolt period. The temporal distribution of recoveries showed that nearly all fish that survived the postsmolt period were captured in the sea before their first spawning migration. The exploitation rate was so high that spawning and natural mortality after spawning do not explain the decreased recapture rate, because very few sea trout return to the streams, and about 90% of the fish are caught before they reach maturity. The lowest age at maturity for female sea trout is two sea years in the Baltic Sea, and fish are able to spawn several times (Jutila et al. 2006).

Fig. 7. (*a*) Relationship between the recapture rate (%) of sea trout (*Salmo trutta trutta*) groups and water temperature at the release site and (*b*) relationship between the recapture rate (%) of sea trout groups and the release period. The mean and standard deviation (solid bars) as well as medians and upper and lower quartiles (open bars) of recapture rates are given. Sample sizes (tagged groups) are shown in the columns. The statistical significance of the differences in recapture rates between temperature groups (*a*) and between release period groups (*b*) is indicated by asterisks: *, $P < 0.05$; **, $P < 0.01$ (Kruskal–Wallis test). The Isojoki sea trout groups were tagged in 1970–2001 and released in the Gulf of Finland and in the Bothnian Sea.

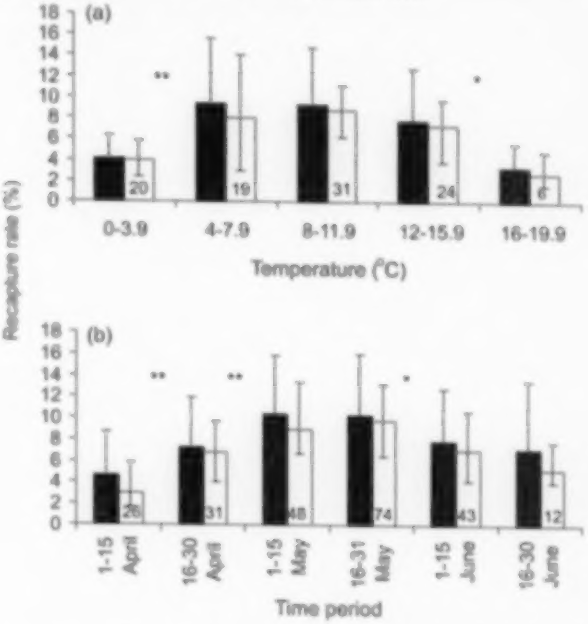

The increase in the length of tagged smolts seemed to lead to a rapid increase in the survival rate in the 1980s, when the smolt size was about 21 cm, but a slower increase in the 1990s, when the smolt size was about 24 cm. The large smolt size and fatness of hatchery-reared fish was aimed at safeguarding against predators and unpredictable marine conditions. This development, however, reached its limit, and the survival of hatchery-reared smolts could no longer be improved by increasing the smolt size. In the 1990s, the recapture rate was very low, independent of the smolt length. It is unlikely that the mortality of large smolts before fishing was higher in the 1990s, but it is more likely that they were

Fig. 8. Median recapture rate (%) (solid bars) with the upper quartiles (solid lines) of sea trout (*Salmo trutta trutta*) groups released in the 1980s and 1990s. The median water temperature (°C) (open diamond) with the quartiles (broken line) at the release site are shown. The sample sizes (number of released groups) are showed in the columns.

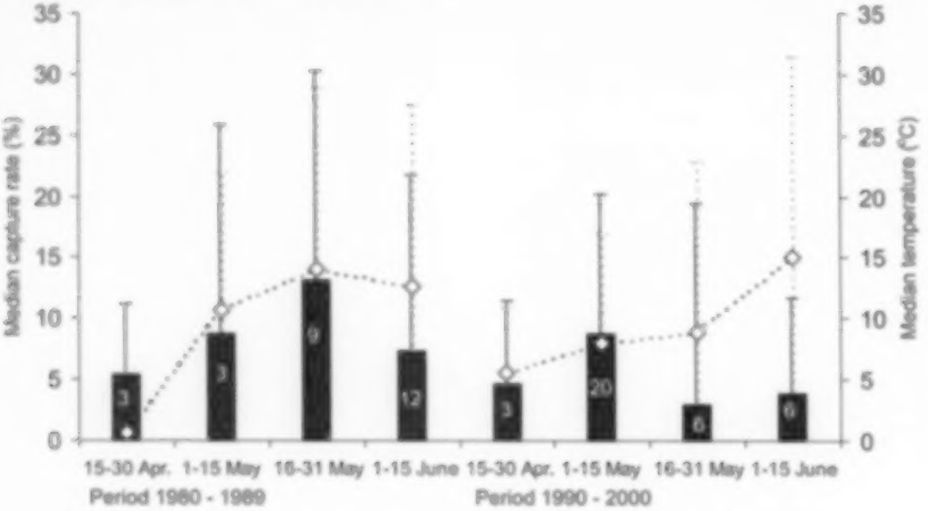

Table 5. Results of trend analyses between the survival rate of sea trout (*Salmo trutta trutta*) groups and smolt and environmental traits for the 1970s and for 1980–2001.

	Regression model					
	1970–1979			1980–2001		
Variable	df	*F*	*P*	df	*F*	*P*
Year	1, 17.2	5.82	0.0272	1, 43.1	33.37	<0.0001
Smolt length	1, 16.9	4.94	0.0401	1, 182	16.84	<0.0001
Release date				1, 179	6.49	0.0117
SST in May				1, 171	0.69	0.4075
Herring in BS				1, 181	10.35	0.0015
Smolt length × herring				1, 182	8.47	0.0041
Smolt length × SST				1, 177	5.37	0.0216
Smolt length × smolt length				1, 167	9.42	0.0025
Release date × SST				1, 179	7.49	0.0068
Year × smolt length	1, 16.9	4.96	0.0398			

Note: SST, sea surface temperature; BS, Bothnian Sea.

taken as undersized fish and were thus not reported. The observation that a large smolt size had no benefit when herring abundance was high suggests that sea trout migrated in good herring years in the areas where they had a high likelihood of disappearing, for example as a nonreported bycatch of fishing for herring, whitefish (*Coregonus* sp.), or Atlantic salmon. The estimated survival based on the return rate of tags does not, therefore, necessarily indicate the real survival from smolt to catch size. Herring abundance was low in the 1980s but high in the 1990s. This suggests that changes in fishing may explain the low return rate of the very large smolts in the 1990s. The low recapture rate of smolts released late (at the end of May or June) in the 1990s may mean that large smolts are targeted by selective net fishing very soon after release. Small trout eat invertebrates near the coast, but large trout soon begin to prey on fish and migrate to deeper waters. The feeding behaviour of sea trout, variability in herring abundance, and behaviour of fishermen might then explain the disappearance of the large smolts. Alternatively, the result could be explained by chance, because the number of the smolts over 26 cm was low. The bottom gill net fishing targeted mostly at whitefish in the BS and pike-perch (*Stizostedion lucioperca*) in the GF is selective in relation to the smolt length of trout released and further increased in the GF and BS during the study period. Sea trout also recruited to the gill net fishery at a younger age, because the mesh size of nets decreased and the release size of trout increased. The increase in bottom gill net fishing in the GF and nonreporting of recaptures may explain the decreasing trend in the recapture rate in the GF. The increase in the legal size from 35 to 40 cm in 1983 did not inevitably decrease the fishing of young fish, but may have reduced the reporting rate.

Fig. 9. Dependence of recapture rate on smolt length, sea surface temperature (SST) in May, and herring abundance when the stocking date is early (*a*) or late (*b*) (model presented in Table 5; 1980–2001). The SST in May classes are 3 °C (circle), 5 °C (triangle), and 8 °C (square). Herring abundance in the Bothnian Sea classes are 7.2 ($\log_{10}$ prey fish abundance) (shaded) and 8.8 (open). The year is 1990; the later the year is, the lower are the curves. The early stocking date is 17 April (day 105 from the beginning of the year) and the late date is 1 June (day 151).

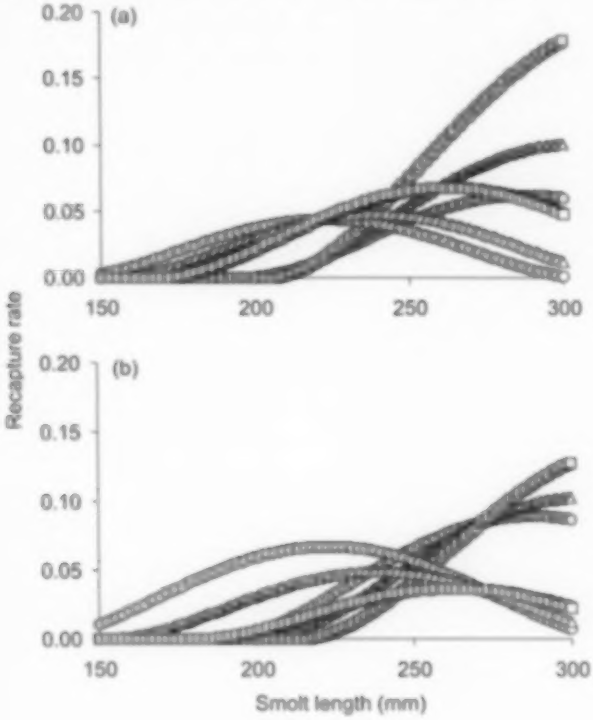

Hatchery-reared smolts are not necessarily physiologically ready to leave freshwater life. The study of Pirhonen et al. (2003) demonstrated that the majority of hatchery-reared sea trout males tagged at age 2+ are mature. In Atlantic salmon, previously mature males have a seven- to eight-fold lower recovery rate after release than immature males (Lundqvist et al. 1994). In the wild, mature males stay in the stream after release until they are ready to migrate or usually do not leave fresh water at all (Jonsson 1985). Parr maturation decreases in the population, which is under domestication selection over many generations (Fleming and Einum 1997). Based on this, 2-year-old reared sea trout with many parental hatchery generations should be ready for migratory life.

Effect of release time and temperature on survival

McCormick et al. (1998) suggested that Atlantic salmon smolt survival is affected by a limited period of readiness (a physiological smolt window) and the timing of seawater entry with environmental conditions, such as temperature, food, and predators (an ecological smolt window). Hansen and Jonsson (1989) showed that the survival of tagged Atlantic salmon smolts was the highest in the spring, and they suggested that heavy predation at times other than spring decreases the survival of smolts. This study demonstrated that there is a thermal window (4–16 °C) for the seawater entry of hatchery-reared sea trout groups. This is in accordance with Pirhonen et al. (2003), who reported that the optimal period for stockings is the spring; sea trout stockings carried out in April and May give better average yields than stockings carried out in June to July. The mean temperatures at the start and end of the run for Atlantic sea trout were 5 and 15 °C, respectively (Byrne et al. 2004).

Warm springs, resulting in a high SST in May, correlated positively with the survival of sea trout smolt groups, as has previously been shown for Atlantic salmon smolts (Friedland et al. 1993; Kallio-Nyberg et al. 2004; Jutila et al. 2005). In addition, the present study revealed that the optimal release time was dependent on the annual SST in May. If the SST in May was warm, an early release date was best, but if the SST was cold, a late release date was best. This study does not imply that the releases were carried out at the wrong time in the 1990s, but that other reasons explained the decrease in survival. As a matter of practice, the breeder cannot in advance predict the optimal release time in relation to the SST in May, and the date of release is difficult to change according to the seasonal climatic conditions. Our model also revealed interdependences among herring abundance, SST, and release date.

Marine conditions

Of the abiotic marine factors, only the SST in May was found to be linked with the survival rate of stocked sea trout groups. Abiotic marine factors such as SST and salinity affect the food resources of sea trout, the recruitment of prey fish, and the abundance of other suitable food (Dippner et al. 2001). The decreasing salinity in the Baltic Sea during a 30-year period has brought a change in zooplankton species composition and abundance (Rönkkönen et al. 2004) and in the diet of planktivorous fish species (Möllmann et al. 2004). The stomach fullness of herring and sprat has decreased and the proportion of the *Pseudocalanus* sp. in the diet of herring and sprat has decreased since 1977 (Möllmann et al. 2004). These calanoid copepods are the most important food items in the spring both for herring and sprat (Möllmann et al. 2004).

This study indicated that sea trout suffered from a low abundance of herring, which is consistent with earlier studies on Atlantic salmon smolts released in the Gulf of Bothnia (Salminen et al. 1995; Kallio-Nyberg et al. 2004). The observation that the groups with a small smolt size (20–25 cm) obtained greater benefit from a high herring recruitment conforms with a report that the years with a high herring abundance are also linked with other suitable conditions for smolts (Dippner et al. 2001). Investigations in Norwegian coastal waters have revealed that sea trout migrate in May and June in the littoral zone at an average depth of 0.6–0.7 m, feeding on invertebrates (Lyse et al. 1998). In the pelagic open water zone in June and July, migrating sea trout (mean fork length 28 cm) fed almost exclusively on fishes, which constituted >99% of the diet, and small-sized herring were the dominant prey (>80%) (Rikardsen and Amundsen 2005).

In Lake Oulujärvi, northern Finland, Hyvärinen and Huusko (2006) found that all brown trout (*S. trutta lacustris*) >30 cm total length (L_T) were piscivorous, and the majority of brown trout <30 cm (17–30 cm) also foraged for fishes, consistently preferring prey from the smallest vendace (*Coregonus albula*) and smelt (*Osmerus eperlanus*) size groups available (4–10 cm L_T). In the Baltic Sea, herring spawn in the spring (Parmanne 1993), being about 70–90 mm long at the end of the summer (Parmanne 1990). In a study on Baltic Sea salmon, Salminen et al. (2001) suggested that 0+ herring are probably not available for salmon postsmolts until July. The 1+ herring, with a length of 90–100 mm in spring (Parmanne 1990), may be too large for predation by the smaller sea trout postsmolts, because the mean prey size was 30% of the predator length (Hyvärinen and Huusko 2006). The large smolts may mainly eat fish, and small smolts mainly eat invertebrates soon after release. The piscivorous trout with a high growth rate probably recruit to the fishery earlier than trout with an invertebrate diet. The results thus suggest that because of the different feeding behaviour of the small and large smolts, they probably migrate in different areas and are thus likely to have a different return rate. In the years with a low herring abundance, which may also indicate low invertebrate abundance, nearly all the small smolts die before recruitment to the fishery. The cause of death may be starvation, but the low survival rate for small smolts may also be a consequence of a high predation rate. Small sea trout feed in the littoral zone, which is also occupied by their highly size-selective main predator, the northern pike (*Esox lucius*) (Hyvärinen and Vehanen 2004).

Release site and conditions

During the 1990s, there was a decreasing trend in the recovery rate of sea trout groups in the GF, but not in the BS. On the other hand, the annual variation in the recovery rate was larger in the BS than in the GF. This suggests that marine conditions or return rates of sea trout differ between these two areas, but unfortunately we were unable to include variables relevant in predicting these differences. A study on Atlantic salmon revealed that the survival rate is higher and less variable in the GF than in the BS (Salminen et al. 1995). The survival rate of salmon postsmolts was associated with good growth conditions (i.e., warm summers and rich food resources and 0+ herring abundance in the BS), but the survival of smolts was independent of annual marine conditions in the GF (Salminen et al. 1995). Our results suggest that marine conditions are also more variable and unpredictable for sea trout smolts in the BS than in the GF.

Salmonids may react or adapt to variable conditions by changing their migration area (Kallio-Nyberg et al. 1999) or their feeding behaviour (Hyvärinen and Huusko 2006). At least Atlantic salmon postsmolts originating from the northern Gulf of Bothnia leave and migrate southwards if the annual herring recruitment is low, but remain in the Gulf if herring abundance is high (Salminen et al. 1994; Kallio-Nyberg et al. 1999). The long feeding distance of the northern Gulf of Bothnia stocks may be an adaptation to the poor feeding conditions near their home rivers. In contrast, Neva salmon postsmolts originating from the GF always feed near the release site (Salminen 1997). The studied Isojoki sea trout may migrate to feed offshore (Kallio-Nyberg et al. 2002), but observation of the feeding behaviour of brown trout suggests that brown trout can also change their prey fish (Hyvärinen and Huusko 2006).

Return activity and sea trout fishing

The proportion of tag recoveries of undersized fish increased in the time period from 1980 to 2001. The recapture rate of undersized fish was about 5%–10% lower when calculated from tag recoveries than from the size distribution of recaptured fish in the groups released in the GF. This suggests that the survival of sea trout smolts released in the GF is higher than shown by the tagging and recapture method. The estimated proportions include some assumptions that contain uncertainty. The size distribution of captured fish did not always follow the normal distribution in every year class. Although not all assumptions are necessarily valid for every release year, the estimated and actual proportions of returned fish diverged in the 1990s. Undersized fish seemed to be missing based on the distribution of the returned fish. The size distributions of recaptured fish have varied from year to year because of changes in fishing and the size of smolts at release. It is likely that the majority of nonreported, undersized fish with a large release size were caught very soon after release by bottom gill nets, which have especially increased in use in the GF. On the other hand, 40 cm long trout may be over-represented in the catch, because fishermen want reported undersized fish to appear legal. Some of the undersized fish are likely to be set free, as the law requires. The possible variation in tag-reporting activity also somewhat increases the uncertainty related to our survival model.

The proportion of the catch taken by bottom gill nets increased during the study period in the GF, and the recapture rate simultaneously decreased. In the bottom gill net fishery, the fast-growing individuals with a large smolt size had a higher likelihood of being caught earlier than slow-growing individuals. In addition, the small mesh size in the nets decreases the recruiting age for sea trout. Throughout the study period, the fishing mortality of sea trout before the first spawning migration was very high. In practise, all sea trout are caught before the end of their natural lifespan. The change in fishing has resulted in sea trout being caught at a younger age. The increased fishing of young fish should have increased the survival estimate based on the recapture rate, but this did not occur. The decreased return rate may be linked with increased, nonprofessional fishing by bottom gill nets and nonreporting of the tag recoveries or with increased postsmolt mortality. Unfortunately, we could not include the fishing variables in the survival analyses, but it is likely that the changes in fishing have also affected the recapture rate.

In conclusion, the survival of hatchery-reared sea trout decreased in the 1990s in the same way as that of Atlantic salmon (Kallio-Nyberg et al. 2004, 2006). The simultaneously decreasing trends in the survival of salmonids suggest that common factors explain these changes. This study demonstrated that a decrease in the reporting activity of tags, the abundance of herring, and the SST partly explained trends in the survival rate, but there were many within-year variables that remained unknown. The smolt year variable may include changes due to fishing, marine conditions, smolt traits (size, quality), or combinations of them. The low genetic variation in the hatchery stock (Jutila et al. 1998) may reduce their success in the wild or weaken their ability to adapt to variable marine conditions. However, the sharp decrease in survival in the 1990s is unlikely to have been due to changes in genetic traits or marine conditions alone. Rather, fishing and reporting activity may explain the declining trend in survival. The increase in bottom gill net fishing in the GF and nonreporting of tags may explain the decreasing trend in the recapture rate of sea trout in the GF. In the survival estimates, the lower than estimated proportion of undersized fish returned suggests that more attention should be paid in the future to the effect of the tagging method and the reporting activity of fishermen.

Acknowledgements

We thank Dr. Matti Salminen for critically reading the manuscript and offering many helpful suggestions, Pekka Alenius (Finnish Institute of Marine Research) for salinity and sea surface temperature data, and two anonymous referees for helpful comments. Dr. Roy Siddall helped correct the English.

References

Berg, O.K., and Berg, M. 1987. Effects of Carlin tagging on the mortality and growth of sea trout *Salmo trutta* L. Fauna Norv. Ser. A, **8**: 15–20.

Byrne, C.J., Poole, R., Dillane, M., Rogan, G., and Whelan, K.F. 2004. Temporal and environmental influences on the variation in sea trout (*Salmo trutta* L.) smolt migration in the Burrishoole system in the west of Ireland from 1971 to 2000. Fish. Res. **66**: 85–94.

Dieperink, C., Bak, B.D., Pedersen, L.-F., Pedersen, M.I., and Pedersen, S. 2002. Predation on Atlantic salmon and sea trout during their first days as postsmolts. J. Fish Biol. **61**: 848–852.

Dippner, J.W., Hänninen, J., Kuosa, H., and Vuorinen, J. 2001. The influence of climate variability on zooplankton abundances in the Northern Baltic Archipelago Sea (SW Finland). ICES J. Mar. Sci. **58**: 569–578.

Fleming, I.A., and Einum, S. 1997. Experimental tests of genetic divergence of farmed from wild Atlantic salmon due to domestication. ICES J. Mar. Sci. **54**: 1051–1063.

Friedland, K.D., Reddin, D.G., and Kocik, J.F. 1993. Marine survival of North American and European Atlantic salmon: effects of growth and environment. ICES J. Mar. Sci. **50**: 481–492.

Friedland, K.D., Hansen, L.P., and Dunkley, D.A. 1998. Marine temperatures experienced by postsmolts and the survival of Atlantic salmon, *Salmo salar* L., in the North Sea area. Fish. Oceanogr. **7**(1): 22–34.

Friedland, K.D., Hansen, L.P., Dunkley, D.A., and MacLean, J.C. 2000. Linkage between ocean climate, postsmolt growth, and survival of Atlantic salmon (*Salmo salar* L.) in the North Sea area. ICES J. Mar. Sci. **57**: 419–429.

Friedland, K.D., Reddin, D.G., and Castonguay, M. 2003. Ocean thermal conditions in the post-smolt nursery of North American Atlantic salmon. ICES J. Mar. Sci. **60**: 343–355.

Haikonen, A., Romakkaniemi, A., Keinänen, M., Linnansaari, T., Mäntyniemi, S., Pasternack, M., and Vatanen, S. 2002. Monitoring of the salmon and trout stocks in the River Tornionjoki in 2001. Finnish Game and Fisheries Research Institute, Helsinki. ISBN: 951-776-366-2. [In Finnish and English.]

Haluch, M., and Skóra, K. 1997. Food of sea trout (*Salmo trutta* m. *trutta* L.) caught in the Gulf of Gdańsk in 1944–1995 (Baltic Sea). Bull. Sea Fish. Inst. **3**(142): 55–71.

Hansen, L.P., and Jonsson, B. 1989. Salmon ranching experiments in the River Imsa: effect of timing of Atlantic salmon (*Salmo salar*) smolt migration on survival to adults. Aquaculture, **82**: 367–373.

Hansen, L.P., and Quinn, T.P. 1998. The marine phase of the Atlantic salmon (*Salmo salar*) life cycle, with comparisons to Pacific salmon. Can. J. Fish. Aquat. Sci. **55**(Suppl. 1): 104–118.

Hurrell, J. 1995. Citing online sources: NAO index data provided by Climate Analysis Section, NCAR, Boulder, USA. Available from www.cgd.ucar.edu/cas/jhurrell/indices.data.html#naostatdifm [accessed 20 March 2005; updated 18 January 2007].

Hyvärinen, P., and Huusko, A. 2006. Diet of brown trout in relation to variation in abundance and size of pelagic prey. J. Fish Biol. **68**: 87–98.

Hyvärinen, P., and Vehanen, T. 2004. Effect of brown trout body size on post-stocking survival and pike predation. Ecol. Freshw. Fish, **13**: 77–84.

ICES. 2005*a*. ICES WGBAST Report 2005. ICES Advisory Committee for Fishery Management. ICES CM 2005/ACFM18. Available from www.ices.dk/reports/ACFM/2005/WGBAST/WGBAST05.pdf [accessed 10 May 2005; updated 8 June 2007].

ICES. 2005*b*. Citing online sources: the estimates of herring and sprat abundances presented in an ICES report. For the Bothnian Sea, available from www.ices.dk/committe/acfm/comwork/report/2005/may/her-30.pdf; for the Main Basin, available from www.ices.dk/committe/acfm/comwork/report/2005/may/her-2532-ex-gor.pdf [accessed 10 May 2005; updated 8 June 2007].

Jonsson, B. 1985. Life history patterns of freshwater resident and sea-run migrant brown trout in Norway. Trans. Am. Fish. Soc. **114**: 182–194.

Jonsson, N., and Jonsson, B. 2004. Size and age of maturity of Atlantic salmon correlate with North Atlantic Oscillation Index (NAOI). J. Fish Biol. **64**: 241–247.

Jutila, E., Ahvonen, A., Laamanen, M., and Koskiniemi, J. 1998. Adverse impact of forestry on fish and fisheries in stream environments of the Isojoki basin, western Finland. Boreal Environ. Res. **3**: 395–404.

Jutila, E., Jokikokko, E., and Julkunen, M. 2005. The smolt run and postsmolt survival of Atlantic salmon, *Salmo salar* L., in relation to early summer water temperatures in the northern Baltic Sea. Ecol. Freshw. Fish. **14**: 69–78.

Jutila, E., Saura, A., Kallio-Nyberg, I., Huhmarniemi, A., and Romakkaniemi, A. 2006. The status of fishing of sea trout on the Finnish coast of the Gulf of Bothnia in the Baltic Sea. *In* Sea Trout: Biology, Conservation and Management. Proceedings of the 1st International Sea Trout Symposium, July 2004, Cardiff, Wales, UK. *Edited by* G. Harris and N. Milner. Blackwell Publishing, Oxford, UK. pp. 128–138.

Kallio-Nyberg, I., and Koljonen, M.-L. 1997. The genetic consequences of hatchery-rearing on life-history traits of the Atlantic salmon (*Salmo salar*): a comparative analysis of sea-ranched salmon with wild and reared parents. Aquaculture, **153**: 207–224.

Kallio-Nyberg, I., Peltonen, H., and Rita, H. 1999. Effects of stock-specific and environmental factors on the feeding migration of Atlantic salmon (*Salmo salar*) in the Baltic Sea. Can. J. Fish. Aquat. Sci. **56**: 853–861.

Kallio-Nyberg, I., Saura, A., and Ahlfors, P. 2002. Sea migration pattern of two sea trout (*Salmo trutta*) stocks released into the Gulf of Finland. Ann. Zool. Fenn. **39**: 221–235.

Kallio-Nyberg, I., Jutila, E., Saloniemi, I., and Jokikokko, E. 2004. Association between environmental factors, smolt size and the survival of wild and reared Atlantic salmon from the Simojoki River in the Baltic Sea. J. Fish Biol. **65**: 122–134.

Kallio-Nyberg, I., Jutila, E., Jokikokko, E., and Saloniemi, I. 2006. Survival of reared Atlantic salmon and sea trout in relation to marine conditions of smolt year in the Baltic Sea. Fish. Res. **80**: 295–304.

Karlsson, L., Ikonen, E., Mitans, A., and Hansson, S. 1999. The diet of salmon (*Salmo salar*) in the Baltic Sea and connections with the M74 syndrome. Ambio, **28**(1): 37–42.

Lundqvist, H., McKinnell, S., Fängstam, H., and Berglund, I. 1994. The effect of time, size and sex on recapture rates and yield after river releases of *Salmo salar* smolts. Aquaculture, **121**: 245–257.

Lyse, A.A., Stefansson, S.O., and Fernö, A. 1998. Behaviour and diet of sea trout post-smolts in a Norwegian fjord system. J. Fish Biol. **52**: 923–936.

McCormick, S.D., Hansen, L.P., Quinn, T.P., and Saunders, R.L. 1998. Movement, migration, and smolting of Atlantic salmon (*Salmo salar*). Can. J. Fish. Aquat. Sci. **55**(Suppl. 1): 777–792.

McKinnell, S.M., and Karlström, Ö. 1999. Spatial and temporal covariation in the recruitment and abundance of Atlantic salmon populations in the Baltic Sea. ICES J. Mar. Sci. **56**: 433–443.

McKinnell, S.M., and Lundqvist, H. 2000. Unstable release strategies in the reared Atlantic salmon, *Salmo salar* L. Fish. Manag. Ecol. **7**: 211–224.

Möllmann, C., Kornilovs, G., Fetter, M., and Köster, F.W. 2004. Feeding ecology of central Baltic Sea herring and sprat. J. Fish Biol. **65**: 1563–1581.

Parmanne, R. 1990. Growth, morphological variation and migration of herring (*Clupea harengus* L.) in the northern Baltic Sea. Finnish Fish. Res. 10.

Parmanne, R. 1993. Larval abundance and catch composition of Baltic herring in the Gulf of Finland. Aqua Fenn. **23**: 75–84.

Pirhonen, J., Valkeajärvi, P., Thorpe, J.H., and Soivio, A. 2003. Effect of stocking time on yield and location of recapture in two forms of brown trout (*Salmo trutta*) when stocked in respect to migration activity. Aquaculture, **222**: 189–201.

Rikardsen, A.H., and Amundsen, P.A. 2005. Pelagic marine feeding of Arctic charr and sea trout. J. Fish Biol. **66**: 1163–1166.

Rönkkönen, S., Ojaveer, E., Raid, T., and Viitasalo, M. 2004. Long-term changes in Baltic herring (*Clupea harengus membras*) growth in the Gulf of Finland. Can. J. Fish. Aquat. Sci. **61**: 219–229.

Salminen, M. 1997. Relationships between smolt size, postsmolt growth and sea age at maturity in Atlantic salmon ranched in the Baltic Sea. J. Appl. Ichthyol. **13**: 121–130.

Salminen, M., Kuikka, S., and Erkamo, E. 1994. Divergence in the feeding migration of Baltic salmon (*Salmo salar* L.); the significance of smolt size. Nord. J. Freshw. Res. **69**: 32–42.

Salminen, M., Kuikka, S., and Erkamo, E. 1995. Annual variability in survival of sea-ranched Baltic salmon, *Salmo salar* L.: significance of smolt size and marine conditions. Fish. Manag. Ecol. **2**: 171–184.

Salminen, M., Erkamo, E., and Salmi, J. 2001. Diet of post-smolt and one-sea-winter Atlantic salmon in the Bothnian Sea, Northern Baltic. J. Fish Biol. **58**: 16–35.

Saloniemi, I., Jokikokko, E., Kallio-Nyberg, I., Jutila, E., and Pasanen, P. 2004. Survival of reared and wild Atlantic salmon smolts: size matters more in bad years. ICES J. Mar. Sci. **61**: 782–787.

SAS Institute, Inc. 2001. SAS/STAT™ user's guide. Version 8.2. SAS Institute Inc., Cary, N.C.

Revisiting evolutionary dead ends in sockeye salmon (*Oncorhynchus nerka*) life history

Scott A. Pavey, Troy R. Hamon, and Jennifer L. Nielsen

Abstract: This study challenges recent hypotheses about sockeye salmon (*Oncorhynchus nerka*) colonization based on life history and broadens the pathways that investigators should consider when studying sockeye colonization of novel habitats. Most sockeye populations exhibit lake-type life histories. Riverine populations are thought to be more likely to stray from their natal stream to spawn and therefore colonize new habitat. We examined genetic relationships among five geographically proximate sockeye populations from the Aniakchak region of the Alaska Peninsula, Alaska. Specifically, we sought to determine if the genetic population structure was consistent with the hypothesis that a riverine population colonized a recently available upriver volcanic caldera lake, and whether recent volcanism led to genetic bottlenecks in these sockeye populations. Heterozygosity and allelic richness were not higher in the riverine population. Patterns of genetic divergence suggested that the geographically proximate riverine sockeye population did not colonize the lake; the caldera populations were more genetically divergent from the downstream riverine population (F_{ST} = 0.047) than a lake-type population in a different drainage (F_{ST} = 0.018). Our results did not suggest the presence of genetic bottlenecks in the caldera populations.

Résumé : Notre étude remet en question quelques hypothèses récentes sur la colonisation du saumon rouge (*Oncorhynchus nerka*) basées sur le cycle biologique et ouvre de nouvelles perspectives que les chercheurs devront prendre en considération lorsqu'ils étudient la colonisation de nouveaux habitats par le saumon rouge. La plupart des populations de saumons rouges ont des cycles biologiques de type lacustre. On croit que les populations d'eau courante sont plus susceptibles de s'éloigner de leur cours d'eau natal lors de la fraye et ainsi de coloniser de nouveaux habitats. Nous examinons les relations génétiques de cinq populations de saumons rouges rapprochées géographiquement dans la région d'Aniakchak de la péninsule de l'Alaska, Alaska. En particulier, nous cherchons à savoir si la structure génétique des populations s'accorde avec l'hypothèse qui veut qu'une population d'eau courante ait colonisé un lac volcanique de caldeira d'amont qui est récemment devenu disponible; nous voulons aussi voir si l'activité volcanique récente a produit des goulots d'étranglement génétiques chez ces populations de saumons rouges. L'hétérozygotie et la richesse allélique ne sont pas plus élevées dans la population d'eau courante. Les patrons de divergence génétique laissent croire que la population d'eau courante de saumons rouges située a proximité n'a pas colonisé le lac; les populations de la caldeira divergent plus génétiquement de la population d'eau courante d'aval (F_{ST} = 0,047) que d'une population de type lacustre d'un autre bassin versant (F_{ST} = 0,018). Nos résultats n'indiquent aucun goulot d'étranglement génétique chez les populations de la caldeira.

[Traduit par la Rédaction]

Introduction

Anadromous sockeye salmon (*Oncorhynchus nerka*) are thought to have two general life history strategies. The first strategy (lake-type) includes the use of a lake as a nursery where young sockeye rear for 1–2 years after emergence. Populations are often locally adapted to spawning sites within a lake (Foerster 1968; Burgner 1991; Wood 1995). The second strategy (sea- and river-type) includes the use of riverine habitats, instead of lakes, for rearing. These sockeye migrate to the ocean either several months (sea-type or ocean-type; Gilbert 1913) or 1–2 years (river-type; Semko 1954) after emergence. All of these strategies involve migration to the ocean for the majority of growth, so the important habitat differences among these strategies are in the freshwater phase.

A number of investigators have studied these alternative life histories (e.g., Wood et al. 1987; Eiler et al. 1992; Wood et al. 1994). River-type and sea-type (both hereafter "riverine") sockeye spawn in glacial runoff habitat and rear

Received 1 September 2006. Accepted 24 May 2007. Published on the NRC Research Press Web site at cjfas.nrc.ca on 28 August 2007. J19513

S.A. Pavey.[1,2] Katmai National Park and Preserve, P.O. Box 7, King Salmon, AK 99613, USA, and University of Alaska Anchorage, Biological Sciences Department, 3211 Providence Drive, Anchorage, AK 99508, USA.
T.R. Hamon. Katmai National Park and Preserve, P.O. Box 7, King Salmon, AK 99613, USA.
J.L. Nielsen. USGS Alaska Science Center, 1011 E Tudor Road, Anchorage, AK 99503, USA.

[1] Corresponding author (e-mail: spavey@sfu.ca).

[2] Present address: Simon Fraser University, Department of Biological Sciences, 8888 University Drive, Burnaby, BC V5B 1K3, Canada.

doi:10.1139/F07-091

downstream in "side-channel river habitat" (Gustafson and Winans 1999). This contrasts with lake-type sockeye that typically spawn in tributaries, outlets, or beaches and rear in the adjacent lake (Burgner 1991). In broad-scale genetic studies, there is less genetic differentiation among riverine than among lake-type populations, suggesting that natal homing may be less precise in riverine sockeye (Wood 1995; Gustafson and Winans 1999; Beacham et al. 2004). However, a different pattern was observed in the Kamachatka Peninsula where riverine populations were genetically distinct (Beacham et al. 2006*a*). Riverine sockeye populations tend to have higher levels of genetic diversity than lake-type populations, measured as heterozygosity and allelic richness (Gustafson and Winans 1999; Beacham et al. 2004, 2006*b*). Wood (1995) suggested that riverine sockeye were the principal colonists of new habitats following the retreat of glaciers.

During periods of glacial maxima, coastal Alaska and Canada were mostly covered by ice. The majority of freshwater lakes in this area arose since the last glaciation (Imbrie and Imbrie 1979; Pielou 1991). Hence, most lower lying areas that lake-type sockeye presently use to spawn and rear were probably blocked by glaciers, and thus suitable habitat for sockeye to exhibit a lake-type life history was limited. Riverine sockeye persisted in glacial refugia in northern and southern refuges and possibly in other areas (Varnavskaya et al. 1994*a*; Wood et al. 1994; Beacham et al. 2006*a*). As the retreat of the Cordilleran ice sheet opened coastal habitats about 10 000 years ago, sockeye rapidly colonized new freshwater habitats and, in many cases, adopted a lake-type life history (Wood 1995). Colonization and establishment of new sockeye populations occurs when, instead of homing to their natal habitats, individuals stray and spawn in a freshwater location previously uninhabited by sockeye. Straying to new habitats may not result in the establishment of new populations in all cases, as the potential colonists may be maladapted to the new freshwater environments. Lake-type sockeye specialize in the use of freshwater habitats more than any other Pacific salmon species (Burgner 1991). Lake-type sockeye use many lake habitats for spawning, including tributaries, outlets, outwash fans, upwelling zones, and beaches (Burgner 1991; Wood 1995). Compared with lake-type, riverine sockeye are thought to be the persistent, parental lineage, which colonize new habitat more readily because of higher rates of straying. Lake-type sockeye are specialized for temporary environments and are thought to be less able to colonize because of their low straying rates. As a result, they have been referred to as evolutionary dead ends (Wood 1995).

Sockeye have diversified within the past 10 000 years from very few populations residing in glacial refugia to thousands of locally adapted populations along the entire coast of the North Pacific Ocean. Several factors can affect population size and structure in sockeye salmon. First, populations may become established via the colonization of only a few individuals (Wood 1995; Milner et al. 2000). Small initial size may lead to founder effects and genetic bottlenecks impacting the population structure of sockeye populations (Ramstad et al. 2004). Second, geologic events have the potential of obstructing returning salmon from reaching their natal sites to spawn or affecting the survival of eggs and juveniles (Ricker 1950; Leider 1989). Third, natural barriers such as waterfalls and rapids have been found to reduce effective population size (N_e) in sockeye spawning above barriers (Habicht et al. 2004). Severe reductions in N_e can result in a genetic bottleneck that may be detectable for decades after the demographic constriction (Cornuet and Luikart 1996; Ramstad et al. 2004).

Many studies have examined genetic structure of sockeye populations that were colonized 7000 – 10 000 years ago (e.g., Varnavskaya et al. 1994*b*; Habicht et al. 2004; Ramstad et al. 2004), but few studies have addressed systems colonized more recently (Burger et al. 1997; Woody et al. 2000). In the present study, we investigated the genetic relationships among five geographically proximate sockeye salmon populations on the Alaska Peninsula. This area contains both recently colonized lake-type populations, as well as a downriver population that exhibits the riverine life history. Using microsatellite markers, we addressed two questions. (*i*) Are genetic relationships consistent with patterns suggesting that the riverine population colonized lake habitats within a volcanic caldera? (*ii*) Do the caldera populations show genetic indications of recent bottlenecks?

Materials and methods

Study area

Aniakchak National Monument and Preserve (ANMP) in southwestern Alaska provides a unique system in which to study the interactions of sockeye life history strategies. Several recent cataclysmic geologic events have taken place within ANMP (Fig. 1). A massive volcanic eruption 3650 years ago formed a large caldera (Aniakchak Caldera) that filled with water creating a lake similar to Crater Lake in Oregon (McGimsey et al. 1994; Pearce et al. 2004). Approximately 1800 years ago (VanderHoek and Myron 2004), the caldera wall collapsed resulting in a large flood and the formation of the Aniakchak River, which connects the caldera lake (Surprise Lake, elevation 321 m) with the Pacific Ocean through "The Gates", a chasm breaching the caldera wall (Hubbard 1931; see Fig. 1). A large fluvial plain was established when the passing flood waters dropped sediment as the water velocity slowed where the Aniakchak emerges from more deeply incised bedrock channels to relatively flat lowlands. Several smaller eruptions have occurred, including well-documented events approximately 500 years ago and in 1931 (Hubbard 1931; McGimsey et al. 1994; Neal et al. 2001). These smaller eruptions probably affected spawning, rearing, and incubating conditions and may have impacted or eliminated any sockeye populations present in the caldera during that time (Hubbard 1932). Sockeye salmon spawning habitat of current populations in the Aniakchak caldera may have been available for colonization of current populations as early as about 1800 years ago (based on access following the flood) or as recently as 76 years ago (based on the timing of the most recent eruption). Adult sockeye caldera populations are all lake-type, although some spawn along Surprise Lake beaches and some spawn in the Surprise Lake outlet in riverine habitats (Fig. 1).

The only other known sockeye population in the Aniakchak River drainage spawns in Albert Johnson Creek (Fig. 1), the largest tributary of the Aniakchak River. This

Fig. 1. Map of Aniakchak National Monument and Preserve and Black Lake showing the five study populations (inset: location in Alaska, USA): MESH, Meshik Lake; BL, Black Lake; SLB, Surprise Lake beaches; SLO, Surprise Lake outlet; AJC, Albert Johnson Creek.

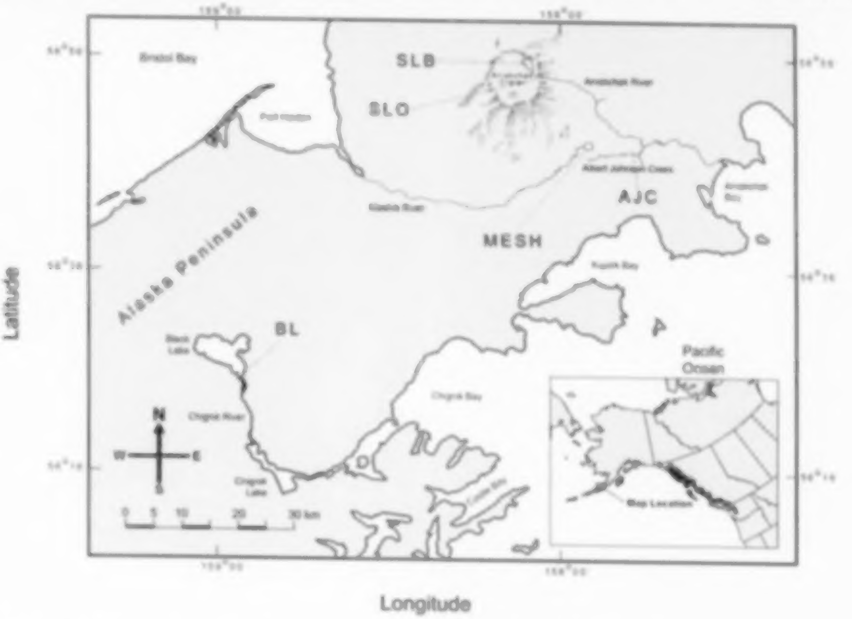

creek is located at the base of the volcano (~27 m elevation) and cuts east through the fluvial flood plain. Adults of these sockeye are riverine, having no juvenile access to Surprise Lake, which is the only lake in the drainage. Another sockeye salmon population occurs in Meshik Lake near the headwaters of Albert Johnson Creek. This lake is on the other side of the peninsular divide and drains into the Bering Sea (Fig. 1). Although Meshik Lake is geographically proximate to Albert Johnson Creek (3.5 km), mouth-to-mouth distance between the two drainages around the Alaska Peninsula is approximately 1200 km. A fifth population, Black Lake, is part of the Chignik River drainage and has a large, commercially important, lake-type sockeye run. The mouth of the Chignik River is located approximately 120 km southwest of the mouth of the Aniakchak River (Fig. 1). Black Lake and Meshik Lake populations serve as ecological outgroups providing perspective on the genetic relationships found among Aniakchak River drainage populations.

Sample collection

We conducted the genetic sampling of spawning sockeye adults in both Albert Johnson Creek and the caldera (Surprise Lake beaches and outlet) in early August (2001–2003). The Alaska Department of Fish and Game sampled Black Lake sockeye adults in July (2002–2003) at the Black Lake outlet. A National Park Service field crew sampled Meshik Lake juveniles in July (2003). A small amount (approximately1 cm^2) of fin tissue was collected from each adult fish. In the case of Meshik Lake, whole juvenile fish were collected. All fish were sampled using a beach seine. Samples were stored in 100% ethanol and brought to the USGS Molecular Ecology Laboratory (Alaska Science Center, Anchorage, Alaska) for DNA analyses.

Molecular data collection

Total genomic DNA was extracted from intact fin clips using Puregene DNA Isolation Kits© (Gentra Systems, Inc.). Six tetranucleotide microsatellites were analyzed: *One102*, *One105*, *One108*, *One109*, *One110*, and *One115* (Olsen et al. 2000). Multiplexes for these markers were developed by G.K. Sage (USGS Alaska Science Center, Anchorage, Alaska). Polymerase chain reaction (PCR) amplifications were conducted in 10 µL volumes using approximately 50 ng of genomic DNA, 0.1–0.2 µL of Taq© DNA polymerase (Perkin Elmer), and buffer (Scribner et al. 1996) for 35–40 cycles (Table 1). Gel electrophoresis and visualization of microsatellite alleles were performed using LI-COR Model 4200© and IR2 automated fluorescent DNA sequencers (Middendorf et al. 1992). Sizing was performed using Gene ImageIR version 3.00 (LI-COR, Lincoln, Nebraska). All allele size standards were calibrated to the M13 ladder and other known sockeye standards. Every gel was independently proofed by other researchers, and all questionable samples were rerun. Ten percent of all samples were independently amplified a second time and visualized for quality control purposes.

Molecular data analysis

Genotypic disequilibrium and Hardy–Weinberg equilibrium (HWE) tests were conducted using GENEPOP version 3.4 (Raymond and Rousset 1997). Statistical significance levels for multiple comparisons were set using sequential Bonferroni tests (Rice 1989). ARLEQUIN version 1.1 (Schneider et al. 1997) was used to test for differences between sampling years at the same location. If no significant interannual differences were detected, sampling years were pooled and reanalyzed with ARLEQUIN to test for differences in

Table 1. Loci and multiplexes used with thermal regime for PCR amplifications, size range, number of alleles, and expected heterozygosity.

Locus	Thermal regime		Size range	No. of alleles	H_e
Multiplex 1	94° 2 min				
One102	94° 15 s	40 cycles	197–261	17	0.853
One105	56° 15 s		128–152	7	0.558
One115	72° 30 s		179–243	17	0.898
	72° 30 min				
Multiplex 2	94° 2 min				
One108	94° 15 s	35 cycles	177–257	21	0.890
One109	54° 15 s		124–180	15	0.871
One110	72° 30 s		220–304	27	0.910

pairwise allele frequencies between populations. Values of expected heterozygosity for each locus were generated using Microsatellite Analyzer (MSA; Dieringer and Schlotterer 2003). Populations were then compared in a pairwise fashion, and in each comparison, a paired *t* test was conducted with the pairs of locus heterozygosity values in SAS version 8 (SAS Institute Inc., Cary, North Carolina).

Genetic distance values reflecting the proportion of shared alleles between individuals and groups of individuals can be used to graphically depict genetic relationships and population structure. Allele frequency data were used to create 2000 genetic distance matrices based on Cavalli-Sforza and Edwards' (1967) genetic chord distance using GENEDIST from PHYLIP (Felsenstein 1993). Neighbor-joining (NJ) trees were generated using the NEIGHBOR application of PHYLIP from each distance matrix. A consensus tree was created using CONSENSE from PHYLIP. SEQBOOT from PHYLIP was used to bootstrap allelic relationships creating 2000 trees depicting the five populations (Felsenstein 1985). TreeView version 1.6.6 (Page 1996) was used to visualize the consensus NJ tree with bootstrap values.

To compare our data with those of other recent sockeye salmon studies from different localities (Withler et al. 2000; Ramstad et al. 2004; Habicht et al. 2004), five different measures were used to detect a bottleneck signature. These tests were conducted with sampling years pooled for populations with multiple samples. Genotypic disequilibrium was tested using GENEPOP to infer gametic phase disequilibrium (Waples and Smouse 1990), which may be present in populations that have experienced a recent and acute bottleneck (Habicht et al. 2004). Differences in allelic diversity (Nei et al. 1975; Allendorf 1986) were estimated using FSTAT version 2.9.3.2 (Goudet 1995) to calculate population allelic richness (alleles per population adjusted for number of individuals sampled), as rare alleles may be lost after a bottleneck. This test requires comparing possibly bottlenecked populations with a putatively non-bottlenecked population. Pairwise comparisons of populations were estimated for differences in allelic richness using paired *t* tests in SAS. We calculated Garza and Williamson's *M* values using AGAR$_{ST}$ version 2.9 (Garza and Williamson 2001). This metric measures allelic "vacancies" within the allelic range and is expressed as a decimal between zero and one. Bottlenecked populations are expected to have more vacancies than non-bottlenecked populations. Any loci exhibiting alleles outside the four-base-pair repeat motif were excluded from this test (Garza and Williamson 2001). Mode shifts in allele frequency class distributions (Luikart et al. 1998) and heterozygosity excess (Cornuet and Luikart 1996) due to the loss of rare alleles were tested in comparison to Nei's allelic diversity (Nei et al. 1975) using BOTTLENECK (Piry et al. 1998). BOTTLENECK employs the Wilcoxon signed-rank test to detect heterozygosity excess. The output consisted of results obtained under two different mutation models to calculate the comparison expected heterozygosity if the populations were in mutation-drift equilibrium: the infinite allele model (IAM) and the stepwise mutation model (SMM; Cornuet and Luikart 1996).

Genotypic disequilibrium, mode shift in allele frequency class distribution, and heterozygosity excess are best at detecting recent and acute bottlenecks, whereas reduced allelic diversity and Garza and Williamson's *M* value are capable of detecting less severe bottlenecks for a longer time after the demographic constriction (Habicht et al. 2004; Ramstad et al. 2004). All results were analyzed for evidence of bottlenecks and compared with other sockeye studies that used similar analyses (Withler et al. 2000; Habicht et al. 2004; Ramstad et al. 2004).

Results

All five sockeye populations were polymorphic at all loci (total of 576 individuals; Table 2). Allelic polymorphism ranged from 7 to 27, and allelic size ranged from 124 to 304 base pairs over all loci (Table 1). Number of alleles per locus ranged from 2 to 19 (Table 2). Of 72 tests performed, only five were out of HWE ($P < 0.05$; Table 2). No interannual genetic variation was detected in any population ($P > 0.05$), so years were combined for populations with multiple collections for pairwise F_{ST} comparisons, bottleneck tests, and genetic diversity comparisons. All five populations were significantly genetically differentiated ($P < 0.001$). Pairwise F_{ST} values ranged between 0.0112 and 0.0570 (Table 3). The Black Lake population had higher average heterozygosity than Surprise Lake, Albert Johnson Creek, and Meshik Lake populations (Table 4), though this difference was not statistically significant in the paired *t* tests between pairs of loci

Table 2. Microsatellite data collection summary.

		Number of genotyped individuals per locus					
Population and year		*One102*	*One105*	*One108*	*One109*	*One110*	*One115*
Surprise Lake beaches							
2001	*n*	44	54	53	54	54	51
	A	10	3	15	10	14	13
	H–W	+	+	+	+	+	+
2002	*n*	42	41	43	43	43	40
	A	10	3	15	8	14	10
	H–W	–	+	+	+	+	+
2003	*n*	53	53	51	52	49	54
	A	11	3	13	10	13	13
	H–W	+	+	+	+	+	–
Years combined	*n*	139	148	147	149	146	145
	A	12	3	18	12	15	14
	H–W	+	+	+	+	+	–
Surprise Lake outlet							
2001	*n*	18	26	25	28	28	24
	A	9	3	11	11	16	13
	H–W	+	+	+	+	+	+
2002	*n*	35	43	43	43	41	41
	A	12	4	10	10	13	12
	H–W	+	+	+	+	+	+
2003	*n*	47	48	46	48	46	48
	A	9	5	10	8	13	12
	H–W	–	+	+	+	+	+
Years combined	*n*	100	117	114	119	115	113
	A	12	5	13	12	17	13
	H–W	–	+	+	+	+	+
Albert Johnson Creek							
2001	*n*	21	29	28	29	29	27
	A	9	2	10	10	12	13
	H–W	–	+	+	+	+	+
2002	*n*	27	26	34	34	30	25
	A	10	4	11	11	11	12
	H–W	+	+	+	+	+	+
2003	*n*	52	55	55	56	54	51
	A	11	4	10	12	18	15
	H–W	+	+	+	+	+	+
Years combined	*n*	89	85	100	101	95	88
	A	14	4	12	12	19	15
	H–W	+	+	+	+	+	+
Black Lake							
2002	*n*	40	50	48	49	50	45
	A	11	4	16	12	14	16
	H–W	+	+	+	+	+	+
2003	*n*	40	43	44	43	43	38
	A	12	4	16	12	17	12
	H–W	+	+	+	+	+	+
Years combined	*n*	91	97	108	104	107	99
	A	13	5	18	13	19	16
	H–W	+	+	+	+	+	+
Meshik Lake							
2003	*n*	85	91	91	91	91	91
	A	11	4	14	11	13	15
	H–W	+	+	+	–	+	+

Note: *n*, number of individuals genotyped; *A*, number of alleles; H–W, Hardy–Weinburg equilibrium (+, no significant deviation; –, significant deviation; $\alpha = 0.05$).

Table 3. Pairwise F_{ST} values ($P < 0.00001$).

Population	SLO	AJC	BL	MESH
Surprise Lake beaches (SLB)	0.0112	0.0426	0.0184	0.0409
Surprise Lake outlet (SLO)		0.0385	0.0200	0.0473
Albert Johnson Creek (AJC)	0.0385		0.0341	0.0570
Black Lake (BL)	0.0200	0.0341		0.0375
Meshik Lake (MESH)	0.0473	0.0570	0.0375	

Table 4. Sample size, expected heterozygosity, observed heterozygosity, mean number of alleles per population, and *M* values including and excluding *One110*.

Population	Sample size	H_e	H_o	No. of alleles	*M* values
Surprise Lake beaches	151	0.8094	0.7919	12.33	0.923
Surprise Lake outlet	120	0.8056	0.8059	12.00	0.915
Albert Johnson Creek	119	0.7951	0.7925	12.67	0.880
Black Lake	95	0.8261	0.8325	14.00	0.936
Meshik Lake	91	0.7967	0.7982	11.33	0.900

Table 5. Population comparisons of expected heterozygosity and *P* values (initial $\alpha = 0.0083$).

Comparison	Paired mean difference	*P*
Black Lake vs.		
Albert Johnson Creek	0.0309	0.0235
Meshik Lake	0.0295	0.2929
Surprise Lake outlet	0.0205	0.3203
Surprise Lake beaches	0.0167	0.3867
Albert Johnson Creek vs.		
Surprise Lake beaches	0.0142	0.4785
Surprise Lake outlet	0.0104	0.6152

(Table 5). No locus pairs exhibited genotypic disequilibrium after correcting for multiple comparisons (Rice 1989).

In the unrooted neighbor-joining tree based on Cavalli-Sforza and Edwards' chord distances, Albert Johnson Creek sockeye formed a group separate from all other study populations with 100% bootstrap support (Fig. 2). Multiple sampling years of the same locations grouped together with 57%–100% bootstrap support. The caldera populations, Surprise Lake beaches and Surprise Lake outlet, formed a group with 96% bootstrap support. Meshik Lake and Albert Johnson Creek populations formed a weakly supported group with 36% bootstrap support. Although NJ trees of this type lack statistical rigor, the F_{ST} values obtained through ARLEQUIN largely reflect relationships depicted in the tree.

No strong evidence of a bottleneck in the extant caldera populations was detected. Heterozygosity excess was significant in all five populations under the IAM (all populations $P = 0.007$), but not under the SMM ($P = 0.945–0.992$). No mode shift in allele frequencies was detected in any population (Fig. 3). Compared with Black Lake sockeye (i.e., the population with the greatest number of alleles), pairwise comparisons detected reduced allelic richness in the sockeye of Surprise Lake beaches but not Surprise Lake outlet (Table 6). However, when the Albert Johnson Creek population was the standard of comparison, neither Surprise Lake beaches nor Surprise Lake outlet populations showed any reduction in allelic richness (Table 6). Results for *M* values were reported excluding *One110* because of the two-base-pair variant detected in this locus (Garza and Williamson 2001). *M* values were all well above the conservative significance threshold of $M = 0.68$ (Garza and Williamson 2001) and ranged between 0.880 and 0.936 (Table 4). Results including *One110* were still well above the significance threshold ($M = 0.814–0.854$).

Fig. 2. An unrooted neighbor-joining tree based on Cavalli-Sforza and Edwards' chord distance: SLB, Surprise Lake beaches; SLO, Surprise Lake outlet; BL, Black Lake; MESH, Meshik Lake; AJC, Albert Johnson Creek. The numbers represent the percent of 2000 trees that supported the node.

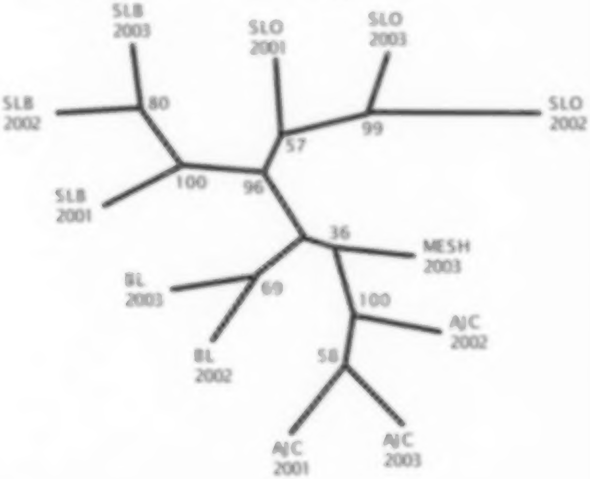

Discussion

Our hypothesis that Albert Johnson Creek riverine sockeye colonized the caldera and rapidly adapted a lake-type life history is not consistent with the data. Black Lake sockeye were a more likely source for the caldera population. In addition, there is little genetic evidence for a bottleneck associated with colonization in the caldera populations.

Fig. 3. Allele class frequency distribution for each population.

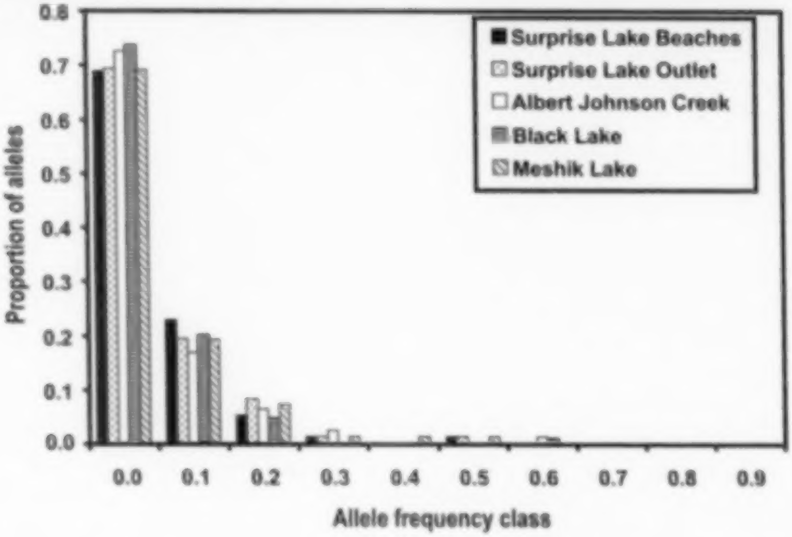

Table 6. Population comparisons of allelic richness and P values (bold = significant; initial α = 0.0083).

Comparison	Paired mean difference	P
Black Lake vs.		
Surprise Lake beaches	2.359	**0.0008**
Meshik Lake	2.493	0.0165
Surprise Lake outlet	2.255	0.0337
Albert Johnson Creek	1.611	0.1437
Albert Johnson Creek vs.		
Surprise Lake outlet	0.644	0.2264
Surprise Lake beaches	0.747	0.5119

Microsatellite polymorphism

The levels of allelic variability found in populations in this study were within the normal range of variation described previously for Bristol Bay sockeye salmon populations (Habicht et al. 2004; Olsen et al. 2004) with the exception of *One110*. This locus exhibited more variability than previously reported because of a two-base-pair variant that is present in all of the Pacific Ocean populations sampled in our study. This variant was not reported by other investigators.

Colonizing population of the caldera

Beacham et al. (2004) found a riverine population that grouped closely with three upriver lake-type populations in a NJ tree based on Cavalli-Sforza and Edwards' chord distance. They also found that riverine populations had more alleles and increased heterozygosity compared with lake-type populations in the same drainage. In the present study, we found the caldera populations to be more genetically similar to a lake-type population in an adjacent drainage, Black Lake, than to a riverine population in the same drainage (Albert Johnson Creek). We also found that numbers of alleles and observed levels of heterozygosity were not significantly higher for riverine sockeye than for lake-type sockeye in this system.

The caldera populations are more genetically similar to Black Lake sockeye than Albert Johnson Creek or Meshik Lake populations, despite the fact that Albert Johnson Creek is within the Aniakchak Drainage. Several circumstances could explain this pattern. First, the actual colonizing population may have been a riverine population that was not included in the populations surveyed. However, Albert Johnson Creek contains the only known riverine sockeye in Aniakchak National Monument and Preserve, and there are no other documented riverine populations within 250 km of the Aniakchak River mouth. Second, Albert Johnson Creek sockeye may stray less than typical riverine sockeye. Albert Johnson Creek is spring fed, which differs from many studied riverine systems in which sockeye spawn in glacial runoff habitat (Gustafson and Winans 1999). Quinn (1984) found that lake-type sockeye that spawn in glacially influenced habitats were more likely to stray than lake-type sockeye that spawn in streams with less year-to-year variability in habitat quality. Third, even if Albert Johnson Creek individuals strayed to the Caldera, they may be maladapted to this new and different environment and unable to successfully colonize. Fourth, straying in riverine sockeye populations may occur frequently among riverine populations but rarely with lake-type populations, as suggested by Gustafson and Winans (1999). Fifth, Black Lake sockeye were sampled on a single day as they entered Black Lake at the outlet. Black Lake is a silty, shallow lake that is not conducive to beach spawning, but there are multiple tributary spawning aggregates identified (Phinney 1970). The vast majority of these identified spawning populations are in the Alec River drainage on the east side of Black Lake (G. Ruggerone, Natural Resources Consultants Inc., 1900 West Nickerson Street, Suite 207, Seattle, WA 98119, USA, personal communication, 2004). This drainage is fed from snowmelt runoff and may have variable year-to-year flow. These sockeye may exhibit an increased straying rate compared with that of other lake-type populations in response to this habitat variability. Sixth, Black Lake contains a much larger population of sockeye. The annual escapement at Black Lake is on the order of a million fish, whereas aerial surveys of the Aniakchak River drainage indicate typical returns for Albert Johnson Creek, the Surprise Lake Outlet, and the Surprise Lake Beaches of fewer than 10 000 fish each. If the Black Lake population has a greater than typical lake-type straying rate in addition to a very large population size, it may exert a powerful genetic influence through migration to the Aniakchak drainage, despite the geographic distance between these drainages. This influence may overwhelm migrants originating from Albert Johnson Creek, which is a much smaller population in nonglacially influenced habitat.

These results suggest that lake-type populations may not always be evolutionary dead ends. Large lake-type populations may also be the colonizers of newly accessible habitats. Our results, unlike previously published accounts (Wood 1995; Beacham et al. 2004, 2006*b*), suggest that riverine sockeye may not be fully responsible for the long-term persistence of this species over evolutionary time. The interaction of both of these life history strategies working in concert may contribute to long-term persistence through oscillating climate patterns. Wood (1995) suggested that although all extant populations are important, riverine sockeye should receive special conservation emphasis compared with lake-type sockeye because of their colonizing role. Beacham et al. (2006*a*), as well as the results of this study, question the universal colonization role of riverine sockeye. We suggest that lake-type populations may also colonize new habitats. Thus managers and investigators must consider multiple pathways in sockeye colonization.

Bottlenecks and geologic activity

The results for heterozygosity excess under the two mutation-model assumptions (IAM and SMM) were contradictory. Microsatellites, in general, and tetranucleotide repeat markers, in particular, which were the basis of the present study, are expected to conform closer to the SMM (Shiver et al. 1993). Using the SMM, no heterozygosity excess was depicted. Also, all five of the study populations, including Black Lake, exhibited significant heterozygosity excess under the IAM. This contradicted all other bottleneck measures, indicating that this mutation model may not be appropriate for the markers used in this study. Taken together, these results indicate that the caldera populations did not go through a bottleneck as a result of the 1931 eruption (15 generations ago).

The reduced allelic richness in the Surprise Lake beach spawning population in relation to Black Lake sockeye may be an effect of (*i*) a bottleneck after the much larger eruption that occurred 500 years ago (100 generations ago), (*ii*) the original colonization after the flood (360 generations ago), (*iii*) the tendency for larger populations to exhibit higher genetic diversity (Wright 1940; Rosensweig 1995; Vellend 2003), or (*iv*) the result of the 300 m elevation climb that is necessary to reach the caldera. Habicht et al. (2004) found that populations above migration barriers (waterfalls and rapids) exhibited reduced heterozygosity compared with populations below the barriers, but neither of the caldera populations had significantly lower allelic richness compared with that of Albert Johnson Creek. This test for genetic bottlenecks is the only test of the five tests used in this study that involved comparison with another population, and results could vary depending on the population chosen for the comparison.

The lack of strong evidence for recent bottlenecks in the caldera populations is surprising in a system with recent volcanic disturbance. Our results differed from those obtained by Ramstad et al. (2004) in an analysis of Lake Clark sockeye (another drainage in southwestern Alaska). Lake Clark was formed after a glacial retreat 12 000 – 15 000 bp (Stilwell and Kaufman 1996), though at least one population may have been established only 100–200 bp (Ramstad et al. 2004). Six out of 11 populations surveyed had reduced *M* values, and the investigators attributed this reduction, along with reduced allelic diversity, to founder effects (Ramstad et al. 2004).

Withler et al. (2000) found no evidence to support a substantial genetic effect of rock slides that severely disrupted sockeye runs in a Fraser River drainage, British Columbia, between 1913–1914. These authors state: "… it is not clear whether the apparent lack of genetic bottlenecks is due to the fact that population sizes did not become as small as estimated after the rockslides, whether effective population sizes were bolstered by increasing gene flow among streams at low fish densities, or whether rapid expansion of population sizes once recovery was initiated prevented a great loss of genetic diversity (p. 1996)". Any one of these situations could apply to the sockeye that spawn at Surprise Lake beaches. Also, demographic bottlenecks caused by single-year events may be difficult to detect in sockeye salmon because of their overlapping generations (Waples 1991; Habicht et al. 2004).

This study of sockeye salmon in the Aniakchak River drainage sheds new light on genetic population structure found between different life history strategies and among populations. Populations that spawn in a volcanic caldera with documented eruptions 76 and 500 years ago left no genetic evidence of population bottlenecks. A large lake-type population appears to have greater genetic association with a population in a recently colonized lake than a more proximate riverine population. This result may indicate that large lake-type populations are more important in colonization events than previously reported.

Several other studies have documented subdivision of sockeye salmon populations over short time scales (e.g., Hendry et al. 2000; Woody et al. 2000; Kinnison et al. 2002), after natural colonization events (e.g., Wilmot and Burger 1985; Varnavskaya et al. 1994*b*; Habicht et al. 2004), and across major life history groupings (e.g., Wood 1995; Gustafson and Winans 1999; Beacham et al. 2006*a*). This is the first study to document population genetic structure covering all three aspects in the same group of sockeye salmon. Our study was conducted on a small number of populations at one locality, but our findings are similar to those of other recent research showing genetic differentiation between populations spawning in different habitats of the same lake (Beacham et al. 2004, 2006*b*). However, unlike the findings in the Beacham et al. (2006*b*) study, the Aniakchak riverine sockeye population did not exhibit increased heterozygosity and allelic richness compared with lake-type populations in the same area. Wood (1995) suggested that riverine sockeye populations stray more frequently and, therefore, are most likely to colonize new areas. Results from this study bring into question these expectations when looking at factors contributing to genetic population structure in sockeye salmon during colonization events. These results should broaden the colonization pathways considered by other investigators when looking at genetic population structure, sockeye colonization, and restoration in novel habitats.

Acknowledgements

We thank E. Wang, M. McBurney, J.E. Krebs, B. Girard, K. Bunney, T. Tingey, J.L. Miller, J. Marcus, J. Nelson, B. Chasco, G. Pappas, K. Bouwens, and the staff of Katmai National Park for field assistance. We also thank I. Williams, S. Graziano, K. Sage, J.R. Gust, S.L. Talbot, J.V. Jackson, J.R. Rearik, C.E. Zimmerman, T. Hamazaki, A.M. Ramey, E. Crispo, J. Meka, A.P. Hendry, J.E. Krebs, F.A. von Hippel, and the Evolution Discussion Group at Simon Fraser University (FAB-Lab) and two anonymous reviewers for timely reviews and advice. We thank I. Williams, S. Graziano, and G.K. Sage for help in the lab. We thank M.E. Whalen and D. Noon for help with graphics. We thank the National Park Service, USGS Alaska Science Center, Alaska EPSCoR, National Science Foundation, and University of Alaska Anchorage for funding.

References

Allendorf, F.W. 1986. Genetic drift and the loss of alleles versus heterozygosity. Zool. Biol. **5**: 181–190.

Beacham, T.D., McIntosh, B., and MacConnachie, C. 2004. Population structure of lake-type and river-type sockeye salmon in transboundary rivers of northern British Columbia. J. Fish Biol. **65**: 389–402.

Beacham, T.D., McIntosh, B., MacConnachie, C., Miller, K.M., Withler, R.E., and Varnavskaya, N. 2006*a*. Pacific rim populations structure of sockeye salmon as determined from microsatellite analysis. Trans. Am. Fish. Soc. **135**: 174–187.

Beacham, T.D., Varnavskaya, N.V., McIntosh, B., and MacConnachie, C. 2006*b*. Population structure of sockeye salmon from Russia determined with microsatellite DNA variation. Trans. Am. Fish. Soc. **135**: 97–109.

Burger, C.V., Spearman, W.J., and Cronin, M.A. 1997. Genetic differentiation of sockeye salmon subpopulations from a geologically young Alaskan lake system. Trans. Am. Fish. Soc. **126**: 926–938.

Burgner, R.L. 1991. Life history of sockeye salmon. *In* Pacific salmon life histories. *Edited by* C. Groot and L. Margolis. University of British Columbia Press, Vancouver, B.C. pp. 3–117.

Cavalli-Sforza, L.L., and Edwards, A.W.F. 1967. Phylogenetic analysis: models and estimation procedures. Evolution, **32**: 550–570.

Cornuet, J-M., and Luikart, G. 1996. Description and power analysis of two tests for detecting recent population bottlenecks from allele frequency data. Genetics, **144**: 2001–2014.

Dieringer, D., and Schlotterer, C. 2003. Microsatellite analyser (MSA): a platform independent analysis tool for large microsatellite data sets. Mol. Ecol. Notes, **3**: 167–169.

Eiler, J.H., Nelson, B.D., and Bradshaw, R.F. 1992. Riverine spawning by sockeye salmon in the Taku River, Alaska and British Columbia. Trans. Am. Fish. Soc. **121**: 701–708.

Felsenstein, J. 1985. Confidence limits on phylogenies: an approach using bootstrap. Evolution, **39**: 783–791.

Felsenstein, J. 1993. PHYLIP (Phylogeny Inference Package). Department of Genetics, University of Washington, Box 357360, Seattle, WA 98105, USA.

Foerster, R.E. 1968. The sockeye salmon, *Oncorhynchus nerka*. Fish. Res. Board Can. Bull. No. 162.

Garza, J.C., and Williamson, E.G. 2001. Detection of reduction in population size using data from microsatellite loci. Mol. Ecol. **10**: 305–318.

Gilbert, C.H. 1913. Age at maturity of the Pacific coast salmon of the genus *Oncorhynchus*. Ann. Rep. Brit. Col. Fish Dep. **1912**: 57–70.

Goudet, J.C. 1995. FSTAT. Version 1.2. A computer program to calculate F-statistics. J. Hered. **86**: 485–486.

Gustafson R.G., and Winans, G.A. 1999. Distribution and population genetic structure of river- and sea-type sockeye salmon in western North America. Ecol. Freshw. Fish, **8**: 181–193.

Habicht, C., Olsen, J.B., Fair, L., and Seeb, J.E. 2004. Smaller effective population sizes evidenced by loss of microsatellite alleles in tributary-spawning populations of sockeye salmon from the Kvichak River, Alaska drainage. Environ. Biol. Fishes, **69**: 51–62.

Hendry, A.P., Wenberg, J.K., Bentzen, P., Volk, E.C., and Quinn, T.P. 2000. Rapid evolution of reproductive isolation in the wild: evidence from introduced salmon. Science (Washington, D.C.), **290**: 516–519.

Hubbard, B.R. 1931. A world inside a mountain. Natl. Geogr. Mag. **60**: 319–345.

Hubbard, B.R. 1932. Aniakchak: the moon crater explodes. The Saturday Evening Post, 2 January 1932.

Imbrie, J., and Imbrie, K.P. 1979. Ice ages: solving the mystery. Harvard University Press, Cambridge, Mass.

Kinnison, M., Benzen, T.P., Unwin, M.J., and Quinn, T.P. 2002. Reconstructing recent divergence: evaluating nonequilibrium population structure in New Zealand chinook salmon. Mol. Ecol. **11**: 739–754.

Leider, S.A. 1989. Increased straying by adult steelhead trout, *Salmo gairdneri*, following the 1980 eruption of Mount St. Helens. Environ. Biol. Fishes, **24**: 219–229.

Luikart, G., Allendorf, F.W., Cornuet, J-M., and Sherwin, W.B. 1998. Distortion of allele frequency distributions provides a test for recent population bottlenecks. J. Hered. **89**: 238–247.

McGimsey, R.G., Waythomas, C.F., and Neal, C.A. 1994. High stand and catastrophic draining of intracaldera Surprise Lake, Aniakchak Volcano, Alaska. *In* Geologic studies in Alaska by the US Geological Survey. *Edited by* A.B. Till and T.E. Moore. US Geological Survey Bulletin No. B2107. pp. 59–71.

Middendorf, L.R., Bruce, J.C., Bruce, R.C., Eckles, R.D., Grone, D.L., Roamer, S.C., Sloniker, G.D., Steffens, D.L., Sutter, S.L., Brumbaugh, J.A., and Patonay, G. 1992. Continuous, on-line DNA sequencing using a versatile inferred laser scanner/electrophoresis apparatus. Electrophoresis, **13**: 487–494.

Milner, A.M., Knudsen, E.E., Soiseth, C., Robertson, A.L., Schell, D., Phillips, I.T., and Magnusson, K. 2000. Colonization and development of stream communities across a 200-year gradient in Glacier Bay National Park, Alaska, USA. Can. J. Fish. Aquat. Sci. **57**: 2319–2335.

Neal, C., McGimsey, R.G., Miller, T.P., Reichle, J.R., and Waythomas, C.F. 2001. Preliminary volcano-hazard assessment for Aniakchak Volcano, Alaska. US Geological Survey Open-File Report No. OF 00-0519.

Nei, M., Maruyama, T., and Chakraborty, R. 1975. The bottleneck effect and genetic variability in populations. Evolution, **29**: 1–10.

Olsen, J.B., Wilson, S.L., Kretchmer, E.F., Jones, K.C., and Seeb, J.E. 2000. Characterization of 14 tetranucleotide microsatellite loci derived from sockeye salmon. Mol. Ecol. **9**: 2155–2234.

Olsen, J.B., Habicht, C., Reynolds, J., and Seeb, J.E. 2004. Moderately and highly polymorphic microsatellites provide discordant estimates of populations divergence in sockeye salmon, *Oncorhynchus nerka*. Environ. Biol. Fishes, **69**: 275–285.

Page, R.D.M. 1996. TREEVIEW: an application to display phylogenetic trees on personal computers. Comput. Appl. Biosci. **12**: 357–358.

Pearce, N.J.G., Westgate, J.A., Preece, S.J., Eastwood, W.J., and Perkins, W.T. 2004. Identification of Aniakchak (Alaska) tephra in Greenland ice core challenges the 1645 BC date for Minoan eruption of Santorini. Geochemistry Geophysics Geosystems, **5**: Q03005, doi:10.1029/2003GC000672.

Phinney, D.E. 1970. Spawning ground catalog of the Chignik River system, Alaska. US Fish and Wildlife Service Data Report No. 41, Washington, D.C.

Pielou, E.C. 1991. After the ice age: the return of life to glaciated North America. The University of Chicago Press, Chicago, Ill.

Piry, S., Luikart, J., and Cornuet, J-M. 1998. BOTTLENECK: a program for detecting recent effective population size reductions from allele data frequencies. Available at http://ensam.inra.fr/~piry.bottleneck.pub.html.

Quinn, T.P. 1984. Homing and straying in Pacific salmon. *In* Mechanisms of migration in fishes. *Edited by* J.D. McCleave and G.P. Arnold. Plenum Press, New York. pp. 357–362.

Ramstad, K.M., Woody, C.A., Sage, G.K., and Allendorf, F.W. 2004. Founding events influence genetic population structure of sockeye salmon (*Oncorhynchus nerka*) in Lake Clark, Alaska. Mol. Ecol. **13**: 277–290.

Raymond, M., and Rousset, F. 1997. GENEPOP. Université de Montpellier II, 34095 Montpellier CEDEX 05, France.

Rice, W.R. 1989. Analyzing tables of statistical tests. Evolution, **43**: 223–225.

Ricker, W.R. 1950. Cycle dominance among Fraser sockeye. Ecology, **31**: 6–26.

Rosensweig, M.L. 1995. Species diversity in time and space. Cambridge University Press, Cambridge, Mass.

Schneider, S., Kueffer, J.J-M., Roessli, D., and Excoffier, L. 1997. ARLEQUIN: an exploratory population genetics software environment. Available at http://anthropoligie.unig.ch/arlequin.

Scribner, K.T., Gust, J.R., and Fields, R.L. 1996. Isolation and characterization of novel microsatellite loci: cross-species amplification and population genetic applications. Can. J. Fish. Aquat. Sci. **53**: 833–841.

Semko, R.S. 1954. The stocks of West Kamchatka salmon and their commercial utilization. Izvestiia TINRO **41**: 3–109. [In Russian; English translation: Fish. Res. Board Can. Translation Series No. 288, 1960.]

Shiver, M., Jin, D.L., Chakraborty, R., and Boerwinkle, E. 1993. VNTR allele frequency distributions under the stepwise mutation model: a computer simulation approach. Genetics, **134**: 983–993.

Stilwell, K.B., and Kaufman, D.S. 1996. Late Wisconsin glacial history of the northern Alaska Peninsula, southwestern Alaska, USA. Arct. Alp. Res. **28**: 817–829.

VanderHoek, R., and Myron, R. 2004. Cultural remains from a catastrophic landscape: an archaeological overview and assessment of Aniakchak National Monument and Preserve. US Department of the Interior, National Park Service, Alaska Region, Katmai National Park and Preserve, King Salmon Mall, Suite 1, King Salmon, AK 99613, USA.

Varnavskaya, N.V., Wood, C.C., and Everett, R.J. 1994*a*. Genetic variation in sockeye salmon (*Oncorhynchus nerka*) populations of Asia and North America. Can. J. Fish. Aquat. Sci. **51**(Suppl. 1): 132–146.

Varnavskaya, N.V., Wood, C.C., Everett, R.J., Wilmot, R.L. Varnavsky, V.S., Midanaya, V.V., and Quinn, T.P. 1994*b*. Genetic differentiation of subpopulations of sockeye salmon (*Oncorhynchus nerka*) within lakes of Alaska, British Columbia, and Kamchatka, Russia. Can. J. Fish. Aquat. Sci. **51**(Suppl. 1): 147–157.

Vellend, M. 2003. Island biogeography of genes and species. Am. Nat. **162**: 358–365.

Waples, R.S. 1991. Genetic methods for estimating the effective size of cetacean populations. *In* Genetic ecology of whales and dolphins. *Edited by* A.R. Hoelzel. Rep. Int. Whal. Comm. (Spec. Iss. No. 13). pp. 279–300.

Waples, R.S., and Smouse, P.E. 1990. Gametic disequilibrium analysis as a means of identifying mixtures of salmon populations. Am. Fish. Soc. Symp. **7**: 439–458.

Wilmot, R.L., and Burger, C.V. 1985. Genetic differences among populations of Alaskan sockeye salmon. Trans. Am. Fish. Soc. **114**: 236–243.

Withler, R.E., Le, K.D., Nelson, R.J., Miller, K.M., and Beacham, T.D. 2000. Intact genetic structure and high levels of genetic diversity in bottlenecked sockeye salmon (*Oncorhynchus nerka*) populations of the Fraser River, British Columbia, Canada. Can. J. Fish. Aquat. Sci. **57**: 1985–1998.

Wood, C.C. 1995. Life history variation and population structure in sockeye salmon. *In* Evolution and the aquatic ecosystem: defining unique units in population conservation. *Edited by* J.L. Nielsen. Am. Fish. Soc. Symp. **17**: 195–216.

Wood, C.C., Riddell, B.E., and Rutherford, D.T. 1987. Alternative juvenile life histories of sockeye salmon (*Oncorhynchus nerka*) and their contribution to production in the Stakine River, northern British Columbia. *In* Sockeye salmon (*Oncorhynchus nerka*) population biology and future management. *Edited by* H.D. Smith, L. Margolis, and C.C. Wood. Can. Spec. Publ. Fish. Aquat. Sci. No. 96. pp. 12–24.

Wood, C.C., Riddell, B.E., Rutherford, D.T., and Withler, R.E. 1994. Biochemical genetic survey of sockeye salmon (*Oncorhynchus nerka*) in Canada. Can. J. Fish. Aquat. Sci. **51**(Suppl. 1): 114–131.

Woody, C., Olsen, A.J., Renolds, J., and Bentzen, P. 2000. Temporal variation in phenotypic and genotypic traits in two sockeye salmon populations, Tustumena Lake, Alaska. Trans. Am. Fish. Soc. **129**: 1031–1043.

Wright, S. 1940. Breeding structure of populations in relation to speciation. Am. Nat. **74**: 232–248.

Evidence for the existence of a native population of sockeye salmon (*Oncorhynchus nerka*) and subsequent introgression with introduced populations in a Pacific Northwest watershed

Ingrid B. Spies, Eric C. Anderson, Kerry Naish, and Paul Bentzen

Abstract: The Lake Washington watershed (Washington, USA) has been the recipient of numerous transplantations of nonnative *Oncorhynchus nerka* (both sockeye salmon and their landlocked form, kokanee) over the past century and currently contains self-sustaining populations of both ecotypes. Microsatellite DNA markers were used to identify native and introduced groups while characterizing population structure. This study confirmed that Baker Lake sockeye transplantations during the 20th century contributed to three current sockeye populations: Cedar River, Issaquah Creek, and Pleasure Point Beach in the Lake Washington watershed. Distinctive allele distributions at two loci, *One101* and *One114*, provide evidence that a fourth Lake Washington sockeye population, Bear Creek, is divergent from other Lake Washington sockeye and may be of substantially native origin despite heavy stocking activity in the watershed over the past century. Data from these loci also suggest the presence of native genes in populations that had been regarded as entirely of introduced origin.

Résumé : Le bassin versant du lac Washington (Washington, É.-U.) a reçu de nombreux empoissonnements d'*Oncorhynchus nerka* (tant des saumons rouges que des kokanis non anadromes) non indigènes depuis un siècle; aujourd'hui, il contient des populations autosuffisantes des deux écotypes. Des marqueurs microsatellites de l'ADN nous ont servi à identifier les groupes indigènes et introduits et à caractériser du même coup la structure des populations. Notre étude confirme que les empoissonnements de saumons rouges du lac Baker au cours du 20e siècle ont contribué aux trois populations actuelles de saumons rouges, celles de Cedar River, d'Issaquah Creek et de Pleasure Point Beach dans le bassin versant du lac Washington. Des distributions distinctes d'allèles à deux locus, *One 101* et *One 114*, donnent des indications de l'existence d'une quatrième population de saumons rouges au lac Washington, celle de Bear Creek, qui diverge des autres saumons rouges du lac Washington et qui peut avoir une importante origine indigène malgré les nombreuses activités d'empoissonnement dans le bassin versant au cours du dernier siècle. Des données provenant de ces locus indiquent aussi la présence de gènes indigènes dans ces populations qui ont été considérées comme étant d'origine entièrement extérieure.

[Traduit par la Rédaction]

Introduction

Introductions of nonnative species to new environments may result in a range of outcomes, such as failure to reproduce, establishment of self-sustaining populations, and interbreeding with wild conspecifics. Such effects are relevant to conservation and management groups interested in preventing loss of biodiversity, but these effects are difficult to predict. Difficulty in prediction is true in the case of Pacific salmon, despite a history of stock transplantations extending back to the 1870s (Moberly and Lium 1977).

The Lake Washington watershed of Washington State, USA (Fig. 1), represents one of only three known cases where sockeye have been successfully transplanted within their native range (Wood 1995). The watershed has a complex history of nonnative introductions of anadromous sockeye salmon (*Oncorhynchus nerka*) and its landlocked form, kokanee, throughout the last century and currently supports several self-sustaining populations of both sockeye and kokanee. Recorded sources of introductions into the Lake Washington watershed include sockeye from Baker Lake and Cultus Lake and kokanee from Lake Whatcom

---

Received 26 July 2006. Accepted 13 June 2007. Published on the NRC Research Press Web site at cjfas.nrc.ca on 31 August 2007.
J19443

I.B. Spies,[1,2] K. Naish, and P. Bentzen.[3] School of Aquatic and Fishery Sciences, University of Washington, Box 355020, Seattle, WA 98195-5020, USA.
E.C. Anderson. Southwest Fisheries Science Center, Fisheries Ecology Division, 110 Shaffer Road, Santa Cruz, CA 95060, USA.

[1] Corresponding author (e-mail: ingrid.spies@noaa.gov).

[2] Present address: Molecular Ecology Research Lab, NOAA Fisheries, Alaska Fisheries Science Center, 7600 Sand Point Way NE, Seattle, WA 98115, USA.

[3] Present address: Department of Biology, Dalhousie University, 1355 Oxford Street, Halifax, NS B3H 4J1, Canada.

Can. J. Fish. Aquat. Sci. **64**: 1209–1221 (2007) doi:10.1139/F07-086

Fig. 1. Sampling locations for *Oncorhynchus nerka*, sockeye salmon (S) and kokanee (K). Sampling sites within the Lake Washington watershed were (1) Bear Creek (S), (2) Laughing Jacobs (K), (3) Issaquah Creek (S, K), (4) Pleasure Point Beach (S), (5) Wetland 79 (S), and (6) Cedar River (S). Locations sampled outside the watershed were (7) Cultus Lake (S), (8) Lake Whatcom (K), (9) Baker Lake (S), and (10) Lake Iliamna, Alaska (S). Other landmarks are (*a*) Lake Washington, (*b*) Lake Sammamish, (*c*) Lake Washington Ship Canal, and (11) North Creek.

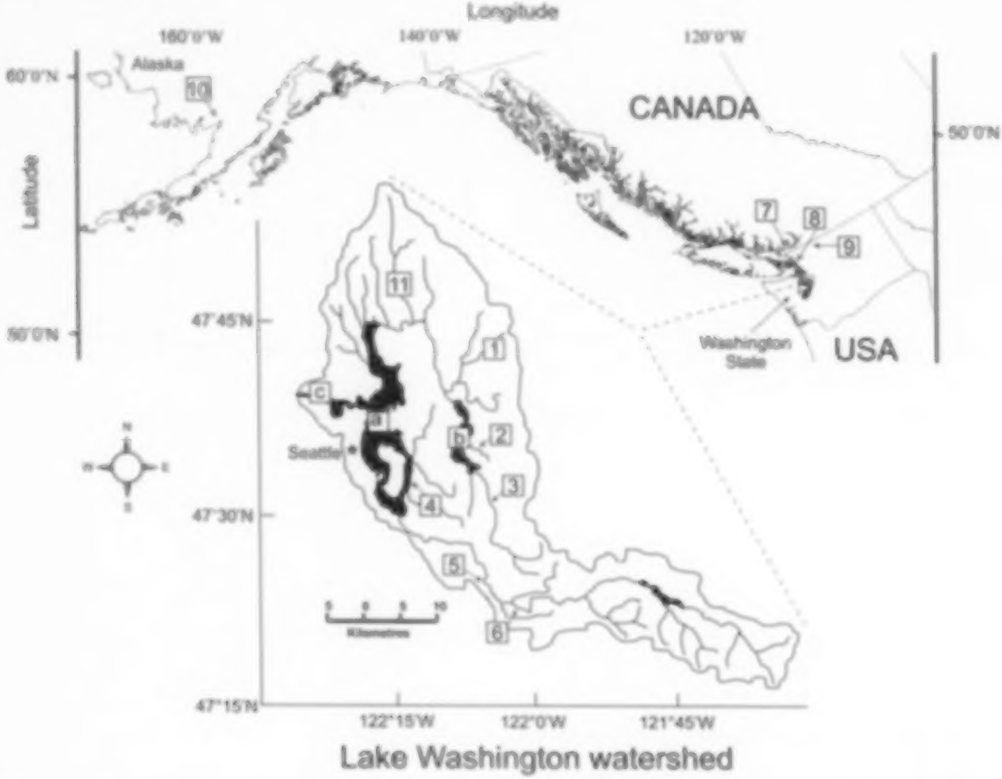

(Fig. 1). Sockeye in the watershed currently spawn in several locations, including the Cedar River at the south end of Lake Washington, Issaquah Creek at the south end of Lake Sammamish, Bear Creek at the north end of the drainage, and Pleasure Point Beach in Lake Washington.

Historical records and genetic data indicate that the kokanee currently existing in the watershed are of native origin (Pfeifer 1992; Young et al. 2004); however, the origin of sockeye in the watershed is not as clear. In 1940, over 400 sockeye returned to the Cedar River and 9000 returned to Issaquah Creek; however, the distribution of sockeye populations in the Lake Washington watershed prior to 1940 is uncertain (Gustafson et al. 1997; Anderson 1999; Hendry et al. 1996). Several studies near the end of the 19th century reported limited numbers of anadromous sockeye in the region (Evermann and Meek 1898; Rathbun 1900), while another study failed to find any (Hammond 1886). Prior to the construction of the Lake Washington ship canal in 1917, spring flooding on the Cedar River commonly caused the Black River to back up into the south end of Lake Washington at the lake outlet, which may have inhibited smolt outmigration. After 1917, the Cedar River was rerouted to flow into Lake Washington, the Black River dried up, and the ship canal became the only route for salmon to migrate between the Pacific Ocean and the Lake Washington watershed (Gustafson et al. 1997). Sockeye salmon were stocked in the Lake Washington watershed as early as 1917, but the majority came from the Baker Lake system between 1935 and 1954. During this time, 1 066 000 fry and fingerling sockeye were transplanted into the Cedar River, 576 000 into Bear Creek, 1 613 000 into Issaquah Creek, 41 000 into Lake Washington, and 24 000 into North Creek (Fig. 1). Between 1917 and 1979, 42 336 kokanee were transplanted into Lake Washington from Lake Whatcom, and between 1977 and 1979, 3765 sockeye fry were transplanted into Lake Washington from an unknown location (Kemmerich 1945; Pfeifer 1992).

Three allozyme studies that examined the origin of sockeye in the Lake Washington watershed (Seeb and Wishard 1977; Hendry et al. 1996; Gustafson et al. 1997) concluded that contemporary sockeye populations in the watershed are probably of two origins. Owing to their similarity to Baker Lake sockeye, Cedar River sockeye were believed to have originated from introductions of Baker Lake sockeye. Conversely, sockeye spawning in Bear Creek and its tributaries were judged to be of native origin because they were genetically distinct from recorded sources of introductions (Baker Lake and Cultus Lake sockeye and Lake

Table 1. Sockeye salmon (*Oncorhynchus nerka*) and kokanee (landlocked sockeye) samples used for genetic analyses in this study.

Collection site (abbreviation)	Classification	Form	n	Year collected
Bear Creek (BC)	Lake Washington watershed	Sockeye	48	1999
Cedar River (C93)	Lake Washington watershed	Sockeye	48	1993
Cedar River (C99)	Lake Washington watershed	Sockeye	48	1999
Issaquah Creek (IS)	Lake Washington watershed	Sockeye	47	1992, 1993
Pleasure Point Beach (PP)	Lake Washington watershed	Sockeye	39	2001
Wetland 79 (CS)[a]	Lake Washington watershed	Sockeye	48	2000
Issaquah Creek (IK)	Native kokanee	Kokanee	13	1993
Laughing Jacobs Creek (LJK)	Native kokanee	Kokanee	48	2000
Lake Iliamna (AK)	Out-group	Sockeye	48	2000
Baker Lake (BK)	Putative donor population	Sockeye	48	1992, 1993
Cultus Lake (CU)	Putative donor population	Sockeye	45	1992
Lake Whatcom (WH)	Putative donor population	Kokanee	48	1999

[a] A side channel of Cedar River.

Whatcom kokanee) and from other Lake Washington sockeye populations, but genetically similar to native kokanee.

The possibility that a native sockeye population persists in Lake Washington after several million nonnative sockeye introductions and major physical changes to the drainage (Gustafson et al. 1997) over the past century is intriguing on biological, management, and historical levels. In 1997, a biological review team concluded that available evidence was insufficient to determine evolutionarily significant unit (ESU) status of sockeye from Bear Creek (Gustafson et al. 1997). To examine this question, we assessed genetic variation at 14 microsatellite loci, a marker type that commonly exhibits many more alleles than allozymes and thus offers much more power to resolve relationships among populations (Avise and Walker 2000; Kalinowski 2002). The aim of this study was to resolve the relationships among Lake Washington drainage sockeye populations, and in particular, to elucidate the most likely origin of the Bear Creek population.

Materials and methods

Sample collection

Tissue samples were obtained from three categories of populations: Lake Washington drainage sockeye, native Lake Washington drainage kokanee, and donor populations of sockeye and kokanee that were the source of historical introductions to the Lake Washington drainage. Sockeye samples were obtained from five spawning locations within the Lake Washington watershed (Table 1): Bear Creek, Issaquah Creek, Pleasure Point Beach, Cedar River, and Wetland 79 (a side channel of the Cedar River). Samples of native kokanee were taken from two remnant native populations, Laughing Jacobs Creek (Young et al. 2004) and Issaquah Creek early run kokanee (Pfeifer 1992; Hendry et al. 1996). Samples were acquired from three donor populations, Baker Lake sockeye, Cultus Lake sockeye, and Lake Whatcom kokanee. Sockeye from Lake Iliamna, Alaska, were included in the study as an out-group for comparative purposes.

DNA extraction and microsatellite amplification

Samples consisted of muscle or fin, and most were stored in 95% nondenatured ethanol prior to DNA extraction. Baker Lake, Issaquah Creek, and Cedar River (1993) samples were taken from frozen tissue archived at the University of Washington, Seattle, Washington. Cultus Lake samples were extracted using Chelex 100 (Sigma-Aldrich, St. Louis, Missouri), desiccated, then resuspended in low TE buffer (10 $\text{mmol}\cdot\text{L}^{-1}$ Tris–HCl, 0.1 $\text{mmol}\cdot\text{L}^{-1}$ EDTA, pH 8.0) prior to analyses; DNA from all other samples was extracted using Qiagen DNeasy 96-well silica membrane-based kits, according to manufacturer's instructions (Qiagen, Valencia, California). DNA samples were diluted to approximately 12–50 $\text{ng}\cdot\mu\text{L}^{-1}$ with low TE (10 $\text{mmol}\cdot\text{L}^{-1}$ Tris–HCl, 0.1 $\text{mmol}\cdot\text{L}^{-1}$ EDTA, pH 8). The polymerase chain reaction (PCR) was used to amplify the following 14 microsatellite loci: *One1*, *One2*, *One8*, *One11*, (Scribner et al. 1996); *Ssa85* (O'Reilly et al. 1996); *Ots103* (Beacham et al. 1998); *Omy77* (Morris et al. 1996); *Ots3* (Banks et al. 1999); *Ots107* (Nelson and Beacham 1999); and *One101*, *One108*, *One109*, *One112*, and *One114* (Olsen et al. 2000). Reactions were carried out in 10 μL volumes and consisted of ~100 ng template, 50 $\text{mmol}\cdot\text{L}^{-1}$ KCl, 10 $\text{mmol}\cdot\text{L}^{-1}$ Tris–HCl, 0.1% Triton® X-100, 0.2 $\text{mmol}\cdot\text{L}^{-1}$ each dNTP, 10 $\text{pmol}\cdot\text{L}^{-1}$ each primer (forward primer 5′ end fluorescently labeled), and 1 U Promega *Taq* (1 U = 16.67 nkat) (Promega Corp., Madison, Wisconsin). In addition, for all loci 3.0 $\text{mmol}\cdot\text{L}^{-1}$ $MgCl_2$ was used, except for *Omy77* and *Ots107*, which were amplified using 1.5 $\text{mmol}\cdot\text{L}^{-1}$ $MgCl_2$. Annealing temperatures (T_M) varied among loci: 47 °C (*Omy77* and *Ots107*), 51 °C (*One114* and *Ots3*), 56 °C (*One101*, *One108*, *One109*, and *One112*), 58 °C (*One1*, *One2*, *One8*, *One11*, and *Ots103*), and 60 °C (*Ssa85*). The following PCR profile was used for all loci: 1 cycle of 94 °C (2 min); 5 cycles of 94 °C (1 min) + $[(T_M + 5\ ^\circ\text{C})(1\ \text{min} - 1\ ^\circ\text{C per cycle}) + 72\ ^\circ\text{C}]$ (1 min); 25 cycles of 94 °C (30 s) + (T_M) (30 s) + 72 °C (30 s); 1 cycle of 72 °C (10 min).

Genotyping was conducted with a MegaBACE 1000 automated sequencer (Amersham Pharmacia Biotech, Inc., Piscataway, New Jersey) according to manufacturer's protocols using a 900 base pair (bp) molecular weight standard and Genetic Profiler software (Molecular Dynamics™,

Table 2. Allele numbers (A), sample sizes (n), expected and observed heterozygosity (H_E and H_O), and P_{HWE} (probability after test for goodness of fit to Hardy–Weinberg equilibrium) for 12 *Oncorhynchus nerka* populations.

Locus		BL (S)	BC (S)	C93 (S)	C99 (S)	CU (S)	PP (S)	IK (K)	IS (S)	AK (S)	LJ (K)	WH (K)	CS (S)
One112	n	47	33	48	48	34	37	13	48	47	46	41	45
134–242	A	10	14	17	19	4	14	9	19	20	13	14	16
H_O: 0.823	H_E	0.80	0.88	0.89	0.89	0.39	0.88	0.85	0.90	0.87	0.85	0.88	0.88
A = 28	H_O	0.74	0.88	0.90	0.88	0.47	0.92	0.85	0.94	0.83	0.89	0.90	0.96
	P_{HWE}	0.529	0.437	0.925	0.283	0.891	0.096	0.178	0.539	0.617	0.003*	0.448	0.555
One114	n	47	44	34	43	35	35	12	48	45	42	46	48
206–304	A	14	29	19	23	16	19	10	19	18	15	16	19
H_O: 0.877	H_E	0.88	0.95	0.92	0.92	0.91	0.92	0.81	0.91	0.93	0.87	0.91	0.92
A = 40	H_O	0.83	0.93	0.94	0.91	0.83	1.00	0.83	0.94	0.93	0.90	0.91	0.92
	P_{HWE}	0.164	0.006	0.324	0.179	0.118	0.002*	0.768	0.642	0.631	0.062	0.670	0.360
Ots3	n	45	44	48	43	39	35	13	48	46	47	48	48
75–107	A	5	6	5	6	7	5	3	9	4	4	7	7
H_O: 0.502	H_E	0.69	0.60	0.62	0.63	0.67	0.58	0.21	0.63	0.14	0.29	0.42	0.65
A = 13	H_O	0.58	0.43	0.58	0.58	0.64	0.77	0.23	0.46	0.15	0.21	0.35	0.63
	P_{HWE}	0.010	0.007	0.192	0.516	0.122	0.000*	1.000	0.029	1.000	0.021	0.137	0.859
One101	n	48	45	48	43	36	31	13	48	36	47	45	48
148–368	A	18	25	34	27	28	25	13	22	26	21	41	29
H_O: 0.930	H_E	0.90	0.93	0.96	0.92	0.95	0.94	0.89	0.93	0.94	0.90	0.96	0.92
A = 73	H_O	0.96	0.93	0.88	0.93	0.89	0.94	1.00	0.94	0.86	0.94	0.96	0.90
	P_{HWE}	0.618	0.777	0.130	0.919	0.177	0.044	0.903	0.604	0.102	0.074	0.165	0.422
Omy77	n	47	43	47	47	43	32	12	47	47	32	46	45
92–138	A	5	10	6	10	6	8	5	9	4	6	10	9
H_O: 0.723	H_E	0.61	0.87	0.77	0.87	0.57	0.77	0.75	0.85	0.52	0.70	0.84	0.85
A = 18	H_O	0.62	0.81	0.77	0.83	0.60	0.72	0.75	0.83	0.53	0.55	0.80	0.82
	P_{HWE}	0.864	0.449	0.947	0.229	0.550	0.192	0.054	0.916	1.000	0.011	0.152	0.647
Ots107	n	48	48	43	48	44	39	13	48	47	48	48	48
75–137	A	4	6	8	8	5	6	3	8	4	5	3	6
H_O: 0.399	H_E	0.45	0.50	0.51	0.48	0.23	0.56	0.41	0.64	0.16	0.23	0.56	0.53
A = 14	H_O	0.40	0.52	0.47	0.46	0.23	0.54	0.23	0.75	0.09	0.21	0.54	0.54
	P_{HWE}	0.026	0.888	0.235	0.624	0.133	0.107	0.077	0.768	0.003*	0.167	0.532	0.858
One1	n	46	43	48	47	37	36	12	48	45	45	45	47
106–114	A	2	3	3	3	1	3	2	4	2	3	3	3
H_O: 0.254	H_E	0.48	0.27	0.36	0.42	0.00	0.40	0.38	0.37	0.14	0.16	0.04	0.44
A = 4	H_O	0.48	0.30	0.33	0.40	0.00	0.44	0.33	0.33	0.16	0.18	0.04	0.38
	P_{HWE}	1.000	1.000	0.743	0.807	–	0.741	1.000	0.007	1.000	1.000	1.000	0.529
One11	n	47	46	48	37	45	36	13	44	44	45	47	44
128–154	A	3	4	3	6	6	4	4	3	6	5	3	3
H_O: 0.501	H_E	0.35	0.64	0.59	0.55	0.64	0.61	0.57	0.55	0.62	0.64	0.27	0.52
A = 10	H_O	0.45	0.63	0.56	0.57	0.49	0.69	0.62	0.52	0.59	0.60	0.28	0.50
	P_{HWE}	0.152	0.001*	0.860	0.342	0.000*	0.587	0.123	0.524	0.133	0.008	1.000	0.653

Table 2 *(concluded).*

Locus		BL (S)	BC (S)	C93 (S)	C99 (S)	CU (S)	PP (S)	IK (K)	IS (S)	AK (S)	LJ (K)	WH (K)	CS (S)
One2	n	46	44	48	47	43	35	13	45	45	44	43	46
230–286	A	7	11	11	13	10	11	6	14	8	10	8	11
H_O: 0.814	H_E	0.73	0.85	0.85	0.82	0.75	0.86	0.73	0.87	0.76	0.77	0.76	0.83
A = 15	H_O	0.78	0.89	0.88	0.87	0.70	0.94	0.92	0.91	0.80	0.70	0.86	0.80
	p_{HWE}	0.033	0.900	0.792	0.257	0.008	0.607	0.663	0.834	0.994	0.004*	0.001*	0.827
One8	n	48	45	48	48	43	39	13	43	46	45	46	48
188–232	A	7	12	12	11	10	11	4	12	12	9	7	12
H_O: 0.667	H_E	0.62	0.78	0.81	0.83	0.53	0.83	0.57	0.81	0.75	0.81	0.58	0.83
A = 19	H_O	0.63	0.76	0.85	0.92	0.42	0.92	0.54	0.79	0.72	0.73	0.67	0.83
	p_{HWE}	0.011	0.105	0.997	0.281	0.069	0.508	1.000	0.440	0.839	0.000*	0.961	0.715
Ots103	n	48	48	43	48	34	24	13	48	45	44	46	48
267–357	A	13	20	18	16	17	16	8	19	16	17	20	19
H_O: 0.885	H_E	0.83	0.93	0.91	0.89	0.90	0.86	0.75	0.90	0.91	0.88	0.94	0.87
A = 26	H_O	0.79	0.94	0.95	0.92	0.91	1.00	0.85	0.92	0.93	0.77	0.96	0.90
	p_{HWE}	0.679	0.256	0.808	0.032	0.615	0.004*	0.770	0.490	0.715	0.001*	0.874	0.489
Ssa85	n	47	28	42	47	36	25	11	42	27	45	47	44
128–206	A	13	12	15	15	10	14	12	16	13	17	16	16
H_O: 0.816	H_E	0.72	0.88	0.91	0.89	0.72	0.91	0.88	0.89	0.88	0.84	0.89	0.87
A = 31	H_O	0.68	0.86	0.90	0.83	0.64	0.92	0.91	0.90	0.78	0.82	0.72	0.93
	p_{HWE}	0.081	0.049	0.989	0.346	0.106	0.342	0.449	0.086	0.211	0.187	0.000*	0.545
One108	n	48	47	48	47	36	33	13	48	48	46	47	45
148–264	A	10	27	22	22	12	18	10	21	15	18	24	19
H_O: 0.864	H_E	0.84	0.94	0.90	0.90	0.78	0.91	0.86	0.92	0.88	0.90	0.93	0.90
A = 41	H_O	0.85	0.94	0.88	0.87	0.61	0.97	0.85	0.96	0.85	0.87	0.89	0.87
	p_{HWE}	0.757	0.649	0.347	0.093	0.019	0.037	0.236	0.451	0.472	0.111	0.337	0.178
One109	n	34	32	48	43	23	39	13	26	47	46	48	47
118–198	A	12	17	9	11	8	7	5	10	12	9	10	12
H_O: 0.705	H_E	0.75	0.90	0.70	0.73	0.65	0.64	0.66	0.76	0.87	0.76	0.80	0.77
A = 24	H_O	0.74	0.63	0.65	0.70	0.78	0.64	0.46	0.69	0.87	0.80	0.79	0.85
	p_{HWE}	0.062	0.000*	0.193	0.308	0.923	0.561	0.132	0.317	0.870	0.654	0.092	0.863

Note: Allele ranges and H_O for each locus and total number of alleles for that locus are given below locus names; p_{HWE} values representing significant ($p < 0.05$) HWE departures, after population-wide sequential Bonferroni correction for the number of loci scored in any given population, are represented by an asterisk. Abbreviations for the 12 populations are defined in Table 1. S, sockeye salmon; K, kokanee.

Fig. 2. Allele frequency histograms for (*a*) *One114* and (*b*) *One101*.

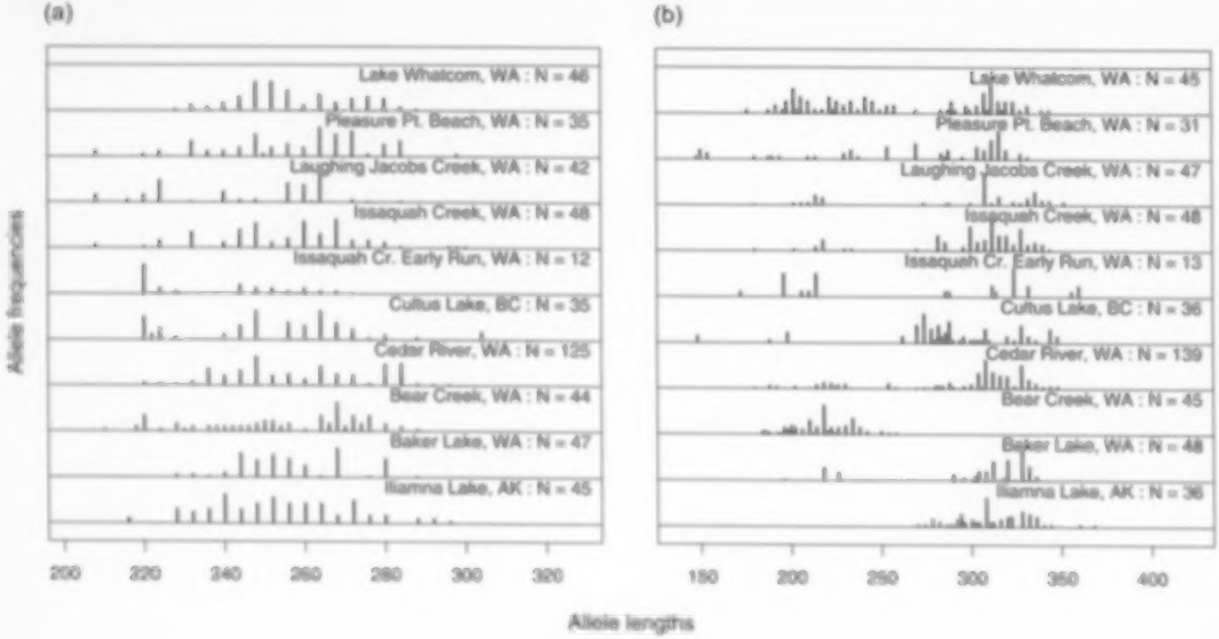

Amersham Pharmacia Biotech, Inc.). A microsatellite macro (Park 2001) was used in Excel (Microsoft Corp., Redmond, Washington) to identify duplicate samples or anomalous allele calls and to convert the data into GENEPOP 3.1 format (Raymond and Rousset 1995).

Data analyses

Tests for the presence of null alleles, upper allele dropout, or errors due to stutter in the data were performed using MICRO-CHECKER software (www.microchecker.hull.ac.uk), using the standard number of bootstrap simulations (1000) and a 95% confidence interval (Oosterhout et al. 2004). Observed and expected heterozygosities were calculated using Genetix 4.02 (Belkhir et al. 2000). The analog of Wright's F_{IS}, $\hat{f}$, was estimated using GENEPOP. Tests of linkage disequilibrium, two-tailed exact tests of departures from Hardy–Weinberg equilibrium (HWE) (Table 2), and exact tests of genic (allelic) differentiation were carried out for each locus and sample combination using GENEPOP with specified Markov chain parameters of 5000 dememorization steps followed by 500 batches of 2000 iterations per batch. Allele frequency data is shown for two loci of interest, *One114* and *One101* (Figs. 2*a* and 2*b*, respectively).

Three tests were employed to test whether any of the 14 microsatellite loci were subject to selection: an F_{ST} test implemented by FDIST2 software (Beaumont and Nichols 1996), a population-specific divergence F test implemented by the program DetSel 1.0 (Vitalis et al. 2003), and the lnRV test statistic (Schlötterer 2002). The FDIST2 F_{ST} test was used to determine whether loci showed unusually high or low levels of differentiation. The test generated limits within which 95% of F_{ST} estimates are expected to lie. These limits were calculated under the assumption of an infinite allele and island migration model with 60 000 iterations of 100 hypothetical populations with samples sizes of 50 individuals. The second test, the F test (Vitalis et al. 2003), uses a coalescent-based simulation approach to model a simulated population that splits in two and diverges by pure random drift to generate the expected joint distribution of two population-specific parameters, F_{pop1} and F_{pop2}. Loci that fall outside simulated joint distributions are potentially affected by selection. The following nuisance parameters, parameters defined by the user, were implemented: mutation rate (infinite alleles model), 0.01, 0.001, 0.0001; time since population split, 500 generations; population size before split, 500; ancestral population size, 500, 1000, 10 000; time since bottleneck event, 50, 100, 200 generations. Because such parameters are often unknown in population genetics, the model is robust to these nuisance parameters, and they are simply used to generate a similar number of allelic states as in the original model. Expected joint distributions of F_{pop1} and F_{pop2} were generated by performing 10 000 coalescent simulations for all 45 population pairs (the three Cedar River samples were pooled for a total of 10 population samples). The joint distribution of F_{pop1} and F_{pop2} becomes tighter as the number of alleles increases; thus loci with greater than 18 alleles were analyzed separately from those with fewer than 18 alleles. For the third test, the lnRV test statistic (Schlötterer 2002), the variance in repeat number of each microsatellite locus was generated using MICROSATELLITE ANALYSER software (Dieringer and Schlötterer 2003). The ratio in variance was calculated for all 45 possible population pairs for each microsatellite locus. Average and standard deviation were then calculated from

Fig. 3. Observed F_{ST} values for loci used in this study, plotted against expected heterozygosity (triangles). The median (middle line) and 95% confidence limits (upper and lower lines) for the expected relationship between heterozygosity and F_{ST} for microsatellites not subject to selection are shown, generated with the program FDIST.

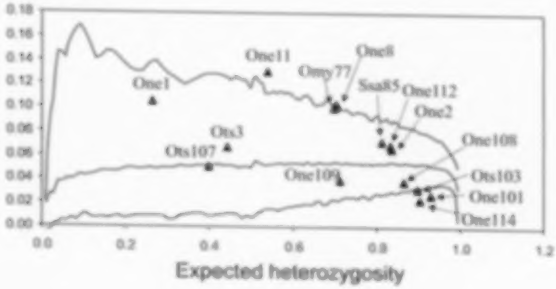

lnRV values, and the lnRV test statistic was applied to lnRV values at each locus to test the null hypothesis of neutral evolution at a significance level of $p = 0.05$.

Probability values for genic tests were summed over population pairs using Fisher's combined method (Sokal and Rohlf 1969). Pairwise $\hat{\theta}$ values (Reynolds et al. 1983), used as an estimator of F_{ST} (Weir and Cockerham 1984), were calculated using Genetix, and the significance of those estimates was assessed using 1000 data permutations. Hierarchical analysis of variance using AMOVA in Arlequin, ver. 2.000 (available at anthro.unige.ch/software/arlequin/) examined divergence among samples. Where appropriate, a Bonferroni correction was applied to provide an $\alpha = 0.05$ level for multiple tests (Rice 1989).

Two different statistical tests were devised to test the null hypothesis that sockeye in Bear Creek descended exclusively from Baker Lake transplants. The first such test used a parametric bootstrap method to compare the observed value of an F_{ST}-like statistic between Baker Lake and Bear Creek with the distribution expected under the null hypothesis. This method (described in Appendix A) accounts for the statistical variation in allele frequency differences arising both from sampling and from genetic drift. It is implemented in the computer program NERKA (available at http://swfsc.noaa.gov/staff.aspx?Division=FED&id=740).

The second test was performed by computing the probability of observing the bimodal allele frequency distribution seen in the combined samples from Baker Lake and Bear Creek at the *One101* locus. In brief, the alleles at *One101* were assumed to derive either from a short-allele lineage or a long-allele lineage, as suggested by the allele frequency ranges observed across all the populations (Fig. 2*b*). The frequencies of these two lineages in the ancestral Baker Lake population 50 years ago were modeled using their posterior distribution given the present-day sample from Baker Lake. Using simulation, we estimated the probability that a present-day sample drawn from a population that descended from such an ancestral Baker Lake population would carry no gene copies belonging to the long-allele class. Since no gene copies from the long-allele class are observed in the Bear Creek sample, this probability provides a measure of how improbable the data are, given a Baker Lake origin for Bear Creek, and hence it provides a measure of evidence against the hypothesis that the Bear Creek sockeye are derived from Baker Lake. The probability calculations rely on elementary properties of the neutral coalescent and are described in Appendix B.

Both the binomial frequency and the parametric bootstrap methods require that an independent estimate of the effective population size (N_e) of the Baker Lake and Bear Creek populations be available. Simulations in Anderson (1999) parameterized by run-size records for Baker Lake and Bear Creek populations indicate that the historical N_e of Baker Lake (since the time of Lake Washington introductions) is probably greater than 200, while the historical N_e of Bear Creek may be as high as 100, but is likely smaller than that (run-size data obtained from the Washington Department of Fish and Wildlife, 600 Capitol Way North, Olympia, WA 98501-1091, USA). A simpler approach, using arithmetic mean (N) and harmonic mean (N_h) population sizes for Baker Lake (1930–2004) and Bear Creek (1982–1996), yielded similar results. Shrimpton and Heath (2003) used temporal changes in allele frequency to estimate N_e/N and N_e/N_h for five stocks of upper Fraser River Chinook salmon (*Oncorhynchus tshawytscha*) and found that N_e/N values ranged from 0.021 to 0.566 and that N_e/N_h values ranged from 0.022 to 0.765. Applying the lower of these values to N and N_h yields conservative estimates of N_e. For Baker Lake, these estimates were $N_e = 511$ and $N_e = 214$, respectively, and for Bear Creek, they were $N_e = 311$ and $N_e = 180$, respectively. However, run-size data for Bear Creek sockeye is limited, and years with smaller return numbers would effectively lower N_e estimates; thus N_e is likely smaller than 180 for Bear Creek. For both statistical tests, assuming a smaller N_e makes the test more conservative (less likely to reject the null hypothesis). Thus, for the parametric bootstrap test, an N_e of 200 was used for Baker Lake and 120 for Bear Creek. For the binomial frequency test, an even more conservative estimate was used: 75 for Baker Lake and 25 for Bear Creek.

Results

The 14 loci used in this study exhibited a broad range of polymorphism, ranging from 4 to 73 alleles per locus across all populations, and observed heterozygosities ranged from 0.50 to 0.93 (Table 2). None of 92 tests for linkage disequilibrium between loci were significant ($p \leq 0.05$), indicating independence among genotypes at all loci. Significant deviations from HWE were detected in 13 of 168 tests, five more than expected by chance alone. Deviation was due to heterozygote deficiency in eight samples and heterozygote excess in five others. All loci and populations were considered in subsequent analyses, since no more than two populations per locus or four loci per population showed significant departures from HWE.

MICRO-CHECKER results showed evidence for null alleles at 9 out of 168 sample–loci combinations, with no particular locus showing evidence for null alleles in more than 2 out of 12 samples. At the 95% confidence interval, 8.4 positive results are expected by chance alone; thus, all loci were considered negative for the presence of null alleles.

Table 3. F_{ST} values estimated following Weir and Cockerham (1984).

	Bear Creek (S)	Cedar River (S)	Issaquah Creek (S)	Lake Iliamna (S)	Baker Lake (S)	Cultus Lake (S)	Issaquah Creek (K)	Laughing Jacobs Creek (K)	Lake Whatcom (K)
Pleasure Point (S)	0.027	0.009	0.015	0.052	0.064	0.068	0.083	0.055	0.064
Bear Creek (S)		0.026	0.024	0.048	0.085	0.085	0.060	0.050	0.035
Cedar River (S)			0.010	0.057	0.044	0.077	0.078	0.060	0.062
Issaquah Creek (S)				0.060	0.066	0.089	0.070	0.055	0.054
Lake Iliamna (S)					0.115	0.088	0.124	0.050	0.076
Baker Lake (S)						0.147	0.158	0.136	0.145
Cultus Lake (S)							0.156	0.108	0.115
Issaquah Creek (K)								0.089	0.090
Laughing Jacobs Creek (K)									0.068

Note: All data were significant ($p < 0.001$). S, sockeye salmon; K, kokanee.

Fig. 4. Parametric bootstrap test of common origin of Bear Creek and Baker Lake sockeye salmon (*Oncorhynchus nerka*) based on different effective population sizes (N_e). The region of the graph showing rejection of the null hypothesis at $p < 0.05$ is to the right of the 0.05 curve.

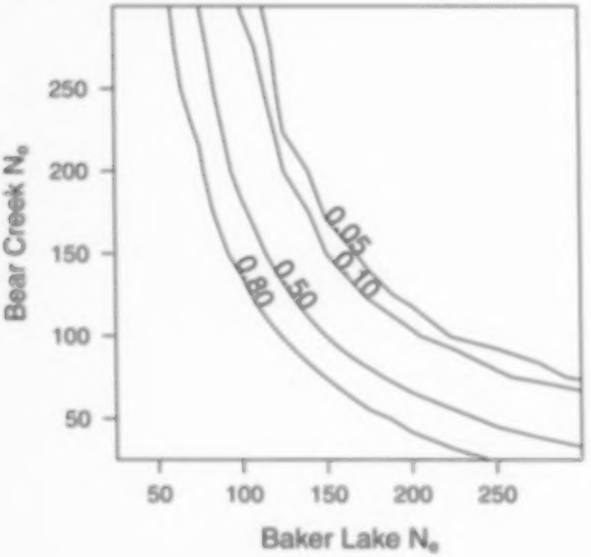

Tests for error due to stutter and upper allele dropout were negative in all cases.

The F_{ST} test of FDIST2 showed that three loci fell outside 95% confidence limits: *One101*, *One114*, and *One11* (Fig. 3). Loci suspected of being under selection with the population-specific divergence *F* test of DetSel differed from those in the FDIST2 analysis. Eleven of the fourteen loci fell outside of the joint distribution in more than 5% of the 45 simulations. The loci with the highest number of comparisons that fell outside of the joint distribution were *One8* (34/45), *Ssa85* (29/45), *One109* (26/45), *One112* (22/45), and *Ots103* and *One108* (both 17/45); all other loci were ≤10/45). Results from the lnRV test showed that none of the loci violated the null hypothesis of neutral evolution. For each microsatellite locus, there were 45 lnRV values. The largest number of significant lnRV values was at *One11*, which had seven significant lnRV values, followed by *One2* with six, *One108* with five, and *One107* with four. Because such a small proportion of lnRV values were significant at any one locus, no locus was considered to be under selection with the lnRV test statistic. If selection were acting on a locus, it is likely that this signal would be apparent using all three tests. However, since no one locus consistently tested positive for selection, no loci were discarded from further analyses because of selective pressures.

Exact tests of genic differentiation among temporally replicated samples in 1992 and 1993 showed that neither Issaquah Creek sockeye nor Baker Lake sockeye samples from those years displayed a significant difference in allele frequency over time at the 5% significance level ($p = 0.320$ for Issaquah Creek and 0.059 for Baker Lake), and samples were pooled in subsequent analyses. Pairwise genic tests revealed significant heterogeneity ($p < 0.05$) among the 12 samples listed in Table 1, with the exceptions of Cedar River 1999 vs. Cedar River 1993 ($p = 0.646$) and Cedar River 1999 vs. Wetland 79 (2000; $p = 0.117$). Although a third Cedar River comparison, Cedar River 1993 vs. Wetland 79, was significantly different ($p = 2.86 \times 10^{-5}$), they are both genetically homogeneous to Cedar River 1993, and for simplicity, the three Cedar River samples (1993, 1999, and Wetland 79) were combined in all subsequent analyses and referred to as the Cedar River sample for a total of 10 samples. All genic comparisons as well as all pairwise F_{ST} estimates among these 10 samples were significant ($p < 0.001$), and F_{ST} values ranged from 0.009 to 0.158 (Table 3).

The analysis of molecular variance (AMOVA) was used to determine whether there are significant differences between putative donor populations and Lake Washington sockeye populations believed to be descended from Baker Lake (Pleasure Point sockeye, Issaquah Creek Sockeye, and Cedar River sockeye). Cultus Lake sockeye were significantly different from this group ($p < 0.0001$), as was Lake Whatcom kokanee ($p = 0.00391$). However, Baker Lake sockeye were not significantly different from these Lake Washington sockeye ($p = 0.76246$).

Two loci, *One101* and *One114*, displayed strong allele frequency differences between Bear Creek and Baker Lake samples. At *One114*, Bear Creek alleles occurred primarily in 2 bp increments, whereas Baker Lake alleles occurred exclusively in 4 bp increments (Fig. 2*a*). Other *O. nerka* populations followed the tetranucleotide repeat pattern observed in Baker Lake, with the exception of a few rare alleles following the 2 bp pattern in Cedar River and Pleasure Point (Fig. 2*a*). At *One101*, Bear Creek allele sizes ranged from 184 to 258 bp, while the majority of allele sizes in the Baker Lake sample were between 290 and 336 bp (Fig. 2*b*). Other Lake Washington sockeye populations, notably Cedar River and Pleasure Point, also had small alleles not seen in the Baker Lake sample.

The parametric bootstrap test that indicated Bear Creek sockeye are descended from Baker Lake sockeye was sensitive to the assumptions made about the N_e of the populations. We therefore present the results of this test in terms of the p value as a function of the assumed N_e values (Fig. 4). Definitive N_e values are not known for these populations; thus, the data are presented within a range of reasonable estimates. With a conservative estimate of Baker Lake's N_e ($= 200$), this test would fail to reject the null hypothesis of common origin between Bear Creek and Baker Lake if Bear Creek's long-term N_e is ≥ 120, which is within the range of historical estimates.

The test based on the distribution of alleles at *One101* provided considerably more evidence against a Baker Lake origin for Bear Creek sockeye. Even with the very conservative assumption that Bear Creek has an historical N_e of 25 and Baker Lake of 75, the probability of observing zero alleles in the long allele category at locus *One101* in the Bear Creek sample was 0.0008. Since this test was performed on 1 of 12 loci that were examined for genetic variation between the populations, we computed the probability that we would see no Bear Creek samples out of 12 loci with zero long-class alleles. (This is analogous to a Bonferroni correction.) The resulting probability was $1 - (1 - 0.0008)^{12} = 0.0096$. This correction is also quite conservative. In summary, even with extremely conservative assumptions, there was lower than a 1 in 100 probability of observing no long-class alleles in Bear Creek, if the Bear Creek sample was derived from Baker Lake transplants.

Discussion

Fourteen microsatellite loci encompassing a total of 356 alleles were used to investigate the origins of sockeye salmon populations in the Lake Washington drainage. Contemporary sockeye populations were compared with three sources of *O. nerka* introductions to the watershed (Baker Lake sockeye, Cultus Lake sockeye, and Lake Whatcom kokanee), as well as to two native kokanee populations (Issaquah Creek early run and Laughing Jacobs Creek).

Loci did not show evidence for null alleles or upper allele dropout, were in linkage equilibrium, and displayed no significant deviations from Hardy–Weinberg expectations. One F_{ST} test for selective neutrality (FDIST2) suggested that three loci (*One114*, *One101*, and *One11*) might have been influenced by selection. It has been shown that FDIST2 does not account for cases where high mutation rates may depress F_{ST} values (Vitalis et al. 2003). The second test for selective neutrality, the population-specific divergence test (implemented in DetSel), suggested that a different set of loci were under selection, while a third test, the lnRV test statistic, demonstrated no evidence for selection in any locus. Disagreement among approaches has been observed in other data sets (e.g., Vasemagi et al. 2005); the most conservative approach to interpreting evidence for selection would be to select those loci that are detected using a range of tests (Beaumont 2005). Discrepancy among the three approaches suggests that the evidence for selection acting on these loci is not definitive; thus, we considered all loci in subsequent tests.

Overall, the data revealed significant genetic differentiation between all tributary and lake spawning sites for sockeye and kokanee in the drainage, and six of the seven temporal comparisons revealed that the differentiation is stable over time. Thus, whatever their origins, contemporary *O. nerka* in the Lake Washington drainage appear to form a series of discrete populations according to spawning location and life history type, a result consistent with previous allozyme studies. Within the drainage, the two kokanee populations were the most genetically divergent; the mean pairwise F_{ST} estimates between these populations and sockeye populations were 0.064, whereas sockeye populations were more closely related, with mean $F_{ST} = 0.019$. Potential explanations for this pattern include strong reproductive isolation between life history types, greater genetic drift associated with the kokanee populations (because of small population sizes), and possible differences in the historical origins of kokanee and sockeye populations.

In general, our results support conclusions from previous studies based on much more limited genetic data that the Cedar River, Pleasure Point, and Issaquah Creek sockeye populations are descended at least in large part from introductions of Baker Lake sockeye, and this conclusion is supported by the timing of reproduction in these populations. AMOVA results showed that Baker Lake sockeye are not significantly different from the Lake Washington sockeye populations (Pleasure Point, Issaquah Creek, and Cedar River); however, both Cultus Lake and Lake Whatcom samples were significantly different from these Lake Washington sockeye. Run timing also supports a Baker Lake origin; Cedar River sockeye enter fresh water between late June and August and spawn from September through December–January, which is similar to the migratory and reproductive timing of Baker Lake sockeye, whereas Cultus Lake sockeye enter fresh water in early October and spawn in late November, and Lake Whatcom kokanee spawn from late October through December. Studies have shown that run timing in sockeye has a genetic basis (Stewart et al. 2002), although it should be noted that variation in run timing may also reflect environmental differences.

The microsatellite data also supports the conclusions of previous studies that Bear Creek sockeye are genetically distinct from the other Lake Washington sockeye populations. Notable divergence was evident in pairwise estimates of F_{ST}, which were 0.024–0.027 (mean = 0.026) between Bear Creek and the other sockeye populations, whereas pairwise F_{ST} between Cedar River, Pleasure Point, and Issaquah Creek sockeye were 0.009–0.015 (mean = 0.011). Most significantly, Bear Creek displayed distinctive allele distributions at two microsatellite loci, *One114* and *One101*. At locus *One101*, Bear Creek alleles occurred exclusively in a size range (184–256 bp) that was very distinct from the 290–336 bp size range that accounted for nearly all the alleles in the Baker Lake sample. A statistical test based on simulations that accounted for genetic drift and sampling error under different scenarios for effective population size led us to conclude that the likelihood that the contrasting allele frequencies between Baker Lake and Bear Creek at *One101* resulted from genetic drift or a population bottleneck was very low, even when conservative assumptions were made about the historical effective sizes of the populations between the time of introductions and the present. Thus, evidence from microsatellite loci, based on several different analyses, strongly suggests that Bear Creek sockeye are of native ancestry.

Previous studies found a genetic similarity between Bear Creek sockeye and native kokanee populations and used that evidence to assert that Bear Creek sockeye are of native origin (Seeb and Wishard 1977; Hendry et al. 1996; Gustafson et al. 1997). However, microsatellite data do not indicate strong genetic similarity between these two groups. We present several explanations: first, small sampling size and small population size are likely to have inflated F_{ST} estimates associated with Issaquah Creek kokanee in this study. Second, the native kokanee populations we surveyed may have changed over time because of migration, genetic drift, or selection, and thus may not reflect the genetic profile of native kokanee as they existed in the past. Third, we did not have the opportunity to survey a broader range of native kokanee, given that many of the watershed's native kokanee populations have been extirpated. Interviews with Snoqualmie tribal elders (Pfeifer 1992) indicated that in 1900 there were substantial populations of kokanee in at least eight Lake Sammamish tributaries, enough for personal subsistence by Native Americans. Thus, even though Bear Creek sockeye do not show genetic similarity to the two native kokanee samples used in this study, they still appear to be of native rather than introduced origin, a conclusion that does not preclude the possibility that Bear Creek sockeye may the result of nonanadromous ancestry.

In general, we concur with previous analyses and offer the strongest evidence to date that Bear Creek sockeye have a native origin. However, our data, and in particular the evidence from microsatellite loci *One101* and *One114*, suggest further interactions between native and introduced populations. Although Bear Creek appears genetically distinct, the genetic differentiation between Bear Creek and the other Lake Washington sockeye populations (mean $F_{ST} = 0.026$) is less than what might be expected for populations descended from different sources. For example, this average value is less than that between the other Lake Washington sockeye populations and Baker Lake (mean $F_{ST} = 0.077$), despite the fact that those populations were apparently derived from the Baker Lake ~50 years ago. This relatively large F_{ST} value could be due to population bottlenecks and genetic drift that may have occurred since the population introductions. Likewise, the relatively small F_{ST} between Bear Creek and the other sockeye populations in the drainage could be explained by gene flow among Lake Washington drainage sockeye populations.

Allele frequency data at *One101* and *One114* show alleles in the Bear Creek sample that are not present in Baker Lake sockeye sample, but that are present to some extent in the other Lake Washington sockeye samples. Substantial gene flow of Baker Lake-origin genes into Bear Creek is belied by the absence of large Baker Lake-type alleles at *One101* in Bear Creek. We showed that the probability that Bear Creek sockeye descended from Baker Lake introductions is very low; this low probability extends equally to substantial descent from fish of indirect Baker Lake origin (i.e., the other sockeye populations in the drainage). Likewise, genetic drift seems unable to account for the presence of small size range (Bear Creek-type) alleles at low–moderate frequencies in the Lake Washington drainage sockeye populations, most notably Cedar River and Pleasure Point. An alternative explanation that appears consistent with the data is that there has been gene flow from the Bear Creek sockeye population into the other sockeye populations in the drainage. Such gene flow could account for the small *One101* alleles in Cedar River, Pleasure Point, and Issaquah Creek sockeye, as well as the presence in the same populations of some 2 bp alleles at *One114*. It would also promote the divergence of these populations from Baker Lake and increase their similarity to Bear Creek. This scenario of unidirectional gene flow from (native) Bear Creek sockeye into (introduced) sockeye populations elsewhere in the drainage seems unlikely from an ecological perspective, since one would expect gene flow to be bidirectional, but it appears to be the only scenario that is fully consistent with the genetic data. This explanation introduces a new perspective to the historical origins of sockeye salmon populations in the Lake Washington drainage. Instead of the recent paradigm that Lake Washington drainage sockeye are primarily derived from Baker Lake introductions, with some limited evidence of the persistence of native genes in a single lake tributary, our data suggest the prospect of a remarkably resilient native population that has not only resisted the genetic influx from introduced populations, but has actually introgressed unidirectionally into those populations. It should be noted that the native population in question need not exclusively comprise Bear Creek; it could include other sockeye aggregations not included in our study.

For fisheries management, the use of genetic markers offers insight into population structure as well as identification of native and introduced groups. The complex history in the Lake Washington drainage of habitat alterations, population introductions, genetic drift, and possible introgression among populations have all acted to obscure the origins of sockeye salmon populations in the drainage; nonetheless, genetic markers have consistently identified Baker Lake sockeye as a primary donor population for most Lake Washington sockeye populations. Similarly, both microsatellite and allozyme markers have provided evidence of unique attributes to the Bear Creek population that appear to point to a native origin. Our conclusions therefore support those of previous allozyme markers, but also provide indications of further complexity in the recent evolution of these populations that were unavailable from previous studies.

Acknowledgements

The authors thank Bruce Bachen and Rand Little at City of Seattle and the University of Washington School of Aquatic and Fishery Sciences for funding this research. I.S. was also supported by an H. Mason Keeler scholarship from the School of Aquatic and Fisheries Science. Bruce Bachen, Terry Beacham, Kurt Fresh, Julie Hall, Andrew Hendry, Jim Shaklee, and Jennifer Vanderhoof contributed samples.

References

Anderson, E.C. 1999. Inferring the ancestral origin of sockeye salmon, *Oncorhynchus nerka*, in the Lake Washington basin: a statistical method in theory and application. M.Sc. thesis, School of Aquatic and Fishery Sciences, University of Washington, Seattle, Wash.

Avise, J.C., and Walker, D. 2000. Abandon all species concepts? A response. Conserv Genet, **1**: 77–80.

Banks, M., Baldwin, M., Rashbrook, V., Fitzgerald, H., Blakenship, S., and Hedgecock, D. 1999. Isolation and inheritance of novel microsatellites in Chinook salmon (*Oncorhynchus tshawytscha*). J. Hered. **90**: 281–288.

Beacham, T., Margolis, L., and Nelson, R. 1998. A comparison of methods of stock identification for sockeye salmon (*Oncorhynchus nerka*) in Barkley Sound, British Columbia. North Pac. Anad. Fish. Comm. Bull. **1**: 227–239.

Beaumont, M. 2005. Adaptation and speciation: what can F_{st} tell us? Trends Ecol. Evol. **20**(8): 435–440.

Beaumont, M., and Nichols, R. 1996. Evaluating loci for use in the genetic analysis of population structure. Proc. R. Soc. Lond. B Biol. Sci. **263**: 1619–1626.

Belkhir, K., Borsa, P., Goudet, J., Chikhi, L., Bonhomme, F. 2000. GENETIX 4.02, logiciel sous Windows TM pour la genetique des populations. Laboratoire Genome, Populations, Interactions, CNRS UPR 9060, Universite de Montpellier II, Montpellier, France.

Dieringer, D., and Schlötterer, C. 2003. MICROSATELLITE ANALYSER (MSA): a platform independent analysis tool for large microsatellite data sets. Mol. Ecol. Notes, **3**(1): 167–169.

Evermann, B., and Meek, S. 1898. A report upon salmon investigations in the Columbia River Basin and elsewhere on the Pacific Coast in 1896. U.S. Fish Comm. Bull. **17**: 15–84.

Gustafson, R., Wainwright, T., Parker, L., and Waples, R. 1997. Status review of sockeye salmon from Washington and Oregon. US Department of Commerce, NOAA, NMFS, Seattle, Wash.

Hammond, J.P. 1886. Fish in Puget Sound. U.S. Fish Comm. Bull. **6**: 195–196.

Hendry, A.P., Quinn, T., and Utter, F.M. 1996. Genetic evidence for the persistence and divergence of native and introduced sockeye salmon (*Oncorhynchus nerka*) within Lake Washington, Washington. Can. J. Fish. Aquat. Sci. **53**: 823–832.

Kalinowski, S.T. 2002. How many alleles per locus should be used to estimate genetic distance? Heredity, **88**: 183–201.

Kemmerich, J. 1945. A review of the artificial propagation and transplantation of the sockeye salmon of Washington conducted by the federal government from 1896–1945. (Available from West Coast Sockeye Salmon Administrative Record, Environmental and Technical Services Division, National Marine Fisheries Service, 525 N.E. Oregon Street, Portland, OR 97232, USA.)

Moberly, S.A., and Lium, R. 1977. Japan salmon hatchery review. Fisheries, **2**: 2–7.

Morris, D., Richard, K., and Wright, J. 1996. Microsatellites from rainbow trout (*Oncorhynchus mykiss*) and their use for genetic study of salmonids. Can. J. Fish. Aquat. Sci. **53**: 120–126.

Nelson, R., and Beacham, T. 1999. Isolation and cross species amplification of microsatellite loci useful for study of Pacific salmon. Anim. Genet. **30**: 228–229.

Oosterhout, C.V., Hutchinson, W.F., Wills, D., and Shipley, P. 2004. MICRO-CHECKER: software for identifying and correcting genotyping errosr in microsatellite data. Mol. Ecol. Notes, **4**: 535–538.

O'Reilly, P.T., Hamilton, L., McConnell, S., and Wright, J. 1996. Rapid analysis of genetic variation in Atlantic salmon (*Salmo salar*) by PCR multiplexing of dinucleotide and tetranucleotide microsatellites. Can. J. Fish. Aquat. Sci. **53**: 2292–2298.

Olsen, J.B., Wilson, S., Kretschmer, E., Jones, K., and Seeb, J. 2000. Characterization of 14 tetranucleotide microsatellite loci derived from sockeye salmon. Mol. Ecol. **9**: 2185–2187.

Park, S.D.E. 2001. Trypanotolerance in West African cattle and the population genetic effects of selection. Ph.D. thesis, University of Dublin, Ireland.

Pfeifer, B. 1992. Fisheries investigations of Lakes Washington and Sammamish 1980–1990. Part V. Wild cutthroat and kokanee in Lakes Washington and Sammamish. Washington Department of Game, Olympia, Wash. (Available from West Coast Sockeye salmon Administrative Record, Environmental and Technical Services Division, National Marine Fisheries Service, 525 N.E. Oregon Street, Portland, OR 97232, USA.)

Rathbun, R. 1900. A review of the fisheries in the contiguous waters of the state of Washington and British Columbia. U.S. Comm. Fish Fish. **25**: 251–350.

Raymond, M., and Rousset, F. 1995. GENEPOP (version 1.2): population genetic software for exact tests and ecumenicism. J. Hered. **86**: 248–249.

Reynolds, J., Weir, B.S., and Cockerham, C. 1983. Estimation of the coancestry coefficient: basis for short-term genetic distance. Genetics, **105**: 767–779.

Rice, W.R. 1989. Analyzing tables of statistical tests. Evolution, **43**: 223–225.

Schlötterer, C. 2002. A microsatellite-based multilocus screen for the identification of local selective sweeps. Mol. Ecol. Notes, **3**(1): 167–169.

Scribner, K.T., Gust, J., and Fields, R. 1996. Isolation and characterization of novel salmon microsatellite loci: cross-species amplification and population genetic applications. Can. J. Fish. Aquat. Sci. **53**: 833–841.

Seeb, J., and Wishard, L. 1977. The use of biochemical genetics in the management of Pacific salmon stocks: genetic marking and mixed fishery analysis. Final report, Service Contract No. 792. Washington Department of Fisheries, Olympia, Wash.

Shrimpton, J.M., and Heath, D. 2003. Census vs. effective population size in chinook salmon: large- and small-scale environmental perturbation effects. Mol. Ecol. **12**: 2571–2583.

Sokal, R.R., and Rohlf, F.J. 1969. Biometry. W.H. Freeman and Company, San Francisco, Calif.

Stewart, D.C., Smith, G., and Youngson, A. 2002. Tributary-specific variation in timing of return of adult Atlantic salmon (*Salmo salar*) to fresh water has a genetic component. Can. J. Fish. Aquat. Sci. **59**: 276–281.

Vasemagi, A., Nilsson, J., and Primmer, C.R. 2005. Expressed sequence tag-linked microsatellites as a source of gene-associated polymorphisms for detecting signatures of divergent selection in Atlantic salmon (*Salmo salar* L.). Mol. Biol. Evol. **22**(4): 1067–1076.

Vitalis, R., Dawson, K., Boursot, P., and Belkhir, K. 2003. DetSel 1.0: a computer program to detect markers responding to selection. J. Hered. **94**(5): 429–431.

Weir, B.S., and Cockerham, C.C. 1984. Estimating F-statistics for the analysis of population structure. Evolution, **38**: 1358–1370.

Wood, C.C. 1995. Life history variation and population structure in sockeye salmon. Am. Fish. Soc. Symp. **17**: 195–216.

Young, S., Downen, M.R., Shaklee, J.B. 2004. Microsatellite DNA data indicate distinct native populations of kokanee, *Oncorhynchus nerka*, persist in the Lake Sammamish Basin, WA. Environ. Biol. Fishes, **69**: 63–79.

Appendix A. The program NERKA

The program NERKA simulates the approximate allele frequency distributions in two different populations under the hypothesis that the two populations have a common origin. This output is then used in a parametric bootstrap (Efron and Tibshirani 1983) test of that null hypothesis of common origin.

Allele frequency simulation

The underlying model upon which NERKA is based is as follows: samples of size n_a and n_b gene copies are drawn from populations a and b, respectively, at the present time 0. Under the hypothesis of common origin, a and b split from a common ancestral population T generations in the past. The inbreeding effective size of populations a and b (N_a and N_b, respectively) between T and the present are assumed known and can be used to define the scaled times since population splitting for each population: $t_a = T/(2N_a)$ and $t_b = T/(2N_b)$, respectively. At each locus, the allele frequencies in the ancestral population from which a and b are presumed to have originated are estimated independently as a weighted average of allele frequencies in the samples from a and b. Writing $\boldsymbol{p}_a = (p_{a,1}, \ldots, p_{a,K})$ with $(\sum_{k=1}^{K} p_{a,k} = 1)$ for the vector of allele frequencies observed in the sample from population a at a locus with K alleles, and using a similar notation for the allele frequencies in population b, the program NERKA estimates the allele frequencies $\boldsymbol{p}_c = (p_{c,1}, \ldots, p_{c,K})$ in the ancestral population as

$$p_{c,k} = \frac{\sigma_b^2 p_{a,k} + \sigma_a^2 p_{b,k}}{\sigma_a^2 + \sigma_b^2}$$

The weights are $\sigma_a^2 = t_a + 1/n_a$ and $\sigma_b^2 = t_b + 1/n_b$. In other words, $\boldsymbol{p}_c$ is an average of $\boldsymbol{p}_a$ and $\boldsymbol{p}_b$, each weighted inversely by the allele frequency variance accrued since time T because of genetic drift and sampling. Though $\boldsymbol{p}_c$ is not the maximum likelihood estimate of the ancestral allele frequencies under the null hypothesis (as would be desired for a formal parametric bootstrap), it is a good approximation and can be rapidly computed.

To simulate new allele frequency distributions in population a given $\boldsymbol{p}_c$, NERKA first simulates the number of lineages ancestral to the n_a gene copies sampled from a by simulating the neutral coalescent (Kingman 1982; Hudson 1983) backward in time, starting with n_a lineages and concluding when the scaled time t_a is reached. The r_a remaining lineages are then assigned allelic types as if they were a multinomial sample with cell probabilities $\boldsymbol{p}_c$. Then those allelic types are inherited by the descendants of those n_a lineages by simulation of a compound Dirichlet – multinomial random variable following Hoppe's (1984) insight that the coalescent process, forward in time, can be modeled using a Pólya urn scheme. Simulation of new allele frequency distributions in population b are simulated similarly. In our analyses, we used $T = 14$ generations between the time of population splitting to the time of sampling. This corresponds to 56 years for a species with an average generation length of 4 years. For each value of N_a and N_b investigated, 5000 simulated allele frequency distributions at all 14 loci in Bear Creek and Baker Lake were simulated using the method described above and used in the parametric bootstrap test described below.

Parametric bootstrap

We compared the data sets simulated under the null hypothesis with the observed data set using a summary statistic F:

$$F = \sum_{\text{alleles } k} \frac{\sigma_b^2 (p_{a,k} - p_{c,k})^2 + \sigma_a^2 (p_{b,k} - p_{c,k})^2}{(\sigma_a^2 + \sigma_b^2)\{p_{c,k}(1 - p_{c,k})\}}$$

which is closely related to F_{ST} (Weir 1996). The sum is over all alleles at all loci. For each value of N_a and N_b assumed, we recorded the proportion of times that the F computed for the data simulated under the null hypothesis was greater than the F value for the observed data set. That proportion provides a p value for rejecting the null hypothesis that Bear Creek sockeye descended exclusively from Baker Lake transplants.

To ensure that the program NERKA yields correct p values, it was tested against numerous sets of data simulated under the null hypothesis. For each simulation replicate, an ancestral population with allele frequencies $\boldsymbol{p}_s$ was simulated at time T, at which point it was split into two populations of sizes n_a and n_b, which were simulated using a Wright–Fisher model, forward in time, to produce samples at time 0. These simulated samples were analyzed using NERKA assuming the correct values of n_a and n_b. For $\boldsymbol{p}_s$ in our simulations, we used the estimate of allele frequencies obtained by pooling the samples of Bear Creek and Baker Lake fish, and we created and analyzed tens of thousands of simulated data sets across a range of values for n_a and n_b. The proportion of these simulated data sets for which NERKA provided a p value less than 0.05 was very close to 5%, as it should be if the p value properly reflects the type I error rate of the test.

Appendix A references

Efron, B., and Tibshirani, R. 1993. An introduction to the bootstrap. Chapman and Hall, New York.

Hoppe, F. 1984. Pólya-like urns and the Ewens sampling formula. J. Math. Biol. **20**: 91–94.

Hudson, R.R. 1983. Porperties of a neutral allele model with intragenic recombination. Theor. Popul. Biol. **23**: 183–201.

Kingman, J.F.C. 1982. On the genealogy of large populations. J. Appl. Prob. **19A**: 27–43.

Weir, B.S. 1996. Genetic data analysis II. Sinauer Associates, Sunderland, Mass.

Appendix B. Calculations concerning locus *One101*

The calculations regarding locus *One101* are motivated by the clearly bimodal allele length distribution across all populations sampled for this study (Fig. 2*b*). From the large number of alleles at this locus, it appears that the mutation rate is quite high; yet even where there is evidence of numerous recent mutations in the recently expanded population of the Cedar River (evidenced by the large number of low-frequency alleles), there is still a solid bimodal pattern, suggesting that at some time long in the past there occurred a mutation that accounts for the separation between the two modes in the allele length distribution, and since then the numerous mutations that have occurred have been much smaller (perhaps single-step) mutations. We assume a model in which there are two different allelic classes, a long class and a short class, and that all alleles ≥270 bp in length have descended from a common ancestor of the long class and all remaining alleles have descended from the short allele class. These allelic classes can then be treated as two alleles. We wish to compute the probability of observing zero long alleles in a sample of 90 gene copies drawn from a population that was itself derived 14 generations ago from a population having allele frequencies like those expected in the Baker Lake population 14 generations ago. Since we in fact observe no long alleles in the sample of 90 gene copies from Bear Creek, this probability, if very low, provides us with evidence that it is unlikely that Bear Creek fish descended from Baker Lake transplants.

Let q_s give the number of short alleles in the sample from the Baker Lake population and q_l give the number of long alleles at locus *One101*. The total sample size for *One101* in Baker Lake will be denoted by $n_B = q_s + q_l$. The effective size of the Baker Lake population since the time of the introduction is assumed to be N_B, and the scaled time since the introduction is thus $t_B = T/(2N_B)$, where we take T to be 14 generations.

The probability, given q_s and q_l, that another population descended from the Baker Lake population could have received no copies of the long allele can be calculated by Monte Carlo simulation in three steps as follows.

Step 1. The neutral coalescent is simulated until scaled time t_B starting with a sample of N_B gene copies. The number of lineages remaining at time t_B is the simulated number of ancestors, A_B, of the sample from Baker Lake. Because of the exchangeability properties of the coalescent process, the allelic length classes of the A_B ancestral lineages can by simulated by adding one short allele and one long allele to a hypergeometric random variable of $A_B - 2$ draws from an urn initially containing $q_s - 1$ and $q_l - 1$ short and long alleles, respectively. We denote the simulated number of short and long alleles among the ancestors by q_s^* and q_l^*, respectively ($q_s^* + q_l^* = A_B$).

Step 2. The ancestral allele frequencies in Baker Lake are simulated: q_s^* and q_l^* can also be thought of as a random binomial sample from the ancestral Baker Lake population having unknown frequencies of the allelic classes p_s^* and p_l^*. Therefore, given q_s^* and q_l^* and a β (0.5,0.5) prior for allele frequencies, the posterior distribution of p_s^* is a β distribution with parameters ($q_s^* + 0.5$, $q_l^* + 0.5$). It is easy to simulate p_s^* from this distribution, and $p_l^* = 1 - p_s^*$.

Step 3. Given the simulated allele frequencies p_s^* and p_l^*, it takes two steps to determine through simulation whether zero or more long alleles would be found in a sample from a second hypothetical descendant population, C. Let this population have effective size N_C, so it split from the ancestral Baker Lake population at a scaled time of $t_C = T/(2N_C)$ generations ago, and let the sample taken from it be of size n_C gene copies. The first step is to simulate A_C — the number of lineages remaining after coalescence for a scaled time of t_C. Second, the numbers, c_s and c_l, of the A_C lineages that belong to the short and the long allelic length classes are drawn from a binomial distribution with cell probabilities p_s^* and p_l^*. If there are no copies of the long allele amongst the A_C lineages, then the sample descended from those lineages will have no copies of the long allele either; otherwise, the sample will have at least one copy of the long allele.

The data we have for Baker Lake show that $q_s = 14$ and $q_l = 82$, and from Bear Creek, the number of genotyped gene copies at *One101* was 90, so $n_C = 90$, and none of the alleles are of the long class. With those parameter values, steps 1 through 3 can be repeated M times. The number of times that the hypothetical, descendant sample contains no long alleles divided by M is an estimate of the probability of obtaining the sample from Bear Creek, if the Bear Creek population had indeed descended from Baker Lake transplants. We used $M = 10^5$.

Long-term polychlorinated biphenyl elimination by three size classes of yellow perch (*Perca flavescens*)

Gord Paterson, Ken G. Drouillard, Todd A. Leadley, and G. Doug Haffner

Abstract: Three size classes of yellow perch (*Perca flavescens*) were dosed with a polychlorinated biphenyl (PCB) mixture and allowed to depurate the chemicals over 1 year while reared in 5000 L experimental tanks maintained under ambient environmental conditions. During the summer, PCB elimination rate constants for small perch (mean = 10.1 g) averaged approximately three times those calculated for medium-sized individuals (mean = 45.9 g) and four times those determined for the largest fish (mean = 86.7 g). Significant differences in PCB congener depuration were observed among the three size classes with negligible elimination of congeners of the octanol–water partition coefficient (log K_{ow}) > 6.5 occurring for the two larger size classes. Over the winter months, medium and large perch eliminated PCB 19 only, the least hydrophobic congener, with no elimination of PCBs of log K_{ow} > 5.8 observed for the smallest individuals. An increase in lipid-normalized PCB concentrations was observed during the overwinter period because of the depletion of lipids as an energetic reserve. For medium and large perch, this increase was sufficient to overwhelm any elimination achieved during the spring and summer seasons. These results demonstrate that the allometry of species bioenergetics and seasonal temperature fluctuations are responsible for the degree of chemical biomagnification observed in aquatic food webs.

Résumé : Nous avons traité trois classes de taille de perchaudes (*Perca flavescens*) avec une préparation de biphényles polychlorés (BPC) et, pour les dépurer de ces produits chimiques, nous les avons maintenues pendant un an dans des réservoirs expérimentaux de 5000 L dans les conditions ambiantes du milieu. En été, les constantes du taux d'élimination des BPC chez les petites perchaudes (moyenne = 10,1 g) sont en moyenne trois fois supérieures à celles calculées chez les poissons de taille moyenne (moyenne = 45,9 g) et quatre fois plus grandes que celles déterminées chez les poissons les plus grands (moyenne = 86,7 g). Nous avons observé des différences significatives dans la dépuration des congénères des BPC entre les trois classes d'âge avec une élimination négligeable des congénères de log K_{ow} > 6,5 chez les deux classes de taille plus grandes. Durant les mois d'hiver, les perchaudes de tailles moyenne et grande éliminent seulement le BPC 19, le congénère le moins hydrophobe; les plus petites perchaudes n'éliminent aucun BPC de log K_{ow} > 5,8. Une augmentation des concentrations de BPC normalisé s'observe dans les lipides au cours de la période hivernale à cause de l'épuisement des lipides servant de réserves énergétiques. Chez les perchaudes de tailles moyenne et supérieure, cette augmentation suffit à compenser toute élimination faite durant les saisons de printemps et d'été. Nos résultats démontrent que l'allométrie de la bioénergétique chez cette espèce et les fluctuations saisonnières de température expliquent le degré de bioamplification observé dans les réseaux alimentaires.

[Traduit par la Rédaction]

Introduction

Allometric models tend to describe negative relationships for the weight-specific rates of physiological processes including consumption, respiration, and growth with increasing body size (Peters et al. 1996). These relationships suggest that for older, larger individuals, toxicokinetic parameters including chemical elimination rates will be slow and substantially limit the potential of biota to achieve steady state with environmental concentrations during their lifetimes. The primary mechanisms considered to result in a reduction of aquatic species' chemical body burden include growth dilution, fecal egestion, and loss across respiratory surfaces (Connolly and Pedersen 1988; Clark et al. 1990). Growth dilution, however, should not be recognized as a true chemical elimination pathway, as no loss of body burden occurs thorough this biological process. Loss across respiratory surfaces is predicted to be substantial for very

Received 2 October 2006. Accepted 15 May 2007. Published on the NRC Research Press Web site at cjfas.nrc.ca on 30 August 2007.
J19572

G. Paterson,[1] K.G. Drouillard, and G.D. Haffner. Great Lakes Institute for Environmental Research and Department of Biological Sciences, University of Windsor, 401 Sunset Avenue, Windsor, ON N9B 3P4, Canada.
T.A. Leadley. Great Lakes Institute for Environmental Research and Department of Biological Sciences, University of Windsor, 401 Sunset Avenue, Windsor, ON N9B 3P4, Canada; and Leadley Environmental Inc., 1354 South Malden Road, R.R. #2, Essex, ON N8M 2X6, Canada.

[1] Corresponding author (e-mail: patersj@uwindsor.ca).

Can. J. Fish. Aquat. Sci. **64**: 1222–1233 (2007) doi:10.1139/F07-088

small individuals only, with fecal egestion being the primary path for physical elimination of the body burden (Connolly and Pedersen 1988). However, experiments conducted to calibrate toxicokinetic parameters in freshwater fish are usually based on young, small individuals (Fisk et al. 1998; Dabrowska et al. 1999; Buckman et al. 2004) because of their wider availability and lesser degree of animal husbandry required for these life stages. This proposes that for species whose bioenergetic rates rapidly decline with increased size, the extrapolation of toxicokinetic constants determined using smaller individuals does not accurately represent the nonlinearity of these processes with respect to body size and variation between individuals.

Existing literature investigating the importance of animal body size on chemical toxicokinetics often fail to consider the importance of body size and associated relationships with biological rate processes (Niimi 1987; Hendriks 1995; Trudel and Rasmussen 1997). Young, small individuals are observed to undergo considerable changes in body mass even over shorter term (6 months) toxicokinetic experiments (Coristine et al. 1996), and chemical elimination rate constants determined in such studies therefore represent an integrated estimate for the range of body mass realized through the study. Further, variability in growth rates and associated species bioenergetics contribute substantially to the variable chemical accumulation patterns observed within age classes of wild fish (Madenjian et al. 1994; Simoneau et al. 2004). Bioenergetic processes such as growth also demonstrate punctuated changes in response to resource availability and seasonal temperature cycles (Roy et al. 2004) rather than the continuous condition expected under laboratory settings. For juvenile fish, such highly variable rate processes likely contribute additional error in the calibration of toxicokinetic rate constants. These factors complicate the extrapolation of lab-derived toxicokinetic rate constants to natural fish populations and confound estimates of contaminant bioaccumulation in older, larger individuals that are often of the greatest concern to risk assessments.

Positive relationships between chemical hydrophobicity, measured as the octanol–water partition coefficient (log K_{ow}), and their respective half-lives have been established for a variety of organisms spanning a range of body sizes (Niimi and Oliver 1983; de Boer et al. 1994; O'Rourke et al. 2004). Such correlations, combined with allometry, suggest for an individual species that the slope of this relationship will become considerably more positive with increasing animal size and the potential that highly hydrophobic compounds will display little or no elimination in larger individuals. Modeling efforts support the latter hypothesis, with little or no elimination of extremely hydrophobic compounds (log $K_{ow} > 6.9$) expected to occur (Sijm and Van der Linde 1995). Half-lives of >1000 days were calculated for PCBs of log K_{ow} ~ 6.5 and higher in large (900 g) rainbow trout (*Oncorhynchus mykiss*) (Niimi and Oliver 1983). For juvenile rainbow trout, half-lives on the order of 100–200 days have been determined in this hydrophobicity range (Fisk et al. 1998; Buckman et al. 2004). These results support the hypothesis of negligible elimination in larger individuals and suggest that the increased degree of biomagnification and proportions of more hydrophobic chemicals measured in large apex predators from aquatic food webs may be more a function of differences in growth rates between trophic levels (Oliver and Niimi 1988). Moreover, large individuals tend to be the longest lived in aquatic food webs, thereby having greater life history exposure and thus potential to biomagnify such chemicals. Quantifying the relationships between fish body size and contaminant elimination will be beneficial for understanding chemical accumulation within species populations and will help to discern the relative importance of processes determining the food-web biomagnification of environmental pollutants.

The objective of this study was to compare the elimination rates of 72 PCB congeners over a 1-year period among three size classes of yellow perch (*Perca flavescens*) spanning approximately an order of magnitude in body size. The log K_{ow} range of the congeners used in this study accurately represents the profiles of those commonly detected in environmental samples and also encompasses the hydrophobicity range of most environmental pollutants. Further, chemical toxicokinetic experiments are typically of shorter duration (3–6 months) and may not allow for the inclusion of important developmental changes such as sexual maturation and reproduction into the experimental design. It has been predicted that such an increase in body size will result in an approximate threefold decrease in chemical elimination rates, with little or no elimination of the more hydrophobic congeners expected for the larger individuals (Sijm and Van der Linde 1995). By simultaneously studying PCB elimination in three perch size classes over a 1-year period, much of the variability and difficulties associated with the completion and comparison of multiple experiments becomes minimized, and chemical toxicokinetic relationships can be developed to include size- and physiology-related changes in bioenergetics exhibited by feral populations.

Materials and methods

Fish husbandry

A total of 462 yellow perch (Table 1) were obtained from a local aquaculture farm (Leadley Environmental Inc., Essex, Ontario, Canada). Fish were measured for total length, mass, and reared in two 5000 L recirculation tanks. Individuals ranged in mass from 2 to 287 g, and fish >20 g in mass were uniquely identified with passive integrated transponder (PIT) tags (EIDAP Inc., Sherwood Park, Alberta, Canada) implanted into the intraperitoneal cavity. All fish <20 g were maintained in one of the experimental tanks, with larger individuals held in the second tank to avoid potential cannibalism. Both of the experimental tanks were kept in an outdoor greenhouse facility, with fish exposed to ambient temperature and light conditions. Four daily water temperatures measurements were recorded using individual temperature loggers (Hoskin Scientific, Burlington, Ontario, Canada) submersed in each tank. Dissolved oxygen, pH, oxidation–reduction potential, and conductivity were measured weekly (Hydrolab™, Campbell Scientific Corp., Edmonton, Alberta, Canada). Fish were fed a low daily maintenance ration (1.5%) of commercial fish food produced from a single production batch (Martin Mills Inc. Elmira, Ontario, Canada) over the duration of the study.

Table 1. Average weight, growth rate, and hepatosomatic indices (HSIs) for yellow perch (*Perca flavescens*) treatment groups.

		Average weight (g)			Average growth rates ($\times10^{-3}$, day^{-1})			HSI (%)	
Size class	Treatment	0 days	365 days	0–60 days	60–300 days	300–365 days	0–365 days	0 days	365 days
Small	Control	8.7±1.7	24.8±1.4	6.1±0.9	2.6±0.1	3.7±0.3	4.2±0.4	2.4±0.1	1.4±0.1
	Dosed	10.1±2.2	27.4±3.4	4.7±1.0	2.1±0.2	4.2±0.3	3.4±0.3	2.1±0.3	1.6±0.2
Medium	Control	33.0±6.9	46.3±1.4	1.1±1.7	1.3±0.4	0.4±0.2	1.1±0.8	1.5±0.2	1.7±0.3
	Dosed	45.9±13.4	57.5±12.3	0.3±0.6	0.6±0.3	0.6±0.2	0.2±0.3	2.5±0.4	2.0±0.4
Large	Control	82.7±5.2	91.2±4.1	–0.2±0.5	0.2±0.2	0.3±0.1	0.1±0.2	2.4±0.4	1.8±0.3
	Dosed	86.7±9.7	87.7±4.5	1.1±1.8	–1.2±0.5	–0.2±0.3	0.3±0.8	2.3±0.2	2.2±0.3

Note: Values indicate mean ± 1 standard error. Growth rates were calculated as per Ricker (1979).

Fish dosing and sampling

A dosing solution consisting of a 1:1:1 mixture of Aroclor® PCB standards (1248, 1254, and 1260; Drouillard et al. 2001) dissolved in safflower oil was injected into the intraperitoneal cavity of each fish. Dosing occurred 14 days prior to the initiation of experimental sampling with an oil-dosing volume of 1.25 μL·g^{-1} used to achieve nominal day 0 concentrations of approximately 2000 ng·g^{-1} total wet weight PCBs. Control fish were injected with an equal volume of clean safflower oil containing no PCB solution, and the soft ray portion of the dorsal fin was clipped on these individuals. To account for potential external PCB sources, chemical recycling, and background food concentrations, control fish were maintained in the experimental tank with dosed individuals.

Using the unique PIT tag identifier codes, size classes of perch were determined by ranking, in order of mass, and subdividing fish >20 g into two experimental groups. Individuals <20 g maintained in the separate experimental tank constituted the smallest size class of fish. Dosed and control treatment groups were removed from the experimental tanks at days 0, 10, 30, 60, 120, 180, 240, 300, 330, and 365 of the experiment, with day 0 of the study occurring on 21 June 2003. For the smallest size class, five dosed and five control fish were collected at each sampling date, with three fish of each treatment group collected for the two larger size groups. Fish were immediately euthanized in a clove oil – ethanol solution and placed in ice-filled coolers. Immediately upon return to the laboratory, fish were processed for total and fork lengths; sex; and gonad, liver, and body weights. Individual fish ≥20 g were ground into a whole body homogenate using a stainless steel blender. From the five fish collected for the smallest size class, the largest individuals were processed singly, with the remaining four fish separated into two samples of similar size and sex, generating three replicates for each sampling date. Animals were maintained and handled following the University of Windsor's Animal Care Committee Guidelines throughout the duration of the study.

PCB analysis

Full details of the analytical procedures are described in Lazar et al. (1992). Briefly, approximately 2.5 g of the whole body homogenate was ground in a glass mortar and pestle containing 35 g sodium sulfate to remove residual water. This mixture was transferred to glass columns containing 50 mL of 1:1 dichloromethane (DCM) – hexane extraction solution. Samples were spiked with 100 μL of an internal recovery standard solution consisting of three ^{13}C PCB congeners (PCBs 37, 52, and 153 at 200 ng·L^{-1}). An additional 250 mL aliquot of the DCM–hexane extraction solution was added to the columns and allowed to stand for 1 h prior to elution. Extracts were concentrated to approximately 10 mL with a 1 mL portion removed for gravimetric lipid determination. Lipid content of the remaining extracts was removed through gel permeation chromatography and samples were cleaned up for PCB analysis through Florisil chromatography (O'Rourke et al. 2004). Extracts were concentrated to 1 mL and transferred to 2 mL gas chromatograph vials for storage at 4 °C until instrumental analysis. Extraction procedures were completed for an in-house reference standard (Detroit River common carp, *Cyprinus carpio*) and method blanks with every five samples. Detection limits for PCB congeners ranged from 0.1 to 0.3 ng·g^{-1}, with concentrations in blanks near or below detection limits; samples were blank-corrected. PCB concentrations for the in-house reference standard averaged 3517 ± 107 ng·g^{-1} (wet weight; mean ± standard error, SE) and were in compliance with the Great Lakes Institute for Environmental Research analytical laboratory's quality assurance guidelines (mean ± 2 standard deviations, SD). Sample recoveries for the three ^{13}C internal standards averaged 98% ± 0.6%, and samples were not corrected for recovery.

PCB analyses were performed on a Hewlett-Packard (HP; Hewlett Packard Company, Palo Alto, California, USA) 5890 gas chromatograph equipped with a 5973 mass selective detector and an HP-7673 autosampler. Samples were run through a 60 m × 0.25 μm DB-5 chromatography column (Chromatographic Specialties, Brockville, Ontario, Canada) with an injection port temperature of 250 °C. Injection volume was 2 μL (splitless) into helium carrier gas at a flow rate of 1 mL·min^{-1} with N_2 as the make-up gas at the detector. The oven temperature was programmed to start and hold at 90 °C for 3 min and ramp to 150 °C at a rate of 7 °C·min^{-1}, then increase at 3 °C·min^{-1} to 280 °C and hold at the final temperature for 5.1 min. Total run time was 1 h. The mass selective detector was run in selected ion monitoring mode for the molecular ion of PCBs. PCBs were identified and quantified against a well-characterized 1:1:1 Aroclor® 1242–1254–1260 PCB standard. Detection limits for PCB congeners ranged from 0.1 to 0.3 ng·g^{-1} (wet weight).

Data analysis

Statistical analyses including analysis of variance (ANOVA) and analysis of covariance (ANCOVA) were completed using SYSTAT version 8.0 for Windows (Wilkinson

1998) with a criterion for significance of $P < 0.05$ used in all cases. For seasonal ANCOVAs, water temperature was the covariate, and for half-life comparison between size classes, body mass was treated as the covariate. All analyses remained significant after treatment for the covariate(s). The nonlinear regression module of SYSTAT was used to determine the polynomial functions describing the temperature and lipid content profiles throughout the duration of the experiment (Fig. 1). Multiple iterations of the regressions were completed to achieve optimal fit to the data. Probability plots were used to test data for normality. For PCBs, logarithmic transformations of congener concentration data were required to normalize distributions. The water temperature data required square root transformation prior to statistical analysis. No other data transformations were required.

The fish growth model of Ricker (1979) (eq. 1) was used to calculate specific growth rates (g; day^{-1}) between sampling events (Table A1):

$$(1)\qquad g = [\ln(W_t / W_0)/t]$$

where W_0 is the average weight (g) of the fish at the initiation of the experiment, W_t is the average weight of the sampled fish on the day of collection, and t is the number of elapsed days. PCB concentrations measured in fish were corrected for growth dilution at each sampling date by multiplying by a factor of $(1 + g \times t)$ (Fisk et al. 1998).

Three distinct chemical elimination periods were identified over the duration of the study, specifically the periods from days 0–60, 60–300, and 300–365, and are herein defined as the summer, fall–winter, and spring elimination periods, respectively. Elimination rate constants (k_2) were derived for individual PCB congeners from the slopes of the least squares regression of natural-log-transformed congener concentration values across these sampling periods. An elimination rate constant was also calculated for the entire experimental duration (0–365 days). Control fish had detectable concentrations of many PCB congeners. For these congeners, the average concentration measured in control fish over the summer, fall–winter, and spring periods of the experiment were subtracted from the concentrations measured in the dosed fish. A general equation describing the calculation is expressed as follows:

$$(2)\qquad \ln[\mathrm{PCB}] = a(t) + b$$

$$(3)\qquad k_2 = |a|$$

where [PCB] is the lipid-, control-, and growth-rate-corrected PCB congener concentration, with a and b representing the regression slope coefficient and constants, respectively. The PCB congener elimination rate constant (k_2) is the absolute value of the slope coefficient (a) and is reported in units of day^{-1}. Elimination rate constants for each PCB congener were determined using the average congener concentration reported at each sampling event. Half-lives ($t_{1/2}$), measured in days, were also calculated for each PCB congener as per eq. 4 following first-order rate kinetics (Table A1).

$$(4)\qquad t_{1/2} = \ln 2 / k_2$$

Fig. 1. (*a*) Average daily tank water temperature profiles recorded across duration of experiment. Values are arithmetic means of four daily readings. Average temperatures for the tank containing small size class are indicated by (◇), with the values for the second tank holding the medium and large size classes indicated by (◆). Curve represents the best-fit polynomial (R^2 = 0.942) for average daily water temperature. (*b*) Average lipid contents of small (◇), medium (×), and large (◆) size classes of yellow perch (*Perca flavescens*) dosed with polychlorinated biphenyl (PCB) at time of sampling. For small perch, values represent arithmetic means of five fish; for medium and large size classes, values are means of three fish each. The solid, dashed, and dotted lines represent the best-fit polynomials describing the changes in lipid content of small, medium, and large perch, respectively, over the duration of the experiment. Error bars in both panels represent ±1 standard error.

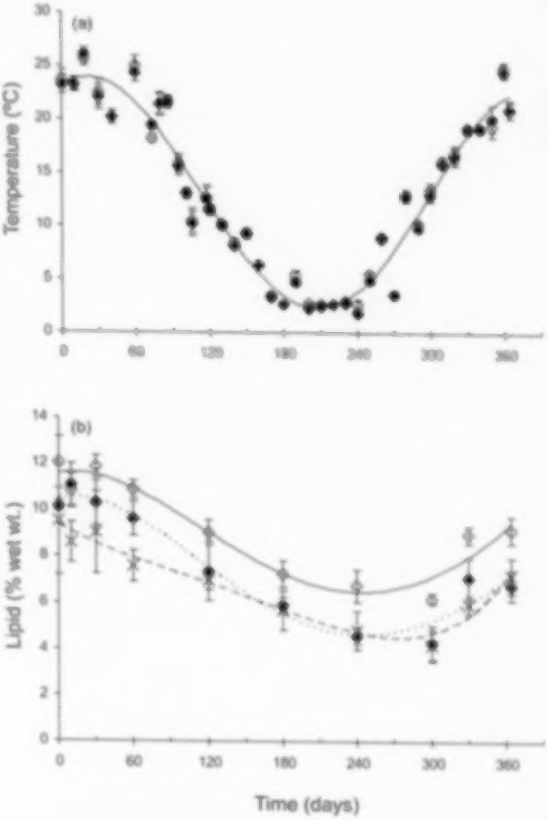

Bioenergetics modeling

The bioenergetics model developed by Kitchell et al. (1977) for yellow perch was used to predict changes expected in biological rate processes for each perch size class over the duration of the experiment due to the influences of body size and water temperature. The processes modeled included consumption, respiration, fecal egestion, excretion, growth rates, and also specific dynamic action. Briefly, the

Table 2. Bioenergetic equation symbol definitions and values used for yellow perch (*Perca flavescens*).

Bioenergetic process (reference equations)	Symbol	Description	Model value
Consumption (C_B), (6, 7)	a_1	Intercept for maximum consumption	0.25
	b_1	Slope for maximum consumption	–0.27
	T_o	Optimum temperature for consumption (°C), juveniles and adults	23
	T_m	Maximum temperature for consumption (°C), juveniles and adults	28
	Q	Slope for temperature dependence of consumption ($\approx Q_{10}$)	2.3
Respiration (R), (8)	a_2	Intercept for maximum standard respiration	0.035
	b_2	Slope for maximum standard respiration	–0.20
	T_o	Optimum temperature for standard respiration (°C), juveniles and adults	28
	T_m	Maximum temperature for standard respiration (°C), juveniles and adults	33
	Q	Slope for temperature dependence of standard respiration ($\approx Q_{10}$)	2.1
	SDA	Specific dynamic action coefficient	0.15
	A	Activity multiplier	1, 2, 3
Fecal egestion (F), (9)	α_1	Intercept for proportion of consumed food egested	0.158
	β_1	Coefficient for egestion vs. temperature	–0.222
	γ_1	Coefficient for egestion vs. feeding level	0.631
Excretion (E), (9)	α_2	Intercept for proportion of consumed food excreted	0.0292
	β_2	Coefficient for excretion vs. temperature	0.58
	γ_2	Coefficient for excretion vs. feeding level	–0.299

Note: Symbols and values are those reported by Kitchell et al. (1977).

basic bioenergetic model defined by Winberg (1956) describes the fate of consumed energy into three basic pathways:

$$(5)\qquad C_B = G + R + W$$

where the total consumed energy (C_B) is designated to be the metabolic costs associated with respiration (R) and waste products (W), while growth (G) represents the available energy once these metabolic costs–losses are accounted for. Consumption (C_B) was modeled as a function of the maximum weight specific consumption rate ($C_{\max}$) as regulated by water temperature (r_{C_B}) and food ration (p):

$$(6)\qquad C_B = C_{\max} p r_{C_B}$$

Maximum weight specific consumption rate is described by the allometric relation in eq (7).

$$(7)\qquad C_{\max} = a_1 W^{b_1}$$

Respiration rate was modeled in a similar manner as a function of body weight ($R_{\max} = a_2 W^{b_2}$), activity (A), water temperature (r_R), and specific dynamic action (SDA).

$$(8)\qquad R = R_{\max} A r_R + \mathrm{SDA}$$

An activity multiplier (A) of 1 was used to simulate laboratory-determined activity respiration (Kitchell et al. 1977), and specific dynamic action was modeled as a constant proportion (0.15) of consumption less energy lost via fecal egestion for yellow perch (Hewett and Johnson 1992).

Fecal egestion (F) and excretory (E) losses were modeled as proportions of feeding rate and water temperature as described below:

$$(9)\qquad F, E = C_B \alpha T^{\beta} e^{\gamma p}$$

with α, β, and γ representing a separate set of regression constants for the temperature dependence of fecal egestion and excretion and p, respectively, as outlined above. Growth rates from the bioenergetics calculations were determined by solving eq. 5 for G. Definitions and values for each variable in the above equations are provided (Table 2; Kitchell et al. 1977). Optimum and maximum temperatures describing the temperature dependence of each bioenergetic relation were those described by Kitchell et al. (1977) for juvenile and adult yellow perch. Model simulations were initiated using the average body mass for each perch size class measured at day 0, with the polynomial function describing changes in water temperature over the course of the experiment used to estimate daily water temperatures for the calculations describing the water temperature dependence of consumption, respiration, fecal egestion, and excretion (Kitchell et al. 1977).

Results

Initial body masses for the three classes of dosed perch, in increasing order of size, averaged 10.1, 45.9, and 86.7 g (Table 1). No significant differences in body mass were observed between control and dosed treatment groups at each sampling day and over the duration of the experiment for all three perch size classes. Small perch demonstrated the greatest growth, increasing in mass from 10.1 to 27.4 g over the duration of the experiment, with medium and large perch exhibiting minimal or no growth, respectively. Growth rates were variable between control and dosed treatment groups for all size classes, with control fish exhibiting marginally higher growth over the duration of the experiment for the small and medium size classes. Hepatosomatic indices (HSIs) were higher in dosed fish than in control individuals by the conclusion of the experiment; however, these differences were not significant. Statistical significance between HSIs for control and dosed treatment groups were found for medium-sized perch only at day 0 of the experiment (P = 0.023). No other significant differences in HSIs were determined over the duration of the experiment. Mortality was limited to a total of 14 fish, consisting of eight dosed and six control individuals over the duration of the study.

An average water temperature of 23.2 °C (±0.5 °C) was recorded for the first 60 days of the experiment and did not exhibit any significant decline over this period (P = 0.719; Fig. 1*a*). Significant changes in water temperature were observed between 60–300 days ($P < 0.001$) and 300–365 days ($P < 0.001$). During the fall–winter period, water temperature declined from 24.4 °C at 60 days to a minimum value of <0.1 °C recorded on day 216 of the experiment. Water temperature averaged 6.8 °C (±0.7 °C) during the fall–winter period. During the final 65 days, water temperature increased from 13.2 to 21.2 °C at the conclusion of the experiment, with a maximum temperature during the spring elimination period of 26.6 °C recorded on day 354. An average water temperature of 19.1 °C (±0.5 °C) was observed during the final 65 days of the study.

No significant differences in lipid content were observed between control and dosed treatment groups within all three size classes over the duration of the experiment (Fig. 1*b*). Among the dosed treatment groups, small perch averaged the highest lipid content at 9.6% (±0.3%), with medium perch averaging 7.2% (±0.4%) and large perch averaging 8.0% (±0.4%) over the duration of the experiment. Lipid content profiles of all three perch size classes followed that observed for water temperature over the duration of the experiment.

PCB elimination rates by yellow perch were negatively correlated with body size, and a significant hydrophobicity effect was observed whereby chemicals of log K_{ow} > 6.5 displayed little or no elimination over an annual period in perch of body size >50 g (Fig. 2). Even gduring the summer period when water temperatures were optimal, an effect of body size was observed. For the 42 PCB congeners exhibiting elimination by all three size classes during this period, elimination rates for the smallest perch ($\bar{x}_{(k_2)}$ = 0.016 day^{-1}) averaged approximately three times those calculated for medium-sized individuals ($\bar{x}_{(k_2)}$ = 0.006 day^{-1}) and were almost fourfold higher than those determined for the largest fish ($\bar{x}_{(k_2)}$ = 0.004 day^{-1}). For the largest perch, minimal elimination of congeners of log K_{ow} > 6.5 was observed during the summer.

Three PCB congeners (PCBs 74, 118, and 108) were used to contrast the elimination profiles observed for the three perch size classes across the duration of the experiment (Fig. 3). These congeners were chosen based on their classification as persistent type PCB congeners that are not readily metabolized by aquatic biota (Boon et al. 1989). These patterns were also compared with predicted changes in respiration and fecal egestion as estimated by the bioenergetics model. Elimination was observed during the summer for all three size classes coincident with bioenergetic rates predicted to be >97% of maximum. PCB half-lives calculated during this period were positively correlated with congener log K_{ow} (Fig. 4); however, elimination of all 72 detectable congeners was observed only in small perch. Chemical half-lives for small perch ranged from 20 to 87 days and averaged 56 ± 2 days, with bioenergetic rates predicted to be the highest of all size classes during the summer. For medium and large perch, elimination occurred for 52 and 44 congeners, respectively, with half-lives averaging >1000 days for congeners of log K_{ow} > 6.5 in these size classes and no elimination of congeners of log K_{ow} ≥ 6.7 observed for large perch. Elimination of such high log K_{ow} congeners occurred in medium perch; however, half-lives typically exceeded 1000 days with a shortest half-life of 369 days calculated for PCB 199 (log K_{ow} = 7.2) in this hydrophobicity range. For the 44 congeners in common to medium and large perch, half-lives averaged 344 ± 103 days and 490 ± 162 days, respectively.

Fig. 2. Relationships between polychlorinated biphenyl (PCB) congener elimination rate constants (k_2, ◆) and yellow perch (*Perca flavescens*) body mass during summer (0–60 days) elimination period and between predicted rates for perch respiration (R) and fecal egestion (F) rates with body mass. Specific values of R and F were predicted separately by the yellow perch bioenergetics model outlined by Kitchell et al. (1977); the broken line represents the sum of these two bioenergetic processes. The solid line describes the nonlinear, allometric relationship between PCB congener elimination rate constant and average perch body mass.

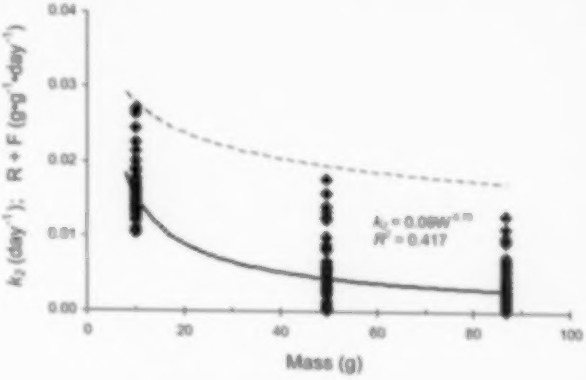

Minimal PCB elimination occurred during the fall–winter period, regardless of perch body mass. Only six PCBs (PCBs16/32, 17, 18, 19, 24/27, 33/20) demonstrated elimination from 60 to 300 days in small perch, and these congeners were all of log K_{ow} < 5.6. Additionally, half-lives for these congeners averaged >1000 days, with a value of 321 days reported for PCB 19, the least hydrophobic congener detected. This congener was also the only PCB displaying elimination during the fall–winter in both medium and large perch, with respective half-lives of 212 and 390 days. The bioenergetics model predicted declines for respiration and fecal egestion rates to their lowest levels during the fall–winter period for all three size classes.

As water temperatures increased into the spring elimination period, bioenergetic rates for respiration and fecal egestion were predicted to increase but averaged <90% of the maxima predicted for the spring period in comparison with an average of >97% modeled for the summer period. During the spring period, PCB elimination was again observed for all three perch size classes. For the smallest perch, elimina-

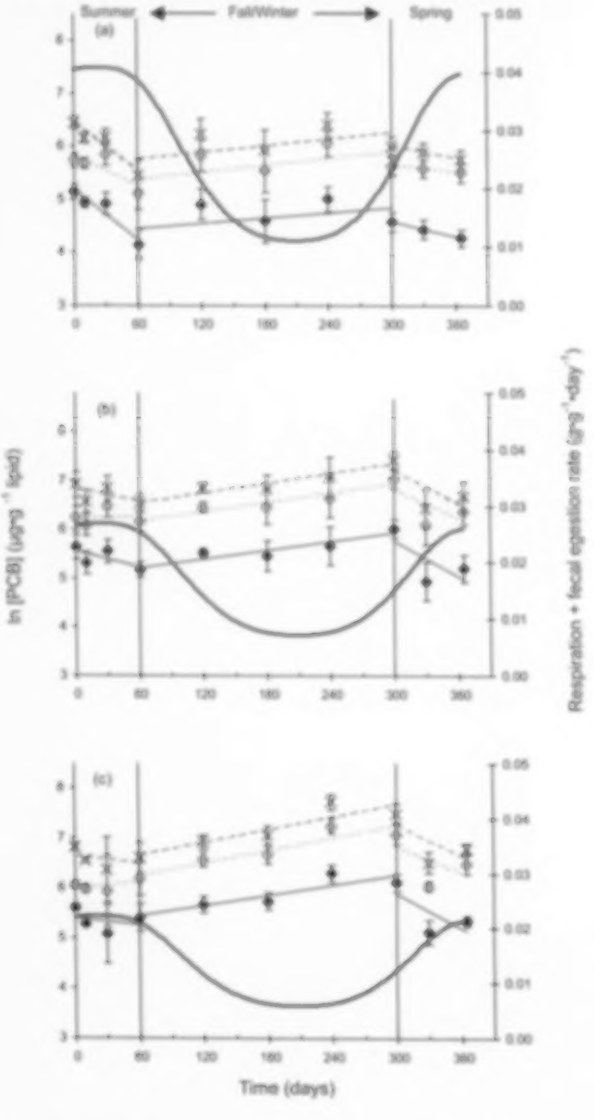

Fig. 3. Concentration (mean ± standard error) profiles for polychlorinated biphenyl (PCB) congeners 74 (◆), 118 (×), and 180 (◇) measured across summer (0–60 days), fall–winter (60–300 days), and spring (300–365 days) elimination periods in (*a*) small, (*b*) medium, and (*c*) large yellow perch (*Perca flavescens*) size classes. In each panel, solid, dashed, and dotted lines represent best-fit linear regressions for PCB congeners 74, 118, and 180, respectively, during each elimination period. The thicker solid line represents the sum of respiration and fecal egestion rates predicted for each perch size class by the bioenergetics model outlined by Kitchell et al. (1977). Vertical bars provided to clarify summer (0–60 days), fall–winter (60–300 days), and spring (300–365 days) elimination periods.

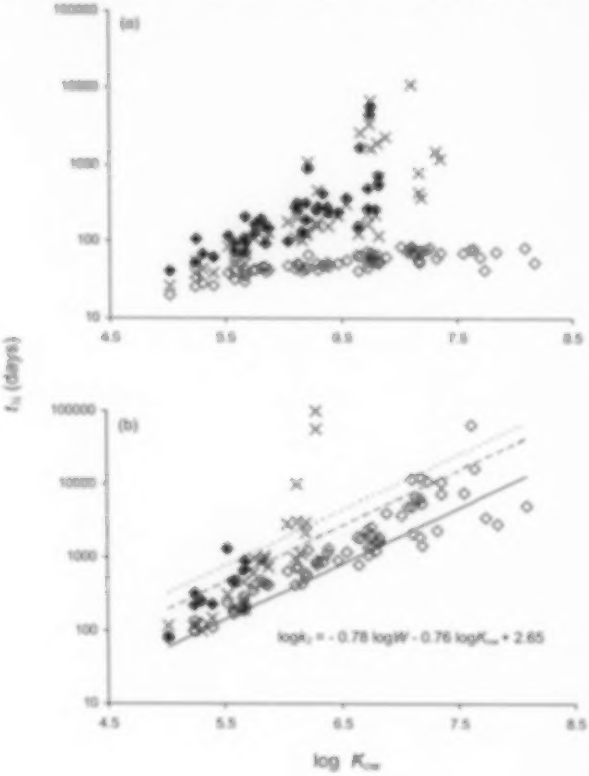

Fig. 4. Relationships between polychlorinated biphenyl (PCB) congener half-lives and octanol–water partition coefficients (log K_{ow}) for small (◇), medium (×), and large (◆) yellow perch (*Perca flavescens*) size classes over (*a*) the summer elimination period (0–60 days) and (*b*) the duration of the experiment (0–365 days). In panel (*b*), solid, dashed, and dotted lines represent multiple linear regressions calculating PCB elimination rate constants in small, medium, and large perch, respectively. Half-lives are calculated from elimination rate constants (k_2) as per eq. 4.

tion of 70 congeners was detected; however, half-lives during the spring averaged 256 ± 46 days and were up to 12-fold longer and significantly different from those calculated during the summer elimination period. Elimination rates of PCBs by both medium and large perch were significantly ($P < 0.001$; ANCOVA) higher in the spring than rates observed during the summer, with elimination of all congeners observed for these size classes. All PCB half-lives for medium and large perch during the spring were ≤125 days, and the average PCB half-life for medium perch was 62 ± 2 days, with an average half-life of 71 ± 2 days calculated for large perch during this period. Half-lives for medium perch were significantly shorter ($P < 0.001$; ANCOVA) than those calculated for the larger perch during the spring period.

Spawning and egg release was observed between 300 and 330 days, with egg masses collected from both experimental tanks. Lipid content of egg masses ($n = 2$) collected from the experimental tank containing the small perch size class averaged 1.2% (±0.1%), with a total PCB concentration of 11.6 $ng \cdot g^{-1}$ (±2.6 $ng \cdot g^{-1}$ wet weight). Egg masses ($n = 3$) collected from the experimental tank housing the medium and large perch averaged 1.0% (±0.1%) lipid content, with a mean total PCB concentration of 62.9 $ng \cdot g^{-1}$ (±14.3 $ng \cdot g^{-1}$).

When calculated over the entire study duration (0–365 days), PCB half-lives averaged >500 days for those congeners that displayed elimination by each size class (Fig. 4*b*; Table A1). In small perch, elimination was observed for 69 of the 72 congeners, with an average half-life of >3400 days. For medium perch, elimination was observed for only 27 of the total congeners, with no elimination for congeners of log $K_{ow} > 6.5$ evident. Half-lives for these 27 congeners averaged >6900 days in comparison with an average of 383 days for these PCBs in small perch. In the largest perch, elimination occurred for only 11 congeners, with no significant elimination of congeners of log $K_{ow} > 5.7$. For these 11 congeners that exhibited significant elimination in all three size classes, half-lives averaged 157, 182, and 509 days in increasing order of size.

Discussion

The results of this study are in agreement with the conclusions of Sijm and Van der Linde (1995), who predicted that an order of magnitude increase in body size would result in a substantial decrease in chemical elimination rates and that negligible elimination of high log K_{ow} chemicals would be observed in individuals larger than approximately 50 g. For hydrophobic chemicals, growth dilution, fecal egestion, and loss across the respiratory surface are considered the primary mechanisms resulting in the elimination of the body burden (Connolly and Pedersen 1988; Clark et al. 1990; Sijm et al. 1992). Fecal production rates in fish are tightly coupled with consumption, and under wild conditions, yellow perch are predicted to consume a maintenance ration during the overwinter months (Kitchell et al. 1977). The declines in lipid content for all three perch size classes as water temperatures declined below 10 °C demonstrates the reliance on this energetic reserve during the fall–winter period and provides evidence for the absence of feeding. Lipid and energy content depletion during overwinter periods is not uncommon for perch species (Henderson et al. 2000; Eckmann 2004), and similar losses of fat reserves occur in other species to meet energy requirements during periods of hibernation, starvation, and physiological transformation (MacDonald et al. 2002; Leney et al. 2006). The most important trend over the fall–winter period, however, was the increase in chemical concentration per unit lipid for each of the perch size classes.

Lipids are the primary tissue where hydrophobic organic pollutants accumulate in biota and represent the capacity of an animal to accumulate these chemicals (Mackay and Paterson 1981). When lipids are mobilized as an energetic resource, chemical concentrations per unit lipid mass, or fugacity, increase resulting in an elevated potential for the chemical to partition from lipid reserves into the bloodstream (de Freitas and Norstrom 1974). This mobilization of chemical may result in potential loss across the respiratory surface; however, during the fall–winter period, gill ventilation rates will be exceedingly low but still dependent on the allometry of respiration (Norstrom et al. 1976). Small perch were able to eliminate marginally higher log K_{ow} congeners, and half-lives for PCB 19 during the fall–winter period increased with perch size, providing evidence for the allometry of elimination, even during such a cold water period. Most importantly, this lack of elimination occurred during a period of major lipid depletion that generated the highest chemical fugacities for the higher log K_{ow} congeners. The absence of PCB elimination, especially for high log K_{ow} congeners, has been observed in starvation-induced silver eels (*Anguilla anguilla*) (Duursma et al. 1991) and in nonfeeding, metamorphosing green frog (*Rana clamitans*) tadpoles (Leney et al. 2006). Such a lack of elimination has been attributed to the decline in metabolic activity associated with starvation (Duursma et al. 1991). Yellow perch metabolic rates are predicted to decrease to near basal levels as water temperatures decline in the fall and winter (Norstrom et al. 1976; Kitchell et al. 1977). Combined with allometric effects, larger poikilothermic species are therefore expected to exhibit minimal chemical elimination during the overwinter period.

Concentrations of PCBs are commonly detected in eggs released by spawning fish (Niimi 1983; Fisk and Johnston 1998), and this behaviour must be considered a potential mechanism contributing to the loss of the body burden in fish species. Lipid content of egg masses collected from this study averaged 1.1% (±0.1%), with congener concentrations at or near detection limits for the small perch size class and being similar to control fish concentrations for eggs collected from the experimental tank housing the two larger perch size classes. The experimental design did not separate control from dosed fish, and eggs masses collected during this study likely represent a composite from both treatment groups. Further, PCB concentrations in yellow perch eggs have been demonstrated to be similar to whole body residues (Niimi 1983; Russell et al. 1999), and the resulting burden lost due to egg release is minimal because of the proportional loss of body mass via egg release for yellow perch (Niimi 1983). With such low lipid content, and thus capacity to contain chemical mass, it is unlikely that substantial loss of the initial PCB dose occurred for female fish through egg deposition. HSIs were observed to decrease over the duration of the study, a trend that has been observed in similar dosing experiments (Muir et al. 1992; Fisk et al. 1998; Buckman et al. 2004). However, only 14 fish died during the course of this study, with mortalities spread approximately equally between the control and dosed individuals that perished. Thus, exposure to the Aroclor dosing solution is not considered to have had a detrimental impact on the health of the fish.

The PCB elimination rates observed for small perch during the summer period were very similar to those reported for juvenile rainbow trout reared at their preferred temperature (12 °C) and fed a diet contaminated with PCBs (Fisk et al. 1998). Similarly, a half-life range of 79–95 days has been reported for small perch reared at 20 °C and fed a diet spiked with PCB 153 (Dabrowska et al. 1999), which compares well with a half-life of 64 days for PCB 153/132 for the smallest perch during the initial 60 days of this study. These results demonstrate that the elimination of chemical body burden proceeds through similar mechanisms, and elimination kinetics determined for similar-sized individuals reared at their preferred temperatures are comparable, regardless of whether exposure occurs through dietary or intraperitoneal injection.

This study simultaneously investigated differences in chemical elimination among multiple size classes of a fish species. The results presented here conform to predictions of very slow elimination rates for larger fish (>50 g) and the lack of elimination of very high log K_{ow} (>6.5) chemicals by these larger individuals (Niimi and Oliver 1983; de Boer et al. 1994; Sijm and Van der Linde 1995). More importantly, however, the results of this study were generated under environmental conditions representative of that experienced by yellow perch under natural conditions and therefore provide important insight into understanding food-web biomagnification of persistent organic pollutants such as PCBs.

Aquatic food webs are typically defined by increasing body size with trophic position, and the allometry of growth rates is well established (Peters et al. 1996). As growth rates are negatively correlated with trophic position, growth must be considered a limited contributor to chemical dilution in large apex predators. Growth dilution is most important for high log K_{ow} chemicals (Connolly and Pedersen 1988), and this study has demonstrated that in the absence of growth, larger individuals have very slow elimination rates for these chemicals. Minimal chemical elimination occurred during the fall–winter seasons for all three perch size classes, which was best explained by slight differences in the allometry of respiration during such a cold-water period. More importantly, the overwinter depletion of lipid reserves generates a fugacity increase that may negate the outcomes of chemical elimination achieved by larger individuals during the spring and summer seasons. Thus, because of the water temperature dependence of species' bioenergetic processes, the length of the overwinter period may be crucial for the extent of biomagnification observed in aquatic food webs. For poikilothermic species, long overwinter periods are expected to generate major increases in chemical potential because of the limited feeding and reliance on somatic lipid reserves that occurs during this time. Coupled with the allometric effects observed in this study, this proposes that much of the food-web biomagnification phenomenon is associated with species bioenergetics and seasonal temperature cycles.

Acknowledgements

The authors thank Ms. Karen Balkwill for completing much of the chemical extraction procedures and Sarah O'Rourke, Denis Roy, Jocelyn Leney, and J. Mark Cook for their assistance with the dosing and sampling of animals during the course of the study. Funding for this project was provided by the Natural Sciences and Engineering Research Council of Canada (NSERC) and Canada Research Chair awards to Dr. G.D. Haffner. Additional funding was also received from NSERC post graduate and University of Windsor tuition scholarships awarded to G. Paterson.

References

Boon, J.P., Eijgenraam, F., Everaarts, J.M., and Duinker, J.C. 1989. A structure–activity relationship (SAR) approach towards metabolism of PCBs in marine animals from different trophic levels. Mar. Environ. Res. **27**: 159–176.

Buckman, A.H., Brown, S.B., Hoekstra, P.F., Solomon, K.R., and Fisk, A.T. 2004. Toxicokinetics of three polychlorinated biphenyl technical mixtures in rainbow trout (*Oncorhynchus mykiss*). Environ. Toxicol. Chem. **23**: 1725–1736.

Clark, K.E., Gobas, F.A.P.C., and Mackay, D. 1990. Model of organic chemical uptake and clearance by fish from food and water. Environ. Sci. Technol. **24**: 1203–1213.

Connolly, J.P., and Pedersen, C.J. 1988. A thermodynamic-based evaluation of organic chemical accumulation in aquatic organisms. Environ. Sci. Technol. **22**: 99–103.

Coristine, S., Haffner, G.D., Ciborowski, J.J.H., Lazar, R., Nanni, M.E., and Metcalfe, C.D. 1996. Elimination rates of selected di-ortho, mono-ortho, and non-ortho substituted polychlorinated biphenyls in rainbow trout (*Oncorhynchus mykiss*). Environ. Toxicol. Chem. **15**: 1382–1387.

Dabrowska, H., Fisher, S.W., Dabrowski, K., and Staubus, A.E. 1999. Dietary uptake efficiency of 2,2′,4,4′,5,5′-hexachlorobiphenyl in yellow perch and rainbow trout: role of dietary lipids. Environ. Toxicol. Chem. **18**: 938–945.

de Boer, J., van de Valk, F., Kerkhoff, M.A.T., and Hagel, P. 1994. 8-year study on the elimination of PCBs and other organochlorines from eel (*Anguilla anguilla*) under natural conditions. Environ. Sci. Technol. **28**: 2242–2248.

de Freitas, A.S., and Norstrom, R.J. 1974. Turnover and metabolism of polychlorinated biphenyls in relation to their chemical structure and the movement of lipids in the pigeon. Can. J. Physiol. Pharmacol. **52**: 1081–1094.

Drouillard, K.G., Fernie, K.J., Smits, J.E., Bortolotti, G.R., Bird, D.M., and Norstrom, R.J. 2001. Bioaccumulation and toxicokinetics of 42 polychlorinated biphenyl congeners in American kestrels (*Falco sparverius*). Environ. Toxicol. Chem. **20**: 2514–2522.

Duursma, E.K., Nieuwenhuize, J., Van Liere, J.M., De Rooy C.M., Witte, J.I.J., and Van der Meer, J. 1991. Possible loss of polychlorinated-biphenyls from migrating European silver eels — a 3 month simulation experiment. Mar. Chem. **36**: 215–232.

Eckmann, R. 2004. Overwinter changes in mass and lipid content of *Perca fluviatilis* and *Gymnocephalus cernuus*. J. Fish. Biol. **65**: 1498–1511.

Fisk, A.T., and Johnston, T.A. 1998. Maternal transfer of organochlorines to eggs of walleye (*Stizostedion vitreum*) in Lake Manitoba and western Lake Superior. J. Gt. Lakes Res. **24**: 917–928.

Fisk, A.T., Norstrom, R.J., Cymbalisty, C.D., and Muir, D.C.G. 1998. Dietary accumulation and depuration of hydrophobic organochlorines: bioaccumulation parameters and their relationship with the octanol/water partition coefficient. Environ. Toxicol. Chem. **17**: 951–961.

Henderson, B.A., Trivedi, T., and Collins, N. 2000. Annual cycle of energy allocation to growth and reproduction of yellow perch. J. Fish. Biol. **57**: 122–133.

Hendriks, A.J. 1995. Modelling non-equilibrium concentrations of microcontaminants in organisms: comparative kinetics as a function of species size and octanol–water partitioning. Chemosphere, **30**: 265–292.

Hewett, S.W., and Johnson, B.L. 1992. A generalized bioenergetics model of fish growth for microcomputers. Version 2.0. University of Wisconsin Sea Grant Institute, Madison, Wis.

Kitchell, J.F., Stewart, D.J., and Weininger, D. 1977. Application of a bioenergetics model to yellow perch (*Perca flavescens*) and walleye (*Stizostedion vitreum vitreum*). J. Fish. Res. Board Can. **34**: 1922–1935.

Lazar, R., Edwards, R.C., Metcalfe, C.D., Gobas, F.A.P.C., and Haffner, G.D. 1992. A simple, novel method for the quantitative analysis of coplanar (non-ortho substituted) polychlorinated biphenyls in environmental samples. Chemosphere, **25**: 493–504.

Leney, J.L., Drouillard, K.G., and Haffner, G.D. 2006. Does metamorphosis increase the susceptibility of frogs to highly hydrophobic contaminants? Environ. Sci. Technol. **40**: 1491–1496.

MacDonald, R., Mackay, D., and Hickie, B. 2002. Contaminant amplification in the environment. Environ. Sci. Technol. **36**: 456A–462A.

Mackay, D., and Paterson, S. 1981. Calculating fugacity. Environ. Sci. Technol. **15:** 1006–1014.

Madenjian, C.P., Carpenter, S.R., and Rand, P.S. 1994. Why are PCB concentrations of salmonine individuals from the same lake so variable? Can. J. Fish. Aquat. Sci. **51**: 800–807.

Muir, D.C.G., Yarechewski, A.L., Metner, D.A., and Lockhart, W.L. 1992. Dietary 2,3,7,8-tetrachlorodibenzofuran in rainbow trout: accumulation, disposition, and hepatic mixed function oxidase enzyme induction. Toxicol. Appl. Pharmacol. **117**: 65–74.

Niimi, A.J. 1983. Biological and toxicological effects of environmental contaminants in fish and their eggs. Can. J. Fish. Aquat. Sci. **40**: 306–312.

Niimi, A.J. 1987. Biological half-lives of chemicals in fishes. Rev. Environ. Contam. Toxicol. **99**: 1–46.

Niimi, A.J., and Oliver, B.G. 1983. Biological half-lives of polychlorinated biphenyl (PCB) congeners in whole fish and muscle of rainbow trout (*Salmo gairdneri*). Can. J. Fish. Aquat. Sci. **40**: 1388–1394.

Norstrom, R.J., McKinnon, A.E., and de Freitas, A.S.W. 1976. A bioenergetics-based model for pollutant accumulation by fish. Simulation of PCB and methylmercury residue levels in Ottawa River yellow perch (*Perca flavescens*). J. Fish. Res. Board Can. **33**: 248–267.

Oliver, B.G., and Niimi, A.J. 1988. Trophodynamic analysis of polychlorinated biphenyl congeners and other chlorinated hydrocarbons in the Lake Ontario ecosystem. Environ. Sci. Technol. **22**: 388–397.

O'Rourke, S.M., Drouillard, K.G., and Haffner, G.D. 2004. Determination of laboratory and field elimination rates of polychlorinated biphenyls (PCBs) in the freshwater mussel, *Elliptio complanata*. Arch. Environ. Contam. Toxicol. **47**: 74–83.

Peters, R.H., Cabana, G., Choulik, O., Cohen, T., Griesbach, S., and McCanny, S.J. 1996. General models for trophic fluxes in animals based on their body size. Ecoscience, **3**: 365–377.

Ricker, W.E. 1979. Growth rates and models. *In* Fish physiology. *Edited by* W.S. Hoar, D.J. Randall, and J.R. Brett. Academic Press, New York. pp. 677–743.

Roy, D., Haffner, G.D., and Brandt, S.B. 2004. Estimating fish production potentials using a temporally explicit model. Ecol. Model. **173**: 241–257.

Russell, R.W., Gobas, F.A.P.C., and Haffner, G.D. 1999. Maternal transfer and in ovo exposure of organochlorines in oviparous organisms: a model and field verification. Eviron. Sci. Technol. **33**: 416–420.

Sijm, D.T.H.M., and Van der Linde, A. 1995. Size-dependent bioconcentration kinetics of hydrophobic organic chemicals in fish based on diffusive mass transfer and allometric relationships. Environ. Sci. Technol. **29**: 2769–2777.

Sijm, D.T.H.M., Selnen, W., and Opperhuizen, A. 1992. Life-cycle biomagnification study in fish. Environ. Sci. Technol. **26**: 2162–2174.

Simoneau, M., Lucotte, M., Garceau, S., and Laliberté, D. 2004. Fish growth rates modulate mercury concentrations in walleye (*Sander vitreus*) from eastern Canadian lakes. Environ. Res. **98**: 73–82.

Trudel, M., and Rasmussen, J.B. 1997. Modeling the elimination of mercury by fish. Environ. Sci. Technol. **31**: 1716–1722.

Wilkinson, L. 1998. SYSTAT for Windows: statistics. Version 8.0 ed. SPSS Inc., Chicago, Ill.

Winberg, G.G. 1956. Rate of metabolism and food requirements of fishes. Fish. Res. Board Can. Transl. Ser. No. 194. Fisheries Research Board of Canada, Nanaimo, B.C.

Appendix A

Table A1 appears on the following pages.

Appendix reference

Hawker, D.W., and Connell, D.W. 1988. Octanol–water partition coefficients of polychlorinated biphenyl congeners. Environ. Sci. Technol. **22**: 382–387.

Table A1. Growth-corrected half-lives ($t_{1/2}$) for 72 polychlorinated biphenyl (PCB) congeners in three yellow perch (*Perca flavescens*) size classes over summer (0–60 days), spring (300–365 days), and annual (0–365 days) seasonal cycles.

		Half-lives (days)								
		0–60			300–365			0–365		
Congener	K_{ow}	Small	Medium	Large	Small	Medium	Large	Small	Medium	Large
PCB 19	5.02	20	27	41	26	NA	17	80	112	77
PCB 18	5.24	26	39	54	26	18	32	96	110	215
PCB 17	5.25	35	56	109	44	30	37	130	122	316
PCB 24/27	5.40	26	39	62	26	32	32	106	144	229
PCB 16/32	5.30	28	44	70	37	26	35	117	96	249
PCB 26	5.66	31	52	72	59	40	43	179	232	668
PCB 25	5.67	42	82	207	51	39	45	198	191	691
PCB 31/28	5.67	36	70	105	65	46	45	205	264	900
PCB 33/20	5.59	32	55	94	57	44	41	167	201	472
PCB 22	5.58	41	49	74	54	42	43	186	202	443
PCB 45	5.53	39	85	119	64	44	50	229	309	>1000
PCB 52	5.84	46	157	157	100	53	60	438	921	NA
PCB 49	5.85	40	105	95	112	54	57	418	>1000	NA
PCB 47/48	5.82	46	173	195	100	54	57	476	875	NA
PCB 44	5.75	43	112	128	88	56	56	348	593	NA
PCB 42	5.76	42	147	170	88	49	57	417	956	NA
PCB 64/41/71	5.87	43	131	146	98	55	60	410	730	NA
PCB 40	5.66	37	77	111	74	51	59	279	452	NA
PCB 74	6.20	44	121	316	146	57	61	542	>1000	NA
PCB 70/76	6.17	41	103	132	108	58	56	419	>1000	NA
PCB 66	6.20	45	132	188	118	55	67	603	>1000	NA
PCB 56/60	6.11	44	112	279	115	61	58	407	975	NA
PCB 95	6.13	53	199	260	113	59	68	717	>1000	NA
PCB 91	6.13	50	199	316	134	59	70	725	>1000	NA
PCB 92	6.35	48	286	420	145	59	67	857	NA	NA
PCB 84	6.04	49	177	101	108	58	61	638	>1000	NA
PCB 101	6.38	54	237	280	156	65	75	>1000	NA	NA
PCB 99	6.39	47	157	236	160	58	70	>1000	NA	NA
PCB 97	6.29	51	156	255	161	62	67	854	>1000	NA
PCB 87	6.29	51	174	268	158	64	70	785	>1000	NA
PCB 85	6.30	43	466	279	176	59	64	876	NA	NA
PCB 110	6.48	52	215	238	147	62	70	894	NA	NA
PCB 118	6.74	46	165	268	180	63	67	>1000	NA	NA
PCB 105	6.65	41	126	159	203	63	65	775	NA	NA
PCB 136	6.22	67	>1000	896	146	64	73	>1000	NA	NA
PCB 151	6.64	68	NA	NA	193	65	76	>1000	NA	NA
PCB 144/133	6.77	63	>1000	>1000	173	64	75	>1000	NA	NA
PCB 149	6.67	65	>1000	>1000	199	65	76	>1000	NA	NA
PCB 134	6.55	57	303	365	272	63	76	>1000	NA	NA

Table A1 *(concluded).*

		Half-lives (days)								
		0–60			300–365			0–365		
Congener	K_{ow}	Small	Medium	Large	Small	Medium	Large	Small	Medium	Large
PCB 146	6.89	62	>1000	NA	191	66	78	>1000	NA	NA
PCB 153/132	6.75	63	>1000	>1000	191	63	77	>1000	NA	NA
PCB 141	6.82	66	>1000	NA	213	69	76	>1000	NA	NA
PCB 130	6.80	55	222	264	204	65	71	>1000	NA	NA
PCB 137	6.83	52	118	710	191	65	77	>1000	NA	NA
PCB 138	6.83	58	679	544	197	64	76	>1000	NA	NA
PCB 158	7.02	86	NA	NA	239	66	77	>1000	NA	NA
PCB 128	6.74	54	220	495	219	67	71	>1000	NA	NA
PCB 156	7.18	54	436	NA	687	68	71	>1000	NA	NA
PCB 157	7.18	58	789	NA	>1000	71	71	>1000	NA	NA
PCB 179	6.73	74	NA	NA	188	67	80	>1000	NA	NA
PCB 176	6.76	71	>1000	NA	188	68	82	>1000	NA	NA
PCB 178	7.14	72	NA	NA	301	67	83	>1000	NA	NA
PCB 187/182	7.19	75	NA	NA	305	68	84	>1000	NA	NA
PCB 183	7.20	75	NA	NA	279	68	83	>1000	NA	NA
PCB 185	7.11	82	NA	NA	327	69	85	>1000	NA	NA
PCB 174	7.11	71	NA	NA	244	68	77	>1000	NA	NA
PCB 177	7.08	74	NA	NA	269	68	79	>1000	NA	NA
PCB 171	7.11	87	>1000	NA	327	68	78	>1000	NA	NA
PCB 172	7.33	60	>1000	NA	525	76	80	>1000	NA	NA
PCB 180	7.36	70	NA	NA	344	72	81	>1000	NA	NA
PCB 170/190	7.37	72	>1000	NA	395	71	83	>1000	NA	NA
PCB 202	7.24	78	NA	NA	307	67	85	>1000	NA	NA
PCB 200	7.27	82	NA	NA	284	64	95	NA	NA	NA
PCB 199	7.20	75	369	NA	416	74	82	>1000	NA	NA
PCB 201	7.62	79	NA	NA	480	79	97	>1000	NA	NA
PCB 196/203	7.65	82	NA	NA	682	81	99	>1000	NA	NA
PCB 195	7.56	72	NA	NA	875	75	88	>1000	NA	NA
PCB 194	7.84	75	NA	NA	376	85	95	>1000	NA	NA
PCB 208	7.71	63	NA	NA	NA	73	109	NA	NA	NA
PCB 207	7.74	43	NA	147	457	88	125	>1000	NA	NA
PCB 206	8.09	82	NA	NA	764	100	121	>1000	NA	NA
PCB 209	8.18	53	NA	NA	NA	66	109	NA	NA	NA

Note: PCB congener half-lives ($t_{1/2}$) are calculated according to first-order kinetics. See Materials and methods for calculations. Experimental period is in days, with day 0 occurring 21 June 2003. Log K_{ow} values are from Hawker and Connell (1988). Half-life values denoted as NA indicate no elimination observed during experimental sampling period. Half-life values denoted as >1000 indicate elimination of congener occurred during experimental sampling period, but half-life was calculated to be longer than 1000 days.

Planktonic linkages among marine protected areas on the south Florida and southeast United States continental shelves

Jonathan A. Hare and Harvey J. Walsh

Abstract: One proposed benefit of marine protected areas (MPAs) is increased larval export, potentially increasing recruitment in unprotected areas. Because most marine species have planktonic larvae, information regarding planktonic transport is needed to evaluate the benefit of larval export. We used satellite-tracked drifters to define planktonic transport routes and rates from three MPAs along the south Florida and southeast United States (US) continental shelves. Drifter tracks indicated both long-distance transport and local retention. A probability model was developed based on drifter releases. The region was broken into zones; zone-specific residence times and movements between zones were defined from the drifter tracks. Transport out of the region in association with the Loop Current – Florida Current – Gulf Stream was the most frequently observed outcome, yet retention was high in the lower Florida Keys and on the Georgia shelf. From the model results, long-distance planktonic transport and local retention are the endpoints of a continuum rather than a dichotomy. Further, the outcome of planktonic transport is spatially heterogeneous with some regions exhibiting more retention and others exhibiting more export. The spatial aspects of planktonic transport described here should be considered in designing MPAs with fishery management objectives in the south Florida and southeast US shelf ecosystems.

Résumé : Un des bénéfices attendus des zones de protection marines (« MPAs ») est l'accroissement de l'exportation de larves, ce qui augmente potentiellement le recrutement dans les zones non protégées. Puisque la plupart des espèces marines ont des larves planctoniques, il faut connaître les déplacements du plancton pour pouvoir évaluer le bénéfice de l'exportation de larves. Nous avons utilisé des balises dérivantes suivies par satellite afin de déterminer les voies et les taux de transport planctoniques à partir de trois MPAs situées le long des plate-formes continentales du sud de la Floride et du sud-est des É.-U. Les tracés des balises représentent à la fois le transport à grande distance et la rétention locale. Nous avons mis au point un modèle basé sur les libérations des balises. Nous avons divisé la région en zones et déterminé les temps spécifiques de séjour dans les zones et les déplacements entre les zones d'après les tracés des balises. Le résultat le plus fréquemment observé est un transport vers l'extérieur en rapport avec le courant Loop, le courant de Floride et le Gulf Stream, mais il y a aussi une forte rétention dans les Keys de Floride inférieurs et la plate-forme de Géorgie. D'après les résultats du modèle, le transport planctonique de grande distance et la rétention locale sont plus les points extrêmes d'un continuum que les points opposés d'une dichotomie. De plus, le résultat du transport planctonique est hétérogène dans l'espace, certaines régions connaissant plus de rétention et d'autres plus d'exportation. Les aspects spatiaux du transport planctonique que nous décrivons devraient être pris en considération dans l'établissement de MPAs pour la gestion des pêches dans les écosystèmes de la plate-forme continentale dans le sud de la Floride et le sud-est des É.-U.

[Traduit par la Rédaction]

Introduction

Larvae of marine fish and invertebrates are collected far from known spawning locations, indicating long-distance transport (Scheltema 1971, 1986; Leis 1985). These observations are supported by calculations made with average current speed and direction indicating long-distance transport of passive planktonic particles (McGowan and Richards 1989; Roberts 1997). Additionally, many marine populations are genetically homogenous over large spatial scales, which is

Received 24 April 2006. Accepted 11 July 2007. Published on the NRC Research Press Web site at cjfas.nrc.ca on 1 September 2007. J19289

J.A. Hare[1,2] and H.J. Walsh.[3] NOAA NOS NCCOS, Center for Coastal Fisheries and Habitat Research, 101 Pivers Island Road, Beaufort, NC 28516, USA.

[1] Corresponding author (e-mail: jon.hare@noaa.gov).
[2] Present address: NOAA NMFS NEFSC, Narragansett Laboratory, 28 Tarzwell Drive, Narragansett, RI 02882, USA.
[3] Present address: Biology Department, Woods Hole Oceanographic Institution, Woods Hole, MA 02543, USA.

Can. J. Fish. Aquat. Sci. **64**: 1234–1247 (2007) doi:10.1139/F07-089

taken as evidence for planktonic exchange among distant locations (Mitton et al. 1989; Bowen and Avise 1990; Shulman and Bermingham 1995).

Long-distance planktonic transport is considered an important element in the management of marine populations (Doherty and Williams 1988; Fogarty et al. 1991; Caley et al. 1996). The scale of many marine populations is hypothesized to be quite large, in part owing to the concept that planktonic larval transport effectively mixes individuals over large distances (see Sinclair 1988). Consequently, the scale of managed units (stocks) is also large; for example, the 73 species in the snapper–grouper complex of the South Atlantic Bight Fishery Management Council are managed as single stocks from the Florida Keys to North Carolina (NOAA 2005), a linear distance of ~1500 km.

The concept of long-distance planktonic transport also has been incorporated into theories of marine protected area (MPA) design and function. MPAs can be designed with different objectives: protect biodiversity, protect specific habitats, act as a buffer against stock collapse or extinction, and contribute to fishery management (National Research Council (NRC) 2001). MPAs designed with fishery management objectives are expected to provide local fishery benefits through the spillover of juvenile and adults (Roberts et al. 2001; Russ et al. 2004). Larger-scale benefits are predicted through increased input to the larval pool, which hypothetically increases recruitment to the population as a whole, again through the thorough mixing of planktonic individuals (Roberts 1995, 1997; Gaines et al. 2003).

Although the concept of long-distance planktonic transport is embedded in views of marine populations, many recent studies indicate local retention of planktonic stages. In some physical systems (e.g., estuaries), there are well-defined biophysical mechanisms that result in local retention (e.g., selective tidal-stream transport; Cronin and Forward 1986; Rowe and Epifanio 1994). Larval behavior may also interact with circulation in the open ocean to promote local retention (Cowen et al. 2000; Paris and Cowen 2004; Hare and Govoni 2005). Biophysical models of larval transport have revealed that local retention may dominate over long-distance transport in some areas (James et al. 2002; Cowen et al. 2003; Paris et al. 2005). Additionally, recent genetic studies have found differences among locations in species with pelagic larvae, thereby indicating limited mixing of individuals among locations (Taylor and Hellberg 2003). Finally, some of the best evidence for local retention comes from larval tagging studies, which use chemical marks on otoliths; these studies have found self-recruitment rates of 5%–60% (Jones et al. 1999, 2005; Almany et al. 2007). With evidence for both long-distance planktonic transport and local planktonic retention, the critical need is to quantify actual planktonic transport and incorporate this knowledge into spatially explicit management strategies (see Hare 2005; Cowen et al. 2006).

Our purpose was to quantify planktonic transport pathways along the continental shelves of south Florida and the southeast United States (US). We used satellite-tracked drifters released at three MPAs to examine site-specific routes and rates of planktonic transport. We then used these drifter tracks and other drifter tracks from the region to develop a model that quantified the probability of planktonic transport among different areas of the south Florida and southeast US shelves. Drifters have been used previously to study planktonic transport routes and rates in the region (Lee et al. 1994; Domeier 2004; Edwards et al. 2006), but this is one of the first attempts to build a region-wide probabilistic model of larval transport (see Zakardjian et al. 2003).

Material and methods

Study area

The marine regions bordering the southeastern US (Texas to North Carolina) can be divided into three systems: the Gulf of Mexico, south Florida, and the southeast US continental shelves. The Gulf of Mexico extends from the Yucatan Peninsula to southern Florida. South Florida extends from the Florida Keys to West Palm Beach, Florida, and is distinguished by near continuous coral reefs on a very narrow continental shelf. The southeast US continental shelf extends from West Palm Beach, Florida, to Cape Hatteras, North Carolina. Our study examines planktonic transport processes in the south Florida and southeast US continental shelf regions (see Fig. 1*a*).

These three marine systems are connected by the western Atlantic Ocean boundary current, which includes the Loop Current, Florida Current, and Gulf Stream (Boicourt et al. 1998). The Loop Current flows northward through the Yucatan Straits into the Gulf of Mexico and then turns 180° to flow south and then 90° to flow east into the Florida Straits. The Florida Current continues to flow east along the Florida Keys reef tract and then turns to the northeast and north around southeastern Florida following the shelf break. The Gulf Stream continues to follow the shelf break along the southeast US continental shelf and detaches from the shelf at Cape Hatteras. Velocities in this western boundary current can exceed 2 $m \cdot s^{-1}$. Given the length scale of the system (westernmost Florida Keys to Cape Hatteras = ~1500 km) and these maximal velocities, planktonic transport can theoretically occur along the entire length in less than 10 days (McGowan and Richards 1989).

Although the Loop Current –Florida Current – Gulf Stream causes downstream transport of plankton from the Gulf of Mexico to Florida and the Carolinas (Ortner et al. 1995; Tester and Steidinger 1997), the current speed and direction at any place along the shelf break is quite variable owing to the occurrence of cyclonic eddies on the inshore side of the current. Along the Florida Keys reef track, large cyclonic eddies form in association with the turning of the Loop Current into the Florida Straits (Lee et al. 1991). Meanders in the Gulf Stream along the southeast US shelf also generate cyclonic frontal eddies that propagate downstream with the current (Bane and Dewar 1988; Lee et al. 1991). Cyclonic eddies have been implicated in the retention of planktonic larvae in the vicinity of the Florida Keys (Paris et al. 1997; Sponaugle et al. 2005), but their importance to larval transport along the southeast US shelf is largely unknown (see Govoni and Hare 2001). Thus, even though the Loop Current – Florida Current – Gulf Stream can be thought of as a conveyor belt transporting plankton downstream, there are features of the system that can provide retention.

Fig. 1. (*a*) Map of the North American eastern coast; the study region is indicated by the box. Approximate path of the Loop Current – Florida Current – Gulf Stream is shown as a shaded dotted line. (*b*) Map of marine protected areas on the south Florida and southeast US continental shelves. MPA designation based on definition used by the US government (Federal Register 2000).

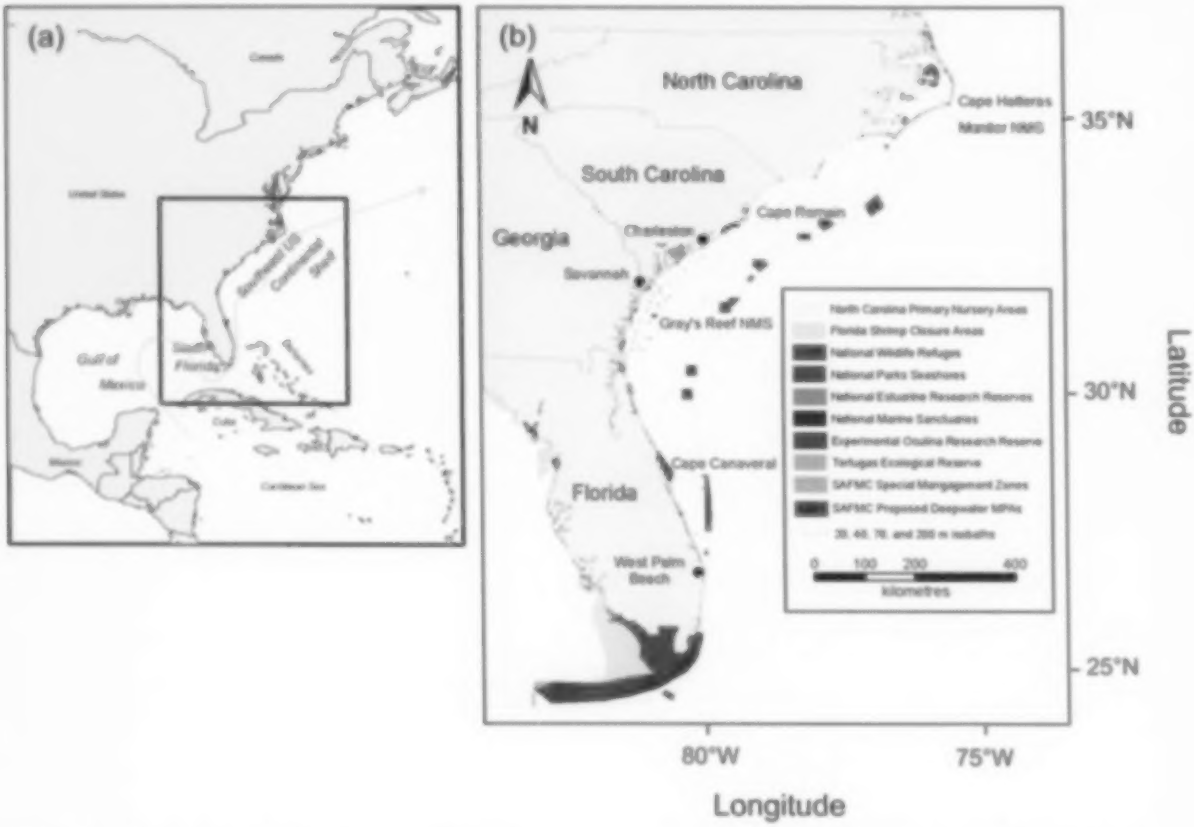
(a)
Canada
United States
Southeast US Continental Shelf
Gulf of Mexico
South Florida
Cuba
Mexico
Caribbean Sea
(b)
N
North Carolina
Cape Hatteras
Monitor NMS
South Carolina
Cape Romain
Charleston
Georgia
Savannah
Gray's Reef NMS
Cape Canaveral
Florida
West Palm Beach
North Carolina Primary Nursery Areas
Florida Shrimp Closure Areas
National Wildlife Refuges
National Parks Seashores
National Estuarine Research Reserves
National Marine Sanctuaries
Experimental Oculina Research Reserve
Tortugas Ecological Reserve
SAFMC Special Mangagement Zones
SAFMC Proposed Deepwater MPAs
20, 40, 70, and 200 m isobaths
0 100 200 400
kilometres
35°N
30°N
25°N
Latitude
80°W
75°W
Longitude

There are a number of MPAs in the south Florida and southeast US shelf systems (Fig. 1*b*). South Florida has a large amount of area protected (but to varying degrees) with the Florida Bay National Park, Biscayne Bay National Park, and the Florida Keys National Marine Sanctuary (NMS). At the westernmost end of the Florida Keys NMS is the Tortugas Ecological Reserve, a large (~520 km^2) no-take marine reserve established in 2001 with the objective of protecting diverse marine life and lush coral reefs in the Dry Tortugas area. The reserve is split into two sections: Tortugas North, which protects coral reef habitat on the Tortugas Bank, and Tortugas South, which protects Riley's Hump, an important snapper and grouper spawning aggregation site.

Much less area is protected along the southeast US continental shelf relative to the south Florida system (Fig. 1*b*). The Experimental Oculina Research Reserve was established in 1994 to protect deepwater coral habitat and grouper spawning aggregations. The Reserve includes 322 km^2 stretched along the east Florida shelf break. The region is closed to bottom fishing, but pelagic fishing is allowed. Gray's Reef National Marine Sanctuary is a small MPA (~58 km^2) located 32 km off the coast of Sapelo Island, Georgia. The Sanctuary is near the boundary between inner- and mid-shelf zones, with depth at the site sloping from 12 m to 20 m. Bottom trawling is prohibited but hook-and-line fishing is allowed.

Drifter releases and tracking

A total of 56 satellite-tracked drifters were released in the three MPAs: Tortugas South Ecological Reserve (Tortugas South ER), Experimental Oculina Research Reserve (Oculina RR), and Gray's Reef National Marine Sanctuary (Gray's Reef NMS) (Fig. 1*b*; Table 1). All drifters were the WOCE SVP design, which includes a surface float attached to a holey sock drogue (Sybrandy and Niiler 1990). Drogues were centered at 15 m for the Oculina RR and Tortugas South ER releases and at 10 m for the Gray's Reef NMS releases. Drogue lengths were between 3.5 and 6.6 m depending on drogue depth and drifter manufacturer. Twenty-one drifters were released in the Tortugas South ER over Riley's Hump; drifters were released in a triangular pattern approximately 2.5 km apart. Only 17 tracks were analyzed because of transmission failures and premature retrievals. Twenty drifters were released in the Oculina RR; on a given date, four drifters were released in a rectangular pattern with a north–south dimension of 24 km and an east–west dimension of 8 km. Nineteen tracks were analyzed because of a premature retrieval. Fifteen drifters were released at Gray's Reef NMS; on a given date, drifters were released in a trian-

Table 1. Summary of drifter releases made in three marine protected areas along the south Florida and southeast US shelves: Tortugas Ecological Reserve (Tortugas ER), Experimental Oculina Research Reserve (Oculina RR), and Gray's Reef National Marine Sanctuary (Gray's Reef NMS).

Release site	Release date	No. of drifters released	No. of drifter tracks analyzed	Drogue depth (m)
Gray's Reef NMS	26 April 2000	3	2*	10
Gray's Reef NMS	21 June 2000	3	2†	10
Gray's Reef NMS	3 October 2000	3	3	10
Gray's Reef NMS	30 January 2001	3	3	10
Gray's Reef NMS	22 March 2001	3	3	10
Tortugas ER	24 June 2000	3	2†	15
Tortugas ER	17 July 2000	3	3	15
Tortugas ER	24 July 2000	3	2†	15
Tortugas ER	31 July 2000	3	3	15
Tortugas ER	8 July 2001	3	2†	15
Tortugas ER	16 July 2001	3	2†	15
Tortugas ER	20 July 2001	3	3	15
Oculina RR	15 February 2002	4	4	15
Oculina RR	12 March 2002	4	4	15
Oculina RR	20 April 2002	4	3†	15
Oculina RR	22 July 2002	4	4	15
Oculina RR	19 August 2002	4	4	15

*Two drifters were tangled after release and treated as one drifter for the analyses presented here.

†Drifter was either retrieved prematurely or stopped transmitting <10 days after release.

Table 2. Larval durations of members of the South Atlantic Fisheries Management Council (SAFMC) snapper–grouper complex (summarized from Lindeman et al. 2000).

Family (or subfamily)	Common name	Approximate larval duration (days)	No. of species in SAFMC snapper–grouper complex
Epinepheline	Groupers	45	21
Lutjanidae	Snappers	30	14
Haemulidae	Grunts	15	10
Sparidae	Porgies	25	9
Labridae	Wrasses	25	2

gular pattern approximately 2.5 km apart near the center of the Sanctuary. Two drifters collided with each other and remained together for an extended period of time; these two drifters were treated as one. Another drifter was retrieved prematurely, so only 13 tracks were analyzed from Gray's Reef NMS releases. Thus, of the 56 drifters released, 49 were included in the analyses.

Drifter location was tracked via Service ARGOS with approximately four fixes per day. Location data from all drifters were quality checked and linearly interpolated to produce tracks at 6-h time intervals. Tracks were truncated when drifters crossed inshore of the 20 m isobath for the drifters drogued at 15 m and at the 15 m isobath for drifters drogued at 10 m.

Data analysis

Three analyses were conducted to provide a general view of planktonic larval transport from the three release locations. First, a simple spaghetti plot was created to provide a general overview of planktonic transport routes along southern Florida and the southeastern US coast. Second, specific transport routes were identified and drifter tracks were classified to these specific routes to provide an estimate of the likelihood of larvae being transported over the various routes. Finally, drifter locations were examined at 15, 30, 45, and 60 days after release. These times correspond to the planktonic duration of many important fishery species in the region (Table 2), and this analysis provides insights into the time scales of the various transport routes.

Planktonic transport model

Overview

A probability model was developed to provide a more quantitative view of larval transport along the south Florida and southeast US continental shelves. The model was, in essence, a box model with the spatial structure based on alongshelf and cross-shelf zones. A probability function of the residence times of drifters in each box was estimated from drifter tracks. The probability of movement from one box to all neighboring boxes also was calculated from drifter tracks. The zone-specific functions of residence times and movements to neighboring boxes were then used to construct a probability model of planktonic transport in the study area.

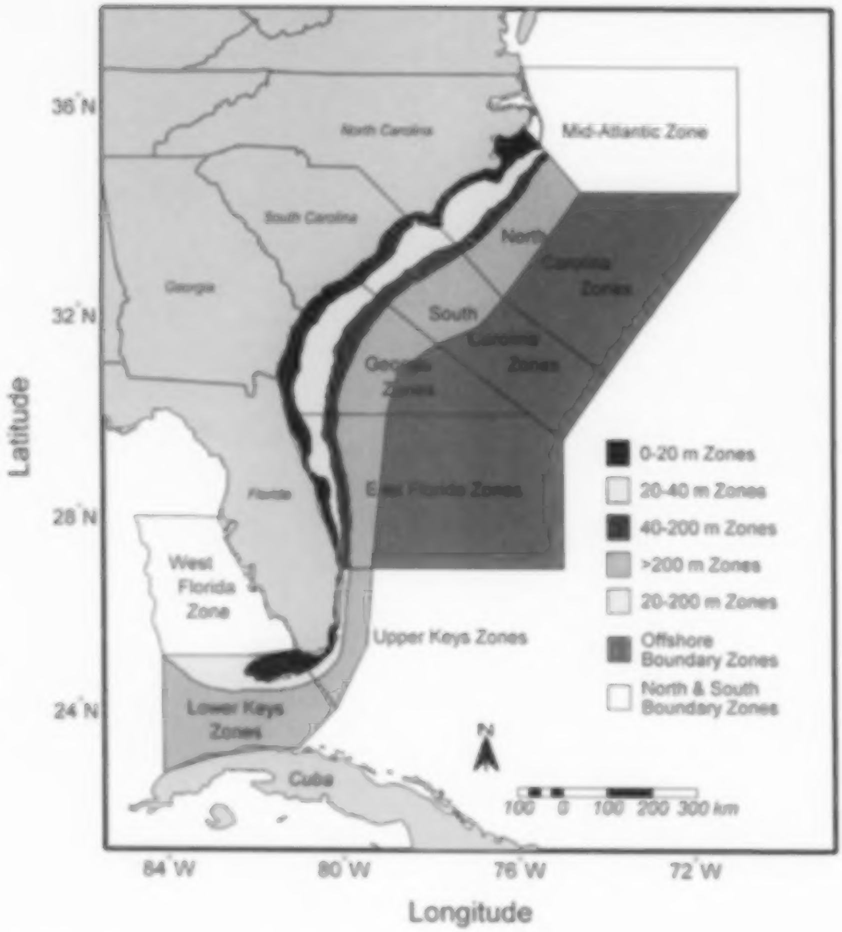
36°N
32°N
28°N
24°N
84°W
80°W
76°W
72°W
Latitude
Longitude
North Carolina
South Carolina
Georgia
Florida
Mid-Atlantic Zone
North Carolina Zones
South Carolina Zones
Georgia Zones
East Florida Zones
West Florida Zone
Upper Keys Zones
Lower Keys Zones
Cuba
0-20 m Zones
20-40 m Zones
40-200 m Zones
>200 m Zones
20-200 m Zones
Offshore Boundary Zones
North & South Boundary Zones
N
100 0 100 200 300 km

Fig. 2. Along-shelf and cross-shelf zones used in the probability model of larval transport along the south Florida and southeast US shelves.

Particles were released in various zones of the model and moved in accordance with the residence-time probability distributions and movement probability distributions. Analyses were conducted of the movement of particles through the spatial domain, including examination of the location of particles from a given release zone over time and the number of particles present in a zone that were released in that zone (a measure of retention).

The model was developed in five steps: (*i*) the study region was divided into along-shelf and cross-shelf zones (i.e., boxes); (*ii*) the position of each drifter at each time was assigned to a zone; (*iii*) zone-specific residence times were calculated and zone-specific movements were tallied for each drifter; (*iv*) probability functions were estimated for residence time and movement for each zone; and (*v*) particles were moved through model domain using probability functions of residence time and movement. These steps are outlined below and more detail is given in Supplemental Appendix S1 (available from the NRC Depository of Unpublished Data).[4]

Division of study region into zones

The study region was divided into zones based on previously defined along-shelf and cross-shelf patterns in circulation (Atkinson and Menzel 1985; Pietrafesa et al. 1985; Lee et al. 1991, 1994). Six along-shelf zones were defined: North Carolina, South Carolina, Georgia, East Florida, Upper Keys, and Lower Keys (Fig. 2). A maximum of five cross-shelf zones were defined for each along-shelf zone: 0–20 m, 20–40 m, 40–200 m, >200 m, and an offshore boundary zone. In addition, zones were designated upstream (West Florida) and downstream (Mid-Atlantic) of the study region; these two zones had no across-shelf structure. Owing to the narrowness of the continental shelf in the Lower and Upper

---

[4] Supplementary data for this article are available on the journal Web site (http://cjfas.nrc.ca) or may be purchased from the Depository of Unpublished Data, Document Delivery, CISTI, National Research Council Canada, Building M55, 1200 Montreal Road, Ottawa, ON K1A 0R6, Canada. DUD 5195. For more information on obtaining material refer to http://cisti-icist.nrc-cnrc.gc.ca/irm/unpub_e.shtml.

Keys region, two continental shelf zones were combined into one: 20–200 m. Further, owing the narrowness of the Florida Straits, with Cuba and the Bahamas to the south and east, the offshore boundary zones were excluded for the Lower and Upper Keys. The boundaries of the along-shelf and cross-shelf zones (Fig. 2) then were converted into polygons.

Assignment of drifter positions to zones

The position of each drifter at every 6-h interval was assigned to a zone using the *inpoly* function of MatLab (The MathWorks Inc., Natick, Massachusetts, www.mathworks.com). The 49 drifters releases analyzed in this study were included (Table 1). Drifters tracks from two additional sources also were included (see Supplemental Appendix S1)[4]. In all, the tracks of 105 drifters were included in the development of the model.

Calculation of residence time and tally of movements

Once the zone assignments were made, the instances of movement between zones were identified. Based on the zone assignments and the instances of movement between zones, the residence time of each drifter in each zone was determined. In addition, when a drifter left a zone, the zone it moved into was determined. This resulted in a list of zones, residence times within these zones, and movement to new zones.

Residence-time and movement probability functions

The list of residence times for each zone was used to calculate a residence-time distribution based on the gamma distribution. The gamma distribution closely approximates the normal distribution with the advantage that it has density only for positive real numbers (i.e., residence times cannot be negative). In addition, for each zone, the frequencies of movement to every other zone were calculated from the tally of movements. Frequencies were expressed from 0 to 1 and, thus, represent the probability of movement from each zone to every other zone (see Supplemental Table S1.1).[4]

Model calculation

Ten thousand particles were started in zones encompassing the shelf and slope of the region. Releases were made in the following zones: 20–40 m, 40–200 m, and >200 m in North Carolina, South Carolina, Georgia, and east Florida and 20–200 m and >200 m in Upper Keys and Lower Keys. Each particle then randomly moved through the model domain based on the probability distribution of residence times and the probability of movement from a zone to every other zone. If a particle moved into a <20 m zone, it stayed there. Similarly, if a particle moved into the Mid-Atlantic zone or the West Florida shelf zone, it remained there. Particles were tracked for 60 days, and the results were used to quantify several aspects of larval transport in the system, including the number of particles transported northward in Gulf Stream flows, the number of particles remaining on the south Florida and southeast US shelves, the number of particles remaining in or returning to their release zones, and the specific movement of particles released in zones containing the three focal MPAs of this study.

Results

Analysis of drifter tracks

General circulation patterns

Most of the drifters were transported downstream in association with the Loop Current – Florida Current – Gulf Stream (i.e., eastward along Florida Keys, northwards along east Florida, and northeastward along Georgia, South Carolina, and North Carolina; Fig. 3). Many of the drifters eventually moved past Cape Hatteras and out of the southeast US continental shelf system. Embedded in this general pattern, however, were several specific aspects of the circulation that are important to planktonic transport in the south Florida and southeast US shelf systems. (*i*) Some drifters released at the Tortugas South ER moved up the west Florida shelf. (*ii*) Large and small cyclonic eddies were evident in the region of the Tortugas and Florida Keys. (*iii*) A retention area on the Georgia shelf was observed. (*iv*) A region of onshore transport both south and north of the Georgia shelf was evident with drifters moving out of Gulf Stream associated flows.

Identification of transport routes

Four transport routes were identified for drifters released at the Tortugas South ER (Fig. 4*a*). (*i*) Some drifters remained in the vicinity of the Florida Keys reef track, often exhibiting cyclonic motions to the west and south of the Florida Keys. (*ii*) Some drifters moved northwards along the west Florida shelf. (*iii*) Three drifters moved downstream in the Florida Current but exited onto the east Florida shelf. (*iv*) Three drifters were caught in the Florida Current and continued northward past Cape Hatteras in the Gulf Stream.

Four transports routes also were evident for drifters released at the Oculina RR (Fig. 4*b*). (*i*) About half of the drifters moved rapidly along the shelf break in Gulf Stream associated flows and moved out of the southeast US shelf system. The remaining drifters moved north in Gulf Stream associated flows, but then exited onto the (*ii*) north Florida – Georgia shelf, (*iii*) the South Carolina shelf, and (*iv*) the North Carolina shelf.

Drifters released at Gray's Reef NMS exhibited three transport routes (Fig. 4*c*). (*i*) A majority of the drifters slowly moved offshore, yet remained on the Georgia shelf. The remaining drifters moved along the shelf to (*ii*) the northeast and (*iii*) the southwest.

Time scale of transport routes

Examining drifter locations at specific time intervals indicated that the various transport routes identified above operated at time scales relevant to planktonic larval transport (Fig. 5). More than half of the drifters released at the Tortugas ER remained in the area at 15 and 30 days, but the percentage dropped to ~20% and ~15% at 45 and 60 days, respectively. The percentage of Tortugas ER drifters occurring on the west Florida shelf increased over time from ~20% at 15 and 30 days to ~45% at 45 and 60 days. The percentage of drifters occurring on the east Florida shelf ranged from about 15% at 15 and 60 days to 20% at 30 and 45 days. These data indicate that larvae spawned at the Tortugas South ER can be transported to the west and east

Fig. 3. Spaghetti plot of drifters released at Tortugas South Ecological Reserve (Tortugas South ER), Experimental Oculina Research Reserve (Oculina RR), and Gray's Reef National Marine Sanctuary (Gray's Reef NMS). Drifter release locations are indicated by stars.

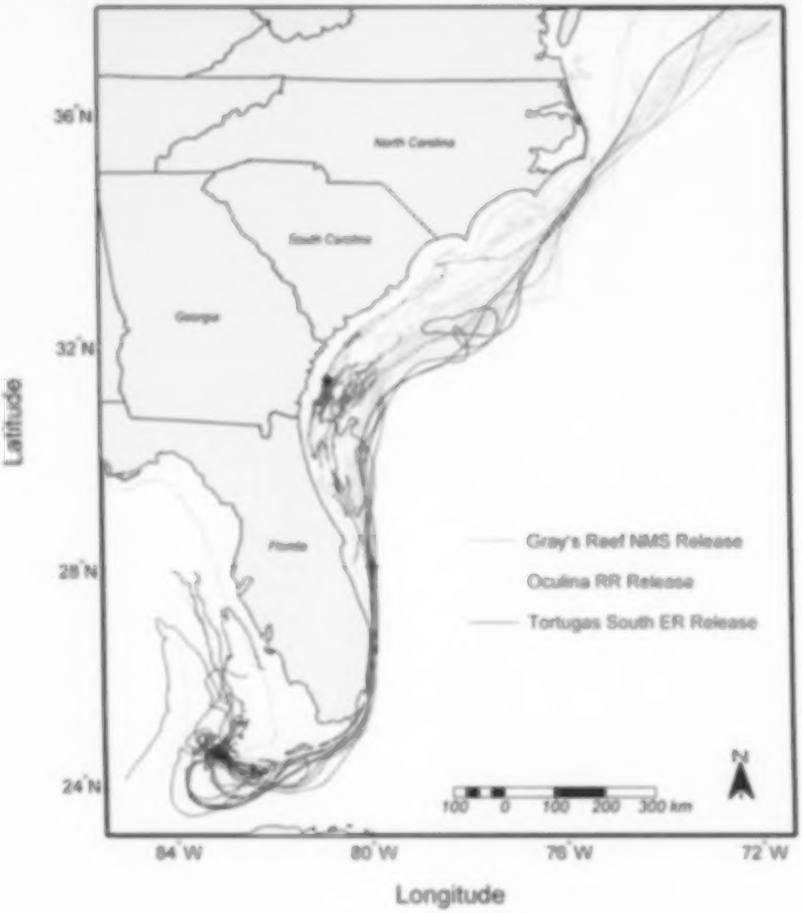

Florida shelves and be retained in the vicinity of the Florida Keys at the time scales of planktonic larval durations.

Many of the drifters released at Oculina RR were rapidly transported north of Cape Hatteras: ~20% of the drifters were north of Cape Hatteras at 15 days, ~40% at 30 days, and ~80% at 45 and 60 days. These data indicate that many of the larvae spawned at Oculina RR are likely lost from the southeast US shelf to the north. However, ~30% of the drifters remained on the southeast US shelf at 15 days. The percentage increased to 50% at 30 days, resulting from the movement of drifters from the Gulf Stream onto the Georgia, South Carolina, and North Carolina shelves. At 45 and 60 days, 20% and 15%, respectively, of the drifters remained on the southeast US shelf. Thus, for larvae spawned at Oculina RR, significant retention on the shelf is likely, albeit to the north of the Oculina RR.

Most of the drifters released at Gray's Reef NMS were retained on the Georgia shelf, and some remained in the area for as long as 60 days. Some transport to the north was evident at 30- and 45-day time intervals and loss to north of Cape Hatteras was evident at 60 days. These data indicate that many of the larvae spawned at Gray's Reef NMS are likely retained on the Georgia continental shelf.

Transport model

The probability model clearly showed that the Loop Current – Florida Current – Gulf Stream influenced particle transport in the region (Fig. 6). The percentage of total particles in the Mid-Atlantic zone was 25%, 48%, 59%, and 65% at 15, 30, 45, and 60 days, respectively. The >200 m South and North Carolina zones also contained large numbers of particles over time as particles moved downstream en route to the Mid-Atlantic zone.

Despite this obvious downstream transport, there was evidence for the retention of particles within the south Florida and southeast US shelf systems. Although most zones lost particles over time, the 20–40 m Georgia zone accumulated particles, and it was not until after day 25 that there were fewer particles than were released in the zone (Fig. 6). Also, the inshore zones (<20 m zones from the Lower Keys to North Carolina zones) accumulated particles over time, particularly in the inshore Georgia and east Florida zones. Parti-

Fig. 4. Examples of transport routes for drifters released at (*a*) Tortugas South Ecological Reserve, (*b*) Experimental Oculina Research Reserve, and (*c*) Gray's Reef National Marine Sanctuary. Each drifter track shown is representative of several similar drifter tracks. Drifter release locations are indicated by stars. Drifter positions every 5 days are shown as black dots overlain on drifter tracks.

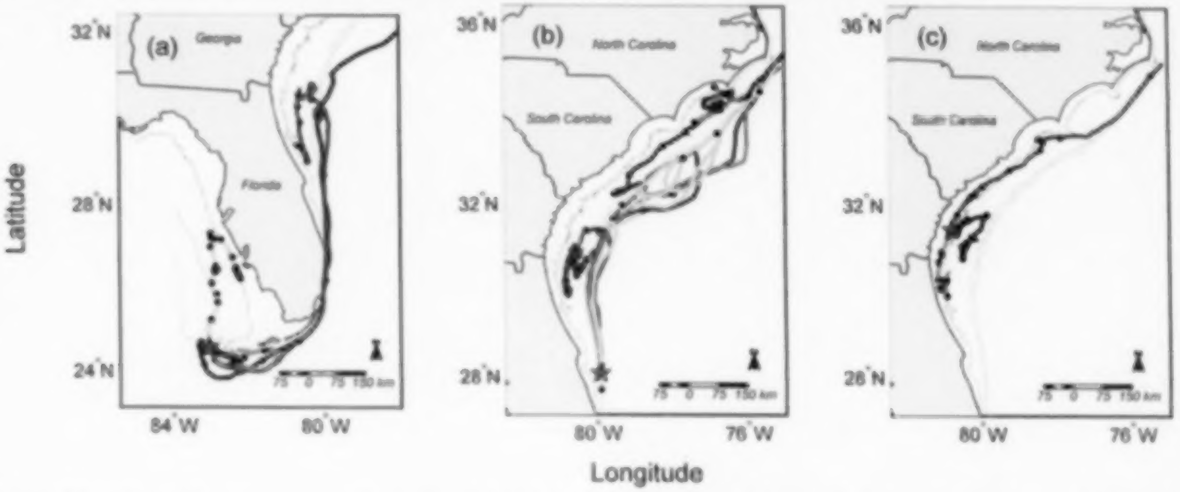

cles could not leave these zones once they entered, but their arrival indicates a consistent supply to inshore areas.

The number of particles on the shelf from each release area also provided evidence for retention (Fig. 7). "On the shelf" is defined as particles moving into or remaining in shelf zones (<20 m, 20–40 m, and 40–200 m) from the Lower Keys to North Carolina. There is a clear inshore–offshore gradient, with more particles released inshore remaining or returning to the shelf over time compared with particles released offshore. There are also along-shelf differences, with more particles from the Lower Keys, east Florida, and Georgia than from the Upper Keys, South Carolina, and North Carolina zones remaining on the shelf.

The number of particles remaining in (or returning to) their release zone provides further evidence for retention and potential self-recruitment (Fig. 8). The 20–40 m zones of North Carolina, South Carolina, and Georgia exhibited higher self-returning, with the Georgia zone exhibiting the highest self-retention. The Lower Keys zone also exhibited relatively high self-returning rates (Fig. 8).

The fate of released particles from zones containing Tortugas South ER, Oculina RR, and Gray's Reef NMS and the source of arriving particles for these zones are provided in Supplemental Figs. S2.1–S2.3.[4] All three MPAs likely supply larvae to adequate settlement habitats; this result was also suggested in the analysis of individual drifter tracks (see above). Thus, from the perspective of larval export, the Tortugas ER is well positioned to support populations in south Florida, on the west Florida shelf, and along the southeast US shelf. Oculina RR and Gray's Reef NMS are positioned to support populations along the southeast US shelf.

Discussion

Implications for MPAs in the south Florida and southeast US regions

For a benefit from larval export to be realized, MPAs need to protect spawning areas that successfully supply larvae to appropriate settlement habitats. Under these criteria, MPA design requires information of the life history of specific species, the location of spawning, the pathways of larval transport from each spawning location, and the spatial and temporal distribution of settlement habitats (Hockey and Branch 1997). As the design criteria for MPAs include more species, the distribution of spawning habitats, larval transport pathways, and settlement habitats begin to encompass the entire continental shelf system (Hockey and Branch 1997; Lindeman et al. 2000). The results of this study could be interpreted within the context of specific species and include details such as spawning locations and juvenile habitat distribution. However, given the number of fishery species present on the southeast US shelf (73 species in the snapper–grouper fishery management unit alone), such an undertaking is well beyond the scope of this study.

The analysis of drifter tracks indicate that the Tortugas ER, Oculina RR, and Gray's Reef NMS likely export larvae to broad areas throughout the region and that the Tortugas ER and Gray's Reef NMS may also be self-recruiting to a degree. Thus, these MPAs could contribute to fishery management through larval export to unprotected areas. Most studies indicate that 20%–50% of a species' habitat needs to be protected (i.e., no-take marine reserve) for MPAs to meet fishery management objectives (DeMartini 1993; Parrish 1999; NRC 2001). The combined area of the Tortugas ER is ~500 km^2 and much of the south Florida shelf is part of the Florida Keys National Marine Sanctuary (9600 km^2), which includes more than 20 no-take zones. However, the total percent area of no-take zones on the south Florida shelf is on the order of 5%, providing only some benefit for fisheries management (Dahlgren and Sobel 2000). MPAs and no-take areas along the southeast US shelf encompass much less area. Gray's Reef NMS is 54 km^2, whereas the inner Georgia shelf is ~15 000 km^2. Oculina RR and recent additions encompass about 1300 km^2, whereas the outer east Florida shelf is ~15 000 km^2. There are other MPAs in the region, with varying degrees of protection, but the amount currently

Fig. 5. Drifter locations (*a*) 15, (*b*) 30, (*c*) 45, and (*d*) 60 days after release at Tortugas South Ecological Reserve (Tortugas South ER), Experimental Oculina Research Reserve (Oculina RR), and Gray's Reef National Marine Sanctuary (Gray's Reef NMS). Drifter release locations are indicated by stars.

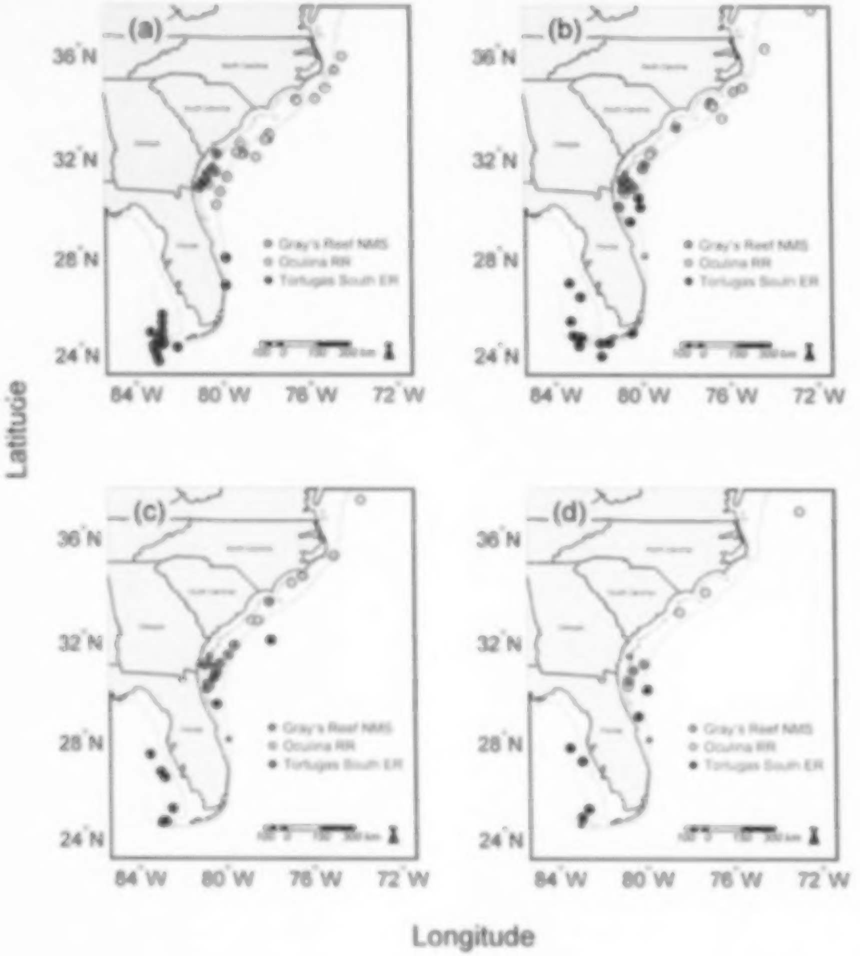

protected in no-take reserves is much less than that generally recommended for fisheries management objectives. Although well positioned, these smaller MPAs are likely to have only marginal influence on the dynamics of exploited fish populations across the regions. That said, these areas do protect reef habitat from destructive fishing practices and spawning aggregation sites (Gilmore and Jones 1992; Koenig et al. 2000; Burton et al. 2005), which are also important objectives of MPAs.

Larval transport processes

The drifter tracks and probability model identified several important larval transport processes in the south Florida and southeast US shelf systems. The role of cyclonic eddies in affecting retention and onshore larval transport in the Florida Keys region has been documented in prior studies (Lee et al. 1994; Paris et al. 1997; Sponaugle et al. 2005). The drifter tracks analyzed here provide further support for the importance of these cyclonic eddies in larval transport.

The drifter tracks also show that even after drifters are entrained in Gulf Stream associated flows, they can be detrained and move onto the southeast US shelf. Similar patterns of entrainment and detrainment have been documented in the Gulf Stream system north of Cape Hatteras (Ashjian 1993; Hare et al. 2002). The consequence is that downstream transport speeds for individual drifters rarely match the average current speeds reported for the Gulf Stream (1.5 $m \cdot s^{-1}$; McGowan and Richards 1989) over periods of time exceeding 5–10 days; by extension, estimates of transport distances based on average current speeds (see McGowan and Richards 1989; Roberts 1997) likely overestimate actual planktonic transport distances.

The drifter tracks also identify the Georgia shelf as a retention area. Some of the drifters released in the 20–40 m Georgia shelf zone remained for up to 60 days, and the probability model showed retention–return rates of 7% at 60 days. These retention times are similar to the estimates of Atkinson et al. (1978) based on flushing rates from freshwater runoff

Fig. 6. Number of particles present in different zones following release calculated from the probability model. Data for the along-shelf zones are included in different panels; data for the cross-shelf zones are defined by different lines in each panel. A schematic of the distribution of particles at day 30 is also shown; along-shelf zones are denoted by lines and cross-shelf zones are from the closest to the coast (<20 m zone) to furthest from the coast (>200 m or the offshore boundary). See Fig. 2 for map of zones.

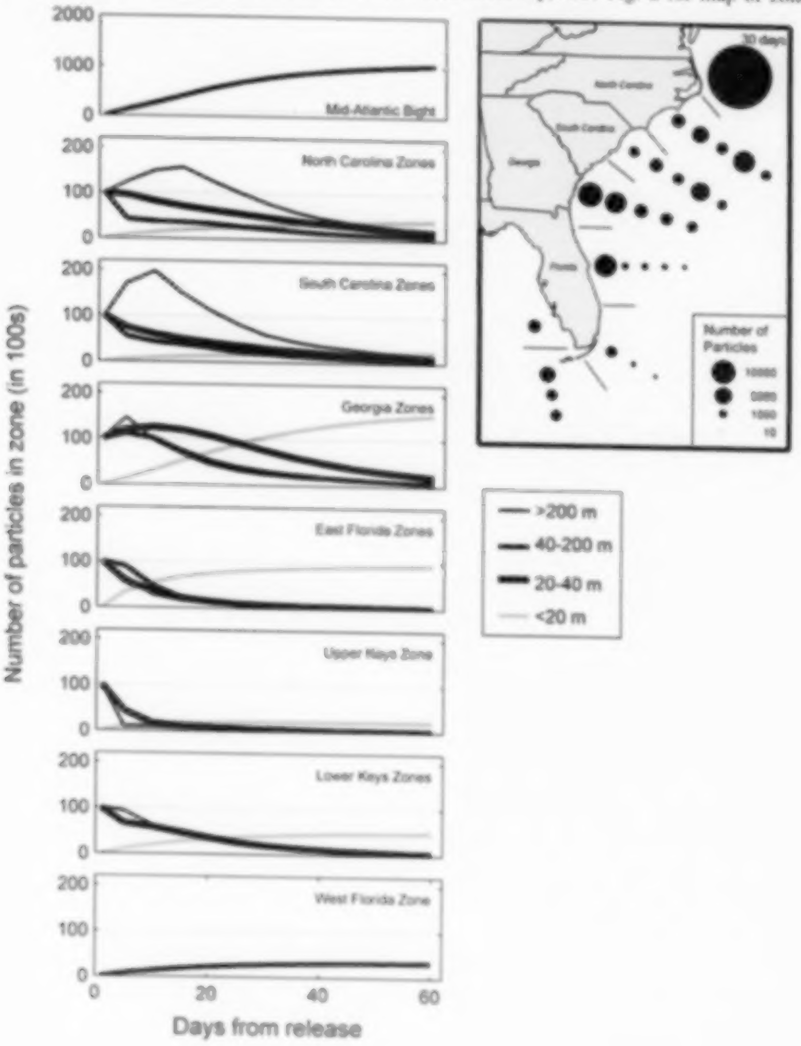

(81 days), as well as Gulf Stream meander frequency and entrainment volume estimates (60–90 days). The agreement between these disparate approaches provides strong evidence for the hypothesis that the Georgia shelf is a retention zone on time scales of most larval durations (15–60 days). The inner shelves (20–40 m) of the South and North Carolina zones also exhibited relatively high retention, but less than the 20–40 m Georgia zone. Further, the Georgia 20–40 m zone experienced less loss from the shelf overall compared with the North and South Carolina 20–40 m zones.

Review of approach

The probability model developed here was based on observational data and assumes constant probabilities of residence time and movement between zones. This assumption is certainly not correct (see Edwards et al. 2006, 2007). Drifters were released in every month of the year, so seasonal variability is incorporated into the probability distributions, but more drifters were released during the summer (Supplemental Fig. S1.2).[4] Another limitation is that the probability model is based on a limited number of releases (105), whereas the model used a large number of particles (10 000 in each zone). However, the drifter releases resulted in more than 500 observations of residence time and movements between zones, and in most cases, the gamma distribution fit the residence-time observations very well (see Supplemental Fig. S1.4).[4] An alternative, widely used approach for quantifying larval transport is three-dimensional circulation models coupled with Lagrangian particle tracking algorithms (Werner et al. 2001). Individ-

Fig. 7. Number of particles released within a zone remaining on the shelf following release. "On the shelf" is defined as in the <20 m, 20–40 m, and 40–200 m zones from the Lower Keys to North Carolina. Data for the along-shelf zones are included in different panels; data for the cross-shelf zones are defined by different lines. A schematic of the distribution of particles at day 30 is also shown; along-shelf zones are denoted by lines and cross-shelf zones are from the closest to the coast (< 20 m zone) to furthest from the coast (>200 m or the offshore boundary). See Fig. 2 for map of zones.

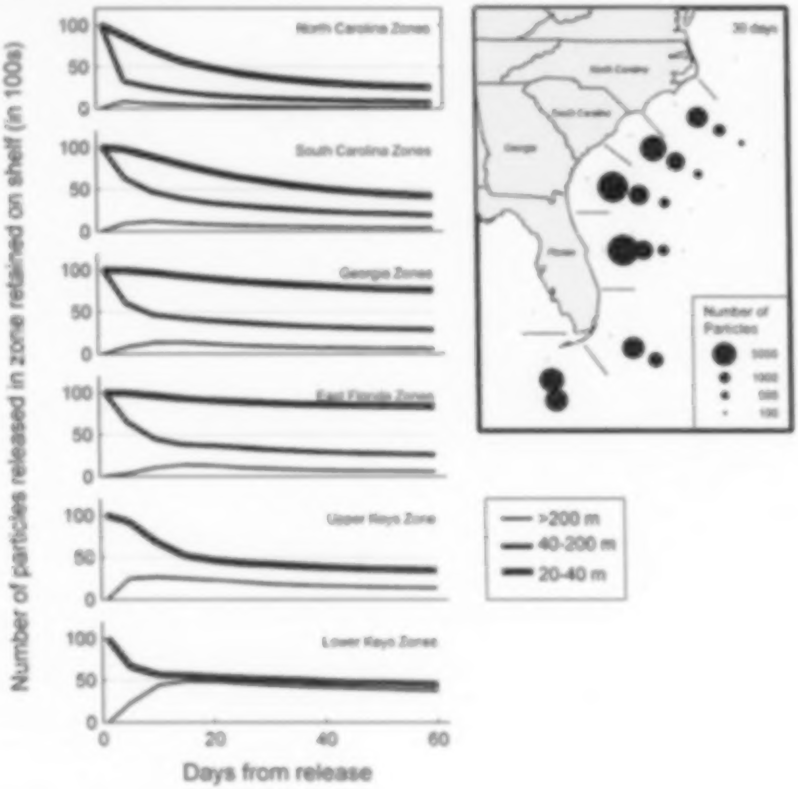

ual drifter tracks are often used to assess the accuracy of circulation models (e.g., Paris et al. 2005; Edwards et al. 2006), so in many instances, the two approaches can be developed simultaneously, with results from the circulation model aggregated spatially to match the resolution of an observation-based probability model (see Zakardjian et al. 2003). Concurrence between the two approaches provides validation of each and supports the application of circulation models at finer spatial scales.

The lack of larval behavior in the probability model deserves special attention. A number of studies have indicated that larval fish can modify their horizontal transport by occupying different vertical levels in the water column (Cowen et al. 1993; Hare et al. 1999; Paris and Cowen 2004). Hare and Govoni (2005) concluded that larvae in surface waters of the southeast US shelf were more likely to be exported to the Gulf Stream; larvae deeper in the water column were more likely to be transported onshore or remain on the shelf (see also Werner et al. 1999). The model developed here was based on surface drifters, so the results favor export, not retention. In addition, evidence that larvae are able to swim horizontally and orient this behavior is growing (Leis 2006). Thus, the amount of retention estimated by the probability model is likely an underestimate of the actual amount of larval retention in the system.

Future directions

The drifter tracks and probability models indicate that both long-distance transport and local retention occur in the south Florida and southeast US shelf systems. Thus, these two outcomes of planktonic transport represent part of a continuum, not a dichotomy. Further, the distribution of outcomes is not spatially homogenous; there are areas that promote retention and areas that promote long-distance transport. Thus, for management applications, it is difficult to generalize: system, region, and site-specific characterizations of actual planktonic transport will be required. There are also a broad variety of life history patterns exhibited by marine species and these species-specific attributes will need to be incorporated into management frameworks.

To understand the actual impact of planktonic transport processes on marine populations, estimates of exchange between spawning locations need to be incorporated into spatially explicit, stage-specific population models (see Fogarty 1998; Yakubu and Fogarty 2006). For most marine fish species, these models need to include exchange during juvenile

Fig. 8. Number of particles released within a zone remaining or returning to that zone following release. Data for the along-shelf zones are included in different panels; data for the cross-shelf zones are defined by different lines. A schematic of the distribution of particles at day 30 is also shown; along-shelf zones are denoted by lines and cross-shelf zones are from the closest to the coast (<20 m zone) to furthest from the coast (>200 m or the offshore boundary). See Fig. 2 for map of zones.

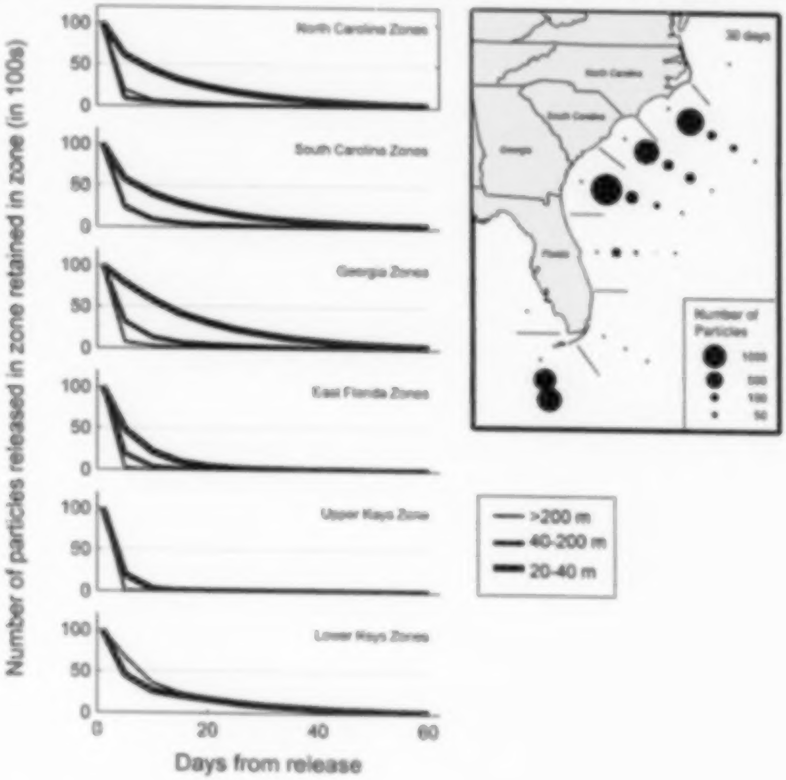

and adult stages, as well as during the planktonic stages (see Hare 2005). This coupling of planktonic transport models and population dynamic models based on real systems will allow the specific design and assessment of spatially explicit management strategies.

Acknowledgements

This work was supported by grants from the NOAA Coral Reef Program through the NOAA NMFS Southeast Fisheries Science Center for research at the Oculina RR, by the Office of National Marine Sanctuaries for research at the Tortugas South ER and Gray's Reef NMS, and by Gray's Reef NMS. Earlier drafts of this manuscript benefited from the input of David Mountain (NOAA, NMFS, Northeast Fisheries Science Center), John Manderson (NOAA, NMFS, Northeast Fisheries Science Center), and Katey Marancik (NOAA, NMFS, Northeast Fisheries Science Center), and two anonymous reviewers. We especially thank all those who participated in drifter deployment, among them John Burke, Craig Bonn, Brian Degan, Siya Lem, Michael Greene, and Katey Marancik, as well as the officers and crews of the NOAA Ship *Oregon II*, NOAA Ship *Ferrel*, and NOAA Ship *Whiting*. We also thank all those who helped track down stranded or prematurely retrieved drifters including Luiz Barbieri, Dan Theisen, Paul Bauersfeld, Don Field, Jim Colvocoresses, David Score, Fritz Wettstein, Steve Baumgardner, Erin McDevitt, and Joy Tatgenhorst. Finally, we thank Bob Cowen for his comments and for the suggestion of including additional drifters in the transport model. Acknowledgement of the above individuals does not imply their endorsement of this work; the authors have sole responsibility for the content of this contribution.

References

Almany, G.R., Berumen, M.L., Thorrold, S.R., Planes, S., and Jones, G.P. 2007. Local replenishment of coral reef fish populations in a marine reserve. Science (Washington, D.C.), **316**: 742–744.

Ashjian, C. 1993. Trends in copepod species abundances across and along a Gulf Stream meander evidence for entrainment and detrainment of fluid parcels from the Gulf Stream. Deep-Sea Res. I, **40**: 461–482.

Atkinson, L.P., and Menzel, D.W. 1985. Introduction: oceanography of the southeast United States continental shelf. *In* Oceanography of the southeastern U.S. continental shelf. *Edited by* L.P. Atkinson, D.W. Menzel, and K.A. Bush. American Geophysical Union, Washington, D.C. pp. 1–9.

Atkinson, L.P., Blanton, J.O., and Haines, E.B. 1978. Shelf flushing rates based on the distribution of salinity and freshwater in the Georgia Bight. Estuar. Coast. Mar. Sci. **7**: 465–472.

Bane, J.M., and Dewar, W.K. 1988. Gulf Stream bimodality and variability downstream of the Charleston Bump. J. Geophys. Res. **93**: 6695–6710.

Boicourt, W.C., Wiseman, W.J., Valle-Levinson, A., and Atkinson, L.P. 1998. Continental shelf of the southeastern United States and the Gulf of Mexico: in the shadow of the western boundary current. *In* The sea. Vol. 11. *Edited by* A.R. Robinson and K.H. Brink. John Wiley & Sons, New York. pp. 135–183.

Bowen, B.W., and Avise, J.C. 1990. Genetic structure of Atlantic and Gulf of Mexico populations of sea bass, menhaden, and sturgeon: influence of zoogeographic factors and life-history patterns. Mar. Biol. **107**: 371–381.

Burton, M.L., Brennan, K.J., Muñoz, R.C., and Parker, R.O. 2005. Preliminary evidence of increased spawning aggregations of mutton snapper (*Lutjanus analis*) at Riley's Hump two years after establishment of the Tortugas South Ecological Reserve. Fish. Bull. **103**: 404–410.

Caley, M.J., Carr, M.H., Hixon, M.A., Hughes, T.P., Jones, G.P., and Menge, B.A. 1996. Recruitment and the local dynamics of open populations. Annu. Rev. Ecol. Syst. **27**: 477–500.

Cowen, R.K., Hare, J.A., and Fahay, M.P. 1993. Beyond hydrography: can physical processes explain larval fish assemblages within the Middle Atlantic Bight? Bull. Mar. Sci. **53**: 567 587.

Cowen, R.K., Lwiza, K.M.M., Sponaugle, S., Paris, C.B., and Olson, D.B. 2000. Connectivity of marine populations: open or closed? Science (Washington, D.C.), **287**: 857–859.

Cowen, R.K., Paris, C.B., Olson, D.B., and Fortuna, J.L. 2003. The role of long distance dispersal versus local retention in replenishing marine populations. Gulf Caribb. Res. **4**: 129–137.

Cowen, R.K., Paris, C.B., and Srinivasan, A. 2006. Scaling of connectivity in marine populations. Science (Washington, D.C.), **311**: 522–527.

Cronin, T.W., and Forward, R.B., Jr. 1986. Vertical migration cycles of crab larvae and their role in larval dispersal. Bull. Mar. Sci. **9**: 192–201.

Dahlgren, C.P., and Sobel, J. 2000. Designing a Dry Tortugas Ecological Reserve: how big is big enough? … To do what? Bull. Mar. Sci. **66**: 707–719.

DeMartini, E.E. 1993. Modelling the potential of fishery reserves for managing Pacific coral reef fishes. Fish. Bull. **91**: 414–427.

Doherty, P.J., and Williams, D.McB. 1988. The replenishment of coral reef fish populations. Oceanogr. Mar. Biol. Annu. Rev. **26**: 487–551

Domeier, M.L. 2004. A potential larval recruitment pathway originating from a Florida marine protected area. Fish. Oceanogr. **13**: 287–294.

Edwards, K.P., Hare, J.A., Werner, F.E., and Blanton, B.O. 2006. Comparison of observed and modeled drifters on the southeast U.S. continental shelf: implications to larval dispersal and transport. Cont. Shelf Res. **26**: 1375–1394.

Edwards, K.P., Hare, J.A., Werner, F.E., and Seim, H. 2007. Using 2-dimensional dispersal kernels to identify the dominant influences on larval dispersal along continental shelf regions: a case-study along the U.S. southeast coast. Mar. Ecol. Prog. Ser. In press.

Federal Register. 2000. Presidential documents. Executive Order 13158 of May 26, 2000. Vol. 65, No. 105, May 31 2000. US Government Printing Office, Washington, D.C.

Fogarty, M.J. 1998. Implications of migration and larval interchange in American lobster (*Homarus americanus*) stocks: spatial structure and resilience. Can. Spec. Publ. Fish. Aquat. Sci. **125**: 273–283.

Fogarty, M.J., Sissenwine, M.P., and Cohen E.B. 1991. Recruitment variability and the dynamics of exploited marine populations. TREE, **6**: 241–246.

Gaines, S.D., Gaylord, B., and Largier, J.L. 2003. Avoiding current oversights in marine reserve design. Ecol. Appl. **13**(Suppl.): S32–S46.

Gilmore, R.G., and Jones, R.S. 1992. Color variation and associated behavior in the epinepheline groupers, *Mycteroperca microlepis* (Goode and Bean) and *M. phenax* Jordan and Swain. Bull. Mar. Sci. **51**: 83–103.

Govoni, J.J., and Hare, J.A. 2001. The Charleston Gyre as spawning and larval nursery habitat for fishes. *In* Island in the stream: oceanography and fisheries of the Charleston Bump. *Edited by* G.R. Sedberry. Am. Fish. Soc. Symp. **25**: 123–136.

Hare, J.A. 2005. The use of early life stages in stock identification studies. *In* Stock identification methods. *Edited by* S. Cardin, K. Friedland, and J. Waldman. Elsevier Academic Press, Amsterdam. pp. 89–117.

Hare, J.A., and Govoni, J.J. 2005. Vertical distribution and the outcome of larval fish transport along the southeast United States continental shelf during winter. Fish. Bull. **103**: 728–736.

Hare, J.A., Quinlan, J.A., Werner, F.E., Blanton, B.O., Govoni, J.J., Forward, R.B., Settle, L.R., and Hoss, D.E. 1999. Larval transport during winter in the SABRE study area: results of a coupled vertical larval behavior – three-dimensional circulation model. Fish. Oceanogr. **8**(Suppl. 1): 57–76.

Hare, J.A., Churchill, J.H., Cowen, R.K., Berger, T., Cornillon, P., Dragos, P., Glenn, S., Govoni, J.J., and Lee, T.N. 2002. Routes and rates of larval fish transport from the southeastern to the mid-Atlantic North American continental shelf. Limnol. Oceanogr. **47**: 1774–1789.

Hockey, P.A., and Branch, G.M. 1997. Criteria, objectives, and methodology for evaluating marine protected areas in South Africa. S. Afr. J. Mar. Sci. **18**: 369–383.

James, M.K., Armsworth, P.R., Mason, L.B., and Bode, L. 2002. The structure of reef fish metapopulations: modeling larval dispersal and retention patterns. Proc. R. Soc. Lond. B, **269**: 2079–2086.

Jones, G.P., Milicich, M.J., Emslie, M.J., and Lunow, C. 1999. Self-recruitment in a coral reef fish population. Nature (London), **402**: 802–804.

Jones, G.P., Planes, S., and Thorrold, S.R. 2005. Coral reef fish larvae settle close to home. Curr. Biol. **15**: 1314–1318.

Koenig, C.C., Coleman, F.C., Grimes, C., Fitzhugh, G., Scanlon, K., Gledhill, C., and Grace, M. 2000. Protection of fish spawning habitat for the conservation of warm-temperate reef-fish fisheries of shelf-edge reefs of Florida. Bull. Mar. Sci. **66**: 593–616.

Lee, T.N., Yoder, J.A., and Atkinson, L.P. 1991. Gulf Stream frontal eddy influence on productivity of the southeast U.S. continental shelf. J. Geophys. Res. **96**: 22 191 – 22 205.

Lee, T.N., Clarke, M.E., Williams, E., Szmant, A.F., and Berger, T. 1994. Evolution of the Tortugas Gyre and its influence on recruitment in the Florida Keys. Bull. Mar. Sci. **54**: 621–646.

Leis, J.M. 1985. Larval fish dispersal and the East Pacific Barrier. Oceanogr. Trop. **19**(2): 181–192.

Leis, J.M. 2006. Are larvae of demersal fishes plankton or nekton? Adv. Mar. Biol. **51**: 57–141.

Lindeman, K.C., Pugliese, R., Waugh, G.T., and Ault, J.S. 2000. Developmental patterns within a multispecies reef fishery: management applications for essential fish habitats and protected areas. Bull. Mar. Sci. **66**: 929–956.

McGowan, M.F., and Richards, W.J. 1989. Bluefin tuna, *Thunnus thynnus*, larvae in the Gulf Stream off the southeastern United States: satellite and shipboard observations of their environment. Fish. Bull. **87**: 615–631.

Mitton, J.B., Berg, C.J., and Orr, K.S. 1989. Population structure, larval dispersal, and gene flow in the queen conch, *Strombus gigas*, of the Caribbean. Biol. Bull. **177**: 356–362.

National Oceanic and Atmospheric Administration. 2005. Stock assessment and fishery evaluation report for the snapper–grouper fishery of the South Atlantic. (Available at http://ocean.floridamarine.org/efh_coral/pdfs/SnapperGrouperSAFE111805.pdf, accessed 17 January 2007).

National Research Council. 2001. Marine protected areas: tools for sustaining ocean ecosystems. National Academy Press, Washington, D.C.

Ortner, P.B., Lee, T.N., Milne, P.J., Zika, R.G., Clarke, M.E., Podesta, G.P., Swart, P.K., Tester, P.A., Atkinson, L.P., and Johnson, W.R. 1995. Mississippi river flood waters that reached the Gulf Stream. J. Geophys. Res. **100**: 13 595 – 13 602.

Pal, B.K., Murthy, R., and Thomson, R. 1998. Lagrangian measurements in Lake Ontario. J. Gt. Lakes. Res. **24**: 681–697.

Paris, C.B., Graber, H.C., Jones, D.L., Ropke, A.W., and Richards, W.J. 1997. Translocation of larval coral reef fishes via submesoscale spin-off eddies from the Florida Current. Bull. Mar. Sci. **60**: 966–983.

Paris, C.B., and Cowen, R.K. 2004. Direct evidence of a biophysical retention mechanism for coral reef fish larvae. Limnol. Oceanogr. **49**: 1964–1979.

Paris, C.B., Cowen, R.K., Claro, R., and Lindeman, K.C. 2005. Larval transport pathways from Cuban snapper (Lutjanidae) spawning aggregations based on biophysical modeling. Mar. Ecol. Prog. Ser. **296**: 93–106.

Parrish, R. 1999. Marine reserves for fisheries management: why not? Calif. Coop. Ocean. Fish. Investig. Rep. **40**: 77–86.

Pietrafesa, L.J., Janowitz, G.S., and Wittman, P.A. 1985. Physical oceanographic processes in the Carolina Capes. *In* Oceanography of the southeastern U.S. continental shelf. *Edited by* L.P. Atkinson, D.W. Menzel, and K.A. Bush. American Geophysical Union, Washington, D.C. pp. 23–32.

Roberts, C.M. 1995. Rapid build-up of fish biomass in a Caribbean marine reserve. Conserv. Biol. **9**: 815–826.

Roberts, C.M. 1997. Connectivity and management of Caribbean coral reefs. Science (Washington, D.C.), **278**: 1454–1457.

Roberts, C.M., Bohnsack, J.A., Gell, F., Hawkins, J.P., and Goodridge, R. 2001. Effects of marine reserves on adjacent fisheries. Science (Washington, D.C.), **294**: 1920–1923.

Rowe, P.M., and Epifanio, C.E. 1994. Tidal stream transport of weakfish larvae in Delaware Bay, USA. Mar. Ecol. Prog. Ser. **110**: 105–114.

Russ, G.R., Alcala, A.C., Maypa, A.P., Calumpong, H.P., and White, A.T. 2004. Marine reserve benefits local fisheries. Ecol. Appl. **14**: 597–606.

Scheltema, R.S. 1971. The dispersal of the larvae of shoal-water benthic invertebrate species over long distances by ocean. *In* Fourth European Marine Biology Symposium. *Edited by* D.J. Crisp. University Press, Cambridge. pp. 7–28.

Scheltema, R.S. 1986. Long-distance dispersal by planktonic larvae of shoal-water benthic invertebrates among Central Pacific islands. Bull. Mar. Sci. **39**: 241–256.

Shulman, M.J., and Bermingham, E. 1995. Early life histories, ocean currents, and the population genetics of Caribbean reef fishes. Evolution, **49**: 897–910.

Sinclair, M. 1988. Marine populations: an essay on population regulation and speciation. Washington Sea Grant Program, Seattle, Washington.

Sponaugle, S., Lee, T.N., Kourafalou, V.H., and Pikard, D. 2005. Florida Current frontal eddies and the settlement of coral reef fishes. Limnol. Oceanogr. **50**: 1033–1048.

Sybrandy, A.L., and Niiler, P.P. 1990. The WOCE/TOGA SVP Lagrangian drifter construction manual. Scripps Institution of Oceanography, University of California, San Diego, SIO Reference No. 90–248.

Taylor, M.S., and Hellberg, M.E. 2003. Genetic evidence for local retention of pelagic larvae in a Caribbean reef fish. Science (Washington, D.C.), **299**: 107–109.

Tester, P.A., and Steidinger, K.A. 1997. *Gymnodinium breve* red tide blooms: initiation, transport, and consequences of surface circulation. Limnol. Oceanogr. **42**: 1039–1051.

Werner, F.E., Blanton, B.O., Quinlan, J.A., and Luettich, R.A. 1999. Physical oceanography of the North Carolina continental shelf during the fall and winter seasons: implications for the transport of larval menhaden. Fish. Oceanogr. **8**(Suppl. 2): 7–21.

Werner, F.E., Quinlan, J.A., Lough, R.G. and Lynch, D.R. 2001. Spatially explicit individual based modeling of marine populations: a review of the advances in the 1990's. Sarsia, **86**: 411–421.

Yakubu, A.-A., and Fogarty, M.J. 2006. Spatially discrete metapopulation models with directional dispersal. Math Biosci. **204**: 68–101.

Yang, H., Weisberg, R.H., Niiler, P.P., Sturges, W., and Johnson, W. 1999. Lagrangian circulation and forbidden zone on the West Florida Shelf. Cont. Shelf Res. **19**: 1221–1245.

Zakardjian, B.A., Sheng, J., Runge, J.A., McLaren, I., Plourde, S., Thompson, K.R., and Gratton, Y. 2003. Effects of temperature and circulation on the population dynamics of *Calanus finmarchicus* in the Gulf of St. Lawrence and Scotian Shelf: study with a coupled, three-dimensional hydrodynamic, stage-based life history model. J. Geophys. Res. **108**: 8016. DOI: 10.1029/2002JC001410.

Overwintering habitat use of shortnose sturgeon (*Acipenser brevirostrum*): defining critical habitat using a novel underwater video survey and modeling approach

Xinhai Li, Matthew K. Litvak, and John E. Hughes Clarke

Abstract: The overwintering habitat use of shortnose sturgeon (*Acipenser brevirostrum*) was investigated from January to March 2005 in the upper Kennebecasis River, New Brunswick, Canada, using a novel underwater video camera system and modeling approach. Following a random sampling procedure, 187 holes were drilled into the ice, and 234 sturgeon were counted and video-recorded. We found that sturgeon concentrated in a 2 ha area at the confluence of the Kennebecasis and Hammond rivers on a flat sandy substrate at a depth of 3.1–6.9 m. Generalized linear models were developed to describe the relationship of shortnose sturgeon density and habitat variables. The model indicated that the shortnose sturgeon had significant preference to deeper areas within this region. The total abundance of shortnose sturgeon in the area was estimated to be 4836 ± 69 (mean ± standard error) using the ordinary kriging method to interpolate sturgeon density at unsampled sites. This overwintering habitat of shortnose sturgeon can be defined as critical habitat following the identification policies of the Canadian Species at Risk Act (SARA).

Résumé : Nous avons étudié l'utilisation de l'habitat en hiver chez l'esturgeon à museau court (*Acipenser brevirostrum*) de janvier à mars 2005 dans le cours supérieur de la Kennebecasis, Nouveau-Brunswick, Canada, à l'aide d'un système nouveau de caméra vidéo et avec une approche de modélisation. Après un échantillonnage aléatoire, nous avons percé 187 trous dans la glace et énuméré et filmé 234 esturgeons. Les esturgeons se concentrent sur une surface de 2 ha au confluent des rivières Kennebecasis et Hammond sur un substrat plat et sablonneux à une profondeur de 3,1–6,9 m. Nous avons mis au point des modèles linéaires généralisés pour décrire la relation entre la densité des esturgeons à museau court et les variables de l'habitat. Le modèle indique que les esturgeons montrent une préférence significative pour les zones les plus profondes dans cette région. Nous estimons l'abondance totale des esturgeons à museau court dans la région à 4836 ± 69 (moyenne ± écart type) en utilisant la méthode ordinaire de krigage pour interpoler les densités de saumons aux sites non échantillonnés. Cet habitat d'hiver de l'esturgeon à museau court peut être désigné comme habitat essentiel d'après les critères d'identification de la loi canadienne sur les espèces en péril (LEP, « SARA »).

[Traduit par la Rédaction]

Introduction

Sturgeons and paddlefishes are among the most endangered fishes in the world, with all 27 species listed on the International Union for Conservation of Nature and Natural Resources (IUCN) Red List: six species are critically endangered, 11 species are endangered, nine species are vulnerable, and one species is at low risk (IUCN 2006). Shortnose sturgeon (*Acipenser brevirostrum*) is one of the nine vulnerable species with a declining population trend (IUCN 2006). This trend has been attributed to blockage of spawning migrations by damming, regulation and dredging of rivers, bycatch from harvest, and pollution (Kynard 1997; National Marine Fisheries Service (NMFS) 1998). It was listed as an endangered species in the United States in 1967 (US Fish and Wildlife Service 1999) and a species of special concern in Canada in 1980 by the Committee on the Status of Endangered Wildlife in Canada (COSEWIC 2005). In spite of the urgent need of protection, there have only been a few studies on shortnose sturgeon habitat use and ecology.

Shortnose sturgeon inhabit 19 rivers along the Atlantic coast of North America, from the Saint John River in New Brunswick, Canada, its only Canadian population, to the St. Johns River in Florida, USA (NMFS 1998). Since

Received 17 July 2006. Accepted 18 April 2007. Published on the NRC Research Press Web site at cjfas.nrc.ca on 1 September 2007.
J19425

X.H. Li[1] and M.K. Litvak.[2] Department of Biology, University of New Brunswick, P.O. Box 5050, Saint John, NB E2L 4L5, Canada.
J.E. Hughes Clarke. Department of Geodesy and Geomatics Engineering, University of New Brunswick, Fredericton, NB E3B 5A3, Canada.

[1] Present address: Institute of Zoology, Chinese Academy of Sciences, Datun Road, Beijing 100101, China.

[2] Corresponding author (e-mail: litvak@unbsj.ca).

Can. J. Fish. Aquat. Sci. 64: 1248–1257 (2007) doi:10.1139/F07-093

Dadswell's (1979) systematic survey of the Saint John River population in the early to mid-1970s, only very basic information on habitat use of shortnose sturgeon has been studied in seven of these rivers (e.g., Kynard 1997; Kynard et al. 2000; Collins et al. 2002). In general, shortnose sturgeon are amphidromous, and their stay in salt water varies with latitude (Kynard 1997). Shortnose sturgeon are bottom feeders; they use their protractile mouths to suck up sand and mud to capture benthic crustaceans, molluscs, polychaetes, and small fishes (Dadswell 1979). Although we do know something of the summer habitat and activity, the overwintering habitat use of shortnose sturgeon is largely unknown.

Dadswell (1979), based on his gill net sampling, suggested that there were seven discrete overwintering sites in the lower Saint John River occurring in deep areas of lakes and river channels or in halocline regions. Hall et al. (1991), using telemetry tracking, concluded that adult and juvenile use the freshwater–saltwater boundary region of the Savannah River during both fall and winter. Based on a telemetry survey and classification of several hierarchical classes of the habitat, Kynard et al. (2000) suggested that Connecticut River shortnose sturgeon increased their use of curves, channels (deep water), and sand substrate in the fall; winter habitat selection continued the fall pattern, but the fish were less mobile. However, the knowledge of the actual habitat utilization of shortnose sturgeon in winter is very limited. Clearly, locating the overwintering habitat and determining habitat preference of shortnose sturgeon is a priority for protecting this species. Thus, the objectives of our study were to locate the overwintering site, discover how shortnose sturgeon use their habitat in winter, and estimate their population size. To accomplish this goal, we developed an underwater video approach that involved calibrating fish density with regard to water turbidity, and this information was used to develop and compare spatial autocorrelation models and calculate shortnose sturgeon population size.

Materials and methods

Study area and sonic telemetry

We tagged three shortnose sturgeon in the fall of 2004 to help us determine a general location of the overwintering habitat. These fish were captured from the upper Kennebecasis River, a tributary of the Saint John River in New Brunswick, Canada, on 21 September 2004. They were each implanted with an ultrasonic transmitter (V16; VEMCO, Shad Bay, Nova Scotia, Canada) and released on that day. These coded transmitters emitted a sonic burst at random intervals of 80–100 s that were detected using both omnidirectional and directional hydrophones attached to a receiver – tag decoder (VR60; VEMCO). The omnidirectional hydrophone was used to detect if the tagged fish were within 800 m radius (maximum detection envelope) of the hydrophone. The directional hydrophone was used to determine the bearing of the fish relative to the location of the observer. Bearings were determined by using a compass aligned with the head of the directional hydrophone to establish the direction of the strongest sound received and decoded by the VEMCO VR60. Global positioning system (GPS) locations were obtained with a Magellan Meridian Marine WAAS (wide area augmentation system) enabled handset at four or five different observer locations (either from boat or shore) over a short period of time. This WAAS-capable receiver provided a position accuracy of better than 3 m 95% of the time (http://www.magellangps.com/en/). The actual fish locations, including 95% confidence interval ellipses, were calculated using the bearing and latitude–longitude of each observer location with the telemetry software Locate III (Nams 2004).

We tracked these fish every other day in late September and October 2004 and found that they gradually moved upstream and stayed at one spot at the confluence of the Kennebecasis River and Hammond River for overwintering from 18 October 2004 (Fig. 1). Before good ice conditions, we occasionally tracked the sturgeon at the overwintering site during the winter by listening for the fish with the VEMCO VR60 at the river's edge. No significant movement of shortnose sturgeon was detected during the winter, so we started the survey at the location of the tracked shortnose sturgeon when ice conditions permitted access to the site.

Underwater video survey

We used an underwater video camera (Atlantis™ underwater viewing system AUW-525C; Atlantis Cameras, Bergenfield, New Jersey) to observe the sturgeon, count the fish, and record the habitat variables at the overwintering site. Visual-based techniques have been used during fish survey for over 40 years. SCUBA divers can quantify fish populations by direct observation using standard visual belt transects (Brock 1954). Remote observation techniques, such as underwater video, have been used in a few aquatic biological studies, such as observing reactions of Atlantic salmon (*Salmo salar*) and whitefish (*Coregonus lavaretus*) to modified trap nets (Toivonen and Hudd 1993) and estimating gill net selectivity (Grant et al. 2004). Recently, sidescan sonar technology has been used to determine spatial distribution of lake sturgeon (*Acipenser fulvescens*) (Thomas and Hass 2002). This is an excellent approach but is limited in its ability to determine species identity of each sonar image, whereas video imaging allows identification to the species level. To our knowledge, no studies have used an underwater camera to observe sturgeon overwintering aggregation and habitat use.

The survey was conducted from January to March 2005 when on-ice survey conditions were safe. We used a 10-inch ice auger (1 inch = 25.4 mm) (Jiffy Legend™ model 31; Jiffy Ice Drills, Sheboygan Falls, Wisconsin) to drill holes into the ice. The underwater video camera was attached to a 7 m long pole and was lowered through the holes in the ice to reach the river bottom. The camera orientation was parallel to the bottom so that we could have a side view and a greater radius of detection. The camera was turned 360 degrees to detect sturgeon within its zone of visibility. The images were recorded on a SONY DCR-HC30 digital video camera. The tapes were played back in the lab, and counts of shortnose sturgeon at each hole were recorded.

Locations of the holes were randomly selected. GPS locations were obtained with a Magellan Meridian Marine handset. Depth at each hole was measured using the long pole. The substrate composition below each hole was visually classified following a classification system based on sediment terminology of the American Geophysical Union (Lane

Fig. 1. Study area of habitat use of shortnose sturgeon (*Acipenser brevirostrum*) in Kennebecasis River. The upper maps show the study area in New Brunswick, Canada. The lower map is the enlarged area of the solid rectangle in the upper map indicating the exact study location (rectangle) and the sonic tracking results from the three adult shortnose sturgeon (SNS) from 19 September 2004 to 16 April 2005.

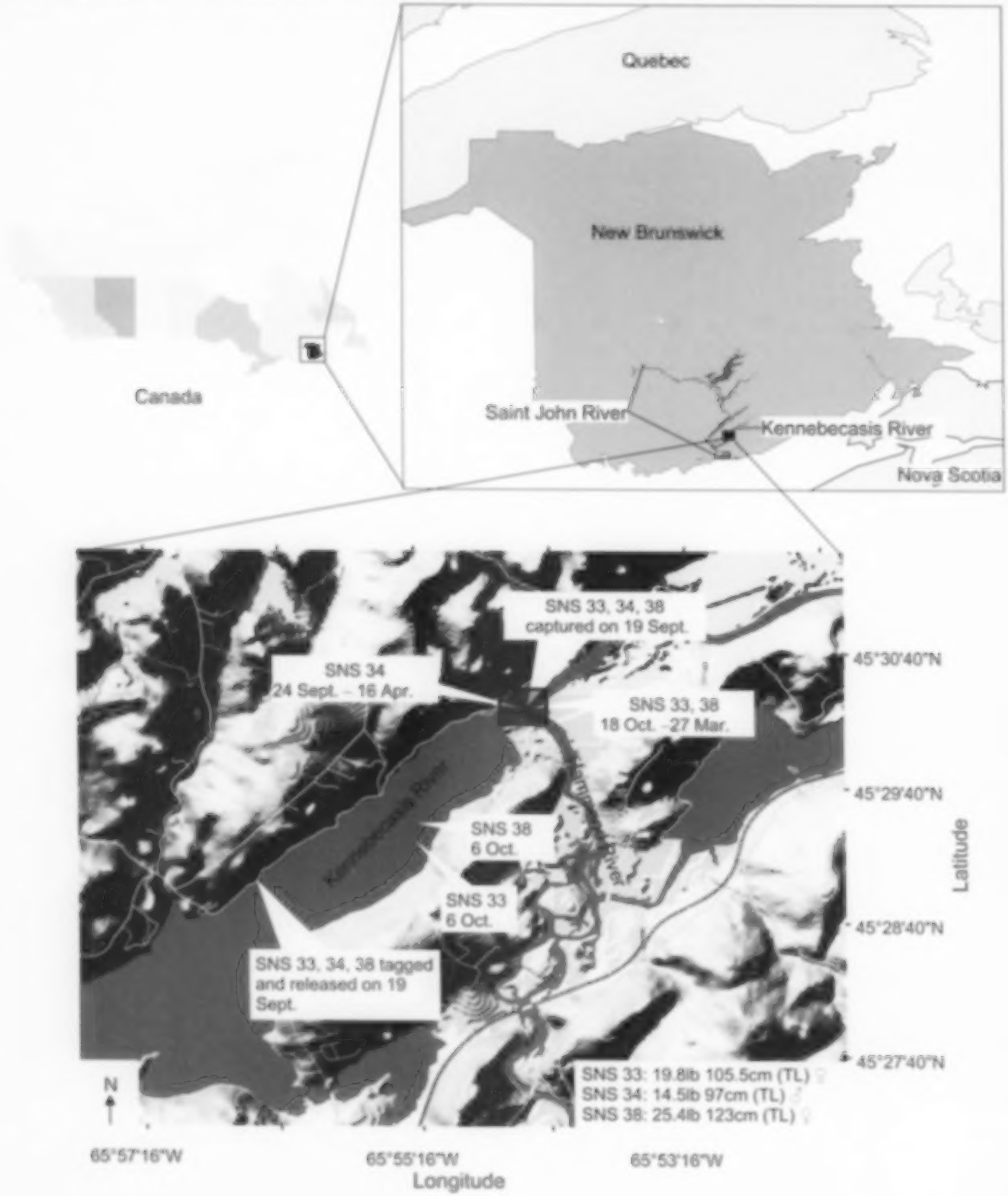
Quebec
New Brunswick
Canada
Saint John River
Kennebecasis River
Nova Scotia
SNS 33, 34, 38 captured on 19 Sept.
SNS 34 24 Sept. – 16 Apr.
SNS 33, 38 18 Oct. –27 Mar.
Kennebecasis River
Hammond River
SNS 38 6 Oct.
SNS 33 6 Oct.
SNS 33, 34, 38 tagged and released on 19 Sept.
SNS 33: 19.8lb 105.5cm (TL) ♀
SNS 34: 14.5lb 97cm (TL) ♂
SNS 38: 25.4lb 123cm (TL) ♀
N
45°30'40"N
45°29'40"N
45°28'40"N
45°27'40"N
Latitude
65°57'16"W
65°55'16"W
65°53'16"W
Longitude

Table 1. The categories of substrate at the confluence of Kennebecasis River and Hammond River, New Brunswick, following classification of stream substrate materials by particle size (Lane 1947; Platts et al. 1983).

Category	Size range (mm)	Index*
Silt	<0.062	1
Sand	0.062–1.0	2
Fine gravel	1–16	3
Coarse gravel	16–64	4
Cobble–boulders	64–4096	5

*The values used in the generalized linear models (GzLMs).

1947; Platts et al. 1983) (Table 1). The temperature at the river bottom was measured, using a VEMCO Minilog, at 5 min intervals for 2 days of deployment. The salinity and dissolved oxygen were measured using a YSI meter (model YSI 85; YSI Incorporated, Yellow Springs, Ohio).

Visibility

Visibility in water, as determined by turbidity and light intensity, has the potential to affect video survey results. We developed a protocol to correct for this effect. We dropped a cuboid lead weight as a scale to the river bottom and then lowered the video camera to the lead weight; while recording we moved the camera away until the lead weight was just out of sight in the turbid water. Still images were exported from the recorded video using software Adobe Premiere 6.5 (www.adobe.com), and the image length of the lead weight in the image when it was close to out of view was measured using image analysis software ImageJ 1.32J (Abramoff et al. 2004). In the lab, a similar procedure was conducted in a tank with clear water. We took images of the lead weight at known distances and then constructed the following simple linear regression model:

$$(1)\qquad D_{\text{water (cm)}} = -97.9L_{\text{image (cm)}} + 1154.4 \qquad (R^2 = 0.92,\ F = 43.1,\ p < 0.01)$$

where $D_{\text{water (cm)}}$ is the distance between the camera and the lead weight in water, and $L_{\text{image (cm)}}$ is the length of the lead weight in images. We calculated maximum visibility radius at each hole sampled by substituting the length when the lead weight almost disappeared in the water into the model.

Testing independence between holes

Spatial autocorrelation was checked using a semivariogram in order to test independence of observation (counts) at each hole. A typical semivariogram has a monotonic increase curve as long as the distance is less than a certain value, the range, indicating the variance between sites increases with the distance between the sites. Correlation exists between samples within the semivariogram range. In the analysis of habitat preference where the independence of sample is required, the holes within the semivariogram range were removed from the data set.

The temporal consistency between different survey days was checked using a paired t test on the same 31 holes over two consecutive days. The power of the test was conducted to avoid the possibility of committing a type II error if the null was not rejected.

Estimation of population size

The sturgeon count was standardized as sturgeon density by being divided by the observation area at each hole using the visibility $D_{\text{water (cm)}}$ as the radius. An ordinary kriging method was used to interpolate density values between the sample plots so that the sturgeon population size at the whole area could be estimated. Kriging is a method of interpolation named after D.G. Krige who developed the technique in an attempt to more accurately predict ore reserves. Over the past several decades, kriging has become a fundamental tool in the field of geostatistics.

Four theoretical semivariance models are commonly used in ordinary kriging: (*i*) Gaussian model: semivariance = nugget + sill{1 – exp[–lag(lag/range × range)]}; (*ii*) spherical model: semivariance = nugget + sill[1.5lag/range – 0.5(lag/range)^3], when lag ≤ range; semivariance = nugget + sill, when lag > range; (*iii*) exponential model: semivariance = nugget + sill[1 – exp(–3lag/range)], when lag > 0; semivariance = 0, when lag = 0; and (*iv*) power model: semivariance = nugget + sill(lag$^{\text{range}}$).

The actual semivariance model of sturgeon density between each hole was calculated using the SAS Variogram procedure (SAS Institute Inc., Cary, North Carolina). The model parameters were estimated as sill = 0.2, range = 10, and nugget = 0. The calculated semivariance, i.e., the experimental semivariance, was compared with the four theoretical semivariance models. The appropriate model was chosen based on the measurement of model fit that minimized the objective function:

$$(2)\qquad \sum_{\text{lag}} [\text{semivariance}(\text{lag}) - \text{semivariance}^{*}(\text{lag})]^2$$

i.e., the residual sum of squares between the theoretical semivariance (indicated by asterisk) and experimental semivariance (Cressie 1993; Mello and Rose 2005). Using the theoretical variogram model with best fit, ordinary kriging predictions were computed as

$$(3)\qquad Z(V) = \sum_{i=1}^{N} \lambda_i Z(\chi_i)$$

where $Z(V)$ is the estimate of density at an unsampled point, N is the number of holes, and λ_i is the weight attributed to sample x_i (Mello and Rose 2005). The ordinary kriging was processed using ArcGIS software (ESRI, Redlands, California), and the output included predictions (sturgeon density) and standard error of the predictions.

Habitat modeling

A generalized linear model (GzLM) was developed to describe the habitat preference regarding associated habitat variables and has the following form (McCullogh and Nelder 1989):

$$(4)\qquad g(\mu) = \beta_0 + \beta_{\text{depth}}\text{depth} + \beta_{\text{substrate}}\text{substrate} + \beta_{\text{depth} \times \text{substrate}}\text{depth} \times \text{substrate}$$

Fig. 2. The density of shortnose sturgeon (*Acipenser brevirostrum*) at the confluence of Kennebecasis River and Hammond River, New Brunswick, Canada, from February to March 2005. The arrows indicate the downstream flow direction.

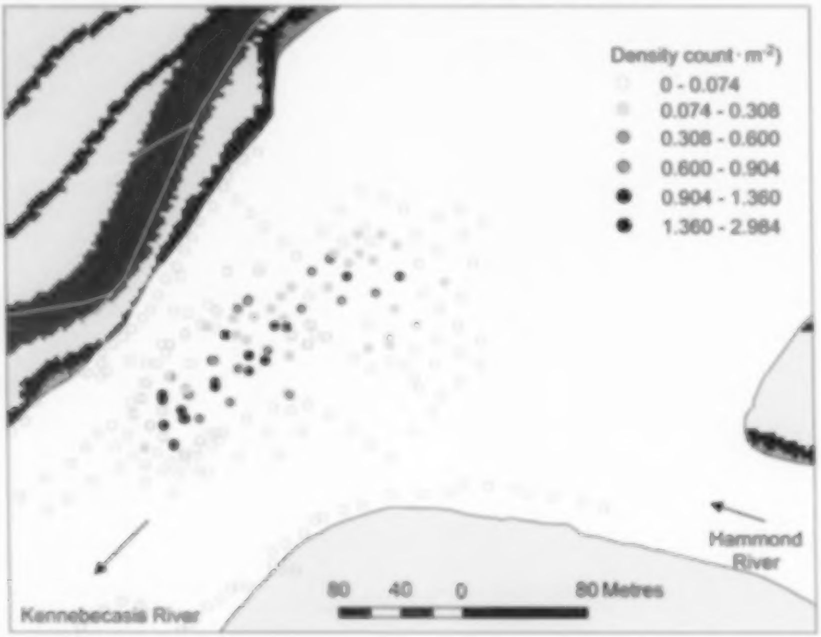

where $\mu = E(Y)$, Y is the density of shortnose sturgeon at each hole, depth and substrate are the covariates for observation Y, β_{depth} and $\beta_{\text{substrate}}$ are the linear coefficients, $\beta_{\text{depth} \times \text{substrate}}$ is the interaction coefficient, and $g()$ is a logarithm link function that links the random component $E(Y)$ to the systematic component $\beta_0 + \beta_{\text{depth}}$ depth + $\beta_{\text{substrate}}$ substrate + $\beta_{\text{depth} \times \text{substrate}}$ depth × substrate. The negative binomial distribution was used to describe the random component $E(Y)$ (Power and Moser 1999).

Results

In total, 187 holes were drilled into the ice, 234 sturgeon were counted (Figs. 2 and 3) and their images were digitally recorded on video. The river bottom habitat within the study area was dominated by sandy substrate, mixed with gravel and silt substrate. At the confluence, the Kennebecasis and the Hammond rivers are 141–340 m and 68 m wide, respectively (Fig. 2). The depth is deeper (6–6.9 m) at the downstream section than the upstream section (3–4 m). The majority of the area is sandy, as 89.3% of the holes are over sandy substrate. The shortnose sturgeon concentrated at the deepest area on this sandy substrate. There is a deeper area with gravel or cobble substrate downstream of this area, but no fish were found there. No sturgeon were found on silt substrate, as all the sample plots with silt substrate were in shallow areas where depth was less then 2 m. Our survey indicated that shortnose sturgeon concentrated within a 2 ha area at the confluence between the Kennebecasis River and Hammond River (Fig. 2) on a flat sandy substrate at the depth of 3.1–6.9 m (Fig. 4).

Fig. 3. Frequency distribution of (*a*) count and (*b*) density of shortnose sturgeon (*Acipenser brevirostrum*) at the 187 holes drilled at the confluence of Kennebecasis River and Hammond River, New Brunswick, Canada, from February to March 2005. In (*b*), the 187 holes are given identity numbers (ID) from 1 to 187.

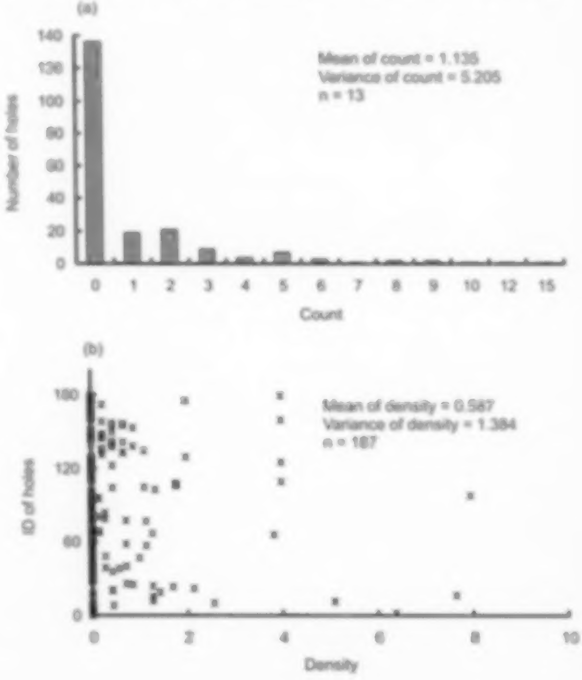

Fig. 4. The density (count·m^{-2}) of shortnose sturgeon (*Acipenser brevirostrum*) at each hole within the range of (*a*) depth and (*b*) substrate.

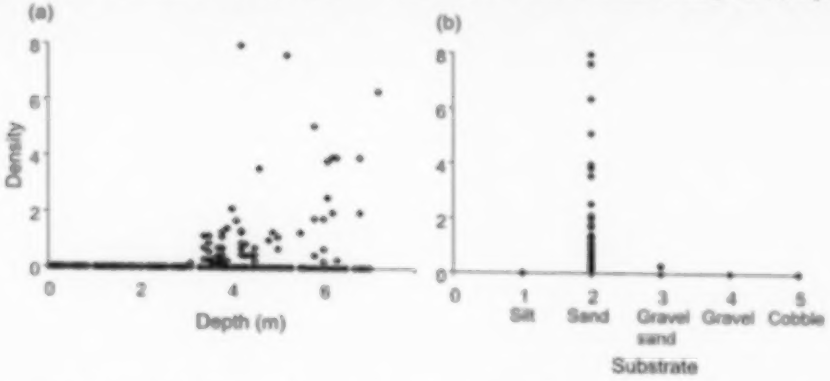

Table 2. Parameter estimates of the generalized linear model (GzLM) for shortnose sturgeon habitat use in the upper Kennebecasis River, New Brunswick, Canada.

Parameter	df	Estimate	SE	χ^2	Pr > χ^2
Model 1					
Intercept	1	–5.9190	1.1746	25.39	<0.0001
Depth	1	1.6942	0.4473	14.34	0.0002
Substrate	1	0.8256	0.4949	2.78	0.0953
Depth × substrate	1	–0.4874	0.2060	5.60	0.0180
Model 2					
Intercept	1	–4.0776	0.5195	61.62	<0.0001
Depth	1	0.6530	0.1061	37.86	<0.0001

Other habitat variables such as temperature, dissolved oxygen, salinity, and current velocity did not show an effect on the habitat use by shortnose sturgeon. The study area is at river kilometre 38. The tide head can reach river kilometre 120 in Saint John River (Metcalfe et al. 1976). The water temperature at river bottom was extremely stable: 0 °C through the tidal cycle. The dissolved oxygen was measured several times with a mean and standard error (SE) of 10.51 ± 0.26 mg·L^{-1}. The salinity was close to zero even at high tide. The current velocity on the river bottom changed with the tidal cycle, estimated in the range of –0.6 to 1 m·s^{-1}, which was determined by calculating the speeds of suspended particles flowing by the camera during video sampling. No evidence showed that current velocity had a strong influence on shortnose sturgeon distribution; however, the sturgeon always kept their body direction against the current (positive rheotaxis) when the water was moving. The water visibility at the river bottom changed with depth and time (range of 20–150 cm).

The distribution of the dependent variable, sturgeon density, appeared to follow a negative binomial distribution (Fig. 3); a log link function was therefore used to associate fish count with depth (Fig. 4) (Power and Moser 1999). A GzLM was built using SAS Genmod procedure: log(density) = –5.92 + 1.69depth + 0.83substrate – 1.49depth × substrate. Depth and substrate had a significant interaction (Table 2), suggesting that the two habitat variables were not independent and should be taken into account separately. When depth was considered, the GzLM is log(density) = –4.08 + 0.65depth, suggesting the shortnose sturgeon had strong preference to deeper area (Table 1). The habitat preference for substrate was consistent, i.e., all sturgeon were found on the sandy bottom (Fig. 4). We limited the GzLM to the sturgeon on the sandy substrate to develop a distribution map of shortnose sturgeon at the overwintering site (Fig. 5).

Spatial autocorrelation of the sturgeon density data was checked. The semivariogram (Fig. 6) indicated that when the distance between two holes was over the range, i.e.10 m, the density of the two holes was not correlated. Because only few among the 187 holes were closer than 10 m, the spatial independence of the density data was satisfied.

We were able to acquire good data on 12 days during February and March 2005 when weather and ice conditions were safe and water visibility permitted visual observations to be made at the sampling holes. To estimate the daily variance of fish density, we checked the same 31 holes on 15 and 16 March (Fig. 7) and found that there was no significant difference between the survey results of two days (paired t test, $t = 1.41$, $p = 0.17$). Power analysis indicated that we had 98% power to detect a mean difference of one fish per hole. Hence we can confidently conclude that sturgeon density did not change during the sampling period, i.e., shortnose sturgeon did not move much. Thus all data from the different survey days were pooled. In fact, it was clear from the video that shortnose sturgeon were not active in winter. Based on our observations, we found that they stayed on the river bottom, never foraged, and only occasionally swam around at slow speeds.

We compared four variogram models for best fit (Fig. 6), and the exponential model was selected for the ordinary

Fig. 5. The predicted density of shortnose sturgeon (*Acipenser brevirostrum*) and substrate index at the confluence of Kennebecasis River and Hammond River in New Brunswick, Canada: (*a*) density of shortnose sturgeon (calculated using generalized linear model (GzLM) log(density) = –4.08 + 0.65depth); (*b*) substrate indices; (*c*) density of shortnose sturgeon (calculated using maps 5*a* and 5*b*; see note below); (*d*) density of shortnose sturgeon calculated using an ordinary kriging method with the exponential semivariance model. Note: The sturgeon density was exp(–4.08 + 0.65depth)/(*k* × abs(substrate – 2) + 1), where exp(–4.08 + 0.65depth) was the sturgeon density calculated by depth using the GzLM (Fig. 5*a*); *k* × abs(substrate – 2) + 1 was used to modified the density by substrate, where *k* is a constant that modifies the changing rate of sturgeon density with substrate; *k* is 20 when the predicted density mostly matched the field survey data (Fig. 5*c*). The favorite substrate for the sturgeon is sand, which was given an index of 2; *k* × abs(substrate – 2) + 1 has the minimum value of 1 when substrate is sand.

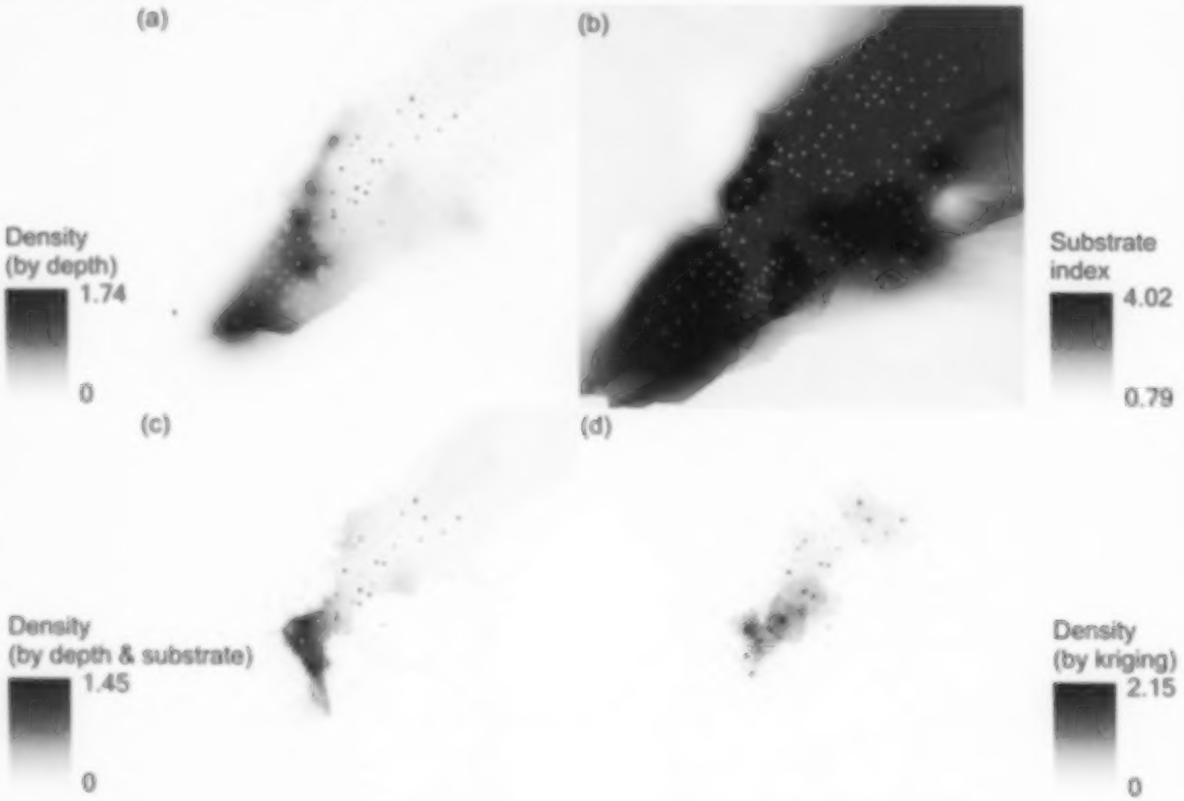

kriging. The total abundance of shortnose sturgeon was calculated to be 4836 using the ordinary kriging method. The standard error of the population size was 69 when the interpolation error of the kriging process was considered exclusively using ArcGIS software (ESRI, Redlands, California).

Discussion

It is not a traditional approach to use an underwater camera to survey the habitat use of shortnose sturgeon because the fish is highly mobile and the visibility of river water in which it occurs is usually low during the spring, summer, and fall; shortnose sturgeon has shown great variation in spring, summer, and fall habitat use (Kynard et al. 2000). However, it is clear from tracking during previous years (M.K. Litvak, unpublished data) in conjunction with the results of this study that shortnose sturgeon aggregate and do not move much in winter. Fortunately, water visibility improves after the river is covered by ice and the surrounding landscape is covered with snow. This cover decreases sediment load from runoff and decreases turbidity in the water allowing us to observe shortnose sturgeon directly. Our study was the first to visually observe overwintering of shortnose sturgeon, and with this approach, we were able to determine that they congregated at high density on a sandy bottom with a salinity close to zero in a small region at the junction of the Kennebecasis and Hammond rivers.

The depth of this overwintering area is rather shallow (3.1–6.9 m) compared with the major sections of Kennebecasis River, which are about 30 m deep on average. The salinity was also very low. Such results are different from all previous studies (e.g., Dadswell 1979; Kynard 1997; Kynard et al. 2000). For the substrate, our results are consistent with those of other studies of shortnose sturgeon inhabitating a sandy bottom. We also found that shortnose sturgeon did move less (Kynard et al. 2000) and that the population aggregated at discrete site(s) (Dadswell et al. 1984), unlike their pattern of habitat use in summer when individuals are found associated

Fig. 6. The semivariogram of the four models used in ordinary kriging of sturgeon density. The experimental model indicates the real data of the semivariance of sturgeon density between holes. Model parameters: sill = 0.2, range = 10, nugget = 0.

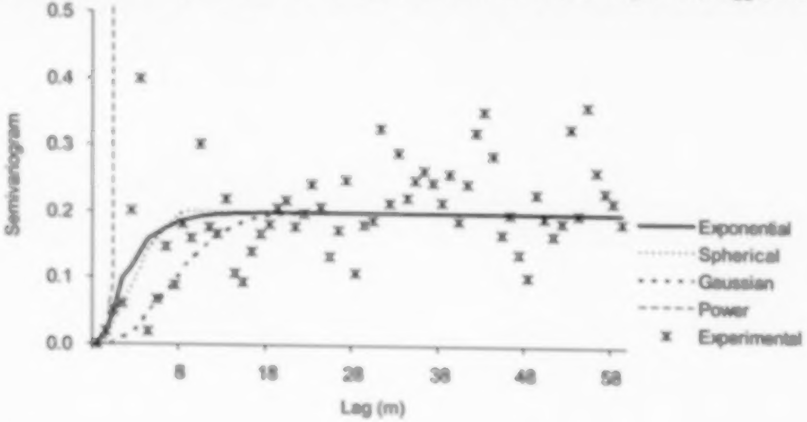

Fig. 7. The counts of shortnose sturgeon (*Acipenser brevirostrum*) at the 31 holes on 15 March (open bars) and 16 March (shaded bars) 2005 at the confluence of Kennebecasis River and Hammond River, New Brunswick, Canada. Each of the 31 holes is given an identity number (ID) from 1 to 31.

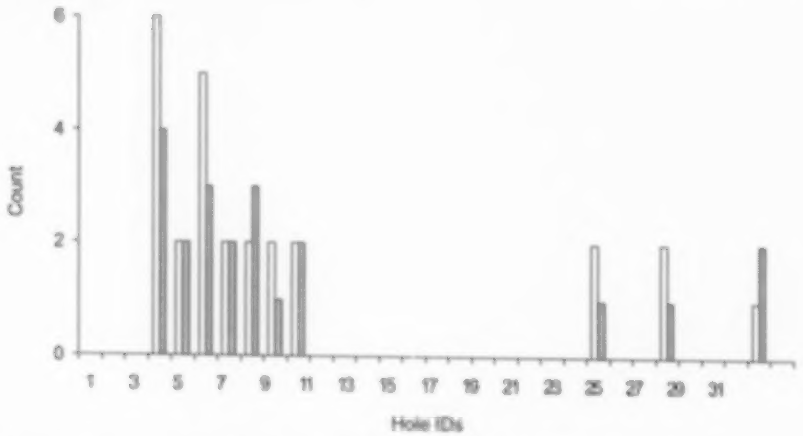

with a variety of habitat types (Kynard et al. 2000). Dadswell et al. (1984) indicated there were seven overwintering sites in lower Saint John River, but our study site belonged to none of them. We were able to check one of the seven sites with our video system, Murphy Cove (3.5 km downstream from our study area), but did not find any sturgeon there. Nor have we ever tracked any of the sonically tagged fish to any of the overwintering sites that Dadswell et al. (1984) had previously discovered 30 years ago. This difference in use may be due to changes in overwintering habit and (or) the increased resolution that is afforded by sonic telemetry and GPS systems available today.

We used GzLMs to study the association of sturgeon density and habitat variables. GzLM is a generalization of the general linear model (Dalthorn 2004). It was developed in the early 1970s (Nelder and Wedderburn 1972; Wedderburn 1974) and has been applied in a number of recent studies on fish ecology (e.g., Dettmers et al. 2001; Jiao et al. 2004*a*, 2004*b*). The GzLM extends the general linear model to include response variables that follow any probability distribution in the exponential family of distributions (McCullogh and Nelder 1989). Hypothesis tests applied to the GzLM do not require normality of the response variables, nor do they require homogeneity of variances. Hence, GzLMs can be used when response variables follow distributions other than the normal distribution and when variances are not constant (McCullogh and Nelder 1989). As to our study, count data would be appropriately analyzed as a negative binomial variable within the context of the GzLM (Power and Moser 1999), because the variance of count (5.205) is much higher than the mean of count (1.135). The same rule applied when the count data was standardized as fish density at each hole.

The heterogeneous habitat at the river bottom at our study area provided many options for habitat use of shortnose sturgeon. However, the exclusive use of deeper sandy areas within this region suggested strong preferences of habitat selection. To date, no evidence was found that habitat variables such as temperature, dissolved oxygen, salinity, and current velocity played a role on habitat use of shortnose sturgeon in the winter. The temperature is extremely stable (0 °C) at our study area and likely throughout the Kennebecasis River. The current velocity, unlike temperature, kept changing with tide, yet the sturgeon did not appear to move out of the area no matter the direction and speed of the current. We are not sure of the effects of dissolved oxygen and salinity. The dissolved oxygen is lower and salinity is higher in the downstream deeper section of the Kennebecasis River. The high dissolved oxygen level and fresh water at the confluence of Kennebecasis River and Hammond River might be preferred by shortnose sturgeon in winter.

We used a kriging method to estimate the population size on the basis of fish count data at the 187 holes covering 848 m^2 to predict the population size in the area of 60 000 m^2. The accuracy of the prediction depends on the variogram model, which measured the spatial correlation by describing how the sturgeon density is related over distance and direction. Geometric anisotropy (i.e., variogram varies with direction) was not taken into account and a default direction, north, was used, as there was not a strong directional pattern of sturgeon density. In spite of the generality of the ordinary kriging method in ArcGIS software, it gave us a much more precise estimation of population size compared with traditional mark–recapture estimation; the population size in Kennebecasis River over a 6-year period was estimated by Litvak's lab as 2068 with lower and upper 95% confidence limits of 801 and 11 277, respectively (COSEWIC 2005), using a Jolly–Seber open population estimation technique (Krebs 1999). Thus our technique of video observation and kriging provides an ideal opportunity to develop a precise determination of the population size of shortnose sturgeon, as well as other species that aggregate under the ice during the winter. This is of vital importance as we try to better manage listed species in Canada and other northern countries.

This overwintering habitat of shortnose sturgeon may be defined as critical habitat following the identification policies of both Canadian Species at Risk Act (SARA) and the Endangered Species Act (EST) of the US. SARA was proclaimed in June 2003 and is one of a three-part Government of Canada strategy for the protection of wildlife species at risk; the identification of critical habitat is a key step in the SARA. The EST was issued in 1973 and provides a program for the conservation of threatened and endangered species and the habitats in which they are found in the US. Both of these Acts suggest that an area occupied by a listed species is critical habitat if physical or geographical features essential to the conservation of said species are found within the habitat. Our underwater videographic study confirms that shortnose sturgeon aggregate at high densities at the confluence of Hammond and Kennebecasis rivers, suggesting the importance of this region to continued persistence of shortnose sturgeon. Additionally, sonic-tagged shortnose sturgeon have been tracked to this area each winter for the past 7 years (M.K. Litvak, unpublished) and stay in this region from October to April. The formal identification of this region in the Public Registry would ensure that further protection takes effect.

Acknowledgements

We especially thank Louis Arsenault and BLee Williams for their excellent help. We thank Remy Rochette, Derek J. Knox, Gilles Lacroix, and Fred G. Whoriskey for letting us use their field survey instruments. We are grateful to Diana Hamilton, Jeff Houlahan, and James Watmough for their comments. We thank Cornel Ceapa, Jamie Crossman, Steve Leadbeater, Jackie Randell, Sean Patrick Doyle, Domika Clarke, Clare Fang, Jie Yang, Cindy Jiang, and Hui Lu for their assistance in the fieldwork. Canadian Digital Elevation Data (CDED) was downloaded from Canadian government website GeoBase (http://www.geobase.ca/); Digital Topographic Database (DTDB), including data of rivers, lakes, roads, and land use, was downloaded from UNB library website (http://www.lib.unb.ca/gddm/maps/SNB). This study was supported by the New Brunswick Innovation Foundation (JHC and MKL) and Natural Sciences and Engineering Research Council of Canada (NSERC) Discovery, WWF Endangered Species Fund, New Brunswick Wildlife Trust Fund, and Mountain Equipment Co-op grants (MKL).

References

Abramoff, M.D., Magelhaes, P.J., and Ram, S.J. 2004. Image processing with ImageJ. Biophotonics International, **11**: 36–42.

Brock, V.F. 1954. A preliminary report on a method of estimating reef fish populations. J. Wildl. Manag. **18**: 299–308

Collins, M.R., Post, W.C., Russ, D.C., and Smith, T. 2002. Habitat use and movements of juvenile shortnose sturgeon in the Savannah River, Georgia – South Carolina. Trans. Am. Fish. Soc. **131**: 975–979.

COSEWIC. 2005. COSEWIC assessment and update status report on the shortnose sturgeon *Acipenser brevirostrum* in Canada. Committee on the Status of Endangered Wildlife in Canada, Ottawa.

Cressie, N.A.C. 1993. Statistics for spatial data. John Wiley & Sons Inc., New York.

Dadswell, M.J. 1979. Biology and population characteristics of the shortnose sturgeon, *Acipenser brevirostrum* LeSueur 1818 (Osteichthyes, Acipenseridae), in the Saint John River Estuary, New Brunswick, Canada. Can. J. Zool. **57**: 2186–2210.

Dadswell, M.J., Taubert, B.D., Squiers, T.S., Marchette, D., and Buckley, J. 1984. Synopsis of biological data on shortnose sturgeon (*Acipenser brevirostrum* LeSueur 1818). NOAA, National Marine Fisheries Service, Tech. Rep. NMFS No. 14.

Dalthorn, D. 2004. The generalized linear model for spatial data: assessing the effects of environmental covariates on population density in the field. Entomol. Exp. Appl. **111**: 117–131.

Dettmers, J.M., Gutreuter, S., Wahl, D.H., and Soluk, D.A. 2001. Patterns in abundance of fishes in main channels of the upper Mississippi River system. Can. J. Fish. Aquat. Sci. **58**: 933–942.

Grant, G.C., Radomski, P., and Anderson, C. 2004. Using underwater video to directly estimate gear selectivity: the retention probability for walleye (*Sander vitreus*) in gill nets. Can. J. Fish. Aquat. Sci. **61**: 168–174.

Hall, J.W., Smith, T.I.J., and Lamprecht, S.D. 1991. Movements and habitats of shortnose sturgeon, *Acipenser brevirostrum*, in the Savannah River. Copeia, 1991: 695–702.

International Union for Conservation of Nature and Natural Resources. 2006. IUCN Red List of threatened species. Available from http://www.iucnredlist.org/ [accessed 7 June 2006].

Jiao, Y., Chen, Y., Schneider, D., and Wroblewski, J. 2004*a*. A simulation study of impacts of error structure on modeling stock–recruitment data using generalized linear models. Can. J. Fish. Aquat. Sci. **61**: 122–133.

Jiao, Y., Schneider, D., Chen, Y., and Wroblewski, J. 2004*b*. An analysis of error structure in modeling the stock–recruitment data of gadoid stocks using generalized linear models. Can. J. Fish. Aquat. Sci. **61**: 134–146.

Krebs, C.J. 1999. Ecological methodology. Benjamin/Cummings, Menlo Park, California.

Kynard, B. 1997. Life history, latitudinal patterns, and status of the shortnose sturgeon, *Acipenser brevirostrum*. Environ. Biol. Fishes, **48**: 319–334.

Kynard, B., Horgan, M., Kieffer, M., and Seibel, D. 2000. Habitats used by shortnose sturgeon in two Massachusetts rivers, with notes on estuarine Atlantic sturgeon: a hierarchical approach. Trans. Am. Fish. Soc. **129**: 487–503.

Lane, E.W. 1947. Report of the subcommittee on sediment terminology. Trans. Am. Geophys. Union, **28**:936–938.

McCullogh, P., and Nelder, J.A. 1989. Generalized linear models. 2nd ed. Chapman and Hall, London.

Mello, L.G.S., and Rose, G.A. 2005. Using geostatistics to quantify seasonal distribution and aggregation patterns of fishes: an example of Atlantic cod (*Gadus morhua*). Can. J. Fish. Aquat. Sci. **62**: 659–670.

Metcalfe, C.D., Dadswell, M.J., Gillis, G.F., and Thomas, M.L.H. 1976. Physical, chemical, and biological parameters of the Saint John River Estuary, New Brunswick, Canada. Fish. Mar. Serv. Tech. Rep. No. 686. ISSN 0701-7626.

Nams, V.O. 2004. Locate III user's guide. Pacer Computer Software, Truro, Nova Scotia, Canada.

Nelder, J.A., and Wedderburn, R.W.M. 1972. Generalized linear models. J. R. Stat. Soc. A, **135**: 370–384.

National Marine Fisheries Service. 1998. Final recovery plan for the shortnose sturgeon (*Acipenser brevirostrum*). Prepared by the Shortnose Sturgeon Team for the National Marine Fisheries Service, Silver Spring, Maryland.

Platts, W.S, Megahan, W.F., and Minshall, G.W. 1983. Methods for evaluating stream riparian and biotic conditions. US Department of Agriculture, Forest Service Gen. Tech. Rep. No. INT-138.

Power, J.H., and Moser, E.B. 1999. Linear model analysis of net catch data using the negative binomial distribution. Can. J. Fish. Aquat. Sci. **56**: 191–200.

Thomas, M.V., and Hass, R.C. 2002. Abundance, age structure, and spatial distribution of lake sturgeon (*Acipenser fulvescens*) in the St. Clair system. J. Appl. Ichthyol. **18**: 495–501.

Toivonen, A., and Hudd, R. 1993. Video tape documentation of salmon (*Salmo salar*) and whitefish (*Coregonus lavaretus*) reacting to a modified whitefish trap net. ICES Mar. Sci. Symp. **196**: 59–61.

US Fish and Wildlife Service. 1999. Endangered and threatened wildlife and plants. Division of Endangered Species, US Fish and Wildlife Service, Washington, D.C.

Wedderburn, R.W.M. 1974. Quasi-likelihood functions, generalized linear models and the Gauss–Newton method. Biometrika, **61**: 439–447.

The influence of family-correlated survival on N_b/N for progeny from integrated multi- and single-generation hatchery stocks of coho salmon (*Oncorhynchus kisutch*)

G.R. Moyer, M.S. Blouin, and M.A. Banks

Abstract: There exist surprisingly few data on the final variance and mean of family sizes for hatchery-born fish at the adult stage. Thus, it is difficult to predict, for a conservation hatchery operation that minimizes the variance in progeny number, how much lower the true effective population size (N_e) of a cohort of hatchery-born adults will be than N_e predicted simply by the number of parents that produced them. We used parentage analysis to estimate the survival and N_e for two integrated stocks of hatchery coho salmon (*Oncorhynchus kisutch*). One hatchery is a multigeneration stock obtained by spawning 70% hatchery with 30% naturally reproducing fish, whereas the second is a single-generation stock derived from naturally reproducing coho. There was no significant difference in average overall survival between stocks, but observed N_e was significantly less than expected for each stock. Family-correlated survival contributed to roughly a 20% reduction in N_e over the freshwater and marine life stages. This reduction is similar to previous estimates and suggests a value that can be used when estimating the effective number of hatchery parents in applications of the Ryman–Laikre formula (at least for programs such as ours that attempt to equalize sex ratios and family sizes).

Résumé : Il existe étonnamment peu de données sur la variance et la moyenne finales des tailles des familles au stade adulte chez les poissons nés en pisciculture. Il est ainsi difficile, dans une pisciculture de conservation qui minimise la variance des nombres dans la progéniture, de prédire de combien inférieure sera la véritable taille effective de la population (N_e) d'une cohorte d'adultes nés en pisciculture par rapport au N_e prédit simplement par le nombre des parents qui les ont produits. Nous utilisons une analyse de parenté pour estimer la survie et le N_e chez deux stocks intégrés de saumons coho (*Oncorhynchus kisutch*) de pisciculture. Une des piscicultures utilise un stock de plusieurs générations obtenu en croisant 70 % de poissons de pisciculture avec 30 % de poissons à reproduction naturelle, alors que l'autre est formé d'un seul stock de saumons coho à reproduction naturelle. Il n'y a pas de différence de survie globale entre les stocks, mais le N_e observé est significativement inférieur à la valeur attendue pour chacun des stocks. La survie en fonction de la famille contribue grosso modo 20 % de la réduction de N_e au cours des stades du cycle en eau douce et en mer. Cette réduction est semblable à celle des estimations antérieures, ce qui fournit une valeur qui peut être utilisée pour calculer le nombre effectif de parents de pisciculture lors de l'application de la formule de Ryman–Laikre (au moins dans les programmes comme le nôtre qui cherchent à égaliser les rapports mâles–femelles et les tailles des familles).

[Traduit par la Rédaction]

Introduction

Fish hatcheries occupy various roles ranging from fish production for commercial harvest to augmentation for recreational purposes. Recently there has been a shift in hatchery programs from merely supplying fish for harvest to incorporating conservation objectives as a means to revive threatened wild populations (Hedrick et al. 2000; Miller and Kapuscinski 2003; Brannon et al. 2004). The goal of a conservation hatchery is to boost the existing adult census size of a wild population by breeding a fraction of the wild population in captivity and releasing their offspring into the natural habitat (also known as supplementation). Although there may be a gain in total production of offspring, one cost associated with such a gain may be a reduction in the effective population size (N_e) of the total population (termed the Ryman–Laikre effect; Ryman and Laikre 1991). The simple formula

$$(1)\qquad \frac{1}{N_e} = \frac{x^2}{N_h} + \frac{(1-x)^2}{N_w}$$

Received 16 October 2006. Accepted 24 May 2007. Published on the NRC Research Press Web site at cjfas.nrc.ca on 1 September 2007.
J19603

G.R. Moyer[1,2] and M.A. Banks. Coastal Oregon Marine Experiment Station, Hatfield Marine Science Center, Department of Fisheries and Wildlife, Oregon State University, 2030 SE Marine Science Drive, Newport, OR 97365-5296, USA.
M.S. Blouin. Department of Zoology, Oregon State University, Corvallis, OR 97331-2914, USA.

[1] Corresponding author (e-mail: Greg_Moyer@fws.gov).
[2] Present address: US Fish and Wildlife Service, Conservation Genetics Laboratory, Warm Springs, GA 31830, USA.

doi:10.1139/F07-099

(Ryman and Laikre 1991) describes the change in the inbreeding effective size of a population that results when a large fraction of the breeders in a population descend from a small number of founders, where N_h is the effective size of the hatchery fish breeding in the wild and N_w is the effective size of the wild fish breeding in the wild. Thus, for application of the Ryman–Laikre equation, it is important to know the effective size of each group of fish. Estimating N_w for wild salmon populations can be quite difficult and has been the subject of much study (Waples 1990, 2002*a*; Shrimpton and Heath 2003). Here we focus on how accurately one can predict the effective size of the hatchery component of a supplemented population, N_h. It is often assumed that the effective size of the hatchery group can be estimated simply from the numbers of males and females used as brood stock to produce that hatchery group. However, few data exist on the realized effective size of a cohort of hatchery fish relative to the effective size as predicted by the number of brood stock that produced them. For example, if 200 male–female pairs are spawned in a hatchery and if variance in family sizes is random through all stages of the life cycle of their offspring, then the inbreeding effective size of that cohort of offspring would equal the census size, $N = 400$. Nonrandom (family-correlated) survival during any stage of the life cycle would cause the N_e of that cohort of returning adults to be less than 400. How much less can be expected for typical conservation hatchery operations remains an open question. Family-correlated survival can occur at any stage of the life cycle but may be particularly high in captivity (Allendorf 1993). Thus, some estimates of the mean and variance in family sizes, and true realized N_e of hatchery cohorts, would be very useful for application of the Ryman–Laikre formula in practice.

Hatcheries have traditionally used broodfish that have been passed for many generations through a hatchery because such stocks perform well in a hatchery environment. In contrast, conservation hatcheries have opted to produce single-generation stocks using naturally born brood stock or have integrated captive with naturally born brood stock (Mobrand et al. 2005). It is unknown whether the mean ($\bar{k}$) and variance (V) in final family size differ between the two brood-stock strategies adopted by conservation hatcheries. Differences, if large, might cause one to substantially under- or over-estimate the effective size for a cohort of single-generation stock, relative to the expectation of an integrated stock.

Here we test whether there is a significant difference in the mean and variance in number of surviving adult progeny between a single-generation and an integrated multigeneration hatchery stock. We also estimate, for two cohorts of each stock, the reduction in realized N_e over that predicted by the number of parents that produced each cohort. We found no significant difference in survival between single-generation and multigeneration stocks, with both stocks experiencing similar reductions in N_e. This reduction was significantly less than expected, indicating that nonrandom survival occurred throughout the freshwater–marine life stage. Our data suggest that the hatchery coho (*Oncorhynchus kisutch*) used in this study experienced about a 20% reduction in N_e over that predicted throughout their freshwater and marine life stages, regardless of the type of hatchery stock.

Materials and methods

Sampling design — year 2001

For at least the past decade, the North Umpqua River hatchery program has been managed as a harvest program, augmenting the recreational and commercial fisheries. The program integrates a random collection and spawning of adults throughout the run by mixing 70% hatchery fish (i.e., adipose-clipped fish) with 30% natural fish. Each fish released from the hatchery is adipose-clipped to ensure the designation "hatchery fish". Therefore, we considered adipose-clipped coho collected in the North Umpqua to be of multigeneration hatchery origin. In fall and early winter 2001, the Oregon Department of Fish and Wildlife (ODFW) collected 100 female and 100 male coho salmon having marked adipose fins (considered multigeneration brood stock; MGHS) from the North Umpqua River at Winchester Dam (Fig. 1). They also collected 94 females and 94 males having unmarked adipose fins (considered single-generation brood stock; SGHS because progeny were reared in a hatchery). Collections were performed randomly with respect to age, run time, and length. Males and females from the multigeneration brood stock were randomly paired and spawned at ODFW's Rock Creek hatchery facility using single-pair matings (i.e., each male and female was used only once). Single-generation broods were spawned following the same protocol. Eggs from each mating pair were incubated separately until the eyed-egg stage. At this stage, we attempted to equalize the variance in progeny number by randomly sampling 140–150 eyed eggs per mating pair and rearing them to the smolt stage (progeny from MGHS and SGHS were reared separately). Although 140–150 eggs per mating pair was a goal, our observed mean in eyed eggs per mating pair was less than expected (see Results) because of high egg mortality from a few mating pairs. As a result, our variance in progeny number was also greater than expected.

Sampling design — year 2002

Sampling design for the 2002 brood stock was similar to that of 2001. However, the SGHS were collected from Calapooya Creek (Fig. 1), which is a tributary of the Umpqua River and considered part of the Umpqua population complex (Ford et al. 2004). Coho inhabiting Calapooya Creek are considered naturally reproducing (i.e., there is no recognized hatchery contribution to this system); however, it is conceivable that some of these fish historically could be of hatchery origin.

In fall and early winter 2002, ODFW personnel collected 100 female and 100 male coho salmon having unmarked adipose fins (SGHS) from Calapooya Creek at Nonpareil Dam (Fig. 1). The MGHS for 2002 consisted of 100 males and 100 females collected at Winchester Dam on the North Umpqua, as before. Collection, mating, and rearing of 2002 brood stock followed the 2001 sampling design protocol.

In spring 2003 and 2004, smolts from respective 2001 and 2002 brood years were released in Calapooya Creek above Nonpareil Dam (Fig. 1). Coho salmon smolts typically migrate to the Pacific Ocean a few weeks after release. Fins from released smolts were clipped adipose left maxillary or adipose right maxillary to designate progeny from MGHS or SGHS, respectively. Coho have a 3-year life cycle. Mature

Fig. 1. Map of the Umpqua basin, Oregon, USA. Our study involved sampling natural and hatchery coho in the North Umpqua at Winchester Dam, spawning and rearing offspring at Oregon's Department of Fish and Wildlife Rock Creek Hatchery facility, and releasing smolts above Nonpareil Dam on Calapooya Creek. All returning progeny were sampled at a fish trap located at Nonpareil Dam, genotyped using 11 microsatellite loci, and assigned to most likely brood stock through parentage analysis.

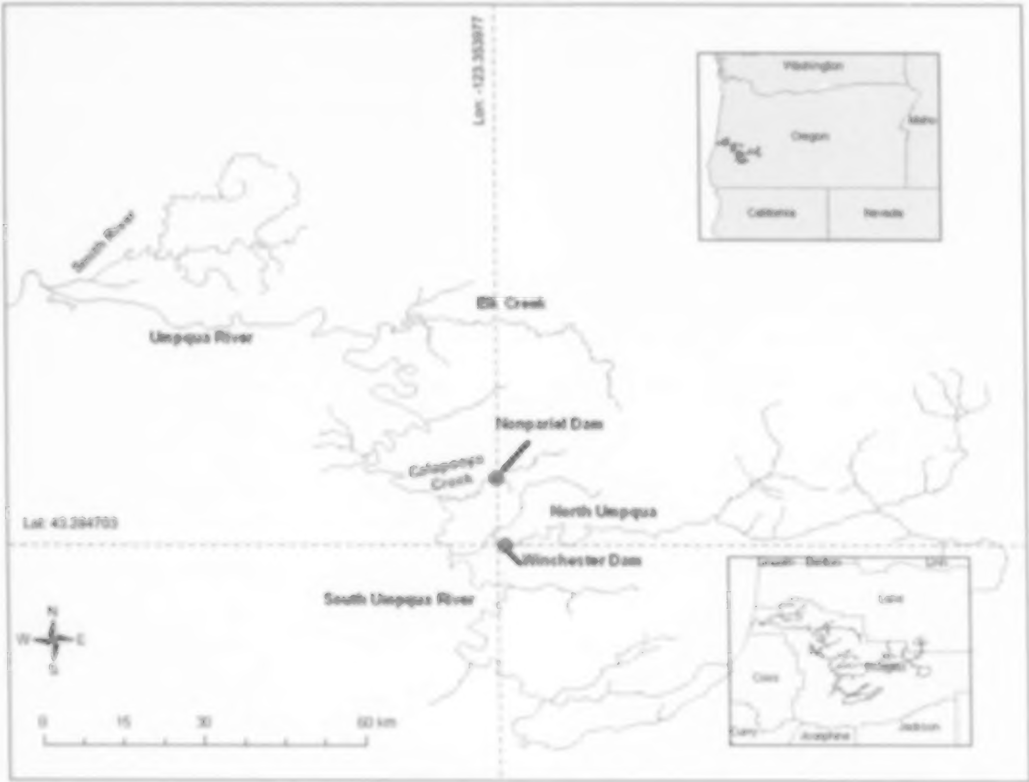

adults typically return to spawn at age 3, but reproductively mature males, called jacks, can return at age 2. Thus, coho salmon released as smolts in 2001 returned to the Calapooya Creek during the fall of 2003 (jacks) and 2004 (adult males and females), and smolts released in 2002 returned in the fall of 2004 and 2005. ODFW constructed a fish trap at the base of Nonpareil Dam (Fig. 1), allowing for the capture, fin-clipping, and above-dam release of all returning adult coho salmon in this study.

Screening, optimization, and identification of microsatellite markers

DNA was extracted using Qiagen DNA extraction kits. DNA concentration (~4–24 ng·µL^{-1}) was quantified using a Victor^{3}V 1420 multilabel counter (PerkinElmer Inc., Boston, Mass.).

Choosing appropriate markers for accurate parentage assignment is a function of population size, number of loci, and number and distribution of alleles per locus (Bernatchez and Duchesne 2000). We took the following strategy for choosing appropriate markers for this study. First, we screened 96 candidate loci known to amplify in salmon species. Of these loci, we successfully amplified 41 candidates for further evaluation. Next, loci were selected based on repeat motif (tetranucleotides were chosen over dinucleotide repeats because of increased scoring error for dinucleotides), allelic diversity, and allelic distribution (Blouin et al. 1996; O'Reilly et al. 1998; Bernatchez and Duchesne 2000). Using these criteria, we narrowed the pool of potential markers to 21 and screened the 2001 pair matings (n = 388) using these markers. Because of inconsistent scoring, presence of null alleles, and deviation from Hardy–Weinberg expectations (HWE), 10 of these loci where excluded from subsequent analyses. Primer information, including range of allele sizes, repeat motif, annealing temperature, and buffer pH, for the remaining 11 loci used in this study are listed in Table 1. Single-locus polymerase chain reaction (PCR) amplifications were performed in 5 µL reactions using 0.175 mmol·L^{-1} each of dNTP, 0.15 µmol·L^{-1} each primer, and 0.025 U *Taq* polymerase (1 U = 16.67 nkat; Promega Corp., Madison, Wis.) (see Table 1 for buffer and $MgCl_2$ concentrations). PCR conditions were an initial denaturation at 94 °C (3 min), followed by a touchdown procedure involving four cycles of denaturing (94 °C), annealing, and extension (74 °C), where the initial annealing temperature was decreased by 1 °C·cycle^{-1} (see Table 1 for initial and final annealing temperatures). After initial cycles, reactions were run for 30 cycles at the final annealing temperature.

Before electrophoresis, 0.8 µL PCR product from three to five separate reactions were combined (Table 1) and mixed

Table 1. Description and polymerase chain reaction (PCR) conditions of microsatellite loci used for this study.

Marker	k	H	Range of alleles	Exclusion probability	Annealing temperature (°C)	MgCl$_2$ (mmol·L^{-1})	Buffer pH	Reference
OTS519^{A}	8	0.72	286–310	0.35	58–54	1.0	9.0[*]	Naish and Park 2002
OTS520^{A}	24	0.87	190–252	0.72	58–54	1.0	8.5[†]	Naish and Park 2002
ONE111^{A}	6	0.84	180–190	0.32	52–48	2.5	9.0[*]	Olsen et al. 2000
P53^{A}	19	0.91	165–197	0.73	58–54	1.0	9.0[*]	de Fromentel et al. 1992
OTS3^{B}	10	0.89	142–162	0.53	58–54	1.0	9.0[*]	Banks et al. 1999
ONEμ2^{B}	25	0.89	196–257	0.72	63–59	1.0	9.0[*]	Currens et al. 1997
OCL8^{B}	20	0.88	90–121	0.65	50–46	1.5	9.0[*]	Condrey and Bentzen 1998
OTS215^{C}	8	0.72	155–160	0.35	60–56	1.0	9.0[*]	M. Banks (unpublished data)
ONEμ13^{C}	15	0.81	194–236	0.57	60–56	1.5	9.0[*]	Scribner et al. 1996
OMY1011^{C}	11	0.84	178–212	0.58	50–46	1.5	9.0[*]	P. Bentzen (unpublished data)[‡]
OKI23^{D}	20	0.80	120–180	0.74	60–56	1.5	8.5[†]	A. Spidle (unpublished data)[§]

Note: The abbreviation k represents the number of alleles per locus, and H is the observed heterozygosity. The exclusion probability is the average probability of excluding a single unrelated candidate parent from parentage of a given offspring. Loci with the same letter designate combined genotyping runs. The first annealing temperature number is the initial annealing temperature and the latter is the final annealing temperature.

[*] 1× *Taq* reaction buffer (Promega).

[†] 20 mmol·L^{-1} Tris, pH 8.5, and 50 mmol·L^{-1} KCl (Williamson et al. 2002).

[‡] P. Bentzen, Department of Biology, Dalhousie University, Halifax, NS B2Y 4J1, Canada.

[§] A. Spidle, Northwest Indian Fisheries Commission, 6730 Martin Way East, Olympia, WA 98516, USA.

with a 4 μL solution containing 98% formamide and 2% Genescan LIZ 500 size standard (Applied Biosystems, Foster City, Calif.). Microsatellite reactions were visualized with an ABI 3730xl Prism (Applied Biosystems) using fluorescently labeled forward primers and analyzed using GeneMapper Software v3.7 (Applied Biosystems). To minimize potential pipetting error (PCR and genotyping were performed using 384-welled plates), DNA and PCR products were transferred using a PlateMate Plus pippetting robot (Matrix Technologies, Hudson, N.H.).

Parentage analysis and estimating mean and variance in progeny number

We assessed the statistical power of our 11 loci for successful parentage analysis (α = 0.20 and 0.05) via simulations as implemented by Cervus v3.0 (Marshall et al. 1998). Cervus uses known allele frequency data to generate a pair of parental genotypes, plus a series of random genotypes representing unrelated candidate parents of one sex. Offspring are then produced by Mendelian sampling of the true parents' alleles. Once simulated parent and offspring genotypes were generated, we obtained an estimate of the number of loci needed for accurate parentage assignment assuming all candidate parents had been accurately genotyped. We estimated the proportion of loci typed (95%) from the known 2001 candidate parents and designated a genotyping error rate of 1.5%. For simulations, we based the genotyping error rate on previous published data sets (Bonin et al. 2004). We confirmed this value by matching known hatchery parents to hatchery returns (n = 384) and assessing the proportion of mistyped loci for each correct assignment. Cervus simulations were run for 10 000 cycles.

Parentage analyses were performed using exclusion and categorical allocation methods (Jones and Ardren 2003). Exclusion was implemented using WhichParent v1.0 (W. Eichert, available at http://www.bml.ucdavis.edu/facresearch/salmonsw.html or by request) where the number of mismatches was set to two. This setting was chosen because it produced the greatest number of true assignments based on preliminary runs that assigned known progeny to known hatchery brood stock. Categorical allocation, which involves calculating a logarithm of the likelihood ratio (LOD score) for any parentage relationship, was implemented using FAMOZ (Gerber et al. 2003). Simulations to calculate the LOD score threshold value for parentage assignment were implemented in FAMOZ as described by Gerber et al. (2003) (the intersection of the distributions was chosen as the threshold value). Simulations and actual parental assignments were conducted assuming a genotyping error rate of 1.5% per locus and an analysis error rate of 0.01% per locus (see Sancristobal and Chevalet (1997) and Gerber et al. (2000) for details about analysis error rate).

Once parent–offspring assignments were confirmed, we estimated the mean ($\bar{k}$) and variance (V) in progeny number per family for MGHS and SGHS (separately for both brood years). We tested the hypothesis that there was no difference in mean progeny number per parent between SGHS and MGHS (each year was analyzed separately) using a two-tailed t test (Sokal and Rohlf 1995). A test for homogeneity of variances between groups was performed using the F test (Sokal and Rohlf 1995).

Assessment of nonrandom survival and realized vs. expected N_e

Crow and Morton 1955) referenced $V/\bar{k}$ as the index of variability (R; Geiger et al. 1997; Waples 2002*b*). To assess whether survival is completely random from eyed-egg to adult life stage in hatchery coho salmon, we scaled R at the eyed-egg stage to the expected value assuming random survival in a population of constant size (i.e., $\bar{k}$ = 2) using the equation

$$(2) \qquad R^{*} = 1 + \bar{k}_2 \frac{(R-1)}{\bar{k}_1}$$

where R^{*} is the scaled index of variability, $\bar{k}_1$ represents the observed mean progeny number per family, and $\bar{k}_2$ is the expected mean progeny number per family (i.e., we assumed $\bar{k}_2$ = 2). If survival was random from egg to adult stage with

Table 2. Count of hatchery coho passed above Nonpareil Dam (Calapooya Creek) for 2004–2005 cohorts.

	Male	Jack	Female	Unresolved	Dropped	Total
2004 cohort						
SGHS	69	23	71	2 (1 M, 1 J)	2 (2 M)	167
MGHS	98	38	78	2 (1 M, 1 F)	2 (2 M)	218
2005 cohort						
SGHS	121	38	169	20 (4 M, 1 J, 15 F)	0	348
MGHS	174	28	189	9 (2 M, 1 J, 6 F)	7 (2 M, 5 F)	407

Note: M, male; J, jack; F, female. Comparisons are between returns from single- and multi-generation hatchery stocks (SGHS and MGHS, respectively). Individuals excluded from analyses are as follows: progeny that were unassigned to a known parental array (Unresolved), and progeny having fewer than eight genotyped loci or were returns from incorrect hatchery matings (Dropped; see text for details).

$\bar{k}_2 = 2$, R^* at the eyed-egg stage (R^*_e) should be similar to the observed value of R at the adult stage (R_a). Therefore, a deviation between these two values (R^*_e and R_a) is an indication of nonrandom survival among families.

An approximate expression for the ratio of expected N_e/N was calculated using the equation

$$(3)\qquad \frac{N_e}{N} = \left[\frac{\bar{k}_2}{1+R^*}\right]$$

where $\bar{k}_2$ is the expected mean progeny number per family (we assumed $\bar{k}_2 = 2$) and N is the census size of the parent population (Waples 2002*b*). Note that N is not the census size of the cohort of adult offspring. Rather it is the census size of the parents that produced them (Waples 2005), and because the number of females equals the number of males, it is also the expected N_e of the offspring cohort given random family survival. Also note that estimates of N_e associated with family size data should be interpreted as estimates of the effective number of breeders (N_b) per year (Waples and Teel 1990; Waples 2005). Depending on whether N_b/N was estimated for egg or adult stages, the parameter R^* was calculated as above using the respective value of $\bar{k}_1$. We assessed confidence in parameters R^*_e, R_a, R^*_a, and N_b/N by bootstrap resampling (Sokal and Rohlf 1995). Randomization tests (Sokal and Rohlf 1995) were used to investigate whether estimates of R^*_e, R_a, and N_b/N were significantly different between SGHS and MGHS (each cohort was analyzed separately).

Results

Parentage simulations using Cervus concluded that our predicted success rate for the 11 loci used in this study (when sexes are known a priori) was 100% at $\alpha = 0.05$. We obtained similar estimates for the number of progeny per parent using exclusion and categorical assignment methods (the LOD threshold value for parentage assignment using FAMOZ was 8.0); therefore, only results from WhichParent are presented.

In 2001, the mean number of eggs per mating pair ($\bar{k}_e$) for SGHS cohort collected for smolt production was 147 ($V = 433.47$), and the mean number of eggs per mating pair sampled for smolt production for MGHS matings was 136 ($V = 397.34$). In April 2003, 12 016 adipose left maxillary clipped (progeny from 2001 MGHS cohort) and 12 357 adipose right maxillary clipped (progeny from 2001 SGHS cohort) smolts were released in the Calapooya Creek above Nonpareil Dam (Fig. 1).

The returning 2004 cohort was comprised of 62 marked jacks (one of which was dropped from subsequent analyses; see below) and 323 marked adults (seven of which were excluded from subsequent analyses) (Table 2). Four of eight fish were deemed dropped and excluded from further analyses. Three were probably due to spilling of gametes during hatchery spawning (WhichParent assigned returns to a male or female but not to a known mating pair), and one had less than eight genotyped loci scored. The last four fish, deemed unresolved, were deleted from further analyses because they could not be assigned to a specific mating pair, indicating that they may be age 4 (but see below) or stray marked fish from another system.

The mean number of eggs per mating pair for 2002 SGHS cohort reared for smolt production was 138 ($V = 276.66$) vs. 139 ($V = 108.16$) for MGHS. In April 2004, 11 018 adipose left maxillary clipped (progeny from MGHS) and 10 979 adipose right maxillary clipped (progeny from SGHS) smolts were released in the Calapooya Creek above Nonpareil Dam. The returning 2005 cohort was comprised of 68 marked jacks (two of which were eliminated from further analyses) and 687 marked adults (35 of which were excluded from subsequent analyses) (Table 2). Seven returns were dropped from subsequent analyses, all a consequence of having mating strategies where WhichParent assigned returns to a male of one mating pair with a female of the next mating pair. Twenty-nine fish could not be assigned to a specific mating pair and were unassigned to the 2001 parental data set, indicating they where not age-4 fish; therefore, we suspect that these fish were marked strays for reasons previously addressed.

The number of returning progeny assigned to the 2004 cohort was 214 MGHS and 163 SGHS. The 2005 cohort contained 391 and 328 assigned progeny, respectively. Calculated $\bar{k}$, V, R^*, and N_b/N for egg and adult stages are reported in Table 3. A statistically greater variance was found in MGHS than in SGHS for the adult 2004 cohort ($V_{\mathrm{MGHS}} = 3.62$, $V_{\mathrm{SGHS}} = 2.52$; $F_{0.05(1)99,93} = 1.43$, $P = 0.04$), but comparison between MGHS and SGHS was nonsignificant for the adult 2005 cohort ($V_{\mathrm{MGHS}} = 6.67$, $V_{\mathrm{SGHS}} = 5.58$; $F_{0.05(1)99,99} = 1.39$, $P = 0.18$). Despite significant vari-

Table 3. Estimated demographic parameters for juvenile and adult coho salmon from 2001 and 2002 hatchery stocks.

	Egg					Adult				
	k_e	V_e	R_e	R_e^*	N_b/N^*	k_a	V_a	R_a	R_a^*	N_b/N^*
MGHS 2001	136	397.34	2.92	0.97 (1.00–1.08)	1.02 (0.96–1.00)	2.14	3.62	1.68 (1.25–2.00)	1.64 (1.27–197)	0.76 (0.66–0.86)
SGHS 2001	147	433.47	2.94	0.97 (1.00–1.09)	1.02 (0.95–1.00)	1.72	2.52	1.46 (1.11–1.79)	1.53 (1.15–1.90)	0.79 (0.69–0.92)
MGHS 2002	139	108.16	0.78	1.00 (n/a–1.02)	1.00 (0.99–n/a)	3.84	6.67	1.73 (1.25–2.13)	1.38 (1.16–1.57)	0.84 (0.77–0.93)
SGHS 2002	138	273.92	1.99	1.01 (n/a–1.05)	0.99 (0.97–n/a)	3.13	5.58	1.67 (1.30–2.05)	1.43 (1.17–1.63)	0.82 (0.76–0.92)

Note: Comparisons are between single- and multi-generation brood stocks (SGHS and MGHS, respectively). Subscripts represent the egg (*e*) and adult (*a*) life stages. Mean and variance in progeny number estimated from parentage analysis are designated as *k* and *V*, respectively. The parameter *R* is the observed index of variability (Crow and Morton 1955) and is calculated as *V*/*k*. The asterisk denotes scaled values of *R* and effective size to census size (N_b/N) obtained from eqs. 2 and 3, respectively. Confidence intervals are reported in parenthesis. The designation "n/a" indicates confidence values that were unascertainable via bootstrapping due to the small variance among replicates.

ances between MGHS and SGHS for the 2004 cohort, estimates of $\bar{k}_a$ between groups were nonsignificant in both cohorts (2004 cohort, $t = 1.66$, $t_{0.05(2),189} = 1.97$, $P = 0.10$; 2005 cohort, $t = 1.80$, $t_{0.05(2),198} = 1.97$, $P = 0.07$). Values of R_e^*, R_a^*, and N_b/N were nonsignificant (all $P > 0.05$) between MGHS and SGHS for each cohort; however, confidence intervals for R_e^* and R_a^* were nonoverlapping for all within-stock comparisons (Table 3), indicating that nonrandom survival occurred between egg and adult stages for the 2004 and 2005 cohorts. Likewise, confidence intervals were nonoverlapping for all egg per adult N_e/N comparisons (Table3).

The expected N_b of the 2004 cohort, given random family survival, was 200 for MGHS and 188 for SGHS. The expected N_b for the 2005 cohort was 200 for both MGHS and SGHS. In contrast, the observed N_b for each cohort was always significantly (i.e., nonoverlapping confidence intervals) less than expected (2004 cohort, $N_{b\ \mathrm{MGHS}} = 152$, $N_{b\ \mathrm{SGHS}} = 148$; 2005 cohort, $N_{b\ \mathrm{MGHS}} = 168$, $N_{b\ \mathrm{SGHS}} = 164$), indicating that on average a 20% reduction in N_b (caused by family-correlated survival) occurred in the life cycle of coho salmon during this study.

Discussion

Our study found no difference in survival between two types of integrated (i.e., managed as a component of a natural population) hatchery programs — one that integrates 30% naturally reproducing fish with 70% hatchery fish vs. one that only uses naturally produced fish as brood stock. These findings seem to contradict those of previous studies (Fleming and Gross 1993; Berejikian et al. 1997, 2001), i.e., that fish maintained in a hatchery for multiple generations generally are less fit (the component of fitness being survival) than fish that have never experienced captive conditions. However, there is quite a distinction between present and previous studies. Previous studies compared segregated hatchery brood fish (i.e., managed as if they are a distinct population relative to natural populations) with naturally reproducing ones; in contrast, our study compares two types of integrated hatchery programs. Furthermore, theoretical studies have indicated that hatchery programs with a one-way gene-flow rate of 10%–20% per generation can quickly achieve the fitness level of the donor population (Ford 2002; Lynch and O'Hely 2001). Our study provides empirical evidence indicating that relative survival of progeny from a multigeneration hatchery stock exposed to an integrated breeding program is similar to that of a naturally reproducing stock experiencing hatchery conditions for the first time. However, we urge caution when applying these findings to other such hatchery programs because conclusions are often context-specific and depend on the type of brood stock used (integrated vs. segregated), the breeding program (in this case, single matings and equalization of family size), the amount of gene flow between stocks, and brood-stock history.

Predictions regarding N_b are often calculated using sex-ratio information of the organism in question (Wright 1938; Waples and Teel 1990). Estimating N_b this way assumes that variance in reproductive success among males (or females) is random. Our data clearly show that this assumption is violated for hatchery-reared coho salmon. Both SGHS and MGHS groups had significantly greater variances in family size than would be expected based on random survival from egg to adult (i.e., confidence intervals for R_e^* do not overlie those of R_s). Comparisons between values of R_s and R_e^* for MGHS and SGHS cohorts were not significantly different, suggesting that the extent of among-family selection, whether occurring in the hatchery or wild (see below), appears similar between MGHS and SGHS. These findings, which corroborate Waples (2002*b*), indicate that even in closely monitored hatchery operations, sex-ratio information may be a poor indicator of N_b for hatchery-reared coho salmon. Fortunately, nonrandom survival was not extreme enough to substantially reduce N_b, a finding similar to that of Waples (2002*b*), who also applied demographic data to predict N_b/N for coho salmon.

It is difficult to discern the exact stage at which family-correlated survival occurred for both groups. Mortality can occur in the hatchery at the egg–presmolt stage, in freshwater as smolts migrate to estuarine habitat, or during estuarine–ocean phases. Although this study was not intended to test where differential survival occurred, minimizing the variance in family size at the egg stage should reduce the effects of selection in captivity (Allendorf 1993). It is interesting that estimated survival from egg to released fry was approximately 89% and 80% for 2004 and 2005 cohorts, respectively (data not shown). As predicted, these estimates leave little room for family-correlated survival to occur at the hatchery stage (at least for the 2004 cohort) and suggest that differential survival among family groups transpired during smolt migration to estuarine habitat or during the ocean stage of their life cycle, a finding similar to those of Hobday and Boehlert (2001) and Linley (2001).

Few studies have examined the demographic parameters necessary to compute N_b and N_b/N for hatchery salmon populations; therefore, the reduction in N_b below N is generally unknown. Summarizing $\bar{k}$ and V in female families for five cohorts of hatchery-reared coho salmon, Waples (2002*b*) showed that N_b/N ranged from 0.59 to 0.94 (mean = 0.76). These estimates may tend to underestimate the overall variance in $\bar{k}$ because V was computed for only females; therefore, N may only approximate the expected N_b for the cohort. Nevertheless, our estimates of N_b/N, which ranged from 0.76 to 0.84 (mean = 0.8), are similar to those of Waples (2002*b*), suggesting that N_b for hatchery salmon might be generally predictable from knowledge of the number of parents used as brood stock, particularly when hatchery practices perform single-pair matings and equalize family size prior to release. In fact, when these data are averaged together (i.e., Waples (2002*b*) and current study), a 22% (±8%) reduction in N_b is predicted in the life cycle of hatchery coho salmon. Scaled adult estimates of N_b/N for other salmon species reared in captivity, which are >0.7 for most cohorts (Hedrick et al. 2000; Waples 2002*b*), are similar to those for coho salmon, suggesting that this value (22%) may be used in conjunction with census data for calculating N_b of other salmon species.

Although a 22% reduction in N_b might be predicted for coho salmon, this value, as a general predictor, should be used with caution. Any factor that causes selection among family groups can increase the variance in family size and subsequently reduce N_b. These factors can include, but are not limited to, artificial selection, size-selected predation, isolated disease outbreaks, and varying freshwater or ocean conditions, none of which is mutually exclusive. It should also be stressed that this study attempted to equalize or minimize the variance in family size at an early life stage and equalize sex ratios. Equalization of these parameters is promoted by conservation hatchery programs as a means to maintain higher N_e; therefore hatchery programs not attempting to equalize these parameters would expect on average a >22% reduction; how much greater depends on the level of variation among family groups and mating design (e.g., full factorial vs. 1:1 pair matings)

In conclusion, our data and data in Waples (2002*b*) suggest a simple calculation for estimating one of three necessary parameters for predicting the Ryman–Laikre effect, N_b. More importantly, this parameter appears stable regardless of the type of integrated hatchery breeding program used by hatchery managers. Predicting the N_e of wild populations of salmon from census data has also been the subject of much study, and a rough rule of thumb for that parameter is also emerging (e.g., Waples 2002*a*). Much fewer data exist on the third parameter, the relative reproductive success of hatchery vs. wild fish when breeding in the wild (but see Araki et al. 2006). Reliable estimates of these parameters will allow fisheries professionals to predict the loss of genetic diversity associated with supportive breeding.

Acknowledgements

Field support was provided by D. Loomis, J. Muck, and L. Jackson (Oregon Department of Fish and Wildlife). Funding was provided by the Oregon Watershed Enhancement Board to M.A. Banks and G.R. Moyer. We thank D. Jacobson and M.L. Moyer for providing laboratory assistance, S. Hampton for providing the Umpqua Basin map, and Oregon Department of Fish and Wildlife personnel and volunteers for making the field portion of this study possible. B. Sloss, K. O'Malley, and M. Camara provided insightful comments, editorial assistance, and helpful discussion. This manuscript benefited from comments provided by M. Ferguson and two anonymous reviewers.

References

Allendorf, F.W. 1993. Delay of adaptation to captive breeding by equalizing family size. Conserv. Biol. **7**: 416–419.

Araki, H., Ardren, W.R., Olsen, E., Cooper, B., and Blouin, M.S. 2006. Reproductive success of captive-bred steelhead trout in the wild: evaluation of three hatchery programs in the Hood River. Conserv. Biol. **21**: 181–190.

Banks, M.A., Blouin, M.S., Baldwin, B.A., Rashbrook, V.K., Fitzgerald, H.A., Blankenship, S.M., and Hedgecock, D. 1999. Isolation and inheritance of novel microsatellites in chinook salmon (*Oncorhynchus tshawytscha*). J. Hered. **90**: 281–288.

Berejikian, B.A., Tezak, E.P., Schroder, S., Knudsen, C.M., and Hard, J.J. 1997. Reproductive behavioral interaction between wild and captively reared coho salmon (*Oncorhynchus kisutch*). ICES J. Mar. Sci. **54**: 1040–1050.

Berejikian, B.A., Tezak, E.P., Park, L., LaHood, E., Schroder, S.L., and Beall, E. 2001. Male competition and breeding success in captively reared and wild coho salmon (*Oncorhynchus kisutch*). Can. J. Fish. Aquat. Sci. **58**: 804–810.

Bernatchez, L., and Duchesne, P. 2000. Individual-based genotype analysis in studies of parentage and population assignment: how many loci, how many alleles? Can. J. Fish. Aquat. Sci. **57**: 1–12.

Blouin, M.S., Parsons, M., Lacaille, V., and Lotz, S. 1996. Use of microsatellite loci to classify individuals by relatedness. Mol. Ecol. **5**: 393–401.

Bonin, A., Bellemain, E., Bronken Eidesen, P., Pompanon, F., Brochmann, C., and Taberlet, P. 2004. How to track and assess genotyping errors in population genetics studies. Mol. Ecol. **13**: 3261–3273.

Brannon, E.L., Amend, D.F., Cronin, M.A., Lannan, J.E., LaPetra, S., McNeil, W.J., Noble, R.E., Smith, C.E., Talbot, A.J., Wedemeyer, G.A., and Westers, H. 2004. The controversy about salmon hatcheries. Fisheries, **29**: 12–31.

Condrey, M.J., and Bentzen, P. 1998. Characterization of coastal cutthroat trout (*Oncorhynchus clarki*) microsatellites and their conservation to other salmonids. Mol. Ecol. **7**: 787–789.

Crow, F.F., and Morton, N.E. 1955. Measurement of gene frequency drift in small populations. Evolution, **9**: 202–214.

Currens, K.P., Hemmingsen, A.R., French, R.A., Buchanan, D.V., Schreck, C.B., and Hiram, W.L. 1997. Introgression and susceptibility to disease in a wild population of rainbow trout. N. Am. J. Fish. Manag. **17**: 1065–1078.

de Fromentel, C.C., Pakdel, F., Chapus, A., Baney, C., May, P., and Soussi, T. 1992. Rainbow trout p53: cDNA cloning and biochemical characterization. Gene, **112**: 241–245.

Fleming, I.A., and Gross, M.R. 1993. Breeding success of hatchery and wild coho salmon (*Oncorhynchus kisutch*) in competition. Ecol. Appl. **3**: 230–245.

Ford, M.J. 2002. Selection in captivity during supportive breeding may reduce fitness in the wild. Conserv. Biol. **16**: 815–825.

Ford, M.J., Teel, D., Van Doornik, D.M., Kuligowski, D., and Lawson, P.W. 2004. Genetic population structure of central Oregon Coast coho salmon (*Oncorhynchus kisutch*). Conserv. Genet. **5**: 797–812.

Geiger, H.J., Smoker, W.W., Zhivotovsky, L.A., and Gharrett, A.J. 1997. Variability of family size and marine survival in pink salmon (*Oncorhynchus gorbuscha*) has implications for conservation biology and human use. Can. J. Fish. Aquat. Sci. **54**: 2684–2690.

Gerber, S., Mariette, S., Streiff, R., Bodenes, C., and Kremer, A. 2000. Comparison of microsatellites and amplified fragment length polymorphism markers for parentage analysis. Mol. Ecol. **9**: 1037–1048.

Gerber, S., Chabrier, P., and Kremer, A. 2003. FAMOZ: a software for parentage analysis using dominant, codominant and uniparentally inherited markers. Mol. Ecol. Notes, **3**: 479–481.

Hedrick, P.W., Rashbrook, V.K., and Hedgecock, D. 2000. Effective population size of winter-run chinook salmon based on microsatellite analysis of returning spawners. Can. J. Fish. Aquat. Sci. **57**: 2368–2373.

Hobday, A.J., and Boehlert, G.W. 2001. The role of coastal ocean variation in spatial and temporal patterns in survival and size of coho salmon (*Oncorhynchus kisutch*). Can. J. Fish. Aquat. Sci. **58**: 2021–2036.

Jones, A.G., and Ardren, W.R. 2003. Methods of parentage analysis in natural populations. Mol. Ecol. **12**: 2511–2523.

Linley, T.J. 2001. Influence of short-term estuarine rearing on the ocean survival and size at return of coho salmon in southeastern Alaska. N. Am. J. Aquac. **63**: 306–311.

Lynch, M., and O'Hely, M. 2001. Captive breeding and the genetic fitness of natural populations. Conserv. Genet. **2**: 363–378.

Marshall, T.C., Slate, J., Kruuk, L.E.B., and Pemberton, J.M. 1998. Statistical confidence for likelihood-based paternity inference in natural populations. Mol. Ecol. **7**: 39–655.

Miller, L.M., and Kapuscinski, A.R. 2003. Genetic guidelines for hatchery supplementation programs. *In* Population genetics: principles and applications for fisheries scientists. *Edited by* E.M. Hallerman. American Fisheries Society, Bethesda, Maryland. pp. 329–355.

Mobrand, L., Barr, J., Blankenship, H.L., Campton, D.E., Evelyn, T.T.P., Flagg, T., Mahnken, C., Seeb, L.W., Seidel, P.R., and Smoker, W.W. 2005. Hatchery reform in Washington State: principles and emerging issues. Fisheries, **30**: 11–23.

Naish, K.A., and Park, L.K. 2002. Linkage relationships for 35 new microsatellite loci in chinook salmon, *Oncorhynchus tshawytscha*. Anim. Genet. **33**: 316–318.

Olsen, J.B., Wilson, S.L., Kretschmer, E.J., Jones, K.C., and Seeb, J.E. 2000. Characterization of 14 tetranucleotide microsatellite loci derived from sockeye salmon. Mol. Ecol. **9**: 2185–2187.

O'Reilly, P.T., Herbinger, C., and Wright, J.M. 1998. Analysis of parentage determination in Atlantic salmon (*Salmo salar*) using microsatellites. Anim. Genet. **29**: 363–370.

Ryman, N., and Laikre, L. 1991. Effects of supportive breeding on the genetically effective population size. Conserv. Genet. **5**: 325–329.

Sancristobal, M., and Chevalet, C. 1997. Error tolerant parent identification from a finite set of individuals. Genet. Res. **70**: 53–62.

Scribner, K.T., Gust, J.R., and Fields, R.L. 1996. Isolation and characterization of novel salmon microsatellite loci: cross-species amplification and population genetic applications. Can. J. Fish. Aquat. Sci. **53**: 833–841.

Shrimpton, M.J., and Heath, D.D. 2003. Census vs. effective population size in chinook salmon: large- and small-scale environmental perturbation effects. Mol. Ecol. **12**: 2571–2583.

Sokal, R.R., and Rohlf, F.J. 1995. Biometry: the principles and practice of statistics in biological research. W.H. Freeman and Company, New York.

Waples, R.S. 1990. Conservation genetics of Pacific salmon. III. Estimating effective population size. J Hered. **81**: 277–289.

Waples, R.S. 2002*a*. Effective size of fluctuating salmon populations. Genetics, **161**: 783–791.

Waples, R.S. 2002*b*. Evaluating the effect of stage-specific survivorship on the N_e/N ratio. Mol. Ecol. **11**: 1029–1037.

Waples, R.S. 2005. Genetic estimates of contemporary effective population size: to what time periods do the estimates apply? Mol. Ecol. **14**: 3335–3352.

Waples, R.S., and Teel, D.J. 1990. Conservation genetics of Pacific salmon. I. Temporal changes in allele frequency. Conserv. Biol. **4**: 144–156.

Williamson, K.S., Cordes, J.F., and May, B. 2002. Characterization of microsatellite loci in chinook salmon (*Oncorhynchus tshawytscha*) and cross-species amplification in other salmonids. Mol. Ecol. Notes, **2**: 17–19.

Wright, S. 1938. Size of population and breeding structure in relation to evolution. Science (Washington, D.C.), **87**: 430–431.

Seasonal changes of dissolved organic carbon photo-oxidation rates in a tropical humic lagoon: the role of rainfall as a major regulator

Albert Luiz Suhett, André Megali Amado, Alex Enrich-Prast, Francisco de Assis Esteves, and Vinicius Fortes Farjalla

Abstract: In this paper, we report the seasonal variation of photo-oxidation rates in a tropical humic lagoon and its relation to annual rainfall regime. Photo-oxidation rates ranged from 8.96 to 415.06 μmol C·L^{-1}·day^{-1}, being higher in the beginning to middle of the rainy season and declining throughout the year. Although dissolved organic carbon (DOC) concentration, water color, and sunlight incidence were generally higher in the rainy season, photo-oxidation rates were not significantly related to any of these parameters. Photo-oxidation seems to be influenced mainly by changes in DOC photoreactivity, which was up to threefold higher early in the rainy season, when inputs of fresh allochthonous DOC take place. In the following months, in addition to being continuously degraded by sunlight, DOC is also removed from the water column by processes such as microbial degradation and sedimentation, leading to a decline in DOC concentration and photoreactivity throughout the year until the next rainy season. Thus, the dynamics of DOC inputs caused by the rainfall regime in Comprida Lagoon lead to a yearly pulse of DOC photoreactivity and photo-oxidation rates. We believe this pulse model also fits other aquatic ecosystems subject to similar seasonal inputs of allochthonous DOC, although rainfall would not necessarily be the driving factor.

Résumé : Notre travail présente la variation saisonnière des taux de photo-oxydation dans une lagune tropicale humique en relation avec le régime annuel des précipitations. Les taux de photo-oxydation varient de 8,96 à 415,06 μmol C·L^{-1}·jour^{-1}; ils sont plus élevés au début et au milieu de la saison des pluies et déclinent au cours du reste de l'année. Bien que les concentrations de carbone organique dissous (« DOC »), la couleur de l'eau et l'incidence solaire soient généralement plus élevées durant la saison des pluies, les taux de photo-oxydation ne sont pas significativement reliés à aucune de ces variables. La photo-oxydation semble être influencée surtout par les changements de photo-réactivité de la DOC qui est jusqu'à trois fois supérieure au début de la saison des pluies lorsqu'ont lieu les apports de DOC allochtone fraîche. Dans les mois suivants, en plus d'être constamment dégradée par la lumière solaire, la DOC est aussi retirée de la colonne d'eau par des processus tels que la dégradation microbienne et la sédimentation, ce qui explique le déclin de la concentration et de la photo-réactivité de la DOC au cours de l'année jusqu'à la prochaine saison des pluies. Ainsi la dynamique des apports de DOC contrôlée par le régime des précipitations dans la lagune de Comprida produit un pic annuel de photo-réactivité de la DOC et des taux de photo-oxydation. Nous croyons que ce modèle avec un pic annuel s'applique aussi à d'autres écosystèmes sujets à des apports saisonniers semblables de DOC allochtone, bien que les précipitations ne soient pas nécessairement le facteur déclencheur.

[Traduit par la Rédaction]

Introduction

Dissolved organic carbon (DOC) is a great carbon pool in the biosphere, similar in magnitude to CO_2 in the atmosphere (Farrington 1992). Because DOC is involved in a multitude of biogeochemical processes linking different compartments of the hydrosphere and biosphere, it is an important component of the global carbon cycle and has the potential to affect global climate changes (Granéli et al. 1998). Recently, DOC mineralization processes have received special attention because of the effect of CO_2 as a greenhouse gas and its role in global warming (e.g., Amado et al. 2003).

In addition to microbial degradation, photochemical degradation has been recognized by many authors as an important carbon-mineralization pathway in both temperate and

Received 4 October 2006. Accepted 14 July 2007. Published on the NRC Research Press Web site at cjfas.nrc.ca on 7 September 2007. J19577

A.L. Suhett and A.M. Amado. Programa de Pós-Graduação em Ecologia (PPGE/UFRJ), Ilha do Fundão, CEP 21941-590, Caixa Postal 68020, Rio de Janeiro, Brazil.
A. Enrich-Prast, F.A. Esteves,[1] and V.F. Farjalla.[1,2] Departamento de Ecologia, Instituto de Biologia, Universidade Federal do Rio de Janeiro (UFRJ), Ilha do Fundão, CEP 21941-590, Caixa Postal 68020, Rio de Janeiro, Brazil.

[1] Present address: Núcleo de Pesquisas em Ecologia e Desenvolvimento Sócio-ambiental de Macaé (NUPEM/UFRJ), Av. Rotary Club S/N°, São José do Barreto, CEP 28970-000, P.O. Box 119331, Macaé, Rio de Janeiro, Brazil.
[2] Corresponding author (e-mail: farjalla@biologia.ufrj.br).

Can. J. Fish. Aquat. Sci. **64**: 1266–1272 (2007) doi:10.1139/F07-103

tropical aquatic systems (Lindell et al. 1995; Amon and Benner 1996; Amado et al. 2006). Through this process, light irradiation leads to the breakdown of bulk DOC into lower molecular mass organic compounds and inorganic molecules such as CO_2 (Moran and Zepp 1997). Thus, photochemical DOC degradation enhances carbon mineralization through direct oxidation to inorganic carbon (hereafter called photo-oxidation) and indirect stimulation of bacterial consumption as a result of photoproduction of labile bacterial substrates (Geller 1986; Lindell et al. 1995; Granéli et al. 1996). These processes are especially relevant in systems where DOC is mostly of allochthonous origin and is more available to sunlight than to bacterial degradation (Amon and Benner 1996; Tranvik and Bertilsson 2001; Amado et al. 2006).

DOC photo-oxidation in natural waters can be influenced by many factors, such as (*i*) the DOC concentration in the water (Granéli et al. 1998), (*ii*) the amount of incident light energy (Bertilsson and Tranvik 2000; Farjalla et al. 2001), (*iii*) the DOC exposure history and (or) diagenetic state of molecules (Amado et al. 2003; Biddanda and Cotner 2003), and (*iv*) the DOC origin and quality (Farjalla et al. 2001; Amado et al. 2006). Because most aquatic ecosystems exhibit some kind of seasonal variation in these features, it is likely that photo-oxidation rates also vary seasonally, although only a few attempts have been made to demonstrate these trends (Lindell et al. 2000; Amado et al. 2006).

Humic substances represent more than 50% of DOC in most aquatic ecosystems (Thurman 1985; Thomas 1997). In certain small aquatic ecosystems, including some tropical coastal lagoons, the humic fraction can be as high as 90% of DOC (Suhett et al. 2004). These humic lagoons are characterized by DOC concentrations exceeding 4 $mmol \cdot L^{-1}$, with seasonal inputs driven by the annual rainfall regime (Farjalla et al. 2002). These features suggest that these lagoons may have high DOC photo-oxidation rates and that these rates may vary seasonally in response to rainfall. Nonetheless, we are not aware of any paper on seasonal variation of DOC photo-oxidation in tropical, highly humic ecosystems.

The aim of the current research was to evaluate the seasonal DOC photo-oxidation rates in a highly humic, tropical coastal lagoon (Comprida Lagoon). Thus, in this paper we addressed the effects of the seasonal rainfall regime on DOC photo-oxidation rates and photoreactivity in Comprida Lagoon. The main result is that the DOC photo-oxidation is closely related to the beginning of the rainy season when inputs of fresh, humic DOC take place.

Materials and methods

Study area

The study was carried out in Comprida Lagoon, a tropical, humic coastal lagoon situated in a coastal sand plain in the Restinga de Jurubatiba National Park at the north of Rio de Janeiro State, Brazil (22°17′S and 41°39′W). Comprida Lagoon has an area of 0.12 km^2 and a high perimeter–volume ratio (because of its dendritic shape) and is considerably influenced by the surrounding brushy vegetation (restinga). DOC concentrations in Comprida Lagoon can reach values close to 5 $mmol\ C \cdot L^{-1}$ (Farjalla et al. 2002), and more than 90% of it can be humic carbon (Suhett et al. 2004). The lagoon is typically shallow (<2 m deep), but because of highly colored water, sunlight is mostly attenuated in the first 0.4 m (Granéli et al. 1998).

The climate in the region is warm and humid, with a mean annual temperature of 26.6 °C and rainfall concentrated between October and March (Henriques et al. 1988; Farjalla et al. 2002).

Sampling and experimental setup

Samples were collected in a central site of Comprida Lagoon on seven different days between March 2003 and November 2004 (in March, July, and October 2003 and February, May, July, and November 2004) and are referred to by month and year (e.g., July 2004). All samples were taken at subsurface (~10 cm deep) in polyethylene bottles prewashed with HCl (10%) and deionized water and rinsed with the lagoon water. Samples were prefiltered through 0.7 µm glassfiber filters (GF/F; Whatman Inc., Florham Park, N.J.) to exclude larger particles and then filtered though 0.2 µm polycarbonate membranes (BA 83; Schleicher & Schuell) immediately before sunlight exposure experiments to exclude bacteria. This procedure was taken to minimize the influence of bacterial activity on DOC mineralization during the experiments.

Filtered samples were poured into eight ultraviolet (UV) transparent culture bags (Nasco Whirl-Pak®, Fort Atkinson, Wis.), which were sealed without internal atmosphere (see Amado et al. 2006). Because these bags transmit about 35% of UV light, photo-oxidation rates were probably underestimated in this study. Four bags were wrapped in aluminum foil and used as dark controls. Samples were incubated under natural sunlight for 6 h around noon in plastic pools filled with running tap water to keep the temperature roughly constant (32 ± 3 °C), similar to the experimental setup from Granéli et al. (1998). During the incubations, we measured the incidence of sunlight every hour in the photosynthetically active radiation (PAR; 400–700 nm), UV-A (320–400 nm), and UV-B (280–320 nm) wavebands with a radiometer (IL 1400; International Light Technologies Inc., Peabody, Mass.). These data were used for further calculation of total incident PAR, UV-A, and UV-B during the incubations by integrating them through time. Total incident radiation was also calculated by adding up the total incident PAR, UV-A, and UV-B.

Rainfall data were obtained from the meteorological station at a local farm (São Lázaro Farm, ~3 km from Comprida Lagoon). The cumulative rainfall for the last 30, 60, and 90 days (CR_{30}, CR_{60}, and CR_{90}, respectively) was calculated for each sampling date.

Chemical analyses

Aliquots of the initial 0.2 µm filtered samples were taken for DOC and absorbance analyses before incubations. The aliquots were transferred to 20 mL glass vials (10% HCl and Milli-Q water rinsed) and kept refrigerated (4 °C) to avoid any biological DOC consumption. After incubations, aliquots for dissolved inorganic carbon (DIC) analysis were carefully transferred into glass vials (5.9 mL exetainers; LabCo Ltd., High Wycombe, Buckinghamshire, England) with rubber-sept Teflon caps, leaving no headspace. To avoid DIC losses by CO_2 diffusion, we used a syringe connected to silicone tubing. The tubing was placed on the bottom of the vial and the water samples were slowly placed in the flask, which was overflowed with at least five times the vial volume (±60 mL). After that, we added $HgCl_2$ (final concentration 0.01%) to stop any biological activity and avoid further CO_2 production. The DOC and DIC analyses were performed within 1 day after experiments in a total organic carbon analyzer (TOC 5000; Shimadzu Scientific Instruments, Columbia, Md.) by the high temperature combustion Pt catalytic method. At least three replicate injections were made for each sample, resulting in coefficient of variation (CV) lower than 2%.

We measured the absorbance at 250, 365, and 430 nm with a 1 cm quartz cuvette in a Beckman DU® 560 spectrophotometer using distilled water as a blank. The absorption coefficients at these wavelengths were expressed in inverse metres (m^{-1}) and calculated as follows (Hu et al. 2002):

$$a_\lambda = 2.303(A_\lambda / L)$$

where A_λ is the absorbance at wavelength λ and L is the optical path length of the cuvette (in metres). We used the absorption coefficient at 430 nm (a_{430}) as an estimate of water color. We also determined the absorption coefficients at 250 (a_{250}) and 365 nm (a_{365}) and the ratio of a_{250} to a_{365}, which can be used as an estimate of relative DOC molecular size. An increase in the ratio indicates an increase in the proportion of smaller molecules and vice versa (Strome and Miller 1978). The specific DOC absorbance at 250 nm (250:DOC) and 430 nm (430:DOC) was also calculated. All these parameters may be well related to DOC photo-oxidation rates (Granéli et al. 1998; Bertilsson et al. 1999; Lindell et al. 2000).

Photo-oxidation rates were estimated by the mean difference of DIC between exposed and control samples after incubation. We express photo-oxidation rates as micromoles of DIC per litre produced per day ($\mu mol\ C \cdot L^{-1} \cdot day^{-1}$), assuming photo-oxidation during the 6-h incubations for the whole day. We also calculated an adimensional DOC photoreactivity index (hereafter called DPI) by normalizing photo-oxidation rates by DOC concentration and solar radiation. The efficiency of the different wavebands of sunlight was also considered in the normalization, according to Granéli et al. (1998), who found PAR, UV-A, and UV-B to account for 44%, 39%, and 17% of DOC photo-oxidation, respectively. The DPI was calculated through the following equation:

$$\mathrm{DPI} = \frac{P_i}{\mathrm{DOC}_i}\left[0.44\frac{\mathrm{PAR}_{\max}}{\mathrm{PAR}_i} + 0.39\frac{\text{UV-A}_{\max}}{\text{UV-A}_i} + 0.17\frac{\text{UV-B}_{\max}}{\text{UV-B}_i}\right]$$

where P_i is amount of photo-oxidized DOC at time i; DOC_i is DOC concentration at time i; $\mathrm{PAR}_{\max}$, $\text{UV-A}_{\max}$, and $\text{UV-B}_{\max}$ represent the highest amount of incident PAR, UV-A, and UV-B, respectively, in samples during the experiments over the months; and PAR_i, UV-A_i, and UV-B_i represent the amount of incident PAR, UV-A, and UV-B, respectively, at time i. The constants 0.44, 0.39, and 0.17 are the proportional contribution of PAR, UV-A, and UV-B, respectively, to total photo-oxidation (from Granéli et al. 1998).

Statistical analyses

For testing the significance of the DIC production after incubations, DIC data were $\ln(x + 1)$-transformed and the mean difference between exposed and control samples was tested with one-tailed unpaired t tests using Prism® 4.0 (GraphPad Software, Inc., San Diego, California). It should be noted that the exposed and control samples were not paired to each other and, therefore, were statistically independent. The standard error (SE) for the mean difference was also estimated (Motulsky 2003). Because DIC data were transformed prior to analysis, SE values were back-transformed to give estimated SE for photo-oxidation rates (Motulsky 2003).

Simple correlations were performed with Statistica 6.0 (StatSoft, Inc., Tulsa, Oklahoma) to search for relationships between photo-oxidation and other limnological variables, as well as among these variables with one another. DOC, pH, absorption coefficients and ratios, specific DOC absorption, PAR, UV-A, UV-B, cumulative rainfall, and DPI were included in these analyses, in addition to photo-oxidation rates. A preliminarily examination of the correlations allowed for the exclusion of strongly redundant variables (e.g., PAR and UV-A radiation) and also redundant correlations based on these variables. Besides presenting strong correlations with one another ($r > 0.90$ and $P < 0.001$), these variables were considered redundant primarily because of their logical relationship. In these cases, only one of the variables or correlations were kept. Logically irrelevant correlations, such as PAR × CR_{30}, were also excluded. A total of 31 correlations of potential interest were used for the analyses.

We adopted a level of significance of $\alpha = 0.10$ for all statistical analyses, as done in other ecological studies with few data points (e.g., McCabe and Cyr 2006). Although the effects of the selected variables on photo-oxidation may be complex and interact with each other, it was not possible to apply a multivariate analysis, as done by Bertilsson and Tranvik (2000), because of our small number of cases ($n = 7$ sampling times).

Results

Rainfall followed the general seasonal pattern for the region, with the rainy season from October to March and the dry season from April to September (Fig. 1). The incidence of solar PAR and UV-A radiation also showed a similar seasonal variation, with higher values during the rainy season, whereas UV-B was much less variable throughout the year (Fig. 1).

DOC concentration and water color in Comprida Lagoon varied seasonally and were, in general, coupled (Fig. 2*a*). The beginning of the rainy season in October 2003 led to an increase in DOC concentration, followed by a decrease through the dry season. A similar decline was observed from March 2003 (end of the rainy season) to July 2003 (dry season). A clear uncoupling of DOC and water color occurred in November 2004, with an even higher water color (59.06 m^{-1}) despite the relatively lower DOC concentration (1.96 $mmol \cdot L^{-1}$; Fig. 2*a*). When this month was excluded from analysis, the correlation was significant ($P = 0.069$, $r = 0.78$; Table 1). Significant relationships were also found between DOC and the absorption coefficients a_{250} ($P = 0.038$, $r = 0.84$; Ta-

Fig. 1. Seasonal variation of monthly rainfall (in mm; bars) in the outskirts of Comprida Lagoon from December 2002 to November 2004 and solar radiation in the photosynthetically active radiation (PAR) (○), ultraviolet (UV)-A (●), and UV-B (▼) wavebands measured during the experiments (J·cm^{-2}). Note the break in the scale of the radiation axis. The dry and rainy seasons are separated by vertical broken lines. Precipitation is not shown for November 2004 as the sampling and experiments were done on 1 November.

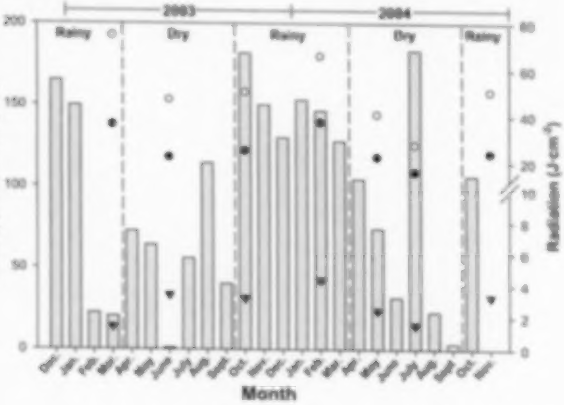

ble 1) and a_{365} (P = 0.042, r = 0.83; Table 1). Until July 2004, the lowest DOC and water color were registered in July 2003 (1.28 mmol·L^{-1} and 17.96 m^{-1}, respectively), whereas the highest values were recorded in February 2004 (4.86 mmol·L^{-1} and 51.81 m^{-1}, respectively). Overall, DOC concentration was positively related to CR$_{60}$ (P = 0.030, r = 0.80; Table 1) and CR$_{90}$ (P = 0.006, r = 0.90; Table 1), and water color was negatively related to pH (P = 0.048, r = –0.79; Table 1).

Photo-oxidation was significant for all experiments, i.e., significant DIC production in irradiated samples relative to nonexposed controls (Table 2). The photo-oxidation rates were associated with the seasonal rainfall regime, with higher values recorded in the beginning to middle of the rainy season and lower values in the dry season (Fig. 2*b*). More specifically, photo-oxidation increased towards October 2003, peaked in February 2004, and decreased in the following periods, peaking again in November 2004 (Fig. 2*b*). The lowest photo-oxidation rate was recorded in July 2003 (8.96 µmol C·L^{-1}·day^{-1}), whereas the highest rate (415.06 µmol C·L^{-1}·day^{-1}) was recorded in November 2004. It should be pointed out that the high monthly rainfall recorded for July 2004 was due to heavy rains from 18 to 23 July. As the sampling and photo-oxidation experiment were carried out on 5 July, the data recorded for July 2004 were not affected by these rain events, as noted by the decrease in DOC and water color (Fig. 2*a*). When all months were analyzed, photo-oxidation rates were correlated only with DPI (P = 0.015, r = 0.85; Table 1). When November 2004 was excluded, photo-oxidation rates were positively correlated with CR$_{60}$ (P = 0.050, r = 0.81; Table 1).

The DPI, in turn, varied from ca. 0.010 to 0.06 in most of the studied period (Fig. 2*b*). However, in October 2003 and November 2004, these values were much higher (0.117 and 0.315, respectively). Even with an increase in DOC and sunlight incidence from October 2003 to February 2004, photo-oxidation rates did not increase in proportion to these parameters, as shown by the decline of DPI in the latter month. The lowest DPI was recorded in July 2003 (0.011; Fig. 2*b*). DPI was positively correlated with 250:DOC (P = 0.070, r = 0.72; Table 1) and 430:DOC (P = 0.060, r = 0.74; Table 1). Moreover, when November 2004 was excluded, a positive correlation was found between DPI and CR$_{30}$, showing that DOC photoreactivity was somehow influenced by cumulative rainfall during the previous month.

Fig. 2. Seasonal changes of (*a*) dissolved organic carbon (DOC) concentration (mmol C·L^{-1}; bars) and water color (m^{-1}; solid circles) and (*b*) DOC photo-oxidation rates (µmol C·L^{-1}·day^{-1}; bars) and DOC photoreactivity index (DPI; solid circles) in Comprida Lagoon from March 2003 to November 2004. Error bars in (*b*) account for estimated standard error of photo-oxidation rates.

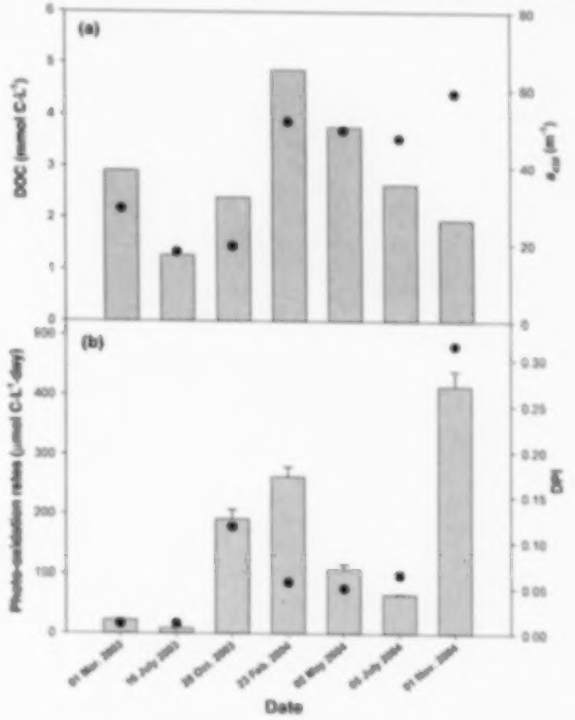

It should be mentioned that although the relationship between photo-oxidation and environmental variables, and among these variables as well, may not necessarily be linear, log-transformed data did not improve correlation coefficients and probability in any consistent way. Therefore, we chose to keep the simple linear correlations.

Discussion

Major climatic factors are known to influence ecological processes either directly or indirectly. In temperate and arctic lakes, the cold winter temperatures inhibit the growth and activity of organisms, with drastic consequences on the functions of the ecosystem (Gaedke 1992; Kirschner and Velimirov 1997; Laybourn-Parry et al. 2004). In these ecosystems, temperature may also indirectly influence ecologi-

Table 1. Significant ($P < 0.10$) correlations between photo-oxidation and environmental variables and among these variables for the whole data set ($n = 7$ sampling times) and without November 2004 ($n = 6$).

All data			Without November 2004		
Correlations	r	P	Correlations	r	P
DPI × photo-oxidation	0.85	0.015	DOC × a_{250}	0.84	0.038
DPI × 250:DOC	0.72	0.070	DOC × a_{365}	0.83	0.042
DPI × 430:DOC	0.74	0.060	DOC × a_{430}	0.78	0.069
CR_{60} × DOC	0.80	0.030	CR_{30} × DPI	0.86	0.028
CR_{90} × DOC	0.90	0.006	CR_{60} × photo-oxidation	0.81	0.050
a_{430} × pH	–0.79	0.048			

Note: For the data set without November 2004, only additional significant correlations (which had not been significant for the whole data set) are presented. DOC, dissolved organic carbon; DPI, DOC photoreactivity index; CR_{30}, CR_{60}, and CR_{90}, cumulative rainfall for the last 30, 60, and 90 days, respectively; 250:DOC and 430:DOC, specific DOC absorbances at 250 and 430 nm, respectively; a_{250}, a_{365}, and a_{430}, the absorption coefficients at 250, 365, and 430 nm, respectively.

Table 2. Probabilities (P), t values, and mean differences (± standard error) for comparisons of mean dissolved inorganic carbon (DIC) concentrations between exposed and control samples after 6-h incubations.

Date of sample	t	P	DIC difference (μmol C·L^{-1})
March 2003	9.260	<0.001	22.75±2.46
July 2003	5.325	0.006	8.96±3.12
October 2003	5.575	<0.001	191.46±34.34
February 2004	7.132	<0.001	262.83±38.35
May 2004	6.624	<0.001	107.42±2.14
July 2004	6.888	0.003	66.00±3.10
November 2004	5.494	0.006	415.06±2.13

Note: For all comparisons, $n = 4$ and degrees of freedom = 6.

cal processes through snowmelt- and rainfall-mediated inputs of allochthonous DOC from early spring to midsummer (Lindell et al. 2000; Pace and Cole 2002; Hongve et al. 2004). Additionally, other factors not directly related to climate, such as the leaching of DOC from highly productive macrophytes and the release of pore-water DOC as a result of wind resuspension, are recognized as important sources of DOC input to lakes (Reitner et al. 1997; Cotner 2000). In tropical lakes and rivers, seasonal rainfalls and flood pulses seem to be major factors regulating inputs of DOC to aquatic systems. Studies developed in tropical floodplain lakes, for instance, have reported considerable inputs of DOC and nutrients to these lakes because of increased connectivity with main rivers during filling-up or high-water periods, with marked effects on bacterial and photochemical degradation (Castillo 2000; Amado et al. 2006; Farjalla et al. 2006).

In the present study, the seasonal dynamics of DOC in Comprida Lagoon was related to the seasonal rainfall regime, more specifically with cumulative rainfall for the previous 1 or 2 months. A similar seasonal pattern for DOC was recorded in four humic coastal lagoons in the same region (including Comprida Lagoon) a few years earlier (Farjalla et al. 2002). These results, together with the coupling between DOC and water color (positive) and between water color and pH (negative), suggest that the DOC input to Comprida Lagoon is dominated by humic substances and is mainly regulated by the seasonal rainfall distribution.

Only a few studies have reported seasonal variation in DOC photo-oxidation. Lindell et al. (2000) showed that photo-oxidation in two temperate lakes was higher in early spring, immediately after snowmelt, as a result of the input of fresh allochthonous DOC and exposure of previously ice-shaded DOC to sunlight. A peak was also observed in winter, due to mixing of the water column and the entering of reactive DOC from deep hypolimnetic waters into the epilimnion, although it is only a measure of potential photoreactivity, as the lake surface is frozen in the winter. Continuous exposure to sunlight makes DOC less photoreactive through summer and fall (Lindell et al. 2000). Amado et al. (2006), working in two Amazonian clear-water ecosystems, observed higher photo-oxidation rates (one order of magnitude higher) in periods of filling-up and high-water level, when allochthonous DOC enters the system as the waters flood forests. Paul et al. (2004) also presented evidence for seasonal variation in DOC photoreactivity in five Scandinavian aquatic ecosystems, expressed as a decreased photoproduction of singlet oxygen, one of the major reactive oxygen species acting in photo-oxidation, from summer to spring.

Here, we observed a wide variation in photo-oxidation rates in Comprida Lagoon throughout the studied period, varying over two orders of magnitude. Basically, photo-oxidation rates showed a seasonal pattern of peaks at the beginning to middle of the rainy season and declined during the year through the dry season. We did not find the usual significant relationships between photo-oxidation rates and DOC concentration, water color, or solar radiation as recorded in other studies with time-punctual approaches (Granéli et al. 1998; Bertilsson et al. 1999; Amado et al. 2003). In the present study, not only photo-oxidation rates, but also the DOC photoreactivity (DPI) varied seasonally, both being positively associated with the seasonal rainfall regime. Because DPI is calculated based on photo-oxidation rates themselves, it seems obvious that these variables are correlated. However, that should not necessarily happen, as this value is normalized by the amount of substrate for photo-oxidation (DOC) and incident sunlight. The positive relationship between DPI and DOC-specific absorption at

250 and 430 nm suggest that DPI reflects the capacity of DOC to interact with sunlight. DOC photoreactivity should be higher when fresh, colored humic DOC enters the lagoon at the beginning of the rainy season. This was illustrated in February 2004, when water color did not increase markedly in relation to October 2003, in spite of increased DOC concentration. Although photo-oxidation increased towards February 2004, it was not as high as expected by the increase in sunlight, because of the lower capacity of DOC to interact with sunlight (lower DOC-specific absorption).

It is interesting to notice that in contrast to October 2003, November 2004 presented a somewhat low DOC concentration but an increased water color. The highest photo-oxidation rate was also measured in this month. This led to a similarly high DPI value. Because of the singularity of this month, some correlations were only significant when it was excluded from analysis. However, the general conclusions drawn from the figures work in quite the same way. We do not believe that the high photo-oxidation rate measured in November 2004 arises from any methodological problem, as we have also measured such high rates in other humic ecosystems in the region, via either DIC production or oxygen consumption methods (A.L. Suhett, A.M. Amado, and V.F. Farjalla, unpublished data). However, we should not discard the possibility of some kind of measurement error (underestimation) for the DOC data in this month, as we found an increased water color and a high photo-oxidation rate.

The photo-oxidation rates reported in the present study are quite high even when compared with those reported in other studies carried out in humic ecosystems (Granéli et al. 1996, 1998; Reitner et al. 1997). In the tropics, sunlight incidence is much less variable and quite high during the year when compared with that of temperate regions. Because of this high light availability throughout the year, any events that cause marked inputs of fresh, highly photoreactive DOC to tropical freshwaters may lead to quite high photo-oxidation rates. This seems to be the case for seasonal rainfall in Comprida Lagoon. In this way, seasonal rainfall may act synergistically with high sunlight incidence to produce atypically high photo-oxidation rates during the rainy period. This may have great implications for the carbon cycle of Comprida Lagoon and other tropical humic ecosystems, rendering photo-oxidation an important pathway for DOC removal, especially when seasonal or punctual inputs of photoreactive DOC take place. This is likely also true for other tropical aquatic ecosystems in which these seasonal inputs occur, such as Amazonian lakes and streams (e.g., Amado et al. 2006). It should also be noted that although sunlight is strongly attenuated in dark waters, Comprida Lagoon (as well as many tropical lakes) is shallow and its water column is constantly mixed by wind action. This mixing may homogenize the effects of photochemical processes through the shallow water column, although sunlight does not penetrate to the bottom.

Fig. 3. Conceptual model of seasonal variation of dissolved organic carbon (DOC) photo-oxidation rates and photoreactivity in Comprida Lagoon. The annual rainfall regime is the main driving factor leading to pulsing dynamics of DOC photoreactivity, with a periodicity of one hydrological year. Peaks of photoreactivity (indicated by the continuous line) occur early in the rainy season driven by the input of fresh allochthonous DOC (indicated by shaded large arrows). Peaks of photo-oxidation rates also occur in the rainy season but do not necessarily coincide with photoreactivity peaks, as high DOC concentration and sunlight incidence may produce high photo-oxidation rates from the middle of the rainy season, even if DOC photoreactivity starts to decline. The following decline of DOC photo-oxidation rates and photoreactivity is attributed mainly to photochemical consumption (continuous thin arrow), but also likely to factors such as bacterial degradation and DOC sedimentation (broken thin arrows).

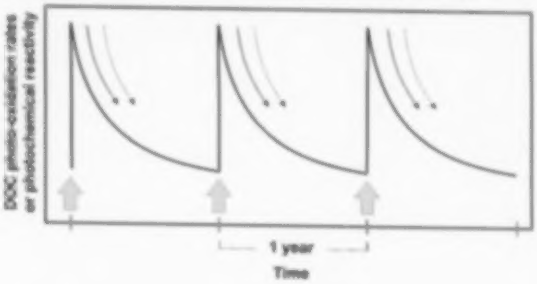

We propose a general conceptual model for the dynamics of DOC photoreactivity and photo-oxidation in Comprida Lagoon (Fig. 3). The annual rainfall regime is the main driving factor leading to pulse-like dynamics of DOC photoreactivity, with a periodicity of one hydrological year. Peaks of photoreactivity occur early in the rainy period as a result of the input of fresh allochthonous DOC. Photo-oxidation rates may peak a little after photoreactivity peaks because of increased DOC concentration and (or) solar incidence. The coincidence of high sunlight incidence with seasonal inputs of photoreactive DOC during rainy season act synergistically to produce high photo-oxidation rates in this season. The following decline of DOC photo-oxidation rates and photoreactivity is attributed mainly to previous photochemical consumption, but other factors such as DOC precipitation to sediments or microbial consumption of photoreactive DOC may also play a role. We strongly believe that this model is also applicable to other tropical humic aquatic ecosystems subjected to seasonal inputs of photoreactive DOC, although rainfall would not necessarily be the driving factor.

Acknowledgements

This work was part of the Project "Carbon sequestration and release in lagoons and reservoirs", coordinated by Bias M. Faria of the Petrobras Research and Development Center (CENPES). The authors are grateful to CENPES/PETROBRAS, CNPq, CAPES, and FAPERJ for financial support and scholarships for the development of this work. We also thank Valéria M. Amado for language review.

References

Amado, A.M., Farjalla, V.F., Esteves, F.A., and Bozelli, R.L. 2003. DOC photo-oxidation in clear-water Amazonian aquatic ecosystems. Amazoniana, **17**(3–4): 513–523.

Amado, A.M., Farjalla, V.F., Esteves, F.A., Bozelli, R.L., Roland, F., and Enrich-Prast, A. 2006. Complementary pathways of dissolved organic carbon removal pathways in clear-water Amazonian ecosystems: photochemical degradation and bacterial uptake. FEMS Microb. Ecol. **56**(1): 8–17.

Amon, R.M.W., and Benner, R. 1996. Photochemical and microbial consumption of dissolved organic carbon and dissolved oxygen in the Amazon River system. Geochim. Cosmochim. Acta, **60**(10): 1783–1792.

Bertilsson, S., and Tranvik, L.J. 2000. Photochemical transformation of dissolved organic matter in lakes. Limnol. Oceanogr. **45**(4): 753–762.

Bertilsson, S., Stepanauskas, R., Cuadros-Hansson, R., Graneli, W., Wikner, J., and Tranvik, L. 1999. Photochemically induced changes in bioavailable carbon and nitrogen pools in a boreal watershed. Aquat. Microb. Ecol. **19**(1): 47–56.

Biddanda, B.A., and Cotner, J.B. 2003. Enhancement of dissolved organic matter bioavailability by sunlight and its role in the carbon cycle of Lakes Superior and Michigan. J. Gt. Lakes Res. **29**(2): 228–241.

Castillo, M.M. 2000. Influence of hydrological seasonality on bacterioplankton in two neotropical floodplain lakes. Hydrobiologia, **437**(1–3): 57–69.

Cotner, J.B. 2000. Intense winter heterotrophic production stimulated by benthic resuspension. Limnol. Oceanogr. **45**(7): 1672–1676.

Farjalla, V.F., Anesio, A.M., Bertilsson, S., and Granéli, W. 2001. Photochemical reactivity of aquatic macrophyte leachates: abiotic transformations and bacterial response. Aquat. Microb. Ecol. **24**(2): 187–195.

Farjalla, V.F., Faria, B.M., and Esteves, F.A. 2002. The relationship between DOC and planktonic bacteria in tropical coastal lagoons. Arch. Hydrobiol. **156**(1): 97–119.

Farjalla, V.F., Azevedo, D.A., Esteves, F.A., Bozelli, R.L., Roland, F., and Enrich-Prast, A. 2006. Influence of hydrological pulse on bacterial growth and DOC uptake in a clear-water Amazonian lake. Microb. Ecol. **52**(2): 334–344.

Farrington, J. 1992. Overview and key recommendations — Marine Organic Geochemistry Workshop, January 1990. Mar. Chem. **39**(1–3): 5–9.

Gaedke, U. 1992. The size distribution of plankton biomass in a large lake and its seasonal variability. Limnol. Oceanogr. **37**(6): 1202–1220.

Geller, A. 1986. Comparison of mechanisms enhancing biodegradability of refractory lake water constituents. Limnol. Oceanogr. **31**(4): 755–764.

Granéli, W., Lindell, M., and Tranvik, L. 1996. Photo-oxidative production of dissolved inorganic carbon in lakes of different humic content. Limnol. Oceanogr. **41**(4): 698–706.

Granéli, W., Lindell, M., Faria, B.M., and Esteves, F.A. 1998. Photoproduction of dissolved inorganic carbon in temperate and tropical lakes — dependence on wavelength band and dissolved organic carbon concentration. Biogeochemistry, **43**(2): 175–195.

Henriques, R.P.B., Araújo, D.S.D., Esteves, F.A., and Franco, A.C. 1988. Análise preliminar das comunidades de macrófitas aquáticas da lagoa Cabiúnas, Rio de Janeiro, Brasil. Acta Limnol. Brasil. **11**: 783–802.

Hongve, D., Riise, G., and Kristiansen, J.F. 2004. Increased colour and organic acid concentrations in Norwegian forest lakes and drinking water — a result of increased precipitation? Aquat. Sci. **66**(2): 231–238.

Hu, C.M., Muller-Karger, F.E., and Zepp, R.G. 2002. Absorbance, absorption coefficient, and apparent quantum yield: a comment on common ambiguity in the use of these optical concepts. Limnol. Oceanogr. **47**(4): 1261–1267.

Kirschner, A.K.T., and Velimirov, B. 1997. A seasonal study of bacterial community succession in a temperate backwater system, indicated by variation in morphotype numbers, biomass, and secondary production. Microb. Ecol. **34**(1): 27–38.

Laybourn-Parry, J., Henshaw, T., Jones, D.J., and Quayle, W. 2004. Bacterioplankton production in freshwater Antarctic lakes. Freshw. Biol. **49**(6): 735–744.

Lindell, M.J., Granéli, W., and Tranvik, L.J. 1995. Enhanced bacterial growth in response to photochemical transformation of dissolved organic matter. Limnol. Oceanogr. **40**(1): 195–199.

Lindell, M.J., Granéli, W., and Bertilsson, S. 2000. Seasonal photoreactivity of dissolved organic matter from lakes with contrasting humic content. Can. J. Fish. Aquat. Sci. **57**(5): 875–885.

McCabe, S.K., and Cyr, H. 2006. Environmental variability influences the structure of benthic algal communities in an oligotrophic lake. Oikos, **115**(2): 197–206.

Moran, M.A., and Zepp, R.G. 1997. Role of photoreactions in the formation of biologically labile compounds from dissolved organic matter. Limnol. Oceanogr. **42**(6): 1307–1316.

Motulsky, H.J. 2003. Prism 4 statistics guide — statistical analyses for laboratory and clinical researchers. GraphPad Software Inc., San Diego, Calif.

Pace, M.L., and Cole, J.J. 2002. Synchronous variation of dissolved organic carbon and color in lakes. Limnol. Oceanogr. **47**(2): 333–342.

Paul, A., Hackbarth, S., Vogt, R.D., Roder, B., Burnison, B.K., and Steinberg, C.E.W. 2004. Photogeneration of singlet oxygen by humic substances: comparison of humic substances of aquatic and terrestrial origin. Photochem. Photobiol. Sci. **3**(3): 273–280.

Reitner, B., Herndl, G.J., and Herzig, A. 1997. Role of ultraviolet-B radiation on photochemical and microbial oxygen consumption in a humic-rich shallow lake. Limnol. Oceanogr. **42**(5): 950–960.

Strome, D.J., and Miller, M.C. 1978. Photolytic changes in dissolved humic substances. Verh. Int. Ver. Limnol. **20**: 1248–1254.

Suhett, A.L., MacCord, F., Amado, A.M., Farjalla, V.F., and Esteves, F.A. 2004. Photodegradation of dissolved organic carbon in humic coastal lagoons (Rio de Janeiro, Brazil). *In* Proceedings of the XII Meeting of the International Humic Substances Society, São Pedro, SP, Brazil. EMBRAPA, Brasília, DF, Brazil. pp. 61–63.

Thomas, J.D. 1997. The role of dissolved organic matter, particularly free amino acids and humic substances, in freshwater ecosystems. Freshw. Biol. **38**(1): 1–36.

Thurman, E.M. 1985. Organic geochemistry of natural waters. Nijhof/Junk, Boston.

Tranvik, L.J., and Bertilsson, S. 2001. Contrasting effects of solar UV radiation on dissolved organic sources for bacterial growth. Ecol. Lett. **4**(5): 458–463.

Stream ecosystems respond to riparian invasion by Japanese knotweed (*Fallopia japonica*)

Antoine Lecerf, Denise Patfield, Anatole Boiché, Miira P. Riipinen, Eric Chauvet, and Michael Dobson

Abstract: There are growing concerns about the rapid spread of exotic plants into riparian zones, yet little information is currently available on their influence on stream ecosystems. This study assessed the impact of riparian invasion by Japanese knotweed (*Fallopia japonica*), an aggressive invader, on leaf litter breakdown and its associated biota (aquatic hyphomycete fungi and benthic invertebrates) in heterotrophic, low-order streams in The Pennines (England) and the Pyrenees (France). Our results suggest that leaf consumers (aquatic hyphomycetes and invertebrate shredders) can readily use knotweed leaf litter even in stream sites where it was not previously present. However, aquatic hyphomycete and invertebrate assemblages differed between stream sites with and without knotweed. Leaf litter breakdown rate and relative abundance of large invertebrate shredders (mainly Trichoptera) were enhanced in the Pyrenean invaded site, whose channel contained a high proportion of knotweed leaf litter, whereas no such effects were observed in The Pennines, possibly because of the less extensive knotweed invasion. Alteration of riparian vegetation by plant invaders could therefore increasingly influence instream community and ecological functions as the severity of invasion rises.

Résumé : En dépit des préoccupations majeures posées par la prolifération rapide de plantes exotiques dans les zones riveraines, il existe actuellement peu de données concernant les conséquences écologiques sur les cours d'eau. Dans cette étude, nous avons évalué l'effet de la renouée du Japon (*Fallopia japonica*), une plante éminemment envahissante, sur la décomposition des feuilles et les organismes biologiques associés (hyphomycètes aquatiques et invertébrés benthiques) dans des petits cours d'eau hétérotrophes de la région des Pennines (Angleterre) et des Pyrénées (France). Nos résultats suggèrent que les consommateurs de feuilles (hyphomycètes aquatiques et invertébrés déchiqueteurs) peuvent aisément utiliser la litière de renouée, même au sein des tronçons de cours d'eau où elle n'était pas présente auparavant. Cependant, les assemblages d'hyphomycètes aquatiques et d'invertébrés diffèrent entre les tronçons de cours d'eau avec et sans renouée du Japon. La vitesse de décomposition des litières et l'abondance relative des invertébrés déchiqueteurs de grande taille (principalement les Trichoptères) ont augmenté au niveau du site pyrénéen envahi où domine la litière de renouée. Ces résultats ne s'observent pas sur le site envahi des Pennines, peut-être en raison de la moindre ampleur de l'invasion par la renouée. Ainsi l'impact des plantes exotiques sur la structure et les fonctions écologiques des communautés aquatiques pourrait être en rapport avec l'intensité de l'invasion.

Introduction

Riparian vegetation strongly influences rivers (Cummins et al. 1989; Wallace et al. 1997; Naiman et al. 2005), and therefore any changes to its structure and composition will have corresponding effects on organisms and ecological processes within the stream channel (e.g., Bärlocher and Graça 2002; Kennedy and Hobbie 2004; Lecerf et al. 2005). Riparian vegetation provides leaf litter as a primary energy supply to most forested low-order streams (Cummins et al. 1989; Wallace et al. 1997). Aquatic hyphomycete fungi and benthic invertebrates rely heavily on leaf accumulations as both food and habitat (Cummins et al. 1989; Bärlocher 1992; Graça 2001). In turn, aquatic hyphomycetes and shredder invertebrates (leaf consumers) play an essential role in the breakdown of leaf litter, a key ecosystem-level process ensuring the transfer of leaf carbon and nutrients toward higher trophic levels (Bärlocher 1992; Gessner et al. 1999; Graça 2001). Besides being controlled by the activity of leaf consumers, litter breakdown rate is also regulated intrinsically

Received 6 November 2006. Accepted 15 May 2007. Published on the NRC Research Press Web site at cjfas.nrc.ca on 18 September 2007.
J19645

A. Lecerf,[1,2] A. Boiché,[3] and E. Chauvet. Laboratoire d'écologie fonctionnelle – EcoLab, Centre National de la Recherche Scientifique (CNRS), University of Toulouse 3, National Polytechnic Institute of Toulouse, 29 rue Jeanne Marvig, 31055 Toulouse CEDEX, France.
D. Patfield, M.P. Riipinen,[4] and M. Dobson.[5] Department of Environmental and Geographical Sciences, Manchester Metropolitan University, Chester Street, M1 5GD Manchester, United Kingdom.

[1] Corresponding author (e-mail: Antoine.Lecerf@ubc.ca).
[2] Present address: Department of Forest Sciences, The University of British Columbia, Vancouver, BC V6T 1Z4, Canada.
[3] Present address: Laboratoire Interations Ecotoxicologie, Biodiversité et Ecosystemes, CNRS, University of Metz, 2 avenue du Géneral Delestraint, 57070 Metz, France.
[4] Present address: APEM Ltd. Aquatic Scientists, Unit A17 Riverview, Vale Road, Heaton Mersey, Stockport, SK4 3GN, United Kingdom.
[5] Present address: Freshwater Biological Association, The Ferry Landing, Far Sawrey, Ambleside, Cumbria, LA22 0LP, United Kingdom.

doi:10.1139/F07-092

by the quality of litter, which varies greatly among plant species (Gessner and Chauvet 1994; Lecerf et al. 2007).

Japanese knotweed (*Fallopia japonica* (Houtt.) Dcne.; syn. *Polygonum cuspidatum* Sieb. & Zucc.; syn. *Reynoutria japonica* Houtt.) originates from East Asia and was introduced to Europe and North America in the 1800s, mainly for ornament. Since then, this species and its congenerics (chiefly, *Fallopia sachalinensis* and *Fallopia × bohemicum*) have been among the most successful plant invaders ever known, becoming widespread in these continents and, more recently, in Oceania (Child and Wade 2000; Weston et al. 2005). Japanese knotweed is an atypical herbaceous plant, being easily distinguished by the gigantic size of its bamboo-like stems (>3 m tall) and the large, deciduous, heart-shaped leaves inserted on the stem by a short stalk (Beerling et al. 1994; Child and Wade 2000). Its rapid spread in the form of dense monospecific stands is ensured by long rhizomes (10–20 m) and a strong competitive ability (Pyšek and Prach 1993; Beerling et al. 1994; Weston et al. 2005).

The detrimental impacts of exotic plants, including Japanese knotweed, invading riparian zones are currently widely appreciated (Pyšek and Prach 1993; Planty-Tabacchi et al. 1996; Tickner et al. 2001), but little is known about their impacts upon the river itself. Animals associated with detritus breakdown could be affected by the alteration of riparian plant communities following knotweed invasion (Maerz et al. 2005). Furthermore, since knotweed produces a series of novel secondary compounds with antimicrobial properties (Beerling et al. 1994; Weston et al. 2005), fungal decomposers could also be susceptible to its invasion along streams. Additionally, litter dynamics in streams could be impaired by the high input rate of leaf litter representing a poor-quality food resource for leaf consumers (Beerling et al. 1994; Dangles et al. 2002). Lastly, it is questionable whether the native leaf consumers can adapt to knotweed leaf litter, because of a lack of coevolutionary history with exotic invaders.

The present study was designed to assess the possible consequences of Japanese knotweed invasion into riparian zones for the composition of leaf standing crop in streams and therefore the quality of food supply to aquatic consumers, the attributes of stream fungal and invertebrate assemblages, and the rate of leaf litter breakdown. For this purpose, we selected stream sites both with and without knotweed establishment in the riparian zone at two European locations. We also compared knotweed, as a nonindigenous species, with a native riparian tree (English oak, *Quercus robur* L.) with slow decomposing leaf litter, in terms of initial quality, breakdown rate, and colonization by aquatic hyphomycetes and invertebrates.

Materials and methods

The study sites

The experiment was carried out in The Pennines, north-central England (53°22'N, 1°49'W; 220–230 m above sea level (a.s.l.)) and the piedmont of the Pyrenees, southwestern France (42°80'N, 0°35'E; 535–580 m a.s.l.). Stream sites were low-order (2–3) reaches with wooded riparian zones and were free of conspicuous anthropogenic stresses. A reference and an invaded site, each approximately 100 m in length, were selected at each location. The reference sites were selected for absence of Japanese knotweed establishment on the banks from the study reach to the source and for their proximity to the paired invaded sites. The site pairs consisted of two adjacent streams (0.5 km apart) immediately upstream their confluence in The Pennines. In the Pyrenees, we selected an upstream and downstream reach 1.5 km apart on a single stream, the upper limit of the knotweed invasion being separated by 0.5 km from the lower limit of the upstream reference site.

Japanese knotweed formed characteristic dense stands in which few other species, mainly trees and shrubs, coexisted. The invaded sites visually differed in the size and occurrence of knotweed stands in riparian zones. In The Pennines, knotweed was present as small clumps (area <20 m^2; mean width 1 m, range 0.5–2 m) appearing recurrently along most the stream. Thus, about 40% of the sampling site was bordered by knotweed stands on at least one stream bank. In the Pyrenees, knotweed overwhelmed the understorey vegetation in riparian zones, with almost contiguous stands forming a 1 km long strip (mean width 3 m, range 0.5–12 m) along a 1 km stretch of both stream banks.

Site description

Species composition and diversity of leaf inputs to streams were monitored in the autumn by collecting 10 naturally accumulated leaf packs in the experimental reaches (Lecerf et al. 2005). These were then pooled to provide approximately 5 L of leaf material. Leaves were washed with tap water, sorted, oven-dried at 105 °C for 48 h, and weighed by species. Leaf species were then assigned to three categories — fast-, medium-, or slow-decomposing — according to their breakdown rate in streams as determined in the literature (Webster and Benfield 1986; Gessner and Chauvet 1994; Lecerf et al. 2007) and from personal observations. Following Dangles et al. (2002), Japanese knotweed leaf litter was assigned to the slow-decomposing category. As the timing of litter fall can differ among plant species, natural leaf packs were sampled on two occasions: early (25 October in France and 17 November in UK) and late (30 November in France and 22 December in UK) autumn.

Water chemistry was monitored on the six dates when leaf packs were added and then retrieved from the streams (see below). Temperature, pH, conductivity, and dissolved oxygen concentration were measured in the field, and filtered water samples were used to determine alkalinity and the concentration of orthophosphate, nitrate, and ammonium following colorimetric standard methods (APHA 1998).

Leaf bag experiment

Freshly fallen leaves of English oak and Japanese knotweed were collected near the study sites in each location. Oak was selected to represent the native plant species given its importance in the riparian community of the study regions and elsewhere in Europe. Oak was also chosen because its leaf litter decomposes at a similar rate to knotweed (Dangles et al. 2002), therefore avoiding sampling bias of leaf-colonizing biota due to different residence time and leaf decomposition stage in streams. The data of Gessner and Chauvet (1994) on leaf litter chemistry and breakdown rate of native plant species from the Pyrenees were included in this study for further comparison with knotweed.

Five grams (±0.05, with exact mass recorded) of air-dried leaves were introduced into 10 mm plastic mesh bags directly after the leaves had been wetted using a spray bottle to prevent breakage during handling. Twenty bags of each leaf species were introduced into each stream site in January 2004 in the Pyrenees and in January 2005 in The Pennines. The leaf bags were secured in streams by nylon lines anchored to iron bars driven into streambed sediments.

Four extra leaf bags of each species from each of the two regions were kept in the laboratory to determine the initial dry mass:ash-free dry mass (AFDM) ratio. In addition, leaf samples of both species were used to determine the content in carbon and nitrogen (CHN-analyser, NA 2100, CE Instruments), phosphorus (ascorbic acid colorimetric method after ash digestion in HCl as described by Flindt and Lillebø 2005), and lignin and cellulose (acid–detergent fibre procedure as described by Gessner 2005*a*). Samples were ground using a Culatti micro hammer mill with a 0.5 mm mesh prior to the analyses.

Four bags of each leaf species were collected from each stream site after 11, 24, 34, 61, and 88 days in the Pyrenees and after 7, 27, 53, 81, and 109 days in The Pennines. Leaf bags were stored individually in plastic ziplock bags and transported to the laboratory in an ice box. Leaves were washed individually to remove sediments and exogenous organic matter along with invertebrates, which were collected in a 0.5 mm screen sieve and then preserved in 70% ethanol until processing. Two sets of five 12 mm diameter discs were cut from five leaves, avoiding the central veins; one set was frozen at −18 °C until processing for ergosterol extraction, and the other was kept fresh to induce fungal sporulation. Fungal samples were not taken from the leaf bags collected after 7 days in The Pennines because of nonavailability of laboratory equipment. The remaining leaf litter was dried at 105 °C for 48 h and weighed to the nearest 0.01 g and ground. Portions of leaf material of about 500 mg were ashed at 550 °C for 4 h and weighed to determine the organic matter content. The leaf mass remaining in bags was expressed as the ratio between final and initial leaf litter AFDM.

The five fresh leaf discs were placed in 100 mL Erlenmeyer flasks filled with 25 mL filtered (Whatman glass fibre GF/F) stream water. Production of fungal asexual spores was stimulated by gentle shaking on an orbital path at 10 °C for 48 h. Thereafter, spore suspensions were transferred into 50 mL polyethylene centrifuge tubes, the flask and discs were rinsed with distilled water to collect spores no longer in suspension, and the volume was adjusted to 35 mL with 2 mL of 37% formalin and distilled water as required. The discs were then oven-dried and weighed to the nearest 0.1 mg.

Processing of aquatic hyphomycetes

Spore suspensions were supplied with 1 mL of Triton X-100 (0.01% solution) and stirred gently to ensure uniform distribution of spores. Aliquots of 5 mL were filtered through a membrane filter (5 µm pore size), and the spores on the filter were stained with 0.1% trypan blue in 60% lactic acid. Two hundred spores per sample were counted and identified to species under the microscope (× 320). Spore production was calculated as the number of spores released per milligram leaf litter AFDM per day.

The frozen leaf discs were used to determine ergosterol content as a measure of fungal biomass (Gessner 2005*b*). The extraction and quantification method is based on solid-phase extraction and high-performance liquid chromatography (adapted from Gessner 2005*b*, with cartridges Waters Oasis HLB, 60 mg, 3 cc). Briefly, leaf material was freeze-dried, weighed to the nearest 0.1 mg, and then lipids were extracted with alkaline ethanol at 80 °C for 30 min. Fungal biomass in leaves was expressed as ergosterol mass per milligram leaf litter AFDM.

Processing of invertebrates

Invertebrates were counted and identified to the lowest practicable level, mostly genus or species for non-Diptera insects and family or order for Diptera and some non-insect taxa (see Supplemental Tables 1 and 2, available online from the NRC Data Depository[6]). Invertebrates assigned to the shredder group were dried (60 °C, 48 h) and weighed to the nearest 0.1 mg. Shredder biomass in leaf bags was expressed per gram AFDM of leaf litter remaining.

Among shredders, we distinguished large species from small species on the basis on their maximum potential body size, anticipating different responses to Japanese knotweed invasion of these two groups (cf. Friberg 1997; Whiles and Wallace 1997). To test this hypothesis, we calculated the odds for having large shredders (as the ratio of large to small shredder abundance) at each site. Odds ratio for invaded:reference sites significantly different from 1 (according to Fisher's exact test, two-tail) indicated differences in large shredder abundance between reference and invaded sites. In the present study, the small shredder species consisted of Plecoptera, while the large shredder species consisted of the case-bearing Trichoptera, *Tipula* (Diptera), and *Gammarus* (Crustacea: Amphipoda).

Statistical analyses

The total number of leaf species found in natural accumulations in streams over the two sampling dates and the Shannon–Wiener diversity index, calculated from percent occurrence (by dry mass) of leaf species at each sampling date, were used as indicators of riparian vegetation diversity (Laitung and Chauvet 2005; Lecerf et al. 2005). Invertebrate taxon richness in leaf bags for each leaf species and stream site was estimated using the individual-based rarefaction method in EcoSim (Gotelli and Entsminger 2006) to correct for difference in number of individuals counted (Gotelli and Colwell 2001). This correction was not required for fungal species richness, as we identified the same number of spores on each occasion (i.e., 200 spores).

Exponential breakdown rate k of English oak and Japanese knotweed in each site was calculated from the proportion of leaf litter AFDM remaining in bags (R) over the time of exposure (t in days) using a nonlinear regression procedure ($R = R_0 \times e^{-kt}$, where R_0 is the initial proportion of leaf

---

[6] Supplementary data for this article are available on the journal Web site (cjfas.nrc.ca) or may be purchased from the Depository of Unpublished Data, Document Delivery, CISTI, National Research Council Canada, Building M-55, 1200 Montreal Road, Ottawa, ON K1A 0R6, Canada. DUD 5205. For more information on obtaining material refer to cisti-icist.nrc-cnrc.gc.ca/irm/unpub_e.shtml.

Table 1. Characteristics of stream sites.

Parameters	The Pennines		Pyrenees	
	Reference	Invaded	Reference	Invaded
Temperature (°C)	6.7 (2.7–8.8)	7.0 (2.8–9.2)	6.1 (1.5–13)	6.2 (1.5–12.5)
pH	6.1 (5.2–6.6)	5.9 (5.1–6.5)	7.6 (7.4–7.8)	7.9 (7.5–7.9)
Conductivity ($\mu S \cdot cm^{-1}$)	143 (95–257)	97 (67–122)	66 (62–70)	80 (72–90)
Alkalinity ($mequiv. \cdot L^{-1}$)	0.07 (0.05–0.09)	0.06 (0.04–0.08)	0.75 (0.72–0.81)	1.05 (1.03–1.92)
O_2 ($mg \cdot L^{-1}$)	11.7 (10.1–13.5)	11.3 (9.8–12.6)	10.4 (9.9–10.8)	10.8 (10.5–11.1)
Phosphate ($\mu g\ P \cdot L^{-1}$)	<1*	<1*	9.6 (3.1–17.7)	11.1 (7.4–15.1)
Nitrate ($\mu g\ N \cdot L^{-1}$)	590 (447–644)	772 (628–858)	970 (760–1150)	1 020 (690–1480)

Note: Mean value (minimum–maximum) of water parameters determined during the leaf bag exposure ($n = 6$ sampling dates).
*Undetectable concentration.

litter AFDM in bags). The best estimates of k were reached when R_0 was not fixed a priori; however, 95% confidence interval indicated that calculated values of R_0 did not significantly differ from the theoretical value of 1.

Results from The Pennines and the Pyrenees were analysed separately because of differences in experimental design (i.e., sampling dates). Two-way multivariate analysis of variance (MANOVA) was used to test for differences in water chemistry across sampling dates and between reference and invaded sites. Leaf litter breakdown rates among combination treatments were compared using analysis of covariance (ANCOVA), with ln-transformed R as the response variable, time of exposure as the covariate, and site type and leaf species as categorical factors; both covariate and categorical factors were fully crossed following the general linear model procedure. Similarly, we used a general linear model to test for differences in fungal spore production, fungal biomass, invertebrate abundance, and shredder biomass in bags among sampling dates, site types, and leaf species. We used analysis of variance (ANOVA) with time as a categorical factor when response variables did not follow a linear trend with time. Otherwise, time was used as covariate in ANCOVA. STATISTICA 6.0 was used to perform these analyses (StatSoft 2001).

Differences in bag-associated assemblages of aquatic hyphomycetes and invertebrates between leaf species and site types in each location were assessed using canonical analyses of principal coordinates (CAP), a flexible and robust eigenvalue-based method consisting of a metric multidimensional scaling followed by a canonical discriminant analysis (Anderson and Willis 2003; Nikolcheva and Bärlocher 2005). Compared with traditional constrained ordination methods (e.g., canonical correspondance analysis), CAP has the advantage that the most appropriate distance or dissimilarity measures can be chosen. Here we used the Hellinger distance, which is sensitive to unimodal patterns of taxon abundance across ecological gradients and give reasonable weight to rare taxa (Legendre and Gallagher 2001). CAP ordination was performed using the original application program written by M.J. Anderson (2004).

When CAP indicated significant differences in aquatic hyphomycetes and invertebrates between leaf species and site types, we then looked for the taxa responsible for multivariate patterns at each location using the IndVal method (Dufrêne and Legendre 1997). Accordingly, the indicator value of the taxon i in the sample of group j, or IndVal$_{ij}$ (in %), was defined as the product of a measure of specificity (formally, $n_{ij}/n_{i\bullet}$ where n is the number of individuals) by a measure of fidelity (formally, $N_{ij}/N_{i\bullet}$, where N is the number of samples containing the taxon i). The significance of the taxon-to-group associations was tested by two resampling methods and was considered when the two tests give $p < 0.05$ (250 permutations; Dufrêne and Legendre 1997). In our study, the IndVal index was used to measure the strength of nonhierarchical association of aquatic hyphomycetes species and invertebrate taxa to site type (reference vs. invaded) or leaf species (oak vs. knotweed). Computation of the IndVal index and of the randomization testing procedure was performed using the program written by M. Dufrêne (biodiversite.wallonie.be/dgrne/sibw/outils/indval/home.html).

Results

Water characteristics

Streams were slightly acid (The Pennines) or circumneutral (Pyrenees) and displayed elevated nitrate concentrations in water (>500 $\mu g\ N \cdot L^{-1}$). Phosphate concentrations were higher in the Pyrenean stream than in the Pennine streams. Water chemistry varied across time in both locations (two-way MANOVAs: Wilks' $\lambda < 0.00001$, $p < 0.01$). It differed significantly between the reference and the invaded site in the Pyrenees (Wilks' $\lambda = 0.0002$, $p = 0.020$) but not in The Pennines (Wilks' $\lambda = 0.016$, $p = 0.213$). Notably, alkalinity was slightly higher in the invaded site in the Pyrenees (Table 1).

Leaf standing crop

All study sites supported a high diversity of leaves, with the species number ranging from 14 to 21 and the Shannon–Wiener index from 1.7 to 2.4. In early autumn, there were large amounts of fast-decomposing leaves in all streams, but more slowly decomposing species dominated at the later sampling date (Figs. 1*a*, 1*b*). In the Pyrenees, slow-decomposing leaves were quite rare at the reference site, whereas they were abundant in the invaded site, partly owing to the presence of Japanese knotweed leaf litter (Figs. 1*a*, 1*b*). Knotweed contributed <10% dry mass of leaf standing crop in The Pennines, whereas it represented approximately 30%–50% of leaf standing crop in the Pyrenees. In the latter location, native hazel (common hazel, *Corylus avellana* L.), which produces medium-decomposing leaves, contributed up

Fig. 1. Composition of leaf standing crop in the Pennine and the Pyrenean streams (Ref, reference stream; Inv, invaded stream) during early (*a*) and late autumn (*b*). The bars represent the relative amount (by dry mass) of each leaf decomposition category (solid bars, slow; grey bars, medium; open bars, fast). Japanese knotweed (*Fallopia japonica*) (hatched bars) is classified as slow-decomposing.

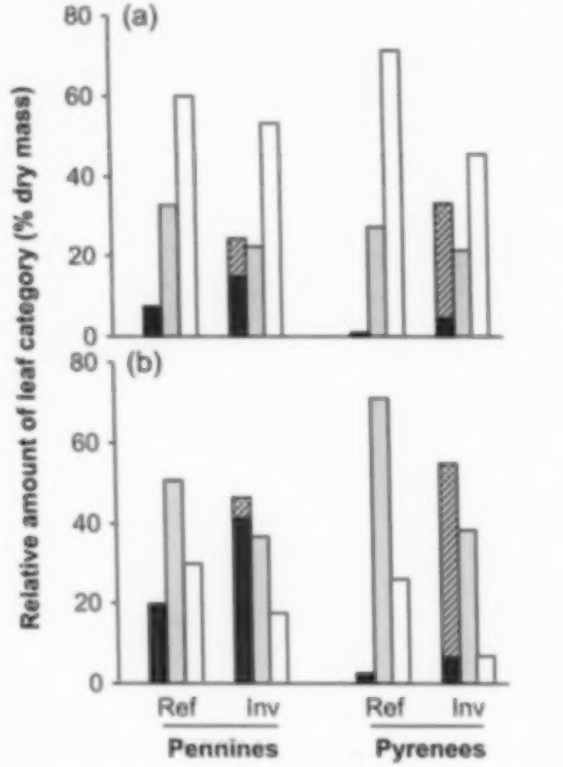

to 64% of leaf standing crop in the reference site but <20% in the invaded site.

Leaf litter quality and breakdown rate

English oak and Japanese knotweed leaf litter used in this study differed in chemistry, with carbon and lignin content being higher in oak than in knotweed (Table 2). In addition, knotweed leaf litter had higher nitrogen and phosphorus contents than oak in The Pennines, but not in the Pyrenees (Table 2). Oak leaf litter contained more lignin and phosphorus in The Pennines than in the Pyrenees (Table 2). Overall, oak and knotweed leaf litter breakdown rates were comparable in The Pennines (ANCOVA: $F = 1.1$, $p = 0.152$), while knotweed disappeared slightly more rapidly than oak in the Pyrenees (ANCOVA: $F = 5.7$, $p = 0.019$; Fig. 2*a*). Within a broad spectrum of leaf litter quality and decomposability, breakdown rates of leaves, including knotweed, and lignin content were well fitted to a power relationship (Fig. 2*b*).

Irrespective of leaf species used in bags, leaf litter breakdown rates were almost the same in the reference and invaded sites in The Pennines (ANCOVA: $F = 0.1$, $p = 0.747$), whereas they were significantly higher in the invaded site than in the reference site in the Pyrenees (ANCOVA: $F = 21.5$, $p <$ 0.001; Fig. 2*a*). Overall, leaf litter disappeared faster in the Pennine streams than in the Pyrenean stream (Fig. 2*a*).

Table 2. Initial chemistry of Japanese knotweed (*Fallopia japonica*) and English oak (*Quercus robur*) leaf litter used in mesh bags.

Constituents	The Pennines		Pyrenees	
	Oak	Knotweed	Oak	Knotweed
Carbon	53.9b	47.4a	53.8b	47.6a
Lignin	20.8c	13.7a	17.8b	13.4a
Cellulose	11.2a	12.8a	12.0a	13.1a
Nitrogen	0.97a	1.82b	0.92a	0.99a
Phosphorus	0.055b	0.119c	0.042a	0.044a

Note: Identical letter indicates no significant difference (one-way analysis of variance followed by Tukey's post hoc test: $p > 0.05$). Mean value ($n = 4$ replicates) of initial concentration of leaf litter constituents (by percent dry mass) were determined for oak and knotweed within each location.

Fig. 2. (*a*) Breakdown rate (*k*) of English oak (*Quercus robur*) and Japanese knotweed (*Fallopia japonica*) (= Knot) leaf litter determined in a reference (open bars) and an invaded (shaded bars) stream site in The Pennines and the Pyrenees. (*b*) Leaf litter breakdown rate as a function of lignin concentration. Values for oak (open circles) and knotweed (shaded triangles) are, respectively, from the reference and the invaded sites of this study, whereas other data (open squares) are from Gessner and Chauvet (1994).

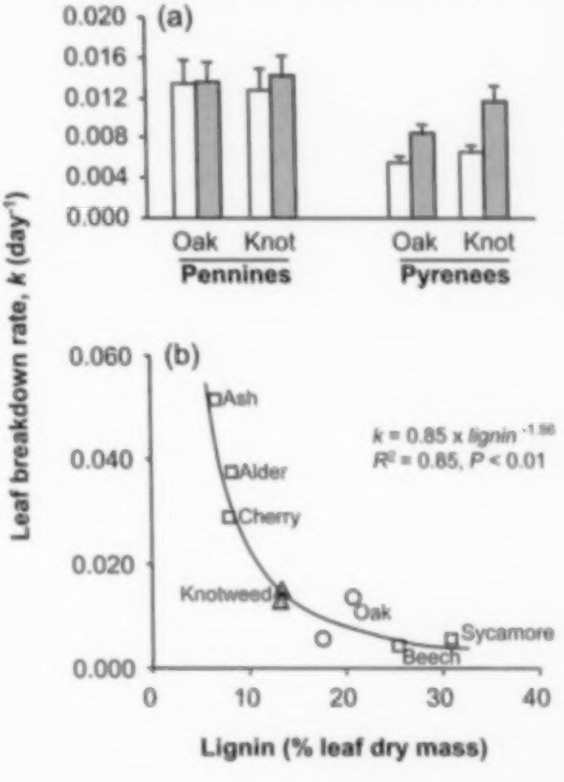

Aquatic hyphomycete assemblages

Spore production of aquatic hyphomycetes varied according to time in both locations (three-way factorial ANOVAs:

Fig. 3. Spore production (*a*, *b*) and biomass as determined by ergosterol content (*c*, *d*) of aquatic hyphomycetes on English oak (*Quercus robur*) (circles) and Japanese knotweed (*Fallopia japonica*) (triangles) leaf litter in a reference (open symbols) and an invaded (shaded symbols) stream site in The Pennines (*a*, *c*) and the Pyrenees (*b*, *d*). Mean and 1 standard error are represented.

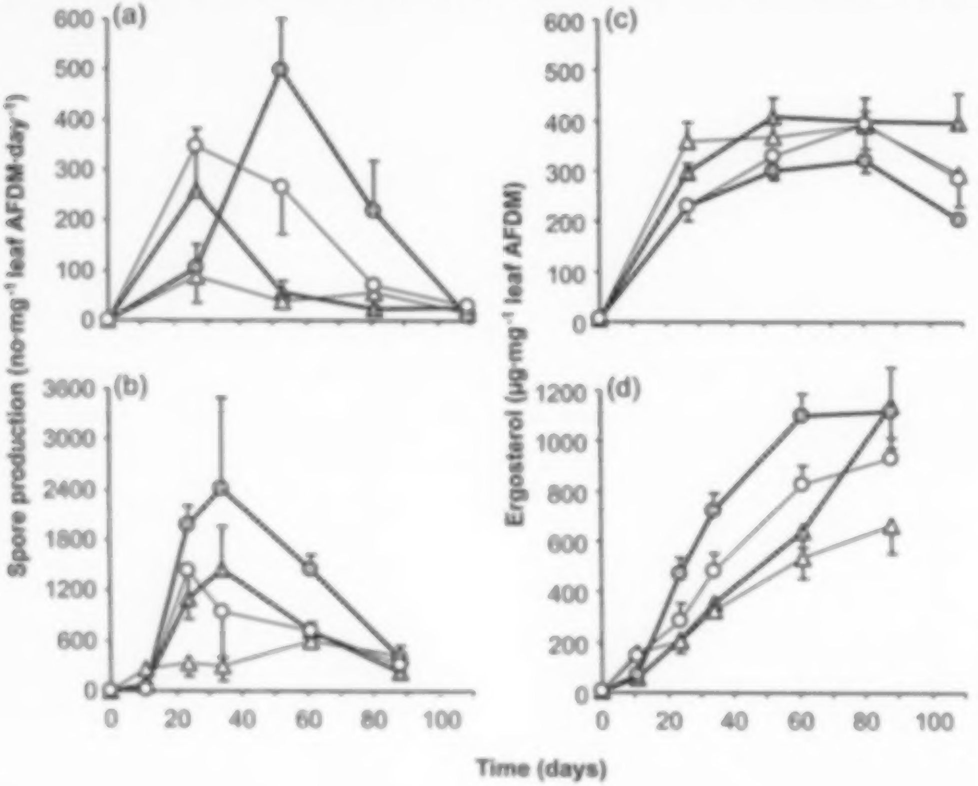

$p < 0.01$; Figs. 3*a*, 3*b*). There was a significant difference between leaf species at all times in The Pennines ($p = 0.015$; Fig. 3*a*) and at certain times in the Pyrenees (leaf species-by-time interaction: $p < 0.001$; Fig. 3*b*). Spore production of aquatic hyphomycetes reached higher values on English oak than on Japanese knotweed (Figs. 3*a*, 3*b*). Spore production on a given leaf species was also higher in the invaded site than in the reference site in both locations (Figs. 3*a*, 3*b*), although the difference was significant in the Pyrenees only ($p = 0.005$). The interactions between leaf species and site type and among time, leaf species, and site type were not significant in either location ($p > 0.12$), yet a peak of spore production was observed in all cases except for knotweed in the reference sites (Figs. 3*a*, 3*b*). There was about a sixfold higher spore production in the Pyrenean stream than in the Pennine streams.

Fungal biomass on leaf litter as determined by ergosterol content increased with time (three-way factorial ANOVAs: $p < 0.001$), and it differed between leaf species ($p < 0.001$), with higher fungal biomass on Japanese knotweed in The Pennines and on English oak in the Pyrenees (Figs. 3*c*, 3*d*). No significant difference between site types was observed in The Pennines (site type only or in interaction with any factors: $p > 0.14$), while higher biomass on leaf litter was found in the Pyrenean invaded site from 20 days (ANOVA, site type-by-time interaction: $p = 0.001$; Fig. 3*d*). Fungal biomass was approximately more than two times higher in the Pyrenees than in The Pennines.

There were more fungal species on Japanese knotweed than on English oak in three of the four sites (Table 3). Irrespective of the leaf species colonized, rare species (relative abundance <0.1%) were more numerous in the invaded site than in the reference site in the Pyrenees (Table 3). Fungal assemblages on leaves were more diverse in the Pyrenees than in The Pennines, with rare species contributing strongly to this difference (Table 3). Whatever the location, assemblages of aquatic hyphomycetes differed among combination treatments (CAP canonical permutation tests, 9999 permutations: $p < 0.01$). The first factorial plane of the CAP analyses separated the reference from the invaded site and, within each site type, oak from knotweed leaves (Figs. 4*a*, 4*c*). Consistent with CAP results, the IndVal method indicated significant associations (randomization tests, 250 permutations: $p < 0.05$) of some fungal species with either reference or invaded site or with either oak or knotweed leaf litter (see Appendix A for details). There were more significant associations in the Pyrenees than in The Pennines, and in both locations most associations were with oak; however, two and four taxa were significantly associated with knotweed in The Pennines and the Pyrenees, respectively.

Table 3. Numbers of aquatic hyphomycete species and invertebrate taxa found in mesh bags of each leaf species (Japanese knotweed (*Fallopia japonica*) and English oak (*Quercus robur*)) exposed in each stream type in The Pennines and the Pyrenees.

	Reference		Invaded	
	Oak	Knotweed	Oak	Knotweed
Hyphomycetes				
The Pennines	19 (2)	18 (2)	16 (2)	18 (1)
Pyrenees	30 (9)	35 (13)	32 (13)	33 (17)
Invertebrates				
The Pennines	25	21	22	20
Pyrenees	27	22	25	27

Note: The number of rare fungal species (relative abundance < 0.1%) is given in parentheses. Individual-based rarefaction curves were used to determine taxonomic richness of invertebrates in virtual samples of 300 and 600 individuals in The Pennines and the Pyrenees, respectively.

Invertebrate assemblages

Abundance of invertebrates in leaf bags in the Pyrenees changed with time (three-way factorial ANOVA: $p < 0.001$) and was slightly lower in the invaded site ($p = 0.075$; data not shown). Variability in invertebrate abundance remained mostly unexplained in The Pennines (all effects: $p > 0.10$). Higher abundance was found in the Pyrenees (mean value = 44.7 individuals·bag^{-1}) than in The Pennines (25.8 individuals·bag^{-1}). Biomass of shredder invertebrates increased linearly with time from origin (Figs. 5*a*, 5*b*). Hence, we compared individual line slopes by using an ANCOVA model without comparing intercepts. In The Pennines, change in shredder biomass occurred more rapidly in English oak leaf bags than in Japanese knotweed leaf bags ($F = 23.9$, $p < 0.001$; Fig. 5*a*), whereas no such difference was observed in the Pyrenees ($F = 0.17$, $p = 0.68$). Irrespective of the leaf species colonized, there was a steeper increase in shredder biomass in the invaded site than in the reference site in the Pyrenees ($F = 5.8$, $p = 0.028$), the difference being significantly more pronounced in oak leaf bags (three-way interaction: $F = 11.2$, $p = 0.004$; Fig. 5*b*). In contrast, there was no significant effect of site type on shredder biomass in The Pennines ($p > 0.60$).

Whatever the location, rarefied taxonomic richness of invertebrates in the reference sites was higher in English oak leaf bags than in Japanese knotweed leaf bags, while this effect was not consistent in the invaded sites (Table 3). Oak supported a more diverse invertebrate assemblage in the reference sites than in the invaded sites. In the Pyrenees, rarefied richness of invertebrates in knotweed leaf bags was higher in the invaded site than in the reference site (Table 3). Whatever the location, assemblages of invertebrates differed among site type-per-leaf species combination treatments (CAP canonical permutation tests, 9999 permutations: $p < 0.01$). However, this was mainly due to differences in invertebrate assemblages between site types (Figs. 4*b*, 4*d*), and the effect of leaf species per se tested by an additional CAP was not significant at either location ($p = 0.10$ and $p = 0.93$ in The Pennines and the Pyrenees, respectively). Consistent with the CAP results, the IndVal method indicated that there were significant associations (randomization tests, 250 permutations: $p < 0.05$) of some invertebrate taxa to either reference or invaded site (see Appendix A for details). In both locations, Chironomidae and Simuliidae were most closely associated with the reference sites. Among the taxa associated with the invaded sites were shredder invertebrates, two small-body-sized species in The Pennines (Plecoptera: *Brachyptera risi* (Taeniopterygiidae) and *Amphinemura sulcicollis* (Nemouridae)) and two large-body-sized species in the Pyrenees (Trichoptera: *Potamophylax latipennis* (Limnephilidae) and *Sericostoma personatum* (Sericostomatidae)).

Odds for having large shredders in leaf bags were similar at the two reference sites (0.080 and 0.074 in The Pennines and the Pyrenees, respectively), but odds for invaded sites differed between regions (0.047 and 0.256 in The Pennines and the Pyrenees, respectively). Moreover, there was a significantly higher occurrence of large shredders in the invaded site than in the reference site in the Pyrenees (odds ratio = 3.34, $p < 0.001$), whereas no such difference was observed in The Pennines (odds ratio = 0.59, $p = 0.0653$).

Discussion

Japanese knotweed leaf litter disappears at a rate comparable with that of common native riparian shrubs or trees that produce slow-decomposing leaf litter (e.g., oak and beech), which is consistent with the quantity of lignin in its leaf tissues (Gessner and Chauvet 1994). The absence of a marked difference in breakdown rate between knotweed and native, slow-decomposing leaf litter stresses the ability of resident aquatic leaf consumers to readily use exotic detritus sources (Graça et al. 2001). Coevolutionary history between riparian plants and aquatic biota is not required to ensure effective trophic dynamics in streams (Thompson and Townsend 2003). This idea is also supported by the absence of leaf substrate specificity of aquatic hyphomycetes in previous studies (Laitung and Chauvet 2005; Nikolcheva and Bärlocher 2005) and by the worldwide distribution of numerous dominant fungal species, but not of the vascular plant species they consume (Bärlocher 1992). Aquatic hyphomycete species may, however, differ in their ability to grow on a given leaf species, resulting in difference in spore production and structure (i.e., species relative abundance) of leaf-associated fungal assemblages between substrate types as observed in the present and previous studies (Gulis 2001; Graça et al. 2002). Similarly, some investigators have found that invertebrates may be sensitive to some traits of the leaf litter they colonize (Richardson et al. 2004; LeRoy et al. 2006), but the similar invertebrate assemblages in oak and knotweed leaf bags in this study suggest no such effect.

Consequences of Japanese knotweed invasion on stream food webs cannot be fully evaluated from observing its short-term exploitation by aquatic biota in comparison with native leaf litter. Indeed, the structure and dynamics of food webs involve a long-term adjustment process of the ecosystem to postinvasion conditions (Belnap et al. 2005; Hoffmeister et al. 2005). Thus, the occurrence of a peak of fungal spore production on knotweed in the invaded sites but not in the references sites may be due to the selection for the fungal species best adapted to growth on knotweed leaf litter. This is consistent with the idea that riparian vegetation is

Fig. 4. First factorial plane of canonical analyses of principal coordinates on aquatic hyphomycete (*a*, *c*) and invertebrate (*b*, *d*) assemblages in English oak (*Quercus robur*) (circles) and Japanese knotweed (*Fallopia japonica*) (triangles) leaf bags exposed in a reference (open symbols) and an invaded (shaded symbols) stream site in The Pennines (*a*, *b*) and the Pyrenees (*c*, *d*).

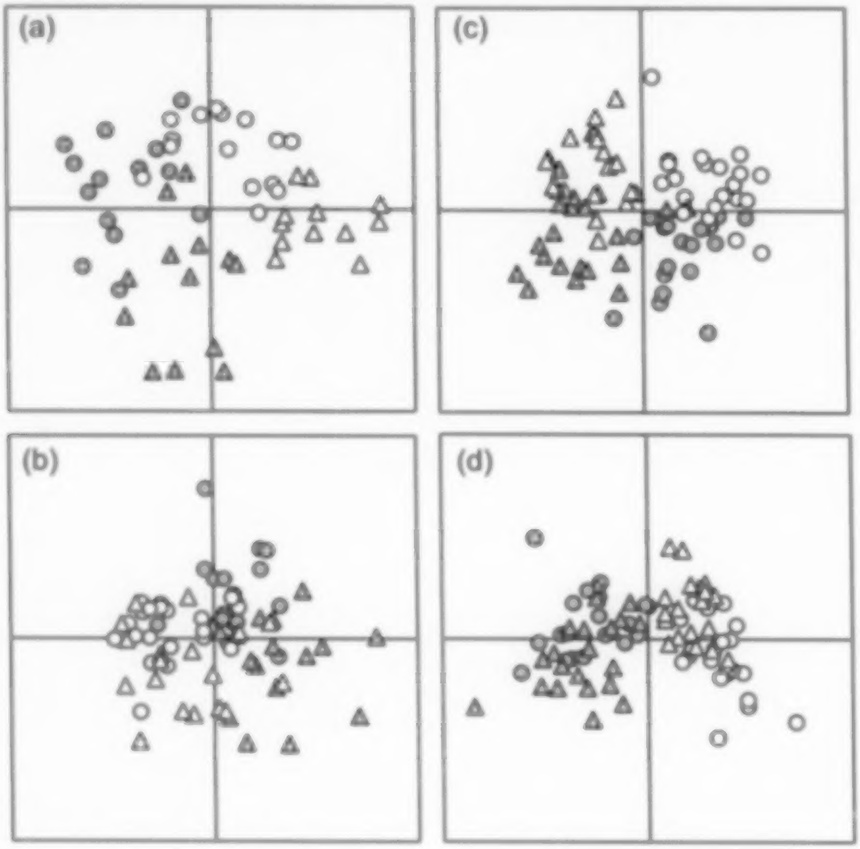

a major factor structuring aquatic hyphomycete assemblages at the stream level (Bärlocher and Graça 2002; Laitung and Chauvet 2005; Ferreira et al. 2006). Similarly, changed shredder assemblages caused by knotweed may partly be the result of selection for the taxa that are most efficient at exploiting a low-quality resource (Cummins et al. 1989; Stout et al. 1993).

In the Pyrenean invaded site, we suspect that change in composition of leaf litter inputs since Japanese knotweed establishment has benefited large shredder species, which in turn has accelerated the breakdown rate of the slow-decomposing leaves (Dangles et al. 2002; Jonsson et al. 2002). A similar causal cascade linking riparian vegetation type, large trichopteran shredders, and litter breakdown emerged from a study on a pine plantation that also produced a low quality leaf litter (Whiles and Wallace 1997). The large size and powerful mouthparts of large trichopteran shredders ensure they can consume sufficient quantities of low-quality litter to meet their nutritional requirements (Friberg and Jacobson 1999; Jonsson et al. 2002). Moreover, large shredders with long life cycles may benefit from slow-decomposing leaves, which remain abundant in streams until they complete their entire development (Cummins et al. 1989; Friberg 1997; Eggert and Wallace 2003). The dependence of large shredders on slow-decomposing leaves may also be explained by a certain degree of trophic specialization, making the late stages of some trichopteran species less prone to use alternative high quality resources, such as benthic algae and moss, than smaller shredders, such as some plecopterans (Dangles 2002).

The fact that leaf litter breakdown rate and odds for having large shredders in leaf bags did not vary across stream sites in The Pennines shows that Japanese knotweed invasion into riparian zones can have variable effects on stream ecosystems. An analogous discrepancy has been reported from the extensive literature dealing with effects of *Eucalyptus* plantations on litter breakdown and invertebrate assemblages in the Iberian Peninsula (Graça et al. 2002). While different shredder assemblages may conceivably differ in their susceptibility to altered riparian vegetation (Dangles et al. 2002), the absence of a stream functional response in the Pennine streams may be better explained by the relatively early stage of the knotweed invasion and hence its minor contribution to leaf standing crops. Alternatively, if evenness among leaf decomposing categories in leaf standing crops in autumn is important for the dynamics of shredder populations, as argued by Cummins et al. (1989), it is possible that the scarcity of slow-decomposing leaves in the Pyrenean streams prior to knotweed invasion had a limiting influence

Fig. 5. Shredder biomass in English oak (*Quercus robur*) (circles) and Japanese knotweed (*Fallopia japonica*) (triangles) leaf bags exposed in a reference (open symbols) and an invaded (shaded symbols) stream site in The Pennines (*a*) and the Pyrenees (*b*). Mean value and regression line (solid lines, oak; dashed lines, knotweed; thin lines, reference sites; thick lines, invaded sites) through the origin are represented.

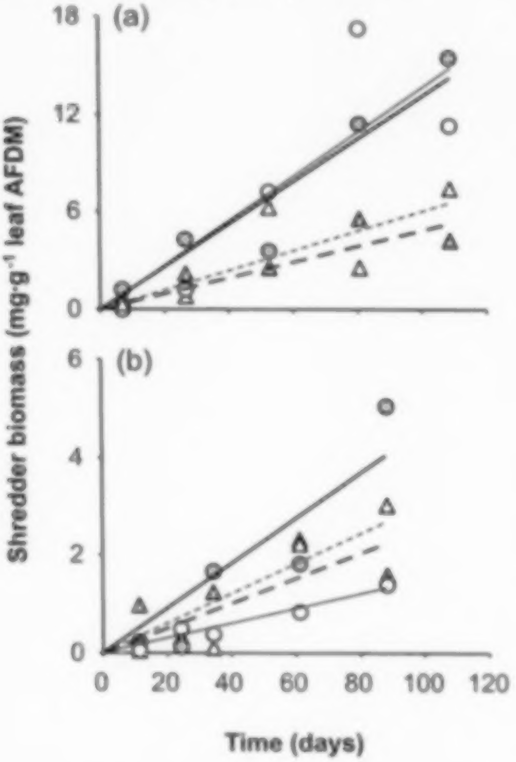

on the production of large shredders. This was not the case in The Pennines, because naturally occurring, slow-decomposing leaves were much more abundant and, hence, probably not limiting.

In this study, the most obvious consequence of Japanese knotweed invasion was the altered species composition of instream leaf standing crops during autumn, resulting in a reduction in average food quality available to aquatic consumers. This negative effect may be exacerbated by the high above-ground productivity of knotweed (Beerling et al. 1994), even though the decrease in food quality may partly be balanced by increased food quantity (Wallace et al. 1997). We feel that a dramatic enhancement of leaf input rate to the two invaded stream sites is unlikely, because either knotweed contributed a small proportion of leaf standing crop (in The Pennines) or it balanced the reduction of native hazel, which naturally contributes greatly to stream leaf input (in the Pyrenees). Whether food quality can compensate for quantity for aquatic consumers remains, however, a critical issue for understanding the consequence of changed riparian vegetation on stream invertebrates (Stout et al. 1993; Lecerf et al. 2005). Other possible consequences of knotweed invasion into riparian zones dominated by herbaceous and shrubby vegetation include the reduction of light available for primary producers because of the dense knotweed canopy and modification of benthic habitats owing to the loss of submerged root systems (e.g., Kennedy and Hobbie 2004).

To conclude, our study indicates that Japanese knotweed can alter the structure and dynamics of stream detritus food webs. Notably, knotweed leaf litter per se has the potential to strongly affect the assemblages and reduce spore production of aquatic hyphomycetes on leaves, which may have a cascading effect on higher consumers relying on stream fungi (Bärlocher 1992; Lecerf et al. 2005). However, knotweed invasion has unpredictable consequences on major ecosystem processes such as leaf breakdown as a result of either long-term adaptive response of stream biota to knotweed litter or a context-dependent effect of invasion determined by the existing structure and composition of the riparian vegetation and the realized extent of knotweed in the invaded community. Accordingly, we can predict that riparian invasion by exotic plants would have limited effects on streams if (*i*) plant invaders do not overwhelm the existing riparian vegetation and (*ii*) the long-term adjustment process of stream ecosystems to changed leaf litter inputs has not been not impaired by any other kinds of disturbance.

Acknowledgements

This research was supported by the European Commission through the Framework 5 programme (Rivfunction: contract EVK1-CT-2001-00088) and travel grants from the British–French cooperation programme ALLIANCE (ref. 07717ZD), administrated by the British Council and the EGIDE association (French agency for international mobility). We thank Sophie Manzi, Didier Lambrigot, and Boris Bracht for their technical assistance in France and Helen Cariss for the selection of sites in UK. Anne-Marie Planty-Tabacchi and Eric Tabacchi provided helpful advices during the experiment, and two anonymous reviewers improved the manuscript.

References

Anderson, M.J. 2004. CAP: canonical analysis of principal coordinates [online]. Available from www.stat.auckland.ac.nz/~mja/prog/CAP_UserNotes.pdf [accessed March 2007].

Anderson, M.J., and Willis, T.J. 2003. Canonical analysis of principal coordinates: a useful method of constrained ordination for ecology. Ecology, **84**: 511–525.

APHA. 1998. Standard methods for the examination of water and wastewater. 20th ed. American Public Health Association, Washington, D.C.

Bärlocher, F. 1992. The ecology of aquatic hyphomycetes. Springer-Verlag, Berlin Heidelberg, New York.

Bärlocher, F., and Graça, M.A.S. 2002. Exotic riparian vegetation lowers fungal diversity but not leaf decomposition in Portuguese streams. Freshw. Biol. **47**: 1123–1136.

Beerling, D.J., Bailey, J.P., and Conolly, A.P. 1994. *Fallopia japonica* (Houtt.) Ronse Decraene. J. Ecol. **82**: 959–979.

Belnap, J., Phillips, S.L., Sherrod, S.K., and Moldenke, A. 2005. Soil biota can change after exotic plant invasion: does this affect ecosystem processes? Ecology, **86**: 3007–3017.

Child, W., and Wade, M. 2000. The Japanese knotweed manual, the management and control of an invasive weed. Packard Publishing Limited, Chichester, UK.

Cummins, K.W., Wilzbach, M.A., Gates, D.M., Perry, J.B., and Taliaferro, W.B. 1989. Shredders and riparian vegetation. Bioscience, **39**: 24–30.

Dangles, O. 2002. Functional plasticity of benthic macroinvertebrates: implication for trophic dynamics in acid streams. Can. J. Fish. Aquat. Sci. **59**: 1563–1573.

Dangles, O., Jonsson, M., and Malmqvist, B. 2002. The importance of detritivore species diversity for maintaining stream ecosystem functioning following the invasion of a riparian plant. Biol. Invasions, **4**: 441–446.

Dufrêne, M., and Legendre, P. 1997. Species assemblages and indicator species: the need for a flexible asymmetrical approach. Ecol. Monogr. **67**: 345–366.

Eggert, S.L., and Wallace, J.B. 2003. Reduced detrital resources limit *Pycnopsyche gentilis* (Trichoptera: Limnephilidae) production and growth. J. North Am. Benthol. Soc. **22**: 388–400.

Ferreira, V., Elosegi, A., Gulis, V., Pozo, J., and Graça, M.A.S. 2006. Eucalyptus plantations affect fungal communities associated with leaf-litter decomposition in Iberian streams. Arch. Hydrobiol. **166**: 467–490.

Flindt, M.R., and Lillebø, A.I. 2005. Determination of total nitrogen and phosphorus in leaf litter. *In* Methods to study litter decomposition: a practical guide. *Edited by* M.A.S. Graça, F. Bärlocher, and M.O. Gessner. Springer-Verlag, Dordrecht. pp. 45–50.

Friberg, N. 1997. Benthic invertebrate communities in six Danish forest streams: impact of forest type on structure and function. Ecography, **20**: 19–28.

Friberg, N., and Jacobson, D. 1999. Variation in growth of the detritivore-shredder *Sericostoma personatum* (Trichoptera). Freshw. Biol. **42**: 625–635.

Gessner, M.O. 2005*a*. Proximate lignin and cellulose. *In* Methods to study litter decomposition: a practical guide. *Edited by* M.A.S. Graça, F. Bärlocher, and M.O. Gessner. Springer-Verlag, Dordrecht. pp. 103–108.

Gessner, M.O. 2005*b*. Ergosterol as a measure of fungal biomass. *In* Methods to study litter decomposition: a practical guide. *Edited by* M.A.S. Graça, F. Bärlocher, and M.O. Gessner. Springer-Verlag, Dordrecht. pp. 171–176.

Gessner, M.O., and Chauvet, E. 1994. Importance of stream microfungi in controlling breakdown rates of leaf litter. Ecology, **75**: 1807–1817.

Gessner, M.O., Chauvet, E., and Dobson, M. 1999. A perspective on leaf litter breakdown in streams. Oikos, **85**: 377–384.

Gotelli, N.J., and Colwell, R.K. 2001. Quantifying biodiversity: procedures and pitfalls in the measurement and comparison of species richness. Ecol. Lett. **4**: 379–391.

Gotelli, N.J., and Entsminger, G.L. 2006. EcoSim, null model software for ecologists. Version 7 [online]. Available from www.garyentsminger.com/ecosim/index.htm [updated 5 January 2006]. Acquired Intelligence, Inc. & Kesey-Bear, Jericho, Vt.

Graça, M.A.S. 2001. The role of invertebrate on leaf litter decomposition in streams — a review. Int. Rev. Hydrobiol. **86**: 383–393.

Graça, M.A.S., Cressa, C., Gessner, M.O., Feio, M.J., Callies, K.A., and Barrios, C. 2001. Food quality, feeding preferences, survival and growth of shredders from temperate and tropical streams. Freshw. Biol. **46**: 947–957.

Graça, M.A.S., Pozo, J., Canhoto, C., and Elosegui, A. 2002. Effects of Eucalyptus plantations on detritus, decomposers and detritivores in streams. The Scientific World Journal, **2**: 1173–1185.

Gulis, V. 2001. Are there any preferences in aquatic hyphomycetes? Mycol. Res. **105**: 1088–1093.

Hoffmeister, T.S., Vet, L.E.M., Biere, A., Holsinger, K., and Filser, J. 2005. Ecological and evolutionary consequences of biological invasion and habitat fragmentation. Ecosystems, **8**: 257–667.

Jonsson, M., Dangles, O., Malmqvist, B., and Guérold, F. 2002. Simulating species loss following perturbation: assessing the effects on process rates. Proc. R. Soc. Lond. B Biol. Sci. **269**: 1047–1052.

Kennedy, T.A., and Hobbie, S.E. 2004. Saltcedar (*Tamarix ramosissima*) invasion alters organic matter dynamics in a desert stream. Freshw. Biol. **49**: 65–76.

Laitung, B., and Chauvet, E. 2005. Vegetation diversity increases species richness of leaf-decaying fungal communities in woodland streams. Arch. Hydrobiol. **164**: 217–235.

Lecerf, A., Dobson, M., Dang, C.K., and Chauvet, E. 2005. Riparian plant species loss alters trophic dynamics in detritus-based stream ecosystems. Oecologia, **146**: 432–442.

Lecerf, A., Risnoveanu, G., Popescu, C., Gessner, M.O., and Chauvet, E. 2007. Decomposition of diverse litter mixtures in streams. Ecology, **88**: 201–209.

Legendre, P., and Gallagher, E.D. 2001. Ecologically meaningful transformations for ordination of species data. Oecologia, **129**: 271–280.

LeRoy, C.J., Whitham, T.G., Keim, P., and Marks, J. 2006. Plant genes link forests and streams. Ecology, **87**: 255–261.

Maerz, J.C., Blossey, B., and Nuzzo, V. 2005. Green frogs show reduced foraging success in habitats invaded by Japanese knotweed. Biodivers. Conserv. **14**: 2901–2911.

Naiman, R.J., Décamps, H., and McLain, N. 2005. Riparia: ecology, conservation, and management of streamside communities. Elsevier Academic Press, Burlington, Mass.

Nikolcheva, L.G., and Bärlocher, F. 2005. Seasonal and substrate preferences of fungi colonizing leaves in streams: traditional versus molecular evidence. Environ. Microbiol. **7**: 270–280.

Planty-Tabacchi, A.M., Tabacchi, E., Naiman, R.J., Deferrari, C., and Decamps, H. 1996. Invasibility of species-rich communities in riparian zones. Conserv. Biol. **10**: 598–607.

Pyšek, P., and Prach, K. 1993. Plant invasions and the role of riparian habitats: a comparison of four species alien to central Europe. J. Biogeogr. **20**: 413–420.

Richardson, J.S., Shaughnessy, C.R., and Harrison, P.G. 2004. Litter breakdown and invertebrate association with three types of leaves in a temperate rainforest stream. Arch. Hydrobiol. **159**: 309–325.

StatSoft, Inc. 2001. Electronic statistics textbook [online]. Available from www.statsoft.com/textbook/stathome.html [accessed March 2007].

Stout, B.M., Benfield, E.F., and Webster, J.R. 1993. Effects of a forest disturbance on shredder production in southern Appalachian headwater streams. Freshw. Biol. **29**: 59–69.

Thompson, R.M., and Townsend, C.R. 2003. Impacts on stream food webs of native and exotic forest: intercontinental comparison. Ecology, **84**: 145–161.

Tickner, D.P., Angold, P.G., Gurnell, A.M., and Mountford, J.O. 2001. Riparian plant invasions: hydrogeomorphological control and ecological impacts. Progress in Physical Geography, **25**: 22–52.

Wallace, J.B., Eggert, S.L., Meyer, J.L., and Webster, J.R. 1997. Multiple trophic levels of a forest stream linked to terrestrial inputs. Science (Washington, D.C.), **277**: 102–104.

Webster, J.R., and Benfield, E.F. 1986. Vascular plant breakdown in freshwater ecosystems. Annu. Rev. Ecol. Syst. **17**: 567–594.

Weston, L.A., Barney, J.N., and DiTommaso, A. 2005. A review of the biology and ecology of three invasion perennials in New York State: Japanese knotweed (*Polygonum cuspidatum*), mugwort (*Artemisia vulgaris*) and pale swallow-wort (*Vincetoxicum rossicum*). Plant Soil, **277**: 53–69.

Whiles, M.R., and Wallace, J.B. 1997. Leaf litter decomposition and macroinvertebrate communities in headwater streams draining pine and hardwood catchments. Hydrobiologia, **353**: 107–119.

Appendix A

Table A1. Indicator fungal species and invertebrate taxa characterizing site types and leaf species in The Pennines and the Pyrenees.

	Reference site	Invaded site	English oak	Japanese knotweed
Fungi				
Pennines	*Mycocentrospora angulata* R.H. Petersen (57.1)	*Tricladium chaetocladium* Ingold (94.0)	*Clavatospora longibrachiata* (Ingold) S. Nilsson (88.2) *Flagellospora curvula* Ingold (87.3) *Mycocentrospora angulata* R.H. Petersen (60.5) *Taeniospora gracilis* Marvanová (31.0)	Non-identified filiform, 60–120 µm (20.0) *Anguillospora* sp1 (12.0)
Pyrenees	*Tumularia aquatica* (Ingold) Descals & Marvanová (32.8)	*Alatospora acuminata* Ingold (82.2)	*Tetrachaetum elegans* Ingold (90.0)	*Anguillospora* sp1 (58.08)
	Tricladium angulatum Ingold (17.2)	*Tetracladium marchalianum* De Wildeman (66.0) *Clavariopsis aquatica* De Wildeman (64.9) *Anguillospora* sp1 (50.6)	*Articulospora tetracladia* Ingold (83.1) *Flagellospora curvula* Ingold (76.3) *Clavatospora longibrachiata* (Ingold) S. Nilsson (71.7) *Tricladium chaetocladium* Ingold (57.6) *Geniculospora inflata* (Ingold) S. Nilsson (53.5) *Mycocentrospora* cf. *aquatica* S.H. Iqbal (49.0) *Lemonniera terrestris* Tubaki (45.0) *Heliscus lugdunensis* Saccardo & Thérry (27.5)	*Anguillospora* sp2 (57.04) Non-identified filiform, > 120 µm (15.8) *Tetracladium setigerum* (Grove) Ingold (15.0)
Invertebrates				
Pennines	Chironomidae (54.4)	*Brachyptera risi* (Morton) (56.4)		
	Simulidae (43.9)	*Amphinemura sulcicollis* (Stephens) (26.1)		
	Hydropsyche instabilis Curtis (18.4)			
Pyrenees	Simulidae (77.5)	*Hydropsyche siltalai* Döhler (78.8)		
	Chironomidae (63.4)	*Elmis* (54.3)		
	Clinocerinae (32.5)	*Ancylus fluviatilis* Müller (45.7)		
	Protonemura (22.9)	Rhyacophilidae (25.5)		
	Ceratopogoninae (20.0)	*Potamophylax latipennis* (Curtis) (16.1)		
		Sericostoma personatum (Spence) (15.0)		

Note: Only taxa for which indicator value (given in parentheses) is significant at $p < 0.05$ according to the two randomized tests are shown (see M. Dufrêne and P. Legendre. 1997. Ecol. Monogr. **67**: 345–366).

Evidence for greater reproductive output per unit area in areas protected from fishing

Michel J. Kaiser, Robert E. Blyth-Skyrme, Paul J.B. Hart, Gareth Edwards-Jones, and David Palmer

Abstract: Marine protected areas are advocated as an essential management tool to ensure the sustainable use of marine resources by providing insurance against over-exploitation and through the provision of refuge for a large biomass of sexually mature adults. Using a unique fishing gear-restriction, voluntary management system as a large-scale experiment, we found that adult scallops (*Pecten maximus*) within areas protected from towed bottom-fishing gear had heavier adductor muscle tissue and gonads that were 19%–24% heavier than those of scallops in fished areas, while other body and age characteristics were similar in both areas. The scallops within the protected area also occurred at a much higher abundance than adjacent, chronically fished (× 12.83) and wider commercially exploited (× 2.18) areas. These results provide evidence that the use of towed bottom-fishing gear can further exacerbate the effects of overfishing through the suppression of the reproductive potential of individuals of similar body size. These findings underline the utility of using closed areas as tools for fisheries conservation of sedentary species of commercial importance.

Résumé : On recommande les zones de protection marine comme outils essentiels de gestion afin d'assurer l'utilisation durable des ressources marines, car elles procurent une assurance contre la surpêche et des refuges pour une importante biomasse d'adultes arrivés à la maturité sexuelle. En utilisant un système de gestion inédit de restriction volontaire des engins de pêche comme expérience à grande échelle, nous observons que, dans les zones protégées où les engins de pêche tirés sur le fond ne sont pas utilisés, les pétoncles adultes (*Pecten maximus*) ont le tissu du muscle adducteur et les gonades de 19 % à 24 % plus lourds que les pétoncles des zones exploitées; les autres caractéristiques du corps et de l'âge sont, par ailleurs, semblables dans les deux zones. Les pétoncles de la zone protégée ont aussi une densité beaucoup plus grande que celles de la zone adjacente soumise chroniquement à la pêche (× 12,83) et des zones plus éloignées exploitées commercialement (× 2,18). Ces résultats montrent que l'utilisation d'engins de pêche traînés sur le fond peut amplifier les effets de la surpêche en réduisant le potentiel reproductif des individus de taille correspondante. Ces observations soulignent l'intérêt d'utiliser les zones fermées comme outils de conservation halieutique chez les espèces sédentaires d'importance commerciale.

[Traduit par la Rédaction]

Introduction

Ecological benefits conferred by marine protected areas (MPAs) are typically measured as an increase in the biomass, abundance, and body size (age) of species that occur within the protected area (Jennings 2000; Halpern 2003). These effects have been demonstrated for a range of phyla, including fish and molluscs (Gell and Roberts 2003). However, in most cases, the species that demonstrated a positive response to protection from fishing were strongly associated with a specific habitat such as a rock or coral reef (Jennings et al. 1995; Willis et al. 2003). In contrast, for species of greater mobility or that utilize a variety of habitats, there is some doubt that MPAs would outperform adequate fishing effort control as a conservation measure (Jennings 2000; Murawski et al. 2000; Steele and Beet 2003). Temperate species with a sedentary lifestyle, such as bivalve molluscs or certain Crustacea, are those most likely to benefit from the exclusion of fishing activities from discrete areas of the sea, as demonstrated by the fourteenfold increase in scallop biomass after a 5-year fishery exclusion off the northeast coast of the USA and as found in a similar study off the Isle of Man, UK (Horwood 2000; Murawski et al. 2000; Beukers-Stewart et al. 2005).

In addition to removing harvesting pressure on the larger individuals within a population, the exclusion of towed bottom-fishing gear also eliminates associated negative ecological effects on nontarget benthic biota and seabed habitats (Jennings and Kaiser 1998; Kaiser et al. 2002). The net benefits accrued in MPAs are therefore considered to result in

Received 9 August 2006. Accepted 18 April 2007. Published on the NRC Research Press Web site at cjfas.nrc.ca on 18 September 2007.
J19476

M.J. Kaiser[1] and R.E. Blyth-Skyrme. School of Ocean Sciences, Bangor University, Menai Bridge, Anglesey, LL59 5AB, UK.
P.J.B. Hart. Department of Biology, University of Leicester, Leicester, LE1 7RH, UK.
G. Edwards-Jones. School of Agriculture and Forestry Science, Bangor University, Deiniol Road, Bangor, LL57 2UW, UK.
D. Palmer. Centre for Environment, Fisheries & Aquaculture Science (CEFAS) Lowestoft Laboratory, Pakefield Road, Lowestoft, Suffolk, NR33 0HT, UK.

[1] Corresponding author (e-mail: michel.kaiser@bangor.ac.uk).

Can. J. Fish. Aquat. Sci. **64**: 1284–1299 (2007) doi:10.1139/F07-090

an increase in the proportion and density of large-bodied mature adults that have higher fecundity resulting in spill-over and potentially propagation into the adjacent fisheries (Gell and Roberts 2003).

We examined the effects of the exclusion of towed bottom-fishing gear and harvesting on a population of great scallops *Pecten maximus* within a management area known as the Inshore Potting Agreement (IPA), Devon, UK (Hart 1998; Blyth et al. 2002). The IPA has been established for over 25 years and is ~500 km^2 of the sea that was subject to a voluntary agreement among different sectors of the fishing industry until 2002, when it was enforced by government legislation (Fig. 1). The area is divided such that a fixed portion is used exclusively by static gear (pots) fishers that target crab and lobster only, while other areas are open seasonally half of the year to towed bottom-fishing gear (trawls and scallop dredges) that target demersal fishes and scallops. Fishing with towed bottom gears occurs throughout the year immediately adjacent to the area. Areas open to commercial scallop fishing activity would be expected to have on average a lower abundance and smaller scallops, but the release of competition for resources might lead to larger somatic growth and investment in reproductive tissues in individual animals. The specific aims of the study were to test for differences in the abundance, body size, and allocation of tissue mass to gonads or soma in scallops sampled in areas subjected to different regimes of fishing activity.

Materials and methods

We sampled scallops from sites that represented a gradient of fishing regimes in August 2002. This gradient comprised of (*i*) fished sites that were open to scallop dredging year round or that were known to have been fished illegally but annually according to the direct observations of fishermen that participated in the IPA, (*ii*) ex-fished sites that had been illegally scallop-dredged 18 months previously but not before this period, and (*iii*) no-fishing sites that were known never to have been fished using towed fishing gear. We have confidence in the accuracy of the information supplied by the fishers involved in the agreement as (1) the fishers have nothing to gain or lose by providing false information, and (2) we have over 10 years of direct working experience with this group of individuals and the local government enforcement body.

The habitat is similar across all sites: a mixed sediment of coarse sand, gravel, and fine mud, punctuated by exposed bedrock. However, the benthic biota associated with the areas of the IPA subjected to different fishing regimes varies accordingly, with the highest diversity and biomass occurring in the no-fishing areas (for a detailed habitat description, see Kaiser et al. 2000; Blyth et al. 2002). Scallops were collected at each site (Fig. 1) from three replicate tows each of 10 min bottom-time duration made with a gang of four Newhaven scallop dredges. The start and end (shot and hauled) positions of each haul were recorded from the ship's navigation system, which enabled the abundance of scallops to be standardized per unit area of seabed. The Newhaven scallop dredge is widely used in northern Europe and consists of a rigid frame approximately 75 cm wide to which a sprung tooth-bar (teeth ~12 cm long) is attached. A net bag with a steel ring belly is attached behind the rigid frame. Gangs (one each side of the vessel) of up to 22 dredges can be fished in some parts of the UK.

Fig. 1. The Inshore Potting Agreement, located off the south coast of Devon, England. Shaded areas denote the officially recognised fishery management system. The light grey areas denote areas from which towed bottom-fishing gear are entirely excluded; the dark grey areas denote seasonal cyclical use by static and towed gear fishers; the unshaded areas are open to all forms of fishing. Numbers denote locations of sampling sites in areas subjected to different fishing regimes as ascertained from interviews with the fishers involved in the agreement. (*i*) Fished sites 1, 2, 3, 4, and 5: note that although site 5 is officially located within a static gear only area, it is known to have been fished by scallop dredgers on an annual basis, even through this is illegal. (*ii*) Ex-fished sites 6 and 7: these sites were supposedly within the static gear only area, but were fished illegally for the first time 18 months prior to the present study. (*iii*) No-fishing sites 8 and 9: for at least 25 years, both of these sites are known never to have been fished with towed gear.

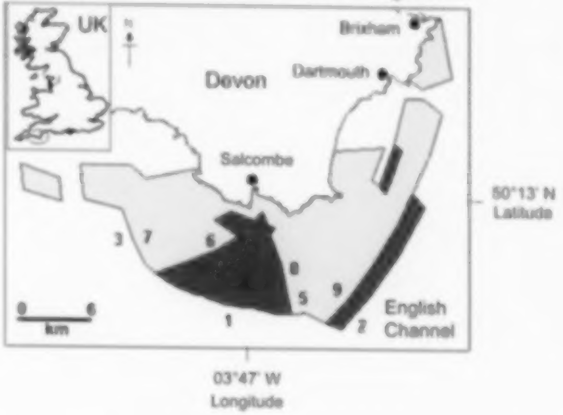

The number of sites sampled may seem relatively few, but this was constrained by the need to get the agreement of pot fishers to move their gear to enable us to sample scallops using towed fishing gear within those areas. Thus, the number of sites sampled reflects the number of collaborating fishers. Catch abundance of scallops above the minimum landing size (100 mm shell height) was standardized to numbers per hectare and tested for significant differences ($\alpha = 0.05$) among fishing regimes using a nested analysis of variance (ANOVA) with sample site nested within fishing regime. Where differences were found, Tukey–Kramer post hoc comparisons were performed. To put this study in the context of a wider geographic area, these data were compared with a much larger field survey of scallop abundance data collected by the Centre for Environment, Fisheries & Aquaculture Science (CEFAS) in August 2004 across the western English Channel. This survey used the same dredges as used in the present study, with standard tows of 15 min. Scallop abundance was standardized to numbers per hectare (see Kaiser et al. 1998).

In the present study, scallops were measured at their right valve for shell height (mm) and clean shell dry weight (g), and the adductor muscle and gonads were dissected out and returned to the laboratory preserved in 4% buffered formalin

Table 1. General linear model nested analysis of variance (ANOVA) to examine variation in scallop (*Pecten maximus*) abundance for those animals >100 mm shell height among different fishing regimes (fished, ex-fished, and no-fishing areas that compose the Inshore Potting Agreement).

Source	*df*	Seq SS	Adj SS	Adj MS	*F*	*P*
Type	2	214.422	214.422	107.211	14.76	0.0001
Site(Type)	6	292.811	292.811	48.802	6.72	0.001
Error	18	130.767	130.767	7.265		
Total	26	638.000				

Note: Seq SS, sequential sum of squares; Adj SS, adjusted sum of squares; Adj MS, adjusted mean square.

in seawater. Age was determined from the annual growth rings that occur in the shell and are amenable to direct quantification. The adductor muscle was chosen because it is used to close the valves of the shell and is the main mechanism of protection from their main predator, the common starfish *Asterias rubens*. Consequently, there is a strong evolutionary selection to invest in tissues that reduce the risk of mortality through predation. The dry weight of these tissues was ascertained by drying to constant weight in an oven set at 90 °C. Condition indices of flesh weight to shell weight and gonad weight were calculated to standardize for differences in body size range that might occur among the different fishing treatments. Damage scars on the right-hand valve of the shell were counted. Scars were defined as irregular indentations at the edge of the shell or that had occurred previously but been repaired by the animal (Ramsay et al. 2000). Data were subjected to ANOVA after testing that the data met the appropriate assumptions using $\log_e$ transformation to stabilize the variance. Differences in the weight of shell, adductor muscle, and gonad per unit shell size were tested (on transformed data) using analysis of covariance (ANCOVA) for the no-fishing and fished sites only. Records of shell scar damage were tested for significance between the different fishing treatments using a Kruskal–Wallis test, as the data did not meet the assumptions for ANOVA.

Results

The mean abundance (per hectare) of scallops was highest in the no-fishing areas and lowest in the fished areas immediately surrounding the IPA (Table 1; mean ± standard error (SE): no-fishing 75.7 ± 30.1; ex-fished 14.5 ± 4.6; fished 5.9 ± 2.3), although there was a significant effect of site nested within fishing regime, which meant that scallop abundance also varied significantly among replicate sample sites. Multiple comparison tests demonstrated that only the abundance of scallops in the ex-fished sites compared with the fished sites were not significantly different (Tukey–Kramer, $P > 0.5$). The abundance of scallops within the no-fishing area was also nearly twice as high as the mean abundance (34.7 ± 3.2) of a sample of 162 stations sampled across the western English Channel (Fig. 2).

As would be expected, scallops collected within the ex-fished areas were on average smaller in shell size and younger (age in years) than scallops sampled in areas either protected from towed bottom-fishing gear or areas open to fishing all year (ANOVA: $F_{[2,191]} = 61.9$, $P < 0.0001$; ex-fished, 5.05 years; fished, 6.6 years; no-fishing, 6.5 years). The lower mean size and age is possibly related to a short burst of intensive and highly targeted illegal fishing in the ex-fished areas. The similar mean ages of scallops found in both fished and no-fishing areas is perhaps explained by the greater sampling effort that was able to be used in the fished areas, in addition to the fact that we were attempting to compare gonads and adductor muscles from scallops of similar shell size (i.e., the primary aim was not to estimate mean age of scallops from the different areas).

Fig. 2. Mean (± standard error) number·ha^{-1} for background, no-fishing, ex-fished, and fished sites. Background densities were calculated from Centre for Environment, Fisheries and Aquaculture Science (CEFAS) scallop survey in summer 2004. Standard tows (15 mins) were made ($n = 162$ sites across the western English Channel) using the same scallop dredges reported in the present paper, and abundance was standardized to number of scallops·ha^{-1}.

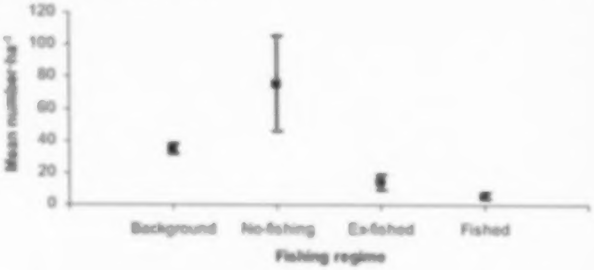

Scallops sampled from the no-fishing areas had the highest mean ratio of gonad dry weight to adductor muscle dry weight, which was 19% and 24% higher than that for the fished and ex-fished areas, respectively (Tukey–Kramer, no-fishing vs. fished, $P < 0.02$; no-fishing vs. ex-fished, $P = 0.01$). ANCOVAs comparing scallops >100 mm shell height between fished and no-fishing sites (i.e., excluding the ex-fished sites) showed that while the shell weights were not different, the increases in weight of adductor muscle and gonad per unit shell length were significantly greater in the no-fishing sites (Fig. 3; Table 2). Shells of scallops collected from the fished areas had a significantly higher median number of scars per shell (2) than shells from the other treatment (median 1 scar per shell) (Kruskal–Wallis, $H = 6.7$, df = 2, $P < 0.035$).

Discussion

The abundance of scallops above the minimum landing size was 12.83 times higher in areas from which towed

Fig. 3. Comparison of (*a*) shell weight, (*b*) dry adductor muscle weight, and (*c*) dry gonad weight against shell height for legal-sized scallops (>100 mm shell height) at no-fishing (solid circles) and fished (open diamonds) sites only. Trend lines show best-fit linear relationships.

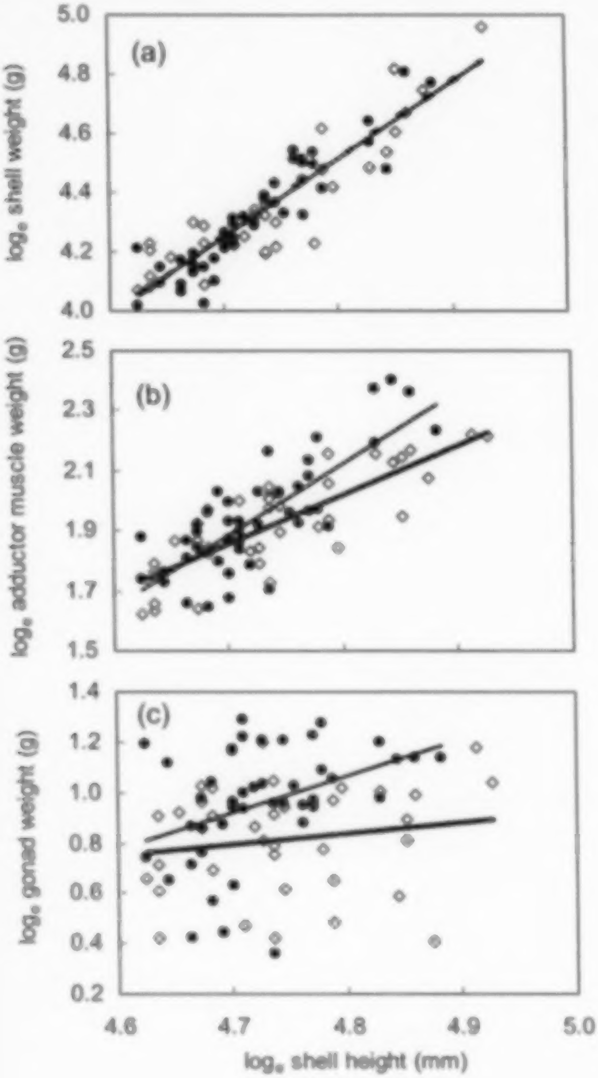

Table 2. Results of analyses of covariance comparing $\log_e$ dry shell, dry adductor muscle, and dry gonad weights against $\log_e$ shell height for scallops >100 mm shell height at no-fishing and fished sites, with $\log_e$ shell height as the covariate.

Source	df	Seq SS	Adj MS	*F*	*P*
$\log_e$ shell weight					
$\log_e$ shell height	1	3.09	3.03	427.6	<0.001
Fishing regime	1	0	0	0.02	0.887
Error	79	0.56	0.01		
Total	81	3.64			
$\log_e$ adductor muscle weight					
$\log_e$ shell height	1	1.5	1.55	128.62	<0.001
Fishing regime	1	0.05	0.05	4.53	0.036
Error	79	0.95	0.01		
Total	81	2.5			
$\log_e$ gonad weight					
$\log_e$ shell height	1	0.21	0.29	6.47	0.013
Fishing regime	1	0.51	0.51	11.24	0.001
Error	79	3.59	0.05		
Total	81	4.31			

Note: The scallops from the ex-fished sites have not been included in this analysis, and no differentiation is made between sites within no-fishing and fished treatments. Seq SS, sequential sum of squares; Adj MS, adjusted mean square.

bottom-fishing gear had been excluded compared with the adjacent areas where fishing occurred either year-round or for 6 months of the year (fished sites). This finding is similar to those from much larger areas closed to fishing of the NE coast of the USA (× 14 increase in biomass) (Murawski et al. 2000) and those off the Isle of Man, UK (× 11 increase in biomass) (Beukers-Stewart et al. 2005). Scallop abundance was also high in those areas that had been protected from towed bottom-fishing gear, but that had been fished illegally during a short period of intensive activity in the last 2 years. However, the mean size of these scallops was much lower, which may be explained in part by the gear selection for only the larger size classes that met the requirements of legal landing-size restrictions and also by the greater sampling effort that we were able to apply in the fished areas, which increased the probability of sampling the less common old scallops. In addition to the greater abundance of scallops within areas protected from fishing, the weight of gonad tissue per unit body size was between 19% and 24% higher in the areas protected from scallop dredging, giving a potential biomass of reproductive output of up to 15.9 times greater than in areas that experience chronic scallop dredging (calculated from the increased abundance and greater gonad tissue (12.83 × 1.24)).

Scallops are sedentary organisms that reproduce by broadcast spawning; hence, reproductive success is likely to be highly density-dependent in this species (Levitan et al. 1992; Yund 2000), especially given the low densities of scallops that were found in the fished areas. Perhaps the most important finding is the previously unreported decrease in reproductive potential of scallops located in areas exposed to chronic fishing activity, as represented by smaller gonad weight per unit body size. Although we were not able to ascertain whether this reduced gonad size equated to fewer or smaller eggs, in either scenario this would result in lower potential successful spawning, as egg size is directly related to egg survival (Martinez and Perez 2003). The reduced adductor muscle mass in the fished areas was not as pronounced as the difference observed in gonad mass. This may reflect the importance of the adductor muscle as an anti-predation strategy against common starfish.

There are a number of factors that might affect gonad production in scallops. It is unlikely that gradients in environmental conditions would have affected gonad size, as the distances among replicate fishing regime sites were similar, thereby controlling for large-scale differences in food supply. Also, water depth across our study sites varied by no

Fig. 4. SeaWIFS imagery of the study area in April and August 2002, with the study site locations overlaid. On neither occasion was there any strong evidence of strong spatial heterogeneity in terms of primary production (i.e., chlorophyll *a* content of the surface water) across the area that might explain differences in gonad and muscle tissues reported in the present study. Data reproduced from www.ifremer.fr/cersat/facilities/browse/del/roses/browse.htm.

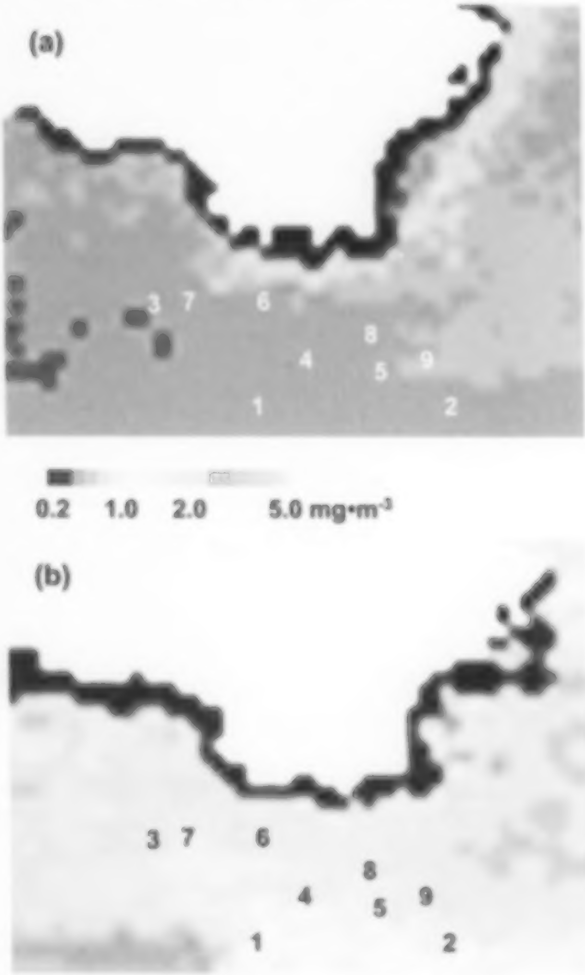

more than 10 m, with an average overall depth of 61.5 m (Kaiser et al. 2000) Furthermore, examination of SeaWIFS imagery (www.ifremer.fr/cersat/facilities/browse/del/roses/browse.htm) of the chlorophyll *a* content of the surface waters of the study site in April and August 2002 indicates no significant gradient in food concentration from inshore to offshore (Fig. 4). The higher abundance of scallops and higher biomass of other sessile, filter-feeding biota within the no-fishing areas might be expected to lead to density-dependent competition for food resources (Gascoigne et al. 2005) within and among species, such that flesh weight would be lower than that in the fished areas, where the biomass of these organisms is lower (Kaiser et al. 2000). Here, we report a result that is entirely the opposite of what might be expected, that is, larger gonad and muscle mass for animals of the same age and size, in areas where competition for resources is highest because of a higher overall biomass of filter feeders (Kaiser et al. 2000).

Newhaven scallop dredges are highly inefficient (41% catch efficiency at most; Beukers-Stewart et al. 2001); hence, scallops located in areas subjected to chronic fishing are more likely to incur repeated injuries from physical contact with fishing gear, which would divert energy from gonad production to the repair of body tissues. The shells of scallops collected from the fished sites in the present study had a higher incidence of shell scars, which provides evidence that these individuals have been subjected to higher levels of physical disturbance than those protected from dredging. In addition, the resuspension of sediments that occurs as a result of bottom fishing can be equivalent to that which occurs during storm events (Planques et al. 2001). Storm events have been shown to lower the availability of suspended particulate matter as a food source for scallops (Cranford et al. 1998; Planques et al. 2001). Both an increased incidence of physical damage and periodic reduction in the availability of food resources could explain the reduced gonad development observed in the present study.

It would appear that areas protected from the effects of bottom fishing not only conserve population abundance and biomass of bivalve molluscs but also maintain reproductive quality (expressed as gonad mass per unit animal size), which is greatly reduced in areas exposed to chronic fishing. This observation suggests that these hitherto unconsidered effects of fishing could further compound the population consequences of depensation for sessile target species such as bivalve molluscs.

Acknowledgements

RB-S was in receipt of an Isle of Man Government studentship. This research was funded in part by Department for Environment, Food and Rural Affairs (DEFRA) contract MF0805. The comments of three anonymous referees, Juan Castilla, and an anonymous colleague helped improve earlier versions of this paper.

References

Beukers-Stewart, B.D., Jenkins, S.R., and Brand, A.R. 2001. The efficiency and selectivity of spring-toothed scallop dredges: a comparison of direct and indirect methods of assessment. J. Shellfish Res. **20**: 121–126.

Beukers-Stewart, B.D., Vause, B.J., Mosley, M.W.J., Rossetti, H.L., and Brand, A.R. 2005. Benefits of closed area protection for a population of scallops. Mar. Ecol. Prog. Ser. **298**: 189–204.

Blyth, R.E., Kaiser, M.J., Edwards-Jones, G., and Hart, P.J.B. 2002. Voluntary management in an inshore fishery has conservation benefits. Environ. Conserv. **29**: 493–508.

Cranford, P.J., Emerson, C.W., Hargrave, B.T., and Milligan, T.G. 1998. In situ feeding and absorption responses of sea scallops *Placopecten magellanicus* (Gmelin) to storm-induced changes in the quantity and composition of seston. J. Exp. Mar. Biol. Ecol. **219**: 45–70.

Gascoigne, J.C., Beadman, H.A., Saurel, C., and Kaiser, M.J. 2005. Density dependence, spatial-scale and patterning in sessile biota. Oecologia, **145**: 371–381.

Gell, F.R., and Roberts, C.M. 2003. Beneftis beyond boundaries: the fishery effects of marine reserves. Trends Ecol. Evol. **18**: 448–455.

Halpern, B.S. 2003. The impact of marine reserves: do reserves work and does reserve size matter? Ecol. Appl. **13**: S117–S137.

Hart, P.J.B. 1998. Enlarging the shadow of the future: avoiding conflict and conserving fish off south Devon, UK. *In* Reinventing fisheries management. *Edited by* T.J. Pitcher, P.J.B. Hart, and D. Pauly. Kluwer, Dordrecht. pp. 227–238.

Horwood, J.W. 2000. No-take zones: a management context. *In* The effects of fishing on non-target species and habitats: biological, social and economic issues. *Edited by* M.J. Kaiser and S.J. de Groot. Blackwell Science, Oxford. pp. 302–312.

Jennings, S. 2000. Patterns and prediction of population recovery in marine reserves. Rev. Fish Biol. Fish. **10**: 209–231.

Jennings, S., and Kaiser, M. 1998. The effects of fishing on marine ecosystems. Adv. Mar. Biol. **34**: 201–352.

Jennings, S., Grandcourt, E.M., and Polunin, N.V.C. 1995. The effects of fishing on the diversity, biomass and trophic structure of Seychelles' reef fish communities. Coral Reefs, **14**: 225–235.

Kaiser, M.J., Armstrong, P.J., Dare, P.J., and Flatt, R.P. 1998. Benthic communities associated with a heavily fished scallop ground. J. Mar. Biol. Assoc. U.K. **78**: 1045–1059.

Kaiser, M.J., Spence, F.E., and Hart, P.J.B. 2000. Fishing gear restrictions and conservation of benthic habitat complexity. Conserv. Biol. **14**: 1512–1525.

Kaiser, M.J., Collie, J.S., Hall, S.J., Jennings, S., and Poiner, I.R. 2002. Modification of marine habitats by trawling activities: prognosis and solutions. Fish and Fisheries, **3**: 114–136.

Levitan, D.R., Sewell, M.A., and Chia, F.S. 1992. How distribution and abundance influence fertilization success in the sea urchin *Strongylocentrus franciscanus*. Ecology, **73**: 248–254.

Martinez, G., and Perez, H. 2003. Effect of different temperature regimes on reproductive conditioning in the scallop *Argopecten purpuratus*. Aquaculture, **228**: 153–167.

Murawski, S.A., Brown, R., Lai, H.-L., Rago, P.J., and Hendrickson, L. 2000. Large-scale closed areas as a fishery-management tool in temperate marine systems: the Georges Bank experiment. Bull. Mar. Sci. **66**: 775–798.

Planques, A., Guilen, J., and Puig, P. 2001. Impact of bottom trawling on water turbidity and muddy sediment of an unfished continental shelf. Limnol. Oceanogr. **46**: 1100–1110.

Ramsay, K., Kaiser, M.J., Richardson, C.A., Veale, L.O., and Brand, A.R. 2000. Can shell scars on dog cockles (*Glycymeris glycymeris* L.) be used as an indicator of fishing disturbance. J. Sea Res. **43**: 167–176.

Steele, J.H., and Beet, A.R. 2003. Marine protected areas in 'nonlinear' ecosystems. Proc. R. Soc. Lond. B Biol. Sci. **270**(Suppl.): S230–S233.

Willis, T.J., Millar, R.B., and Babcock, R.C. 2003. Protection of exploited fishes in temperate regions: high density and biomass of snapper *Pagurus auratus* (Sparidae) in northern New Zealand marine reserves. J. Appl. Ecol. **40**: 214–227.

Yund, P.O. 2000. How severe is sperm limitation in natural populations of marine free-spawners? Trends Ecol. Evol. **15**: 10–13.

Fisheries and Aquatic Sciences
Sciences halieutiques et aquatiques

Photographic Atlas of Fish Otoliths of the Northwest Atlantic Ocean

By / Par Stephen E. Campana

$54.95 CAN. Other countries $54.95 US
54,95 $CAN. À l'étranger 54,95 $US
Softcover / Édition brochée
(*Can. Spec. Publ. Fish. Aquat. Sci. / Publ. spéc. can. sci. halieut. aquat. 133*)
284 pages ISBN 0-660-19108-3 ISSN 0706-6481 NRC / CNRC 46328

Salmonine Introductions to the Laurentian Great Lakes: An Historical Review and Evaluation of Ecological Effects

By / Par Stephen S. Crawford

$42.95 CAN. Other countries $42.95 US
42,95 $CAN. À l'étranger 42,95 $US
Softcover / Édition brochée
(*Can. Spec. Publ. Fish. Aquat. Sci. / Publ. spéc. can. sci. halieut. aquat. 132*)
215 pages ISBN 0-660-17639-4 ISSN 0706-6481 NRC / CNRC 42734

Marine Protected Areas and Fisheries Closures in British Columbia

By Glen S. Jamieson and Joanne Lessard

$69.95 CAN. Other countries $69.95 US
69,95 $CAN. À l'étranger 69,95 $US
Softcover / Édition brochée
(Can. Spec. Publ. Fish. Aquat. Sci. / Publ. spéc. can. sci. halieut. aquat. 131)
414 pages ISBN 0-660-17788-9 ISSN 0706-6481 NRC / CNRC 42846

Workshop on Rebuilding Abalone Stocks in British Columbia

By / Par Alan Campbell

$42.95 CAN. Other countries $42.95 US
42,95 $CAN. À l'étranger 42,95 $US
Softcover / Édition brochée
(*Can. Spec. Publ. Fish. Aquat. Sci. / Publ. spéc. can. sci. halieut. aquat. 130*)
158 pages ISBN 0-660-18292-0 ISSN 0706-6481 NRC / CNRC 42841

To order any of the above titles / Commandez n'importe quel titre ci-dessus à :

Telephone / Téléphone : (613) 990-2254
Fax / Télécopieur : (613) 952-7656
E-mail / Courriel : pubs@nrc-cnrc.gc.ca
Web site / Site web : http://pubs.nrc-cnrc.gc.ca

Order Office / Bureau des commandes
NRC Research Press / Presses scientifique du CNRC
National Research Council / Conseil national de recherches
Ottawa, ON K1A 0R6, Canada

Canadian customers add GST (6%). Prepayment required unless order is accompanied by a purchase order number. Cheques or money orders should be made payable to : "Receiver General for Canada, Credit NRC". For all orders outside Canada, rates are in U.S. Dollars. All sales are final.

Clients du Canada, ajoutez la TPS (6 %). Les commandes doivent être payées d'avance à moins qu'elles ne soient accompagnées d'un numéro de bon de commande. Les chèques ou mandats doivent être libellés au « Receveur général du Canada, crédit du CNRC ». Pour les commandes hors-Canada, les tarifs sont en dollars américains. Toutes les ventes sont finales.

Contents (concluded) / Table des matières (suite et fin)

Antoine Lecerf, Denise Patfield, Anatole Boiché, Miira P. Riipinen, Eric Chauvet, and Michael Dobson 1273–1283 Stream ecosystems respond to riparian invasion by Japanese knotweed (*Fallopia japonica*)

Michel J. Kaiser, Robert E. Blyth-Skyrm, Paul J.B. Hart, Gareth Edwards-Jones, and David Palmer 1284–1289 Evidence for greater reproductive output per unit area in areas protected from fishing

National Research Council Canada
Ottawa, Canada
K1A 0R6

Conseil national de recherches Canada
Ottawa, Canada
K1A 0R6

Postage paid at Ottawa
Publications mail
Registration No. 40062591

Port payé à Ottawa
Poste-publication
Enregistrement n° 40062591

USPS periodical postage paid at Plattsburgh, NY 12901, USA

Canadian Journal of Fisheries and Aquatic Sciences

Journal canadien des sciences halieutiques et aquatiques

Volume 64, Number 9, September 2007

Volume 64, numéro 9, septembre 2007

	ARTICLES	ARTICLES
Richard McGarvey, John E. Feenstra, and Qifeng Ye	1157–1173	Modeling fish numbers dynamically by age and length: partitioning cohorts into "slices"
Michael P. Wilkie, John A. Holmes, and John H. Youson	1174–1182	The lampricide 3-trifluoromethyl-4-nitrophenol (TFM) interferes with intermediary metabolism and glucose homeostasis, but not with ion balance, in larval sea lamprey (*Petromyzon marinus*)
Irma Kallio-Nyberg, Irma Saloniemi, Eero Jutila, and Ari Saura	1183–1198	Effects of marine conditions, fishing, and smolt traits on the survival of tagged, hatchery-reared sea trout (*Salmo trutta trutta*) in the Baltic Sea
Scott A. Pavey, Troy R. Hamon, and Jennifer L. Nielsen	1199–1208	Revisiting evolutionary dead ends in sockeye salmon (*Oncorhynchus nerka*) life history
Ingrid B. Spies, Eric C. Anderson, Kerry Naish, and Paul Bentzen	1209–1221	Evidence for the existence of a native population of sockeye salmon (*Oncorhynchus nerka*) and subsequent introgression with introduced populations in a Pacific Northwest watershed
Gord Paterson, Ken G. Drouillard, Todd A. Leadley, and G. Doug Haffner	1222–1233	Long-term polychlorinated biphenyl elimination by three size classes of yellow perch (*Perca flavescens*)
Jonathan A. Hare and Harvey J. Walsh	1234–1247	Planktonic linkages among marine protected areas on the south Florida and southeast United States continental shelves
Xinhai Li, Matthew K. Litvak, and John E. Hughes Clarke	1248–1257	Overwintering habitat use of shortnose sturgeon (*Acipenser brevirostrum*): defining critical habitat using a novel underwater video survey and modeling approach
G.R. Moyer, M.S. Blouin, and M.A. Banks	1258–1265	The influence of family-correlated survival on N_b/N for progeny from integrated multi- and single-generation hatchery stocks of coho salmon (*Oncorhynchus kisutch*)
Albert Luiz Suhett, André Megali Amado, Alex Enrich-Prast, Francisco de Assis Esteves, and Vinicius Fortes Farjalla	1266–1272	Seasonal changes of dissolved organic carbon photo-oxidation rates in a tropical humic lagoon: the role of rainfall as a major regulator

Continued on inside back cover / Suite au verso

Front cover: Iboko Saito/Toshiyuki Tajima/Dex Image/Getty Images.

Page couverture : Iboko Saito/Toshiyuki Tajima/Dex Image/Getty Images.

Canada

Printed in Canada by / Imprimé au Canada par
NRC Reprographic Services / Service de reprographie CNRC
Page production by / Mise en page par
NRC Research Press / Presses scientifiques du CNRC

0706-652X(200709)64:9;1-G